UNIVERSIDADE DE LISBOA

INSTITUTO SUPERIOR TÉCNICO

Sustainable bio-based resins and fibre-polymer composites for civil engineering structural applications

Mateus de Assunção Hofmann

Supervisor: **Doctor João Pedro Ramôa Ribeiro Correia**
Co-supervisor(s): **Doctor Mário Alexandre de Jesus Garrido**
Doctor João Carlos Moura Bordado

Thesis approved in public session to obtain the PhD Degree in
Civil Engineering

Jury final classification
Pass with Distinction and Honour

2022

UNIVERSIDADE DE LISBOA
INSTITUTO SUPERIOR TÉCNICO

Sustainable bio-based resins and fibre-polymer composites for civil engineering structural applications

Mateus de Assunção Hofmann

Supervisor: **Doctor João Pedro Ramôa Ribeiro Correia**
Co-supervisor(s): **Doctor Mário Alexandre de Jesus Garrido**
Doctor João Carlos Moura Bordado

Thesis approved in public session to obtain the PhD Degree in

Civil Engineering

Jury final classification: **Pass with Distinction and Honour**

Jury

Chairperson: **Doctor Jorge Manuel Caliço Lopes de Brito**, Instituto Superior Técnico, Universidade de Lisboa

Members of the Committee:

Doctor Jorge Fernando Jordão Coelho, Faculdade de Ciências e Tecnologia, Universidade de Coimbra

Doctor Fernando António Baptista Branco, Instituto Superior Técnico, Universidade de Lisboa

Doctor João Pedro Ramôa Ribeiro Correia, Instituto Superior Técnico, Universidade de Lisboa

Doctor Susana Bravo Cordeiro Baptista Cabral da Fonseca, Laboratório Nacional de Engenharia Civil

Funding Institutions

Fundação para a Ciência e Tecnologia (SFRH/BD/139863/2018 and PTDC/ECI-EGC/29597/2017)

Agência Nacional da Inovação (ANI,39769-31/SI/2017)

2022

Resumo

Dado o apelo crescente da sociedade por produtos mais sustentáveis e com menor impacte ambiental, é cada vez mais relevante a busca por alternativas que minimizem a dependência do consumo de recursos fósseis. No contexto da indústria dos compósitos fibra-polímero, o desenvolvimento de polímeros termoendurecíveis baseados em matérias-primas derivadas de recursos renováveis (bio-derivados) pode ajudar a tornar esta indústria mais sustentável e a diminuir a sua atual dependência do petróleo.

Numa primeira fase desta tese, foram desenvolvidas um conjunto de resinas termoendurecíveis inovadoras de poliéster insaturado com elevado bio-conteúdo. A formulação que apresentou maior potencial para substituir as alternativas convencionais derivadas do petróleo foi utilizada como matriz para impregnação de fibras de reforço, de maneira a produzir compósitos fibra-polímero de elevado desempenho, mais sustentáveis e endereçados especialmente para aplicações em estruturas da engenharia civil.

A este respeito, numa segunda fase, a tese apresenta a produção bem-sucedida, por infusão a vácuo, de laminados em compósito de polímero reforçado com fibras de vidro (PRFV) utilizando a resina bio-derivada selecionada, assim como a sua respetiva caracterização. Para além disso, foi produzido, por pultrusão, um protótipo de laminado em compósito de polímero reforçado com fibras de carbono (PRFC), também utilizando a resina bio-derivada selecionada; esta produção foi realizada em ambiente industrial, numa fábrica de laminados de PRFC de elevado desempenho mecânico utilizados no reforço de estruturas de engenharia civil.

Em face das propriedades de processamento das resinas e das propriedades mecânicas e termomecânicas dos compósitos obtidas na extensa campanha experimental realizada nesta tese, foi possível concluir que os compósitos bio-derivados de fibra-polímero aqui desenvolvidos apresentam desempenho equivalente ou, em alguns casos, superior aos alternativos, avaliados sob as mesmas condições, produzidos com resinas convencionais, derivadas do petróleo. Assim, confirma-se que existe uma oportunidade muito relevante para o aumento da sustentabilidade e da competitividade da indústria dos compósitos fibra-polímero, o qual deve ser ainda mais explorado, endereçando um desafio muito importante que este sector enfrenta atualmente.

Palavras-chave: compósitos sustentáveis; resinas de poliéster bio-baseadas; resinas termoendurecíveis bio-baseadas; compósitos bio-baseados de fibra-polímero; matérias-primas renováveis.

Abstract

Given the growing societal demand for more sustainable products with lower environmental impacts, the search for solutions that minimise our dependence on fossil resources is becoming increasingly relevant. In the context of the fibre-polymer composites industry, the development of thermoset polymer matrices based on raw materials derived from renewable resources (bio-based) is key to increase its sustainability and to reduce its current dependence on oil.

In a first stage of this thesis, a set of innovative unsaturated polyester (UP) thermoset resins with high bio-content were developed. The formulation that presented the highest potential to replace its petroleum-derived counterparts was used as impregnation matrix of reinforcing fibres in the production of more sustainable high-performance fibre-polymer composites, specifically targeting applications in civil engineering structures.

In this respect, in a second stage, the thesis presents the successful production, by vacuum infusion, of glass fibre reinforced polymer (GFRP) composites using the above-mentioned bio-based UP resin, and their respective characterisation. In addition, a prototype of a carbon fibre reinforced polymer (CFRP) strip was produced by pultrusion, also using the selected bio-based UP resin; this production was carried out in an industrial pultrusion facility used to manufacture high-performance CFRP strips for strengthening civil engineering structures.

Based on the processing properties of the resins and the mechanical and thermomechanical properties of the composites obtained in the extensive experimental campaign carried out in this thesis, it was possible to conclude that the bio-based fibre-polymer composites developed herein present equivalent or, in some cases, better performance than their petroleum-derived counterparts assessed under the same conditions. Thus, it was possible to confirm that there is a very relevant opportunity to increase the sustainability and competitiveness of the fibre-polymer composites industry, which should be further explored, addressing a very important challenge presently faced by this sector.

Keywords: sustainable composites; bio-based polyester resins; bio-based thermosets; bio-based fibre-polymer composites; renewable raw materials

Acknowledgments

I would like to express my deep gratitude to Professor João Râmoa Correia, scientific supervisor of this thesis, for granting me his trust and freedom in carrying out this research. In addition to the knowledge shared as a Professor and advisor, his enthusiasm and professional dedication is something I had never seen before and has been a great inspiration for my evolution as a student, researcher and engineer.

I would also like to express my gratitude to my co-supervisor Dr. Mário Garrido, who I consider - in addition to a scientific supervisor - a friend for life. The co-supervision of Dr. Mário Garrido was fundamental for the development of this thesis, being a filter of coherence and pragmatism to put my ideas into practice. ”By contrast”, we also had moments of relaxation, mainly those shared on *campus* and, more recently, exchanging tips for playing guitars. I would also like to thank Professor João Bordado, my co-supervisor in the Chemistry area, who I consider the greatest inventor I have ever met. The knowledge and ideas shared by Professor João Bordado were not only fundamental for the execution of this research but will also remain with me for future work. It is worth referring that Professor João Bordado has an office with the most beautiful view of Lisbon, perhaps this is the source of his inspiration.

My thanks to all colleagues and friends of the CORE Group, especially to Abu T. Shahid and Marina Silva, for their help in carrying out the experiments in this thesis. Shahid stayed with me during several extended syntheses, including on weekends, a help I will never forget. Marina also helped me a lot, especially in the final part of this research. My thanks to colleagues, employees and Professors at Instituto Superior Técnico, especially to Professor Fernando Branco, for the moments we shared in the coffee room.

Finally, I would like to thank my wife, Bárbara Silva, who was my emotional support and the biggest motivation to achieve my goals. To my parents, Raquel and José, they are my greatest examples, I thank them for their patience, understanding and unconditional support once again. To my in-laws Kátia and Fernando, for all their help during this period. To my brother-in-law for that special Açaí.

This work was supported by Fundação para a Ciência e a Tecnologia (FCT) and Agência Nacional da Inovação (ANI) through the projects PTDC/ECI-EGC/29597/2017 (Eco-Composite) and Biolam (ANI,39769-31/SI/2017), and through the doctoral grant FCT SFRH/BD/139863/2018, and by the CERIS and CERENA research units of IST.

Table of contents

Resumo i

Abstract iii

Acknowledgments v

Table of Contents vii

List of Figures xv

List of Tables xxi

List of Acronyms xxv

I Introduction and literature review 1

1 Introduction 3

1.1 Context and motivation 3

1.2 Topic overview 6

1.3 Objectives 7

1.4 Methodology 8

1.5 Thesis organisation 9

1.6 References 11

2 Literature review 15

2.1 Introductory remarks 15

2.2 Materials and manufacturing 16

2.2.1 Reinforcing fibres 16

2.2.1.1 Synthetic fibres 16
2.2.1.2 Vegetable fibres 18
2.2.1.3 Basalt fibres 21
2.2.1.4 Comparative critical assessment 24
2.2.2 Polymer matrix 27
2.2.2.1 Conventional thermoset resins 29
2.2.2.2 Bio-based thermoset resins 35
2.2.2.3 Renewable platform 37
2.2.3 Manufacturing techniques 39
2.2.3.1 Hand lay-up 40
2.2.3.2 Vacuum infusion 42
2.2.3.3 Pultrusion 45
2.3 Bio-based composite applications 47
2.3.1 Strengthening of concrete structures 47
2.3.2 Pultruded profiles and FRP laminates 49
2.3.3 Sandwich panels 49
2.3.4 Construction of bridges 49
2.4 Concluding remarks 50
2.5 References 51

II Resins **69**

3 ISO-based unsaturated polyesters **71**
3.1 Introductory remarks 72
3.2 Experimental 74
3.2.1 Materials 74
3.2.2 Prepolymer formulations 75
3.2.3 Synthesis 76
3.2.4 Bio-based content 76
3.2.5 Kinetics 76
3.2.6 Blending process 77
3.2.7 Crosslinking 77

3.2.8 Prepolymer characterisation 78
3.2.9 Crosslinked thermoset characterisation 78
3.3 Results and discussion 79
3.3.1 Bio-based mass and carbon content 79
3.3.2 Prepolymer characterisation 80
3.3.2.1 Kinetics and molecular weight distribution 80
3.3.2.2 Prepolymer viscosity 82
3.3.3 Resin characterisation 83
3.3.3.1 Resin viscosity 83
3.3.3.2 Tensile properties 84
3.3.3.3 Dynamic mechanical analysis 85
3.4 Concluding remarks 91
3.5 References 92

4 DFA-based unsaturated polyester 97
4.1 Introductory remarks 98
4.2 Experimental 102
4.2.1 Materials 102
4.2.2 Prepolymer formulations 102
4.2.3 Synthesis 103
4.2.4 Biobased content 104
4.2.5 Kinetics 104
4.2.6 Crosslinking reactions 104
4.2.7 Prepolymer characterisation 105
4.2.8 UPR characterisation 105
4.3 Results and discussion 106
4.3.1 Preliminary remarks 106
4.3.2 Biobased content 107
4.3.3 Characterisation 107
4.3.3.1 Kinetic and molecular weight 107
4.3.3.2 ^{1}H NMR study 109
4.3.3.3 Viscosity 110

4.3.3.4 Tensile properties 112
4.3.3.5 Thermomechanical properties 114
4.4 Concluding remarks 117
4.5 References 117

5 FDCA-based unsaturated polyester 123

5.1 Introductory remarks 124
5.2 Experimental 126
5.2.1 Materials 126
5.2.2 Synthesis 127
5.2.3 Bio-based content 128
5.2.4 Kinetics 128
5.2.5 Crosslinking reactions 128
5.2.6 Prepolymer characterisation 129
5.2.6.1 Gel permeation chromatography 129
5.2.6.2 Nuclear magnetic resonance 130
5.2.6.3 Viscosity 130
5.2.7 UPR characterisation 130
5.2.7.1 Barcol hardness 130
5.2.7.2 Tensile properties 131
5.2.7.3 Dynamic mechanical analysis 131
5.3 Results and discussion 131
5.3.1 Prepolymers 131
5.3.2 Bio-based content 132
5.3.3 Kinetics 133
5.3.4 Molecular weight 133
5.3.5 ^{1}H NMR study 135
5.3.6 Viscosity 136
5.3.7 Hardness 138
5.3.8 Tensile behaviour 138
5.3.9 Dynamic mechanical analysis 140
5.4 Concluding remarks 143

5.5 References 144

III Composites 149

6 Bio-based GFRP composites 151

6.1 Introductory remarks 152

6.2 Experiments 155

6.2.1 Materials 155

6.2.2 Manufacturing 156

6.2.3 Mechanical characterisation tests 158

6.2.4 Thermomechanical characterisation tests 159

6.3 Results and discussion 159

6.3.1 Tensile and compressive behaviour 159

6.3.2 Shear behaviour 164

6.3.3 Thermomechanical behaviour 166

6.4 Concluding remarks 168

6.5 References 169

7 Bio-based CFRP composite strips 177

7.1 Introductory remarks 178

7.2 Experiments 182

7.2.1 Materials 182

7.2.2 Pultrusion equipment 184

7.2.3 Test methods 187

7.2.3.1 Overview 187

7.2.3.2 Processing parameters 188

7.2.3.3 Calcination tests 188

7.2.3.4 Hardness 189

7.2.3.5 Tensile tests 189

7.2.3.6 Thermomechanical tests 189

7.3 Results and discussion 189

7.3.1 Manufacturing 189

7.3.2 Mechanical behaviour 192
7.3.2.1 Hardness 192
7.3.3 Tensile behaviour 193
7.3.4 Thermomechanical behaviour 195
7.4 Concluding remarks 198
7.5 References 198

IV Conclusions and perspectives 205

8 Conclusions and perspectives 207
8.1 Conclusions 207
8.1.1 General remarks 207
8.1.2 Synthesis of bio-based unsaturated polyester resins 209
8.1.3 Using renewable raw materials 209
8.1.4 Bio-based GFRP composites 211
8.1.5 Bio-based CFRP composites 211
8.2 Future developments 212
8.2.1 Issues regarding the bio-based resins developed here (I) 213
8.2.2 Regarding alternative solutions (II) 213
8.2.3 Other issues (III) 214
8.3 References 215

Appendix 217

Appendix A Prepolymer characterisation 219
A.1 Titration 219
A.2 Kinetics 219
A.2.1 Conversion and degree of polymerisation 220
A.2.2 Theoretical molecular weights 221
A.3 Molecular weight 222
A.3.1 Prepolymers developed in Chapter 4 223
A.3.2 Prepolymers developed in Chapter 5 224

A.4 Bio-based content 225
A.5 ^{1}H NMR study 228
A.6 Viscosity 233

Appendix B Resin characterisation **235**

B.1 Mechanical properties 235
    B.1.1 Barcol hardness test 235
    B.1.2 Tensile tests 235
    B.1.3 Compression tests 236
    B.1.4 In-plane shear tests 237
B.2 Dynamic mechanical analysis 238
B.3 Characterisation of the commercial UPR 239

List of Figures

1.1 Prefabricated components of fibre-polymer composites [4]. 4

1.2 Examples of applications of fibre reinforced polymer (FRP) composites in building construction [4,8]. 4

1.3 FRP composites used in the construction of vehicular bridges and footbridges [8]. 5

1.4 FRPs used in the strengthening of the Maracanã Stadium for World Cup 2014 [10]. 5

2.1 Main forms of plants used as feedstock for processing reinforcement fibres for the manufacture of FRP composite materials, namely: bast (**a.** to **e.**), leaf (**f.** to **h.**), grass/reed (**i.** to **j.**), fruit (**l.**), other (**m.**). 19

2.2 The hierarchical structure of plant cell walls: **a.** to **d.** are reproductions adapted from [27,35]; **a.** shows a section of primary wall composed of macro and microfibril; **b.** presents cell wall layers, comprising one primary wall and three secondary layers (S_1, S_2, and S_3), with a view of the microfibril angle in S_2; **c.** illustrates amorphous and crystalline regions in cellulose microfibrils; and **d.** presents 3D cellulose molecular structure. 20

2.3 Crushed basalt rock production for the manufacturing of basalt fibres [66,67]. 21

2.4 Availability of basalt sources around the world [69,70]. 22

2.5 Continuous basalt fibre (CBF) manufacturing procedures by *Spinneret* technology [78,79]. 24

2.6 Radar plot: plant and synthetic fibres properties. 27

2.7 Example of petroleum- and bio-based polymeric matrices currently available for various industries, such as packaging, biomedical, and composites [102–104]. 28

2.8 Epoxy main chain based on diglycidyl ether of bisphenol A (DGEBA) with terminal oxirane groups for crosslinking reactions either with themselves through catalytic homopolymerisation, or with hardeners, such as amines or acid anhydrides. 30

2.9 Unsaturated polyester main chain based on phthalic anhydride, 1,2-propylene glycol, and maleic anhydride, which provides a double bond for crosslinking reactions with reactive diluents and later orthophthalic polyester resin formation. 31

2.10 Bisphenol A epoxy-based (methacrylate) vinyl ester resin. 33

2.11 Types of phenolic resins. 34

2.12 Hand lay-up technique. 40

2.13 Vacuum infusion technique [202]. 43

2.14 Pultrusion technique (open bath system) [206]. 46

2.15 Strengthening of reinforced concrete (RC) beams using externally bonded FRP sheets with bio-based matrices [212]. 48

2.16 Experimental set-up of sandwich panel manufactured from bio-based resin [218]. 50

2.17 Bio-composite footbridge in Eindhoven across the river Dommel [219], manufactured from flax fibres, bio-based resin, poly(lactic acid) foam, and natural cork. 51

3.1 Graphical abstract of the bio-based unsaturated polyesters. 71

3.2 Kinetics of polyesterification reaction for the polyester prepolymers: a. UP-A; b. UP-B; c. UP-C; d. UP-D; e. UP-E; and f. overlapping of various formulations. 81

3.3 GPC curves for all formulations. 82

3.4 Viscosity of the prepolymers measured at 125 °C. 83

3.5 Representative tensile stress-strain curves for the biobased thermoset polyesters. 84

3.6 Tensile properties of the thermoset polyesters: **a.** tensile strength, **b.** modulus of elasticity, and **c.** strain at break. 86

3.7 Dynamic mechanical analysis curves of the thermoset polyesters: **a.** storage modulus, **b.** loss modulus, and **c.** tan δ. 87

3.8 Definition of different material states and transitions for the UPR-D thermoset. 88

3.9 Cole-Cole plot. 89

4.1 Graphical abstract of the DFA-based unsaturated polyesters. 97

4.2 Chemical structure of DFA. 99

4.3 The tall oil value chain. 100

4.4 Monomers based on renewable raw materials for the UP synthesis. 101

4.5 Kinetics of polyesterification reaction of UPs. 108

4.6 Signal as a function of retention time traces from GPC data for the UPRs. . 109

4.7 Viscosity of the UPs measured at 125 ℃. 112

4.8 Tensile stress-strain curves of the unsaturated polyester resins (UPRs). . . 113

4.9 Scatter plots from the tensile strength, modulus of elasticity, and strain at break results of the UPRs. 115

4.10 DMA curves for the UPRs. 116

5.1 FDCA-based unsaturated polyester graphical abstract. 123

5.2 From lignocellulosic biomass to FDCA monomer production. 124

5.3 Chemical segment structures of the synthesised UPs. 128

5.4 Chemical structures of the synthesised UPRs. 129

5.5 Kinetics of polyesterification reaction of UPs. 134

5.6 Viscosity of the UPs measured at 125 ℃. 137

5.7 Tensile stress-strain curves of the FDCA-based UPRs. 139

5.8 Scatter plots of UPRs tensile results: **a.** tensile strength; **b.** modulus of elasticity; and **c.** strain at break. 141

5.9 Overlapping DMA curves of all UPRs. 142

6.1 Bio-based GFRP laminate graphical abstract. 151

6.2 GFRP manufacturing procedures: **a.** setup, **b.** fibre layup. 157

6.3 Manufacturing of the GFRP plates: **a.** Infusion process for manufacturing of composites (representation for GFRP-B plate); **b.** produced plates; and **c.** cutting plates to obtain specimens for mechanical and thermomechanical characterisation. 158

6.4 Nominal tensile stress-strain curves: **a.** GFRP-C, and **b.** GFRP-B. 160

6.5 Tensile failure modes of representative GFRP-C and GFRP-B specimens. . 160

6.6 Nominal compressive stress-strain curves: **a.** GFRP-C and **b.** GFRP-B. (a premature failure was observed in one of the GFRP-B specimens, and therefore, only the curves of 4 specimens were presented. The same happened for GFRP-C.) . . . 161

6.7 Compressive failure modes of representative GFRP-C and GFRP-B specimens. . . . 162

6.8 Representative nominal axial stress-strain curves of GFRP and resin specimens: **a.** tensile and **b.** compressive. . . . 162

6.9 Representative nominal axial stress-strain curves in tension and compression of GFRP and resin specimens. . . . 163

6.10 Nominal shear stress-distortion curves of GFRP-C and GFRP-B specimens. 164

6.11 Representative shear stress-distortion curves of GFRP and resins specimens. 165

6.12 V-Notched beam shear test failure modes of representative GFRP-C and GFRP-B specimens. . . . 166

6.13 Interlaminar shear tests: **a.** loading configuration (short-beam method), and **b.** failure modes of representative GFRP specimens. . . . 166

6.14 Thermomechanical properties of GFRP and resin specimens. . . . 167

7.1 Bio-based CFRP strip graphical abstract. . . . 177

7.2 CFRP strengthening applications of civil engineering structures [3,4]: **a.** Access ramps of A9 Viaduct Riddes, Switzerland; **b.** Maracanã Stadium, Rio de Janeiro, Brazil; **c.** Aabachbrücke railway bridge, Lachen, Switzerland; and **d.** Cultural Centre of São Lázaro, Lisbon, Portugal (fire damaged structure). . . . 178

7.3 CFRP composites used for strengthening reinforced concrete and masonry building and bridge structures [4]: **a.** and **b.** application of strips and mats in bridges and buildings, respectively, **c.** strips applied in slab, **d.** strips applied in wall, **e.** strip with anchoring plate, **f.** pre-stressed strips, **g.** strips and sheets in beam, **h.** strips in masonry for seismic strengthening, **i.** strips in bottom surface of beam, and **j.** strips in top surface of slab. . . . 179

7.4 From renewable feedstock to the bio-based monomers used in this study. . 183

7.5 Main steps to obtain the bio-based UP resin used in this study: **a.** polyester prepolymer, **b.** polycondensation reaction, **c.** prepolymer incorporation with reactive diluents, and **d.** UP resin and performing the cured resin (more details can be found in [77,78]). . . . 184

7.6 Overview of pultrusion process. . . . 185

7.7 Continuous carbon fibre roving – Tenax® filament yarn: **a.** fibre roving, **b.** fibre roving creels, and **c.** preforming guides. 186

7.8 Preparation for pultrusion process: **a.** metallic tank for resin bath impregnation; **b.** clamps for uniform impregnation; and **c.** clamp opening adjustments.186

7.9 Equipment for pultrusion process: a. two heating zones of the die, and b. temperature and pulling rate controllers. 186

7.10 Pulling system of pultrusion machine: **a.** reciprocating pullers, and **b.** spacers used to control out-of-plane (bearing) stresses applied to the composite strips. 187

7.11 Winders for coiling pultruded strips. 187

7.12 Resin preparation. 190

7.13 Carbon fibre impregnation of the: **a.** CF/VE, and **b.** bio-based CF/UP composites. 191

7.14 Preforming plates: **a.** before and **b.** after tightness adjustments. 191

7.15 Pultruded composite strips: **a.** before and **b.** after linearity adjustments in the clamps. 192

7.16 Bio-based CFRP strip successfully produced: **a.** CF/UP leaving the heating die; **b.** pultruded strip with 22 yarns; and **c.** winding the CF/UP strips into coils. 193

7.17 Nominal tensile stress-strain curves: **a.** CF/VE and **b.** bio-based CF/UP. . . 194

7.18 Failure modes in tension of representative CF/VE and CF/UP specimens. . 194

7.19 Comparison of tensile strength of pultruded CFRP composites mentioned in the literature (CF/PH [84], CF/FA [83], CF/EP [61]), and those developed in this study (CF/VE and CF/UP). 195

7.20 Thermomechanical properties of both types of resin and CFRP specimens. 196

A.1 Titration procedures for AN determination of the polyester prepolymers. . . 219

A.2 GPC tests were performed in a JASCO™ equipment. Initially, polyester samples were dissolved in tetrahydrofuran (THF) with approximate concentration of 1 mg/ml. After filtration, samples were injected into the system with columns filled of a monodisperse standard, namely, polystyrene cross-linked with divinylbenzene (gel). The data processing were performed by ChromNAV® software. 222

A.3 GPC overlapping formulation curves of the DFA-based unsaturated polyester prepolymers. 223

A.4 Molecular weight distribution curves of the DFA-based unsaturated polyester prepolymers from the GPC analysis. 223

A.5 GPC overlapping formulation curves of the FDCA-based unsaturated polyester prepolymers. 224

A.6 Molecular weight distribution curves of the FDCA-based unsaturated polyester prepolymers from the GPC analysis. 224

A.7 NMR test procedures. 228

A.8 ^{1}H NMR spectra of the DFA-based polyester prepolymers: **a.** UP-A; **b.** UP-B; and **c.** UP-C. 229

A.9 ^{1}H NMR spectra of the FDCA-based polyester prepolymers: **a.** UP0; **b.** UP50; and **c.** UP100. 231

A.10 Viscosity tests performed on a Cone & Plate Viscometer Instrument from REL (Research Equipment London Ltd.), by placing only two drops of resin on a surface that is then approached by a rotating cone (constant speed). . 233

B.1 Setup for tensile tests. 236

B.2 Setup for compressive tests. 237

B.3 Setup for in-plane shear tests. 238

B.4 DMA test setup in a TA Instruments Q800 equipment [6]. Test procedures are also illustrated in four main steps: (1) equipment display preparation, (2) set-up assembly, (3) clamp specimen fixing, and (4) inspection and completion preparation. 239

List of Tables

1.1 Thesis core parts organisation and outputs. 10

2.1 Approximate mean values of mechanical properties of synthetic fibres [4,5]. 16

2.2 Physical and mechanical properties of the most widely used plant fibres in engineering applications [36–47]. 20

2.3 Comparison of plant, glass and carbon fibres [84–87]. 26

2.4 Conventional petroleum-based polyester resins [115–117]. 32

2.5 Bio-based monomers to thermoset applications. 38

3.1 Prepolymer formulations. 75

3.2 Bio-based carbon (x_B) and mass (m_B) contents of the prepolymers and their respective thermoset resins, determined according to the procedure outlined in Annex B of ISO 16620 [27] part 4. 79

3.3 Prepolymer composition analysis. 80

3.4 Viscosity of the unsaturated polyester resins. 84

3.5 Dynamic mechanical analysis results for the bio-based thermoset polyesters. 90

4.1 UP prepolymer formulations. 103

4.2 Bio-based carbon (x_B) and mass(m_B) contents of UPs and UPRs, according to ISO 16620 [44] part 4. 107

4.3 Composition analysis of the UPs. 107

4.4 Comparison between ^{1}H NMR results and predicted structure of the UPs. . 111

4.5 Viscosity of the UPRs measured at 25 ℃. .112

4.6 DMA properties of the UPRs. 116

5.1 UP prepolymer formulations. 127

5.2 Bio-based carbon and mass content of UPs and UPRs, according to ISO 16620-4 [41]. . . . 132
5.3 Composition analysis of the UPs. . . . 135
5.4 Comparison between ^{1}H NMR results and predicted structure of the UPs. . . 136
5.5 Viscosity of the UPRs. . . . 137
5.6 dynamic mechanical analysis (DMA) properties of the UPRs. . . . 142

6.1 Mean values of mechanical and thermomechanical properties of Resin-C and Resin-B specimens. . . . 156
6.2 Mechanical properties in tension and compression of GFRP specimens (mean ± standard deviation). . . . 161
6.3 Mechanical properties in in-plane and interlaminar shear of GFRP specimens (mean ± standard deviation). . . . 165

7.1 Mean values of tensile properties and T_g of UP and VE resin specimens. . . 185
7.2 Gel time of conventional and bio-based resins (at 180 °C). . . . 190
7.3 Fibre fraction, mechanical and thermomechanical properties of pultruded CF/VE and CF/UP strips. . . . 195

A.1 Conversion (p) and degree of polymerization (X_n) from the AN values of the DFA-based polyester prepolymers. . . . 220
A.2 Conversion (p) and degree of polymerization (X_n) from the AN values of the FDCA-based polyester prepolymers. . . . 221
A.3 Values used to estimate the theoretical molecular weights (in Chapter 3) from modified Carothers equation. . . . 221
A.4 Theoretical molecular weights from modified Carothers equation of the DFA-based polyester prepolymers. . . . 221
A.5 Theoretical molecular weights from modified Carothers equation of the FDCA-based polyester prepolymers. . . . 222
A.6 Carbon content of raw materials used for the synthesis of bio-based polyester prepolymers developed in Chapter 3. . . . 225
A.7 Carbon content of raw materials used for the synthesis of DFA-based polyester prepolymers. . . . 225
A.8 Carbon content of raw materials used for the synthesis of FDCA-based polyester prepolymers. . . . 225

A.9 Bio-based carbon and mass content of the group (I) formulations developed in Chapter 3. 226

A.10 Bio-based carbon and mass content of the group (II) formulations developed in Chapter 3. 226

A.11 Bio-based carbon and mass content of the DFA-based unsaturated polyester prepolymers. 227

A.12 Bio-based carbon and mass content of the FDCA-based unsaturated polyester prepolymers. 227

A.13 Main resonances from the ^{1}H NMR spectra of the DFA-based polyester prepolymers. 232

A.14 Main resonances from the ^{1}H NMR spectra of the FDCA-based polyester prepolymers. 232

B.1 Mechanical and thermomechanical properties of the commercial UPR. 240

List of Acronyms

AFP automated fibre placement

APC automated preforming cell

ATL automated tape layup

BFRP basalt fibre reinforced polymer

bio-PA bio-based polyamide

bio-PBS bio-based polybutylene succinate

bio-PE bio-based polyethylene

bio-PU bio-based polyurethane

bio-PET bio-based polyethylene terephthalate

bio-PTT bio-based polytrimethylene terephthalate

BPA bisphenol A

CBF continuous basalt fibre

CFM continuous filament mat

CFRP carbon fibre reinforced polymer

CLC combined loading compression

CNC computer numeric control

CMR carcinogenic, mutagenic, and reprotoxic

CNSL cashew nutshell liquid

CTS continuous tow shearing

DFA dimer fatty acid

DGEBA diglycidyl ether of bisphenol A

DMA dynamic mechanical analysis

DSC differential scanning calorimetry

ECH epichlorohydrin

EG ethylene glycol

ELO epoxidized linseed oil

EP epoxidized pine

FA fumaric acid

FDCA 2,5-furandicarboxylic acid

FRP fibre reinforced polymer

FW filament winding

GFRP glass fibre reinforced polymer

GPC gel permeation chromatography

GHG greenhouse gas

HAP hazardous air pollutant

HEMA 2-hydroxyethyl methacrylate

HMTA hexamethylenetetramine

ISO isosorbide

LCM liquid composite moulding

MEKP methyl ethyl ketone peroxide

NMR nuclear magnetic resonance

PA phthalic anhydride

PBS polybutylene succinate

PAN polyacrylonitrile

PBAT polybutylene adipate terephthalate

PCL polycaprolactone

PE polyethylene

PDO 1,3-propanediol

PFA polyfurfuryl alcohol

PG propylene glycol

PHA polyhydroxyalkanoate

PLA polylactic acid

PP polypropylene

PVA polyvinyl alcohol

PVC polyvinyl chloride

RC reinforced concrete

TFP tailored fibre placement

THF tetrahydrofuran

TOFA tall oil fatty acid

TTR through-thickness reinforcement

UD unidirectional roving

UP unsaturated polyester

UPR unsaturated polyester resin

VE vinyl ester

VOC volatile organic compound

RTM resin transfer moulding

VARI vacuum assisted resin infusion

VARTM vacuum assisted resin transfer moulding

Part I

Introduction and literature review

Chapter 1

Introduction

1.1 Context and motivation

The construction sector is one of the world's largest consumers of natural resources, accounting for a significant part of the environmental impact generated by modern society. Given the role of this industry as an economic engine and its importance in enhancing the quality of life of communities, it is essential to find strategies to improve the environmental sustainability of construction. Accordingly, one possible route is the substantial increase in the use of prefabrication in construction. Prefabrication increases constructive efficiency, by allowing for a better sequencing in the building process, and under some circumstances it reduces lead times and construction costs compared to traditional methods [1]. In addition, developing and implementing innovative and more sustainable materials are also a potential route towards the above-mentioned goal, just as important as prefabrication. Nowadays, the emerging solutions for more eco-friendly building materials are numerous and extensive [2], ranging from improving traditional materials to generating new combinations of materials, giving rise to materials with new functionalities [3].

Advanced eco-efficient materials for prefabricated components are one of the main drivers to increase the sustainability of the construction industry [4]. Figure 1.1 shows examples of fibre-polymer – or FRP – composites typically manufactured in a factory and transported to construction sites. FRP composites have several advantages over other materials, due to their lightness, durability, and high stiffness- and strength-to-weight ratios, relevant parameters for structural applications, since the reduction of weight is associated with lower consumption of raw materials [5]. In addition, FRP composites are versatile and multi-functional due to the possibility of being designed to obtain specific properties in different directions, namely by appropriate placement of fibres in various layers and orientations of the laminated structure [6].

FRP composite structures can be modularly produced in a factory and quickly assembled on-site, potentially reducing construction time and waste when compared to other materials,

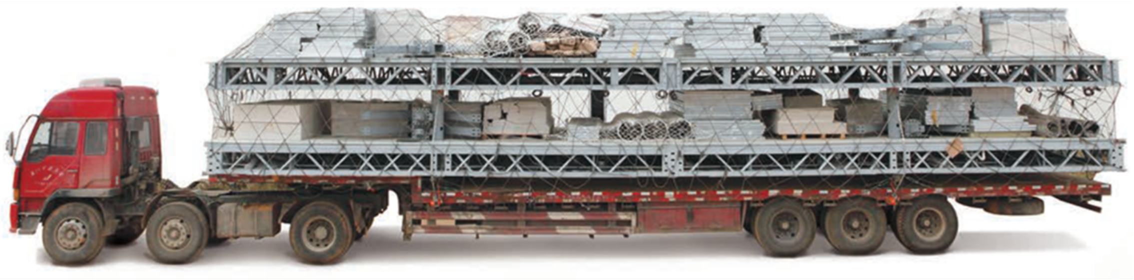

Figure 1.1: Prefabricated components of fibre-polymer composites [4].

such as steel, reinforced concrete, or wood [7]. Figures 1.2a and 1.2b show that off-site manufacturing of parts provides more controlled conditions and allows for better quality and precision in component assembly [4]. Figures 1.2c and 1.2d present The ClickHouse project [8], a recent modular construction for emergency or temporary housing with a frame structure made of pultruded GFRP profiles with built-in bolted connections. Finally, assembly costs and energy consumption involved in the processing of these composites are also lower than those of many traditional materials, making the use of FRPs potentially interesting for various applications of the construction industry [9].

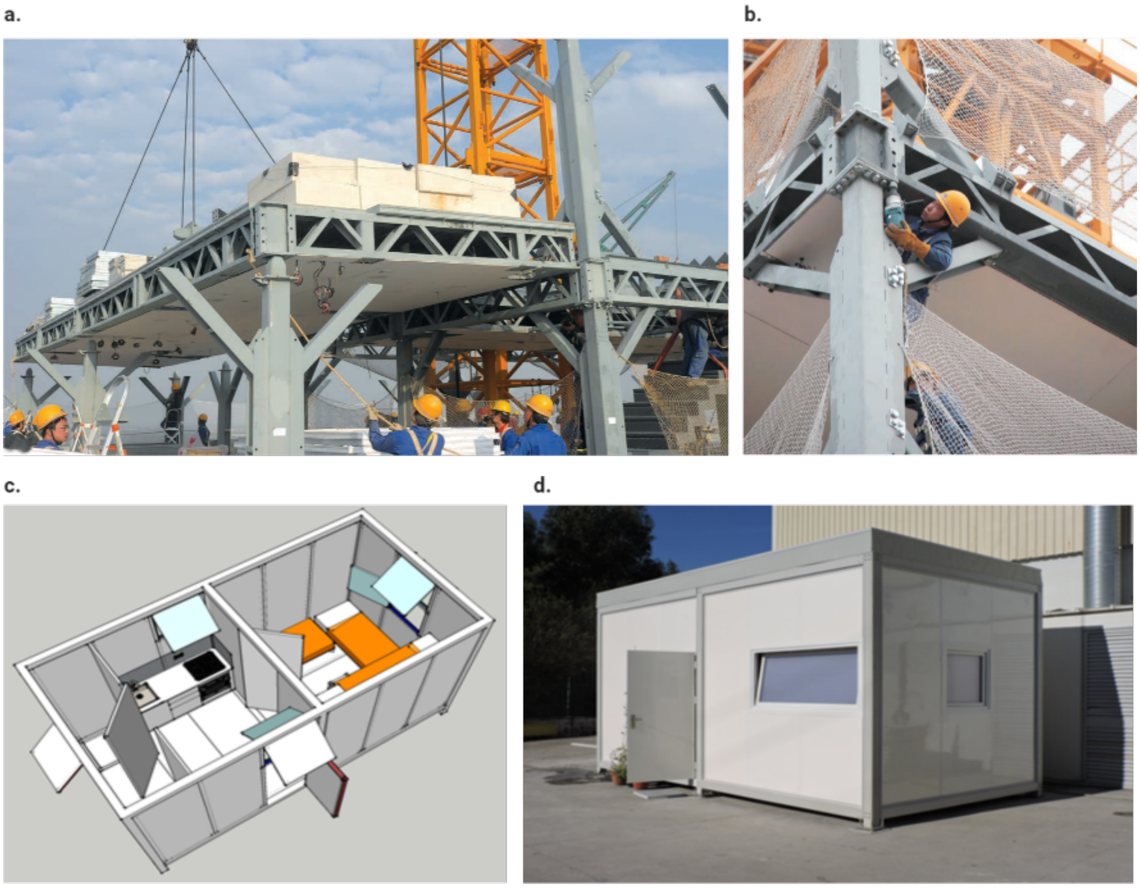

Figure 1.2: Examples of applications of FRP composites in building construction [4,8].

Figures 1.3a and 1.3b show the São Silvestre Footbridge [8], with 11 m of length and 2 m of width, which was installed on-site fully assembled in less than 3 hours; it has a

4 cm thick deck made of steel fibre reinforced self-compacting concrete (SFRSCC) without rebars, supported by 2 pultruded I-shaped GFRP profiles (with 400 mm of height).

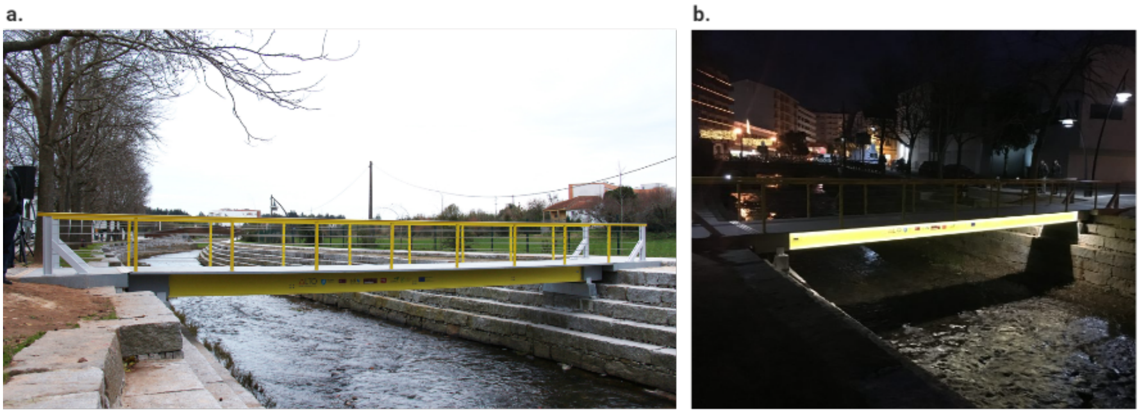

Figure 1.3: FRP composites used in the construction of vehicular bridges and footbridges [8].

Finally, Figure 1.4 shows the Maracanã Stadium's rehabilitation process for the World Cup 2014, illustrating the strengthening work carried out on columns, with carbon-fibre reinforced polymer (CFRP) strips impregnated with epoxy resin as flexural reinforcement and anchors with low modulus carbon sheets (C-Sheets); for shear reinforcement, high modulus C-Sheets were used. Additionally, carbon meshes were applied to the main columns to enable supporting the load of a new stadium roof [10].

Figure 1.4: FRPs used in the strengthening of the Maracanã Stadium for World Cup 2014 [10].

Recent studies have shown that FRP components may have a lower environmental impact compared to conventional structural materials, mainly due to their more extended durability and lower life-cycle maintenance requirements [11–14]. However, FRPs still depend significantly on polymeric matrices produced from oil-based resins, such as unsaturated polyester, epoxy, and phenolic; these typically comprise 30-70% by weight of the FRP material [6] and require significant energy for their production [15]. The fact that petroleum is a non-renewable resource also poses a threat to the long-term sustainability of the FRP composites sector. A possible long-term response to the sector's sustainability requirements is the reduction of petrochemical oil dependence of FRP materials, which can be achieved by partial or almost full replacement of petroleum-based resins with resins synthesised from renewable raw materials [16,17]. This change to resins based on renewable resources will allow to increase the eco-efficiency of FRP composites that are already being used and, mainly, will give an innovative and significant response concerning the sustainability of construction.

1.2 Topic overview

The development of sustainable composites for high-performance applications has shown a relatively slow progression, and much of the efforts to date have focused on replacing synthetic fibres with plant fibres [18–28]. However, plant fibres exhibit lower mechanical properties compared to conventional synthetic fibres (for example, glass, carbon, or aramid), preventing them from being used in structural applications [29,30]. In addition, cellulosic fibres, such as flax and hemp, are also strongly hydrophilic, exhibiting a high moisture absorption rate within the FRP composite, which leads to durability issues [31].

A reasonable compromise between environmental sustainability and adequate structural performance can be achieved by combining synthetic or mineral fibres and "greener" (bio-based) resins; for example, FRPs comprising a bio-based thermoset resin and glass, carbon, or basalt fibres, can have similar performance to traditional composites, offering at the same time the advantage of being derived from renewable resources. Nowadays, the mechanical and thermomechanical properties of some bio-based resins are comparable to those of their conventional petrochemical-derived counterparts. Thus, the industry's current tendency to use "green" composites in heavy structural applications should focus on replacing the matrix (resin) and not the fibres [32].

Among the primary raw materials available to produce these new resins are vegetable oils, sugars, starches, and biomass, as well as forest residues or by-products from agro-food activities, such as sugarcane bagasse and corn cob [33,34]. Like the traditional ones, these new bio-based resins present a wide range of mechanical properties and behaviours, from stiff to flexible, brittle to ductile, and low- to high-strength. However, despite the efforts of producers to develop new more sustainable resins, currently, most bio-based resins commercially available for structural engineering applications still incorporate a small amount of sustainable raw materials, approximately 30-35% [35,36].

Although it is desirable to produce resins derived from entirely renewable sources, this is not always possible, especially in the short-term, namely in the following circumstances: (i) when renewable raw materials have a significantly higher cost than their synthetic alternative; (ii) when the structural and processing properties of a 100% bio-based polymer system are inadequate for high-performance applications; or (iii) when there is a need for the use of reactive diluents, catalysts, and petroleum-derived curing agents. Thus, many times, the best option may be the production of a hybrid blend between renewable sources and oil-based products, aiming to maximise the incorporation of sustainable raw materials.

The synthesis of new monomers based on renewable resources can promote the introduction in the market of more sustainable resins able to compete with petroleum-based resins over the next few years. However, this effort should also focus on the development or improvement of suitable processing properties where conventional processing equipment and techniques used for composites with synthetic resins (such as hand layup, vacuum infusion, and pultrusion) should also be suitable for the processing of eco-friendly resins, facilitating manufacture at an industrial scale [37]. Likewise, bio-based thermoset resins must have improved processing characteristics and properties to become competitive matrices for use in FRP composites. Resins based on renewable sources are gradually being considered for structural applications in civil engineering, and some exploratory studies carried out to date (reviewed in the following chapters) attest their potential.

1.3 Objectives

The central aim of this research is to develop and produce FRP composites with thermoset polymer matrices based on raw materials derived from renewable sources for civil engineering structural applications.

The following objectives were therefore defined:

1. Selecting the most suitable materials and areas of development that must be addressed for sustainable FRP composites, namely, eco-friendlier reinforcement fibres and bio-based thermoset resin alternatives comparable to their petroleum-derived counterparts in terms of mechanical and processing properties;
2. Development of novel bio-based unsaturated polyester resins for high-performance applications constituted partially or almost entirely from raw materials derived from renewable sources;
3. Manufacturing of sustainable GFRP composite laminates through the impregnation of synthetic glass fibres with bio-based resins by using the vacuum infusion technique in a laboratory environment;

4. Further validation of one of the bio-based thermoset polyester resins developed in the thesis, through its use as a polymer matrix in a pilot industrial production, namely in the pultrusion of a CFRP composite strip prototype;
5. Experimental characterisation of the mechanical, thermomechanical, and processing properties of the products manufactured, namely, resins and composites.

1.4 Methodology

The methodology adopted to achieve the objectives set for this research was as follows:

1.a conducting literature and technical reviews to identify a set of materials with the highest potential for developing sustainable FRP composites. A survey of the relevant reinforcing fibres (considering synthetic and plant fibres) and bio-based thermoset resins was also carried out. In this assessment, the processing, mechanical, and thermomechanical properties of the materials, and the compatibility between fibres and resins were considered;

1.b analysis of the raw materials identified in the previous phase, regarding the balance between performance and eco-efficiency. An assessment of the technical requirements of different FRPs manufacturing techniques, such as hand layup, vacuum infusion, and pultrusion, was carried out. Aspects such as viscosity, cure temperature and gel time of the resins were considered;

2. development of novel bio-based unsaturated polyester main chains (prepolymers) able to be incorporated with reactive diluents and form unsaturated polyester resins. Synthesis of different molecular formulations through polycondensation reactions were carried out to obtain bio-based thermoset polyester resins with properties that match or exceed their petroleum-derived counterparts;

3 production of GFRP composite laminates with one of the bio-based unsaturated polyester resins developed in the thesis, namely the one achieving a better balance between mechanical and processing performance, and incorporating a high bio-content. The production cost was also taken into account;

4.a experimental characterisation of the bio-based thermoset resins, including: (i) chemical analysis, titration, gel permeation chromatography (GPC), and nuclear magnetic resonance (NMR); (ii) processing features, viscosity and gel time; (iii) thermomechanical properties, storage and loss modulus, tan δ, and glass transition temperature (T_g), by means of DMA; and (iv) mechanical characterisation tests, strength, modulus of elasticity and strain at failure, in tension;

4.b experimental characterisation regarding the GFRP laminates, and CFRP strips produced by vacuum infusion and pultrusion, respectively. For this purpose, mechanical tests (in tension, compression, and shear) and thermomechanical DMA tests (storage and loss modulus, tan δ, and T_g) were conducted;

5. production of FRP composite strips by pultrusion using one of the resins developed in the thesis. A CFRP composite strip prototype was manufactured by pultrusion in an industrial environment, by a partner company specialised in the manufacture of FRP composite strengthening strips for the construction industry.

1.5 Thesis organisation

The research presented in this thesis is divided into four core parts, comprising six main chapters, which address the objectives introduced in Section 1.3, and two additional chapters, respectively presenting the introduction and summarising the conclusions of the research and future perspectives. The general organisation of the core chapters of the thesis is shown in Table 1.1.

A summary of the main content of each chapter is presented in the following paragraphs.

Part I: Introduction

– Chapter 2: This chapter presents a literature and technical review of the current state of the art about sustainable fibre-polymer composites. The chapter includes the selection of viable alternative materials (fibres and resins) with potential, in terms of mechanical and processing performance, to manufacture eco-friendlier composites. The chapter also describes a critical assessment of available raw materials regarding the development of thermoset polymer resins with high bio-based renewable content incorporation. The main techniques currently used to manufacture fibre-polymer composites addressed for construction are briefly described. Finally, recent studies on applications of bio-based composites in civil engineering structural applications are presented.

Part II: Resins

– Chapter 3: This chapter describes a set of syntheses of different formulations of bio-based unsaturated polyester prepolymers. The prepolymers are evaluated considering their molecular structure, kinetics of polymerisation, and reactive diluents incorporation. Then, an experimental characterisation campaign is described, regarding cured unsaturated polyester resins, which was carried out to determine the mechanical, thermomechanical and processing properties of those resins. In this chapter, isosorbide (ISO) was considered as the main bio-based building block studied, together with fumaric acid (FA) and 1,3-propanediol (PDO);

– Chapter 4: Similar to the campaign carried out in chapter 3, this chapter presents the development of unsaturated polyester resins based on dimer fatty acids and isosorbide building blocks;

– Chapter 5: This chapter presents the development of unsaturated polyester resins based on 2,5-furan dicarxylic acid and isosorbide-derived building blocks. The experimental campaign was carried out according to the procedures previously adopted for prepolymer and resin characterisation.

Part III: Composites

- Chapter 6: This chapter presents the experimental investigation carried out in order to assess the mechanical properties of GFRP laminates manufactured by vacuum infusion with a bio-based unsaturated polyester resin developed in the thesis.
- Chapter 7: In this chapter, one unsaturated polyester resin developed in the thesis is selected to be tested in industrial processing conditions, namely in the manufacturing by pultrusion of carbon fibre reinforced polymer CFRP strips used for structural strengthening. The chapter also presents the mechanical characterisation tests of the resulting bio-based CFRP strips, which allowed validating the CFRP strip prototype.

Conclusions and perspectives

- Chapter 8: The main conclusions of the conducted research are presented and suggestions for future research are formulated.

Supplementary information concerning the main chapters of the thesis is provided in the following two appendices:

- Appendix A: Prepolymer characterisation
- Appendix B: Resin characterisation polyesters.

Table 1.1: Thesis core parts organisation and outputs.

Part	Domain	Subject	Main chapters	Appendices	Papers
I	Introductory	Introduction Literature review	Chapter 1 Chapter 2	–	–
II	Resins	ISO-based polyester	Chapter 3	A,B	3
		DFA-based polyester	Chapter 4	A,B	
		FDCA-bsed polyester	Chapter 5	A,B	
III	Composites	Bio-based GFRP Bio-based CFRP	Chapter 6 Chapter 7	–	2

The main scientific contributions of this thesis have been presented in 5 journal papers and 2 conference presentations, which are listed below and correspond to the main chapters of the thesis.

1. Hofmann, M.; Garrido.; Correia, J.R.; Bordado, J. Compósitos sustentáveis para aplicações estruturais em Engenharia Civil: uma breve revisão da literatura. Tema:

Tecnologias Construtivas - Novos Materiais. *Construção 2018 - reabilitar e construir de forma sustentável.* Universidade do Porto. pages 440-453. 2018.

2. Hofmann, M.: Shahid, A.; Garrido, M.; Bordado, J.; Correia, J. Development of bio-based composites for structural applications. In Jiping Bai, editor. *1^{st} Ibero-American Conference on Composite Materials*, Quântica Editora, pages 38. 2021.
3. Hofmann, M.; Shahid, A.; Garrido, M; Ferreira, M.; Correia, J.R.; Bordado, J. Bio-based thermosetting polyester resin for high-performance applications. *ACS Sustainable Chemistry & Engineering*. Manuscript Accepted 11-Feb-2022.
4. Hofmann, M.; Shahid, A.; Garrido, M; Ferreira, M.; Correia, J.R.; Bordado, J. Development of bio-based thermosetting polyester resins from dimer fatty acids. *European Polymer Journal*. To be submitted in February 2022.
5. Hofmann, M.; Garrido, M; Ferreira, M.; Correia, J.R.; Bordado, J. Iterative way to optimise thermoset polyester structure for high-performance applications in a sustainable approach. *Journal of Applied Polymer Science*. Submitted in January, 2022. Under Review.
6. Hofmann, M.; Shahid, A.; Machado, M.; Garrido, M; Bordado, J.; Correia, J.R. GFRP composite produced by vacuum infusion with a novel high-performance bio-based unsaturated polyester resin: manufacturing and mechanical characterisation. Composites Part A: Applied Science and Manufacturing. To be submitted in March 2022.
7. Hofmann, M.; Shahid, A.; Machado, M.; Garrido, M; Bordado, J.; Correia, J.R. Pultruded CFRP strips produced with a novel bio-based thermoset polyester for structural strengthening. Composites Science and Technology. To be submitted in March 2022.

The research developed herein also resulted in an application for a Patent of Invention concerning an unsaturated polyester resin for FRP composites manufacturing:

- Hofmann, M.; Garrido, M. ; Bordado, J.; Correia, J.R.; Shahid, A. *High performance unsaturated polyester resins based on renewable resources*. Patent of Invention. Number: 117321. Ref. DP/01/2021/77373. Instituto Nacional da Propriedade Industrial. Direção de Marcas e Patentes. Departamento de Patentes e Modelos de Utilidade. Instituto Superior Técnico. Portugal. 2021.

1.6 References

[1] The Modular Building Institute. Improving construction efficiency and productivity with modular construction, with excerpts from: Advancing the competitiveness and efficiency of the U.S. Technical report, National Research Council, Charlottesville, USA, 2010.

[2] European Commission. Smart living, advanced building materials, case study 18. Technical report, Business Innovation Observatory, Luxembourg, 2014.

[3] European Commission. EU R&D scoreboard, The 2014 EU industrial R&D investment scoreboard. Technical report, European Union, Luxembourg, 2014.

[4] World Economic Forum. Shaping the future of construction: Lessons from leading innovators and disruptors. Technical report, Committed to improving the state of the world, Geneva, Switzerland, 2017.

[5] Fazil O. Sonmez. Optimum design of composite structures: A literature survey (1969–2009). *Journal of Reinforced Plastics and Composites*, 36(1):3–39, 2016.

[6] Lawrence C. Bank. *Composites for Construction: Structural Design with FRP Materials*. John Wiley & Sons, Inc., 1 edition, 2006.

[7] J. M. Davies. *Lightweight Sandwich Constructions*. Blackwell Science, Oxford, 1st edition, 2001.

[8] Composites Research Group (CORE Group). The ClickHouse, 2015. `http://coregroup.tecnico.ulisboa.pt/~coregroup.daemon/applied-projects`, accessed on 2020-05-08.

[9] B. C. Mitra. Environment friendly composite materials: Biocomposites and green composites. *Defence Science Journal*, 64(3):244–261, 2014.

[10] S&P Clever Reinforcement Company. Maracanã Stadium refurbishment and reinforcement, 2013. `https://www.sp-reinforcement.ch/en-CH/projects`, accessed on 2020-05-09.

[11] Sebastian G. Maxineasa, Nicolae Taranu, Liliana Bejan, Dorina Isopescu, and Oana M. Banu. Environmental impact of carbon fibre-reinforced polymer flexural strengthening solutions of reinforced concrete beams. *The International Journal of Life Cycle Assessment*, 20(10):1343–1358, 2015.

[12] Valbona Mara, Reza Haghani, and Peter Harryson. Bridge decks of fibre reinforced polymer (FRP): A sustainable solution. *Construction and Building Materials*, 50:190–199, 2014.

[13] Ryszard A. Daniel. A composite bridge is favoured by quantifying ecological impact. *Structural Engineering International*, 20(4):385–391, 2010.

[14] Hirokazu Tanaka, Hitoshi Tazawa, Morio Kurita, and Takumi Shimomura. A case study on life-cycle assessment of environmental aspect of FRP structures. In Amir Mirmiran and Antonio Nanni, editors, *Third International Conference on FRP Composites in Civil Engineering (CICE)*, pages 175–178, Florida, USA, 2006.

[15] Amir Fam and Mak Kenneth. Bio-based FRP composites – Do they have a place in construction? In Kent A. Harries, editor, *Proceedings of the 8th International Conference on Fibre-Reinforced Polymer (FRP) Composites in Civil Engineering (CICE)*, pages 29–38, Hong Kong, China, 2016. International Institute for FRP in Construction.

[16] Ciaran McSwiggan and Amir Fam. Bio-based resins for flexural strengthening of reinforced concrete beams with FRP sheets. *Construction and Building Materials*, 131:618–629, 2017.

[17] Omar Faruk, Andrzej K. Bledzki, Hans-Peter Fink, and Mohini Sain. Biocomposites reinforced with natural fibers: 2000–2010. *Progress in Polymer Science*, 37(11):1552–1596, 2012.

[18] Paul V. Joseph, Kuruvilla Joseph, and Sabu Thomas. Effect of processing variables on

the mechanical properties of sisal-fiber-reinforced polypropylene composites. *Composites Science and Technology*, 59(11):1625–1640, 1999.

[19] Andrzej K. Bledzki and Jochen Gassan. Composites reinforced with cellulose based fibres. *Progress in Polymer Science*, 24(2):221–274, 1999.

[20] Luke CoDyre, Kenneth Mak, and Amir Fam. Flexural and axial behaviour of sandwich panels with bio-based flax fibre-reinforced polymer skins and various foam core densities. *Journal of Sandwich Structures & Materials*, 20(5):595–616, 2016.

[21] Jochen Gassan and Andrzej K. Bledzki. Possibilities for improving the mechanical properties of jute/epoxy composites by alkali treatment of fibres. *Composites Science and Technology*, 59(9):1303–1309, 1999.

[22] Yan Li, Yiu-Wing Mai, and Lin Ye. Sisal fibre and its composites: a review of recent developments. *Composites Science and Technology*, 60(11):2037–2055, 2000.

[23] Pedro J. Herrera-Franco and Alex Valadez-González. Mechanical properties of continuous natural fibre-reinforced polymer composites. *Composites Part A: Applied Science and Manufacturing*, 35(3):339–345, 2004.

[24] Hazizan M. Akil, Mohd F. Omar, Adlan M. Mazuki, Sahnizam Safiee, Zainal M. Ishak, and Azhar A. Bakar. Kenaf fiber reinforced composites: A review. *Materials & Design*, 32(8):4107–4121, 2011.

[25] Harry S. Ku, Hao Wang, N. Pattarachaiyakoop, and Mohan Trada. A review on the tensile properties of natural fiber reinforced polymer composites. *Composites Part B: Engineering*, 42(4):856–873, 2011.

[26] Z. N. Azwa, B. F. Yousif, Allan C. Manalo, and Karu W. Karunasena. A review on the degradability of polymeric composites based on natural fibres. *Materials & Design*, 47:424–442, 2013.

[27] A. Shalwan and B. F. Yousif. In State of Art: Mechanical and tribological behaviour of polymeric composites based on natural fibres. *Materials & Design*, 48:14–24, 2013.

[28] Cristiano Fragassa, Ana Pavlovic, and Carlo Santulli. Mechanical and impact characterisation of flax and basalt fibre vinylester composites and their hybrids. *Composites Part B: Engineering*, 137:247–259, 2018.

[29] Mohammadreza Foruzanmehr, Said Elkoun, Amir Fam, and Mathieu Robert. Degradation characteristics of new bio-resin based-fiber-reinforced polymers for external rehabilitation of structures. *Journal of Composite Materials*, 50(9):1227–1239, 2015.

[30] Robert Quarshie and Joe Carruthers. Technology Overview Biocomposites. Technical report, Accelerating Business Innovation: A Technology Strategy Board Programme, 2014.

[31] Antoine Le Duigou, Peter Davies, and Christophe Baley. Exploring durability of interfaces in flax fibre/epoxy micro-composites. *Composites Part A: Applied Science and Manufacturing*, 48:121–128, 2013.

[32] Yunqing Zhu, Charles Romain, and Charlotte K. Williams. Sustainable polymers from renewable resources. *Nature*, 540(7633):354–362, 2016.

[33] Vijay K. Thakur, Manju K. Thakur, and Michael R. Kessler. *Handbook of Composites from*

Renewable Materials, volume 2. Scrivener Publishing LLC, Beverly, MA, USA, 2017.

[34] Eldridge Amanda and Amir Fam. Environmental Aging Effect on Tensile Properties of GFRP Made of Furfuryl Alcohol Bioresin Compared to Epoxy. *Journal of Composites for Construction*, 18(5):040140–10, 2014.

[35] DuPont Tate & Lyle Bio Products. High-Performance Ingredient for Unsaturated Polyester Resins, 2018. `http://www.duponttateandlyle.com/susterra`, acessed on 2018-03-20.

[36] Sicomin Epoxy Resin. High bio-based content, 2018. `http://www.sicomin.com/products/epoxy-systems/bio-based-epoxy`, acessed on 2018-03-20.

[37] Dipa Ray and Sunanda Sain. Thermosetting bioresins as matrix for biocomposites. In Dipa Ray, editor, *Biocomposites for High-Performance Applications: Current Barriers and Future Needs Towards Industrial Development*, chapter 3, pages 57–80. Woodhead Publishing Series in Composites Science and Engineering, 2017.

Chapter 2

Literature review

2.1 Introductory remarks

As the level of depletion of natural resources, the global warming impact and climate change are becoming increasingly evident, the search for renewable materials able to address the current dependence on oil has gained urgency. Consequently, the development of more sustainable materials has attracted attention in many sectors, and there is an increasing pressure to adopt a circular approach in our economy [1]. Sustainability is especially relevant for the construction industry, which is one of the main contributors to the depletion of natural and mineral resources among all production industries. The paradigm shift in the construction industry towards circular ways of building can meet the ambitions resulting from current legislation [2]. For this, alternative materials and manufacturing techniques need to be found and implemented to guarantee a more sustainable approach.

FRP composites are well established materials in the construction industry due to their mechanical and durability properties. However, although FRP composite materials may perform better in terms of environmental impact than traditional building materials [3], such as steel and concrete, they are generally derived from non-renewable resources and generate hazardous waste during their manufacturing process. In addition, resin prices are strongly linked to the petroleum price, which has undergone significant fluctuations in cost in recent years, causing instability in composite prices.

The use of raw materials based on renewable resources with lower environmental impact can help addressing sustainability issues and reducing dependence on the volatile cost of petroleum for FRP production. However, many currently available bio-based materials have performance limitations for structural applications. Furthermore, even those with suitable features may not be compatible with the current processing techniques, such as in the pultrusion process, which involves at high temperatures. Accordingly, a critical assessment of materials and manufacturing methods is needed to determine the various features that can further promote a more sustainable use of FRP composites.

In this chapter, the main question to be answered by the literature review is whether and how bio-based FRP composite materials can be produced with adequate properties for load-bearing applications, such as structural members for buildings and bridges. For this, alternatives for reducing fossil fuel consumption, preventing raw material depletion, and increasing options for a transition to a more circular economy are presented and discussed.

2.2 Materials and manufacturing

FRP composites are manufactured from two primary raw material constituents: reinforcing fibres and a polymer resin matrix. First, this section reviews the fundamental properties and characteristics of raw materials used to produce eco-friendly FRP products for structural applications; and then, manufacturing methods currently used in the composites industry are investigated.

2.2.1 Reinforcing fibres

2.2.1.1 Synthetic fibres

Synthetic or conventional fibres are still an attractive option mainly due to their superior mechanical properties, low cost, ready availability and consistent properties. Nowadays, synthetic fibres are the materials most often used as reinforcement in FRP composites, particularly in structural applications where the mechanical, thermal, and chemical stability of the finished product are key requirements. The most often used synthetic fibres include carbon, glass, and aramid. Among these, glass is the most widely used type of fibre in composites, mainly due to its low cost and relatively high mechanical properties.

Table 2.1 presents approximate mean values for the mechanical properties of the most used synthetic fibres in structural engineering applications.

Table 2.1: Approximate mean values of mechanical properties of synthetic fibres [4,5].

Fibre	**Grade of fibre**	**Tensile strength (MPa)**	**Elastic modulus (GPa)**	**Ultimate strain (%)**	**Density (g/cm^3)**
E-glass	Electrical glass	3400	72	2.5	2.57
S-glass	Structural glass	4600	88	3.0	2.47
C-glass	Corrosion resistant	2350	74	2.5	2.46
A-glass	Window glass	2760	73	2.5	2.46
Carbon	Standard	3700	250	1.2	1.70
Carbon	High strength	4800	250	1.4	1.80
Carbon	High modulus	3000	500	0.5	1.90
Carbon	Ultrahigh modulus	2400	800	0.2	2.10
Aramid	Kevlar^{TM} 29	2920	70	3.6	1.44
Aramid	Kevlar^{TM} 49	3000	112	2.4	1.44

The following paragraphs describe the main characteristics and properties of synthetic fibres used in structural applications. In general, these fibres are made up of long individual filaments (continuous) and supplied in different architectures.

Glass fibres have a bright white colour to the naked eye and are the most inexpensive among high-performance fibres. In mechanical terms, glass fibres are usually considered to be an isotropic material [6], with a recommended maximum stress in service conditions of about one third of their ultimate strength due to their susceptibility to creep rupture [7]. Besides, glass fibres are sensitive to moisture and need to be well protected by the matrix system, especially in presence of salts and elevated alkalinity. It is important to note that, during the glass fibre manufacturing process, individual filaments are produced with a surface coating called sizing, which aims at protecting the filaments when they are formed into a bundle or a strand [8]. The sizing also contains coupling agents, usually silanes, which improve the bonding between the glass fibre and the polymer matrix [9]. Nowadays, most commercially available glass fibres can be obtained with sizings compatible with the three major thermosetting resins used in structural applications, namely: polyester, vinylester, and epoxy resins [10].

Carbon fibres are mainly used in structural engineering applications, such as (i) FRP strengthening sheets and fabrics, (ii) FRP strengthening strips, and (iii) FRP prestressing tendons [5]. Due to their two-dimensional atomic structure, carbon fibres are considered transversely isotropic, having different properties along the longitudinal and transverse directions of the atomic array [11]. The longitudinal axis gives the fibre its high longitudinal strength and modulus. Similarly to glass fibres, carbon fibres need sizing to be compatible with a resin matrix. Carbon fibres have a charcoal-black colour, and historically have been used primarily with epoxy resins, since suitable sizings for epoxy resin systems are readily available. Nowadays, carbon fibres are also being used with polyester [12] and vinyl ester [13,14] resins for FRP profiles and laminates, although sizing for carbon fibres and polyester or vinyl ester are not as common. Furthermore, carbon fibres are very durable, since they do not absorb moisture and perform very well under elevated temperatures and when subjected to fatigue loads [5]. They have a low coefficient of thermal expansion in their longitudinal direction, giving them excellent dimensional stability. However, previous research has shown that the contact of carbon fibre laminates with metallic materials can lead to the FRP polymer matrix degradation, mainly in the presence of chlorides, and to the corrosion of the metallic material [15,16].

Aramid fibres were first developed and patented by DuPont under the trade name Kevlar$^{\mathrm{TM}}$ [4]. These fibres have a yellow colour and have similar cost to carbon fibres [17]; however, they are the lightest among high-performance fibres. As structural reinforcement, they were used to manufacture the first-generation of FRP prestressing tendons in Europe and Japan, although few manufacturers still produce these FRP components. Occasionally, they are used in specific FRP strengthening applications to wrap columns together with unidirectional glass or carbon fabrics [5]. Due to their relatively high price, high moisture absorption (up to 6% by weight), and relatively poor compressive properties, aramid fibres have been losing attractiveness for use in FRP composites for structural engineering applications.

The different types of aforementioned fibres can be used to reinforce FRP composites in various forms of fibrous materials. The fibre reinforcement forms (or architectures) can be further worked to produce textile products with various reinforcing directions. These multi-axial fabrics are classified either based on fibre linearity and continuity, or directions of their various fibre layers, or based on the fabric formation techniques. Hybrid architectures, comprising different types of fibres, are also supplied by manufacturers for specific purposes, such as to obtain more sophisticated crosswise shapes in FRP components. Normally, the fibre architectures are selected from specific design objectives, for example: (i) either to resist stresses in flexural or shear zones; (ii) or to avoid interlaminar cracking migration; (iii) or to minimise intralaminar cracking propagation, avoiding crack migration phenomena, and/or preventing the crack from jumping between reinforcing layers.

2.2.1.2 Vegetable fibres

Over the last 15 years, the use of natural fibres as eco-friendly substitutes of synthetic fibres in FRPs has been increasing for some specific applications with moderate performance [18]. Natural fibres are extracted from natural sources, such as plants or some living genus, and are classified into three categories: plant (vegetable) or cellulosic, animal and mineral fibres. Plant fibres are the most widely used, due to their renewability and easier availability, whereas animal and mineral fibres have minimal uses [19–21]; however, a notable exception can be found in basalt fibres, which are an increasingly popular type of mineral fibre (as discussed in section 2.2.1.3).

Plant fibres are mainly categorised in two types: primary utility group, which includes, for example, hemp and jute; and secondary utility group, which includes the by-products of plants, such as coir and pineapple. Furthermore, vegetable fibres are available in six different forms [22]: (i) bast fibres (flax, hemp, jute, ramie, kenaf); (ii) leaf fibres (abaca, pineapple, sisal); (iii) grass/reeds (bamboo, bagasse), and stalks (rice, wheat, maize); (iv) fruit fibres (coir, oil palm); (v) seed fibres (kapok, milkweek); and (vi) wood fibres (softwood and hardwood), Figure 2.1. Normally, plant fibres have an uneven and rough surface that provides good adhesion to the resin in a composite material. Bast fibres typically have good mechanical properties, as they provide the mechanical support to the plant stem, which makes them preferred for structural applications in composites [23,24].

Plant fibres present complex structures in microscope view. The different layers of cell walls that wrap the core of lumen are made up of different orientations of microfibrils, as illustrated in Figure 2.2, which provide strength to the fibre subject to different loads

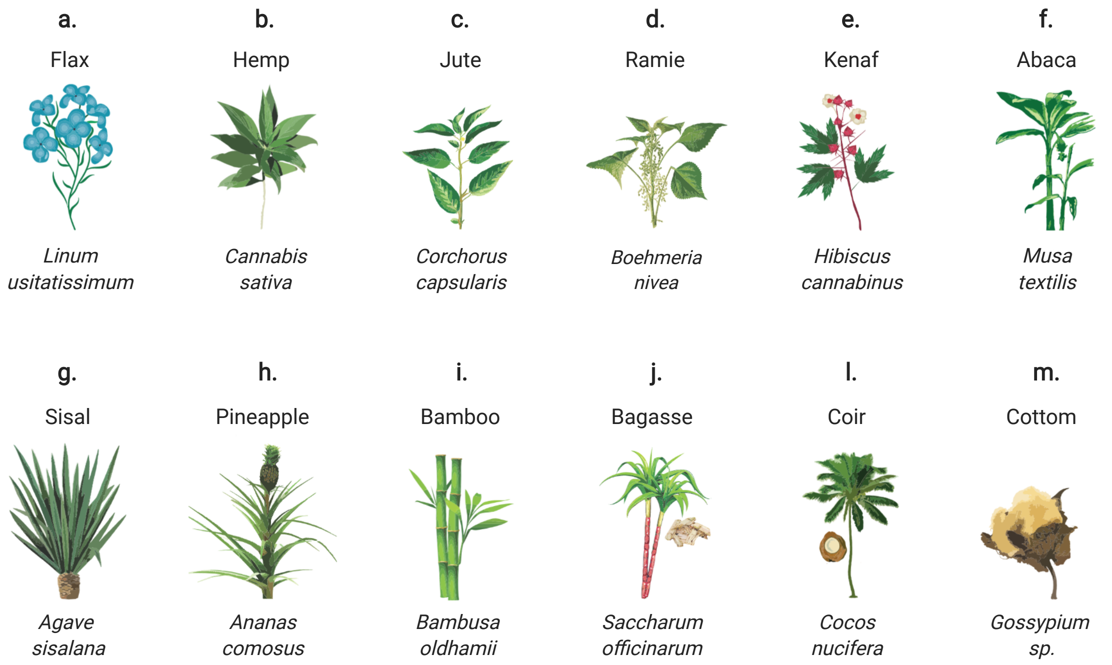

Figure 2.1: Main forms of plants used as feedstock for processing reinforcement fibres for the manufacture of FRP composite materials, namely: bast (**a.** to **e.**), leaf (**f.** to **h.**), grass/reed (**i.** to **j.**), fruit (**l.**), other (**m.**).

[25]. Therefore, similar to other layered systems, the microfibrillar angle governs the tensile strength of plant fibres and the strain at failure increases with microfibrillar angle [26]. According to Lau [27], it is noticeable that the tensile modulus of FRP composites constituted by plant fibres is higher when all microfibrils are aligned along the direction of the tensile loading.

The theoretical mechanical properties of plant fibres would be reasonable enough for their use as a structural material, mainly in fibres with a cellulose content higher than 75% [28]. For example, the theoretical elastic modulus of a cellulose molecule is predicted to be around 138 GPa [29], whereas the theoretical tensile strength of the cellulose available in plant fibres, such as cellulose I, cellulose II and amorphous cellulose is high, about 13 GPa, 9 GPa and 800 MPa, respectively [30–32]. In plant fibres, the higher the cellulose rate, the higher the mechanical properties [33]. However, such performance figures are not reached since plant fibres exist mainly as bundles of smaller primary fibres that contain various microstructural defects. Furthermore, due to their vulnerability to seasonal variations in growing and soil conditions, their mechanical properties typically present a wide scatter, unlike synthetic fibres that have higher consistency in their properties, making the mathematical and numerical modelling of plant fibre composites more difficult (and uncertain) due to the high variability of the input data [28,34].

Table 2.2 presents some physical and mechanical properties of the most widely used plant fibres in engineering applications, and it highlights the large variability among the various properties for a given type of fibre and also for the various fibres.

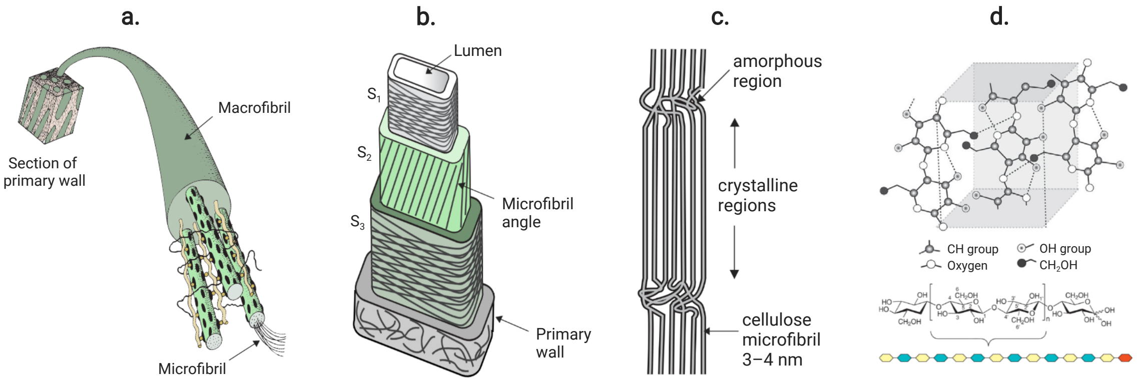

Figure 2.2: The hierarchical structure of plant cell walls: **a.** to **d.** are reproductions adapted from [27,35]; **a.** shows a section of primary wall composed of macro and microfibril; **b.** presents cell wall layers, comprising one primary wall and three secondary layers (S_1, S_2, and S_3), with a view of the microfibril angle in S_2; **c.** illustrates amorphous and crystalline regions in cellulose microfibrils; and **d.** presents 3D cellulose molecular structure.

Table 2.2: Physical and mechanical properties of the most widely used plant fibres in engineering applications [36–47].

Fibre[a]	**Microfibrillar angle (°)**	**Tensile strength (MPa)**	**Elastic modulus (GPa)**	**Ultimate strain (%)**	**Density (g/cm^3)**
Flax	8.3–11.0	345–1035	27.6–50	2.0–3.2	1.3–1.5
Jute	7.0–12.0	200–775	20.0–55	1.5–3.0	1.3
Kenaf	9.0–15.0	930	53.0	1.6	1.4–1.5
Hemp	6.2–11.0	550–690	30.0–70	1.6	1.5
Ramie	7.5	400–938	24.0–128	2.5–3.8	1.5
Sisal	20.0	400–700	9.0–22	3.0–14.0	1.4
Bamboo	2.0–10.7	140–230	11.0–17	4.0–7.0	0.6–1.1
Cotton	20.0–30.0	287–800	5.0–12	7.0–8.0	1.5–1.6

[a] Fibres derived from species mentioned in Figure 2.1.

The main potential contribution of plant fibres used as reinforcement in FRP composites is towards improving sustainability. In this respect, the use of plant fibres in FRP structural applications as an alternative to synthetic fibres has the following advantages, among others [24,38,48,49]: (i) renewable capacity and neutrality with respect to carbon dioxide emissions; (ii) lower density and interesting values of specific moduli, which is advantageous, especially in parts subjected to bending, (iii) lower energy consumption, though fibre processing requires higher amounts of water compared to synthetics, and (iv) thermal recycling is possible, whereas glass need high temperatures and causes problems in combustion furnaces.

However, the use of plant fibres also entails some important drawbacks, which need to be overcome, such as: (i) biodegradability, so the risk of microbial contamination must be taken into account [50,51]; (ii) hydrophilicity, whereas thermoset resins are hydrophobic - the possibility of moisture absorption for composites reinforced by these fibres is thus significant (up to 8% or 10%), together with the inherent degradation of the fibres, which leads to a reduction in performance of the material over time [52,53]; (iii) flammability, since they are not resistant to high temperatures - they lose their stiffness at around 160 ℃ and thermally degrade at a temperature of approximately 200 ℃ [54–58], preventing their use with some matrices and manufacturing techniques, such as pultrusion; and (iv) the tensile strength is lower when compared to conventional fibres, thus they are best suited to produce stiff parts that do not require high strength [59,60].

Regardless of the factors affecting the use of plant fibres as reinforcement in FRP composites, renewability and cost competitiveness are still attractive to all business sectors to explore opportunities to replace traditional synthetic fibres. The research value in this direction is massive, namely, to solve the issues reported for the structural feasibility of natural fibres.

2.2.1.3 Basalt fibres

Basalt fibres have been reported to be a more sustainable alternative for the manufacturing of FRP composites when compared to other synthetic fibres, such as glass and carbon [61]. These mineral fibres are produced by melting crushed basalt rock between 1250 ℃ to 1500 ℃ and drawing the molten material to the subsequent formation of CBF, with nominal diameters in the range of 9 µm to 24 µm and a golden-brown appearance (bronze). Basalt fibre belongs to the group of inorganic nonmetallic fibres; however, unlike glass fibres, the melt is 100% basalt, which is a type of igneous rock formed by the fast cooling of lava at the earth's surface (see Figure 2.3), with no further constituent ingredients or additives, resulting in considerably more eco-friendly fibres than glass fibres [62–65].

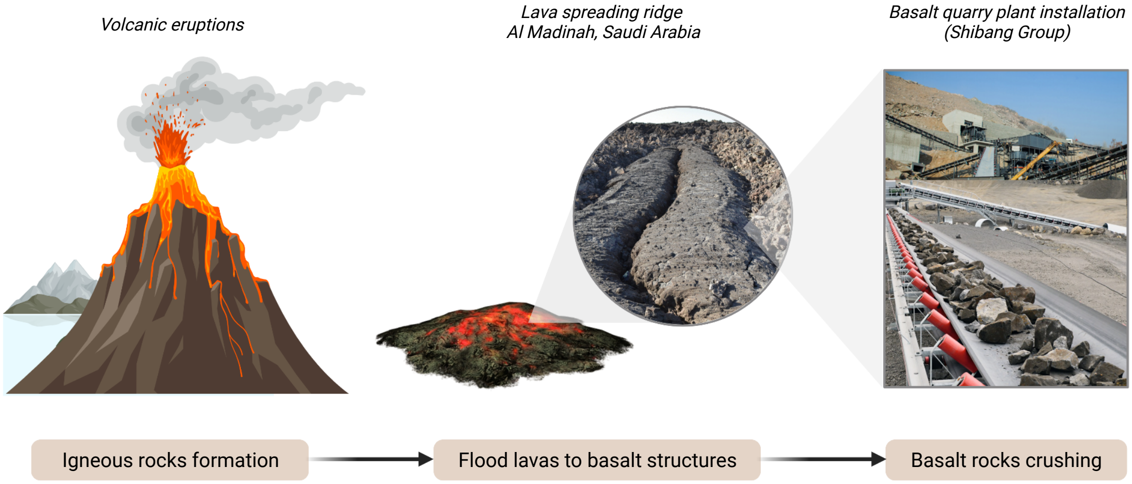

Figure 2.3: Crushed basalt rock production for the manufacturing of basalt fibres [66,67].

Basalt is abundant in nature, being the most common rock in the Earth's crust, since it represents more than 90% of all volcanic rocks. Figure 2.4 shows the world map and landscapes with flood basalt examples, where parts of the same flood basalt event are indicated by outlines or fills of the same colour, and average ages of the flood basalt events (in million years) are also given. Basalt has also an advantage over plant fibres,namely that its physical–chemical properties for production of the CBF are essentially independent from the geographical provenance of the starting raw material, provided that SiO_2 content is in the range of 45% to 50% [68].

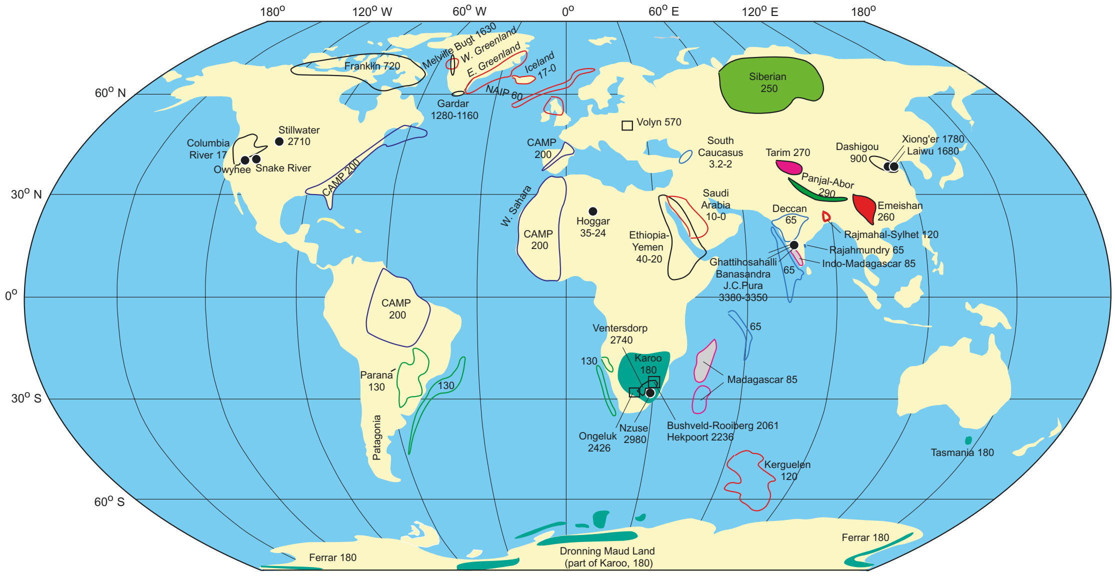

Paraná CFB province, Brazil

The Mesa Range, Victoria Land, Antarctica

Drakensberg Group, Sani Pass, Lesotho

Vatnshlíðarvatn, Varmahlíð, Iceland

The Snake River canyon, USA

Trotternish peninsula, Skye, Scotland

Pliocene basaltic, Kars plateau, Turkey

Upalluk/Giesecke Monument, Greenland

Ponta de São Lourenço, Madeira, Portugal

Figure 2.4: Availability of basalt sources around the world [69,70].

In fact, basalt rock chemical composition depends mainly on the lava source, cooling rate, and historical exposure to the elements. From a mineralogical point of view, basalt is mainly composed of three silicate minerals: plagioclases, pyroxenes and olivines. The nature of the magma influences its chemical composition, where silicon dioxide (SiO_2) is the dominant component, followed by Al_2O_3, FeO + Fe_2O_3, CaO, MgO, Na_2O, K_2O, TiO_2, and so on [71]. These basalt rocks are classified according to the SiO_2 content as: alkaline (SiO_2 up to 42%), mildly acidic (43 to 46% SiO_2) and acidic basalt (over 46% SiO_2); only acidic basalt rocks are suitable for fibre manufacturing, since a high content of SiO_2 allows to obtain good levels of flexibility and chemical stability of the basalt filaments. As regards the other components, Al_2O_3 can increase the chemical resistance of the basalt filaments, and CaO, MgO and TiO_2 promote improvements in water and corrosion resistance [61].

Basalt fibre has higher mechanical and physical properties when compared to glass, with additional advantages, such as lower carbon footprint, no toxic reaction in air or water, increased resistance to elevated temperatures (with continuous work from −269 ℃ to 700 ℃), increased UV resistance, lower hygroscopic property, increased radiation resistance, and resistance to acid and alkaline active environments [72–74]. The major drawbacks of basalt fibres are their higher density and cost compared with E-glass [75].

High-quality basalt fibres are produced from basalt deposits with uniform chemical makeup by selecting the basalt rocks with the richest chemical properties. CBF is typically produced by *Spinneret* technology. Figure 2.5 shows a simplified scheme of continuous basalt fibre manufacturing procedures by *Spinneret* technology, which can be spun in a similar way to that used for glass fibres, with: (1) crushed stone silo, (2) loading station, (3) transport system, (4) batch charging station, (5) initial melt zone, (6) secondary heat zone with precise temperature control, (7) filament-forming bushings, (8) sizing applicator, (9) strand formation station, (10) fibre tensioning station, and (11) automated winding station.

Basalt rock is crushed and washed before being loaded into furnaces heated using air gas mixture or electrically. Some electrodes are generally immersed into the melting bath to promote uniform heating and reduce the time for achieving thermal equilibrium. Once the melting process is completed, molten basalt is poured onto platinum-rhodium heated bushings, from which filaments are drawn under hydrostatic pressure. Filaments are collected together after the cooling process to form a strand, whose integrity and chemical stability are ensured through a preliminary lubrication step. The filament size (in the order of some micrometres in diameter) is controlled by varying the drawing speed and the melt temperature: at gradually decreasing temperature, a yarn is formed whose thickness reduces over the cooling process, and subsequently, it gets twisted into a yarn and plied into a multi-strand roving [76].

CBF can be converted into woven or non-woven textiles or used to reinforce composite structures with techniques similar to those used with continuous filament glass fibres [77].

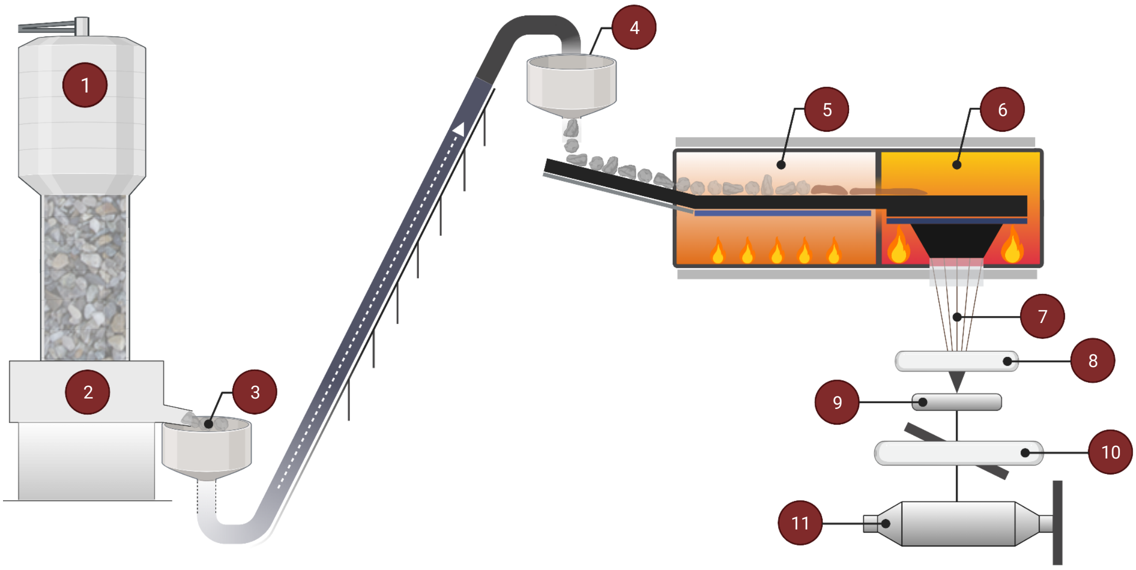

Figure 2.5: CBF manufacturing procedures by *Spinneret* technology [78,79].

Even though basalt rock is a natural (mineral) resource and is currently intensively explored, the concept of basalt fibres as a more sustainable raw material than synthetic ones can be supported by the following aspects [76,77,80,81]: (i) a considerable number of volcanoes keep expelling tons of lava into the Earth's surface, thus providing a continuous source of raw material; (ii) although higher temperatures are required to manufacture fibres from basalt than glass, the production of basalt fibres requires less energy due to the higher uniformity of its heating compared to glass fibres; (iii) basalt fibres can be recycled more efficiently than glass fibres; (iv) no special precautions are required for the disposal of residues after production or at the end of their life cycle, because basalt fibres do not contain any harmful substances.

According to Wu [65], the following three aspects are necessary to boost the use of basalt fibre reinforced polymer (BFRP) composites in structural applications in the future, namely: (i) to promote the large-scale application of existing mature technologies, for example, BFRP reinforcing bars and grids; (ii) to improve recent technologies and accumulate expertise in demonstration projects, including BFRP anchors, intelligent BFRP reinforcement for concrete structures, and BFRP profile-concrete composite structures; and (iii) to explore new application technologies, such as BFRP cables for stayed long-span bridge structures.

2.2.1.4 Comparative critical assessment

In the following, a comparison of the main economic, technical and ecological aspects of various fibres is presented, namely to assist the selection of the most recommended type of fibres to manufacture more sustainable composites within the scope of this thesis.

According to Table 2.3, plant fibres are eco-friendlier and cheaper compared to synthetic fibres and their production worldwide is considerably larger. However, plant fibres require more control on surface treatment (sizing), which involves additional costs, whereas synthetic fibres are already supplied with sizing compatible with most commercial thermoset resins available in the market. Although the potential strength of plant fibres is high if estimated from the theoretical strength of a cellulose molecule, in practice it has not yet been possible to exploit the inherently high properties of cellulose due to naturally occurring structural defects within the fibres (these defects also occur in synthetic fibres, but pose less of a limitation). Defects introduced during processing of the fibres and chemical incompatibilities with the polymer matrix still prevent the adequate stress transfer from the resin to plant fibres. Furthermore, it is difficult to evaluate the quality of plant fibres and thus it is challenging to use existing analytical formulations to predict the mechanical properties of their FRP composites. Hence, despite studies based on hierarchical cellulosic structure [82,83], the interest in plant-fibre composites has until now been somewhat refrained by the acknowledgement that achieving theoretical strengths might not be possible, at least in the near future, due to the aforementioned difficulties.

Plant fibres also have other key limitations, namely the following: (i) high moisture absorption; (ii) poor bonding properties with polymeric resins (hydrophilic fibre and hydrophobic resin); (iii) flammability; (iv) swelling effects that may affect the quality of resulting composites; (vii) biodegradability; and (v) low weatherability. Thus, compared with the widespread acceptance of advanced composites produced with synthetic fibres, the path to adoption of plant-fibre composites in mainstream structural applications will be hindered by technical challenges yet to be overcome.

Alternatively, the development of eco-friendlier and cost-effective basalt fibres for FRP composites has received considerable attention in both academic and industrial fields. In the last decade, FRPs based on basalt fibres have been successfully proved to be an effective and feasible alternative to conventional FRPs both in terms of mechanical performance and of ecological and economical sustainability [89]. When compared with glass and carbon fibres, basalt fibres are easier and cheaper to produce, require lower energy consumption (in electric furnace), and represent an eco-compatible solution, since they do not entail recycling problems [90–92]. From a mechanical point of view, basalt fibres exhibit strength and stiffness properties which allow to manufacture FRP composites with comparable or higher mechanical performance than FRPs based on glass fibres. Furthermore, basalt fibres have larger strain at failure than carbon fibres, and these mineral fibres practically exhibit almost constant mechanical properties in a wide range of temperature values, retaining about 90% of the normal temperature strength up to 600℃ [93]. Due to the high resistance to both corrosion and UV-radiation, combined with good mechanical properties, FRP composites based on woven mats and fabrics of basalt fibres are already successfully employed in structural applications, such as the production of wind turbine blades and in boat building [73,89,94]. For structural applications in construction, CBF has also been already adopted as reinforcement in FRP composites for producing high-strength rovings for pultruded load-bearing parts and concrete-reinforcing bars. In fact, recent experimental and analytical studies [95–101] have shown the feasibility and effectiveness of BFRP for structural applications. Nevertheless, technical standards and design guidelines are still defined and calibrated based on evidence obtained with CFRP and GFRP composites, and therefore they also need to be extended to basalt fibres.

Based on the current inability of plant fibres to be used in structural applications, basalt fibres have emerged to introduce more sustainability to composite materials and structur-

Table 2.3: Comparison of plant, glass and carbon fibres [84–87].

Properties	**Unit**	**Plant**[a]	**Glass**[b]	**Carbon**[c]
Economic				
Annual global production[d]	(tonnes)	31.000.000	4.000.000	55.000
Distribution for FRPs in EU	(tonnes)	Moderate (60.000)	Wide (600.000)	Low (15.000)
Cost of raw fibre	(£/kg)	Low (0.5–1.5)	Low (1.3–20.0)	High (≥ 12.0)
Technical				
Density	(g/cm^3)	Low (1.35–1.55)	High (2.50–2.70)	Low (1.70–2.20)
Tensile strength	(MPa)	Low (≈400–1500)	High (2000–3700)	High (2400–4800)
Elastic modulus	(GPa)	Moderate (≈30–80)	Moderate (70–85)	High (250–800)
Ultimate strain	(%)	Low (1.4–3.2)	High (2.5–5.3)	Low (0.3–2.2)
Specific tensile strength	(GPa/g/cm^3)	Moderate (0.3–1.1)	Moderate (0.7–1.5)	High (0.6–3.7)
Specific elastic modulus	(GPa/g/cm^3)	Moderate (20–60)	Low (27–34)	High (68–290)
Abrasive to machines		No	Yes	Yes
Ecological				
Energy demand of raw fibre	(MJ/kg)	Low (4–15)[e]	Moderate (30–50)	High (≥ 130)
Renewable source		Yes	No	No[f]
Recyclable		Yes	Partly	Partly
Biodegradable		Yes	No	No
Health risk when inhaled		No	Yes	Yes
CO_2 neutral		Yes	No	No

[a] Includes bast, leaf and seed fibres, but does not include wood and grass/reed fibres.

[b] Includes E- and S-glass fibres.

[c] Includes polyacrylonitrile (PAN)- and pitch-based carbon fibres.

[d] Estimated values for the year 2010.

[e] While the energy required in the cultivation of plant fibres is low (4–15 MJ/kg), further processing steps (*e.g.*, retting and spinning) can significantly increase the cumulative energy demand, for instance, to up to 146 MJ/kg for flax yarn [88].

[f] Carbon fibres based on cellulose currently account for only 1–2% of the total carbon fibre market [86].

ally compete with their synthetic counterparts, mainly with glass fibres, which remain the most used to produce FRP composites in the European market, especially E-glass fibres, which have lower cost than carbon fibres and provide similar strength-related properties. However, carbon fibres are often used for specific reinforcement applications, such as FRP composite strengthening strips, because of their higher specific elastic modulus and specific tensile strength compared to glass fibres (see Figure 2.6).

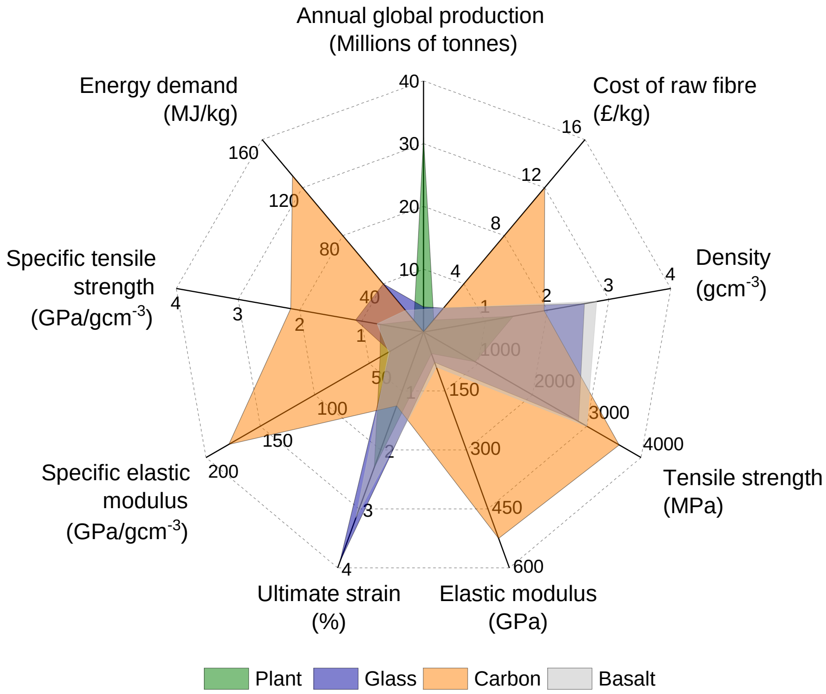

Figure 2.6: Radar plot: plant and synthetic fibres properties.

The analysis described herein about reinforcing fibres allowed the following decisions to be made for the development of FRP composites for more sustainable and eco-friendly structural applications within the scope of this research: (i) plant fibres do not yet have sufficiently consistent mechanical properties and durability to compete with synthetic fibres; (ii) glass fibres will be adopted to produce unsaturated polyester resin matrix composites; (iii) carbon fibres will be used to produce polyester matrix composites; and (iv) aramid fibres will not be used in these activities as they present several drawbacks when compared to the alternatives. Finally, it is worth referring to the fact that basalt fibres have also been selected (by this author) to produce BFRP composites; however, due to time limitations, the manufacturing and characterisation works were not included in this thesis.

2.2.2 Polymer matrix

Polymer matrix, or simply *matrix*, is formed by macromolecular segments or chains with different conformations and arrangements, typically classified as thermoplastics or thermosets. Both these matrices may be petroleum- or bio-based, with biodegradable or non-biodegradable polymeric chains (see Figure 2.7).

Thermoplastics are usually categorised into four groups [102], namely:

1. Petroleum-based and non-biodegradable, such as polyethylene (PE), polypropylene (PP), and polyvinyl chloride (PVC);
2. Entirely or partially bio-based and non-biodegradable, such as bio-based polyethylene (bio-PE), bio-based bio-based polyamide (bio-PA), bio-based bio-based polytrimethylene terephthalate (bio-PTT), and bio-based polyethylene terephthalate (bio-PET);
3. Bio-based and biodegradable, such as polylactic acid (PLA) and polyhydroxyalkanoates (PHAs); and
4. Petroleum-based and biodegradable, such as polybutylene adipate terephthalate (PBAT), polycaprolactone (PCL), and polybutylene succinate (PBS). PBS can be partially bio-based polybutylene succinate (bio-PBS), and it is commercially available at present.

Most research on bio-based polymers has focused on thermoplastics for applications in various industries [103]. However, due to their lower mechanical performance compared to thermosets, they find limitations for high-performance applications. Consequently, thermoplastics are less often used to manufacture materials with higher requirements in terms of load-bearing capacity.

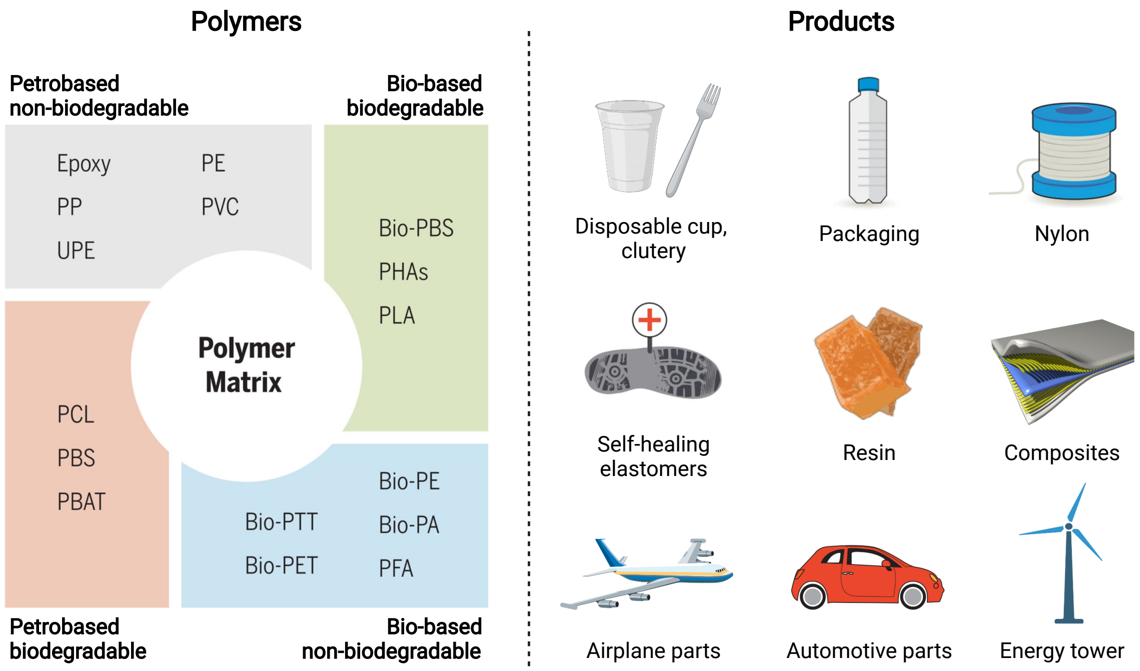

Figure 2.7: Example of petroleum- and bio-based polymeric matrices currently available for various industries, such as packaging, biomedical, and composites [102–104].

Thermoset resins are the non-reinforced part of FRP composites, being used to impregnate and bind the fibres and, after cured, they are responsible for carrying part of some types of loading, particularly those associated with transverse stresses and interlaminar shear stresses [105]. Thermoset resins have good fibre impregnation capacity and excellent adhesive properties. Compared with thermoplastics, they exhibit lower viscosity, allowing higher processing speeds. Furthermore, thermosets have high strength and modulus, good thermal behaviour (at high softening temperatures), better creep properties and more resistance to chemical attack than most thermoplastics [106].

Despite the good properties exhibited by thermosets, they display some shortcomings, including poor cracking, brittleness, and low toughness [107]. In addition, conventional thermosets are petroleum-derived, and their reprocessing is still a challenge to be overcome, since they are a class of amorphous polymers highly crosslinked that become infusible and insoluble when cured by thermal, chemical (catalyst or promoter) or other means. However, the appeal for environmental sustainability, together with current high oil prices and their lower long-term supply availability, may promote the development of more sustainable alternatives to thermoset resins production. Thus, bio-based thermosets can trigger the development of high-performance ecological resins able to produce several high-performance products, such as FRP composites used in different sectors (*e.g.*, construction, automotive, aerospace, marine, energy and consumer goods).

Although bio-based thermoset options have recently emerged, such as polyfurfuryl alcohol (PFA) and bio-based polyurethane (bio-PU), conventional petroleum-based thermosets, such as epoxy, vinyl ester (VE), UP, and phenolic are still dominant in composite applications - the lower cost and the (present) wide availability of crude oil are the main reasons for the slow progress and shift towards greener thermoset polymers.

Since this thesis aims to develop more sustainable FRP composites, the review presented next will focus exclusively on thermoset resins. First, the main characteristics and properties of conventional thermoset resins currently used in the composites industry are presented. Then, recent studies on bio-based alternatives to their petroleum-derived counterparts are presented.

2.2.2.1 Conventional thermoset resins

The most commonly used thermoset resins are epoxy, unsaturated polyester, vinyl ester, and phenolics. They cover a vast class of chemicals and various physical and mechanical properties. In the curing process of these thermosets, the low viscosity resin is converted into a strong, and stiff solid by chemical crosslinking, leading to a tightly bound 3D network while the composite is being formed.

Epoxy is a reactive prepolymer that contains monomers with two or more ring-like epoxide (or oxirane) groups, which react with hydroxyl groups and may be distributed along the macromolecule main chain but are usually terminal [108]. The most popular epoxy monomers are those derived from the reaction of bisphenol A (BPA) and epichlorohydrin

(ECH), in presence of NaOH, resulting in a structure known as DGEBA, see Figure 2.8. The epoxy monomers may be reacted (crosslinked) either with themselves through catalytic homopolymerisation, with a suitable catalyst, such as boron trifluoride and tertiary amine, or with a wide range of reactants of which secondary amines and acid anhydrides are the most important. These reactants are often referred to as hardeners, and the crosslinking reaction is commonly referred to as curing [109,110].

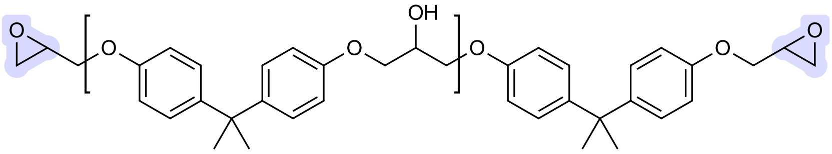

Figure 2.8: Epoxy main chain based on DGEBA with terminal oxirane groups for crosslinking reactions either with themselves through catalytic homopolymerisation, or with hardeners, such as amines or acid anhydrides.

The most characteristic properties of commercial epoxies are related to the reactants used in the synthesis and from the chemical macromolecular structure obtained, resulting in products from low to high T_g materials. When compared with other thermosets (such as polyesters) and using appropriate hardeners, epoxy usually has better chemical resistance to alkalis. Epoxies also present excellent corrosion resistance and high resistance to moisture absorption. Furthermore, due to the absence of styrene, epoxy resins involve significantly less toxic emissions during the curing process than polyester and vinyl ester, making their use eco-friendlier with open-mould techniques, such as hand lay-up or vacuum bagging.

For the civil structures field, epoxy resins are used in structural strengthening applications with stringent strength, stiffness, service temperature, and durability requirements. For example, epoxy resin can be applied to impregnate dry fibre sheets or fabrics in the field and then cured on-site, acting both as a matrix for the FRP composite (impregnating the fibres) and as an adhesive to attach the FRP composite to the substrate, or can be just applied separately as structural adhesive to bond pre-cured FRP strips to concrete (and other materials) in strengthening applications. Furthermore, prefabricated products can be manufactured when epoxy resins are combined with carbon fibres; namely, pre-cured CFRP strips (or sheets) for structural strengthening, CFRP tendons for pre-stressing concrete, and FRP stay cables for bridges.

Unsaturated polyester resin is one of the earliest thermosets, being (the most) widely used in FRP composites [107]. Its main chain (prepolymer) is obtained from the polycondensation reaction of unsaturated and saturated dicarboxylic acids (or anhydrides) with diols, resulting in pale yellow oligomers with a low degree of polymerisation. These oligoesters may have high viscosity, depending on the chemical composition and molecular weight. However, vinyl monomers (usually styrene) are typically used as diluents to decrease the unsaturated polyester oligomers' viscosity and simultaneously to react with their unsaturations (double bonds) using free-radical initiators to the formation of a 3D network.

The solutions of unsaturated polyester prepolymers and reactive diluents are known as UPR, and may be classified based on their chemical structure, with ortho and isophthalic resins being the most common types.

Orthophthalic polyester resins, also known as general-purpose resins, are based on phthalic anhydride, maleic anhydride, and glycols, according to Figure 2.9. Phthalic anhydride is the anhydride of *ortho*-phthalic acid; although phthalic anhydride provides an inflexible link to the main chain, it reduces the thermal and chemical resistance of the polymer. However, it is cheaper compared with isophthalic or terephthalic acids. Additionally, maleic anhydride is the most common olefinic monomer - capable to provide double bonds (unsaturations) - used to synthesise unsaturated polyesters, due to its low cost, large market scale, and high reactivity with diols. However, it is less reactive in subsequent free-radical reactions due to its *cis* configuration when compared to *trans*-fumaric acid. Consequently, fumaric acid is a candidate for replacing maleic anhydride in unsaturated polyesters, as it exhibits *trans* configurations and can be produced biologically from renewable feedstocks [111].

Among the glycols, 1,2-propylene glycol is the most important, mainly due to the presence of the pendant methyl group; the resulting resins are less crystalline and more compatible with commonly used reactive diluent (styrene) than those obtained using ethylene glycol and diethylene glycol. By contrast, resins with high heat and chemical resistance are produced using neopentyl glycol or hydrogenated BPA [112].

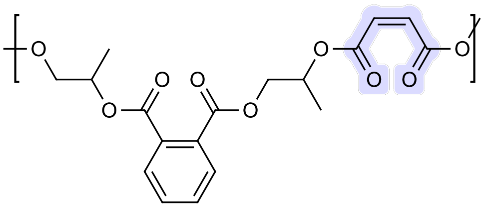

Figure 2.9: Unsaturated polyester main chain based on phthalic anhydride, 1,2-propylene glycol, and maleic anhydride, which provides a double bond for crosslinking reactions with reactive diluents and later orthophthalic polyester resin formation.

UPRs are commonly used to impregnate reinforcing fibres, mainly glass fibres, and cured in the presence of free-radical initiators eventually coupled with accelerators, resulting in a wide range of mechanical, physical and chemical properties, depending on the choice of diacids, diols, crosslinking monomers, initiators and additives [113]. Due to their suitable balance between low cost, versatility of processing, and good mechanical and thermomechanical properties, these resins have been among the most often used thermoset polymers by the FRP composites industry for several years. However, their production still depends significantly on raw materials that are derived from petroleum. Furthermore, despite widespread historical use, styrene (the most common reactive diluent) is toxic to human health [114].

Table 2.4 presents the viscosity and hardness of unsaturated polyester resins currently available on the market for use as matrices in various FRP composite manufacturing techniques, such as hand lay-up, vacuum infusion, and pultrusion.

Table 2.4: Conventional petroleum-based polyester resins [115–117].

Polyester	**Type**	**Application**	**Viscosity**[a] (mPa · s)	**Hardness**[b] (Barcol)
Synolite^{TM} 5410-P-1	ORTHO	Hand lay-up	390	45
Distrition® 135 SX	ISO	Hand lay-up	855	37
Distrition® 110 SXZ	DCPD	Hand lay-up	540	40
Polylite® 33204	ORTHO	Lamination	475	40
Synolite^{TM} 8488-G-2	DCPD	Infusion	85	45
Distrition® 152 S1	ISO-NPG	Infusion	225	44
Crystic® U 904 LVK	ORTHO	Infusion	120	40
Crystic® 701PAX	ISO	Infusion	160	35
Synolite^{TM} 2155-N-1	ORTHO	Pultrusion	275	47
Crystic® 272E	ISO	Pultrusion	350	44
Dion® 31068-00	TERE	Pultrusion	750	–
Aropol^{TM} 7030	ISO	Pultrusion	1200	50
Crestamould® 474PA	ORTHO	Multi-purpose	Thix	48
Polylite® 31054-00	ORTHO	Multi-purpose	700	45

[a] Measurements between 23 °C and 25 °C
[b] Values obtained for different curing schedules, including post-curing for most resins.

Vinyl ester resins are usually formed from unsaturated esters of epoxy prepolymers, combining the improved performance of epoxy with the easier processing and lower cost of polyester. Moreover, vinyl esters offer similar mechanical properties to epoxy resins, low viscosity, and fast cure, equivalent to polyesters [118].

The vinyl ester main chain is usually synthesised by reacting DGEBA, the epoxy resin prepolymer, with an unsaturated acid, such as methacrylic acid (see Figure 2.10). Consequently, they are more expensive than polyesters. By contrast, vinylester prepolymer can also be derived from polyester and urethane prepolymers; but those based on oxirane groups (epoxy) are of particular commercial significance [107]. In addition, compared to epoxy resins, vinyl esters exhibit lower adhesion strength to substrates, and their volumetric shrinkage is higher, ranging from 5% to 10%.

Vinyl esters are often identified as an unsaturated polyester grade because of their similar structure to polyesters and their cure and processing similarity. However, the structural difference of their macromolecules, which partially justifies their improved chemical and mechanical properties, is the presence of reactive double bonds at the ends of the chains. Thus, crosslinking to vinyl esters occurs at the unsaturations (carbon-carbon double bonds)

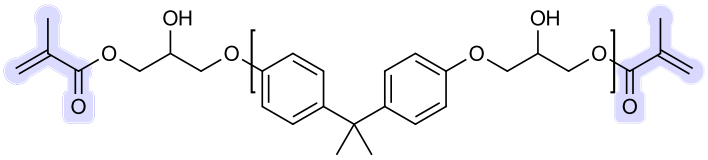

Figure 2.10: Bisphenol A epoxy-based (methacrylate) vinyl ester resin.

positioned at the end of the polymer main chain, meaning that the resulting thermoset contains fewer crosslinked bonds than polyesters; instead, unsaturated polyester resin has reactive double bonds distributed throughout its main chain [119]. Furthermore, although the tensile and flexural properties of cured vinyl ester resins do not vary appreciably with molecular weight, the thermomechanical properties can be improved by using phenolic-novolac-type building blocks for their main chains.

Because of the fewer crosslinking sites, a cured vinyl ester is more flexible and has higher fracture strength than a cured polyester resin. Also, like polyester resins, vinyl esters are dissolved in styrene [120]. Consequently, the crosslinking mechanism is similar to polyesters, presenting the same problems with free radicals during long-term storage. However, unlike polyesters, vinyl ester resins have a low content of ester groups and low vinyl functionality, resulting in better resistance to hydrolysis, lower exothermic temperature peaks, and less shrinkage after curing. Furthermore, vinyl ester resins have good wetting characteristics and excellent adhesion to glass fibres due to the high number of OH (hydroxyl) groups in their main chain, forming hydrogen bonds with similar groups on the glass fibre surface [118].

Vinyl esters are also resistant to strong acids, and strong alkalis [121]. This explains why most commercially available FRP bars used to reinforce concrete elements are made from vinyl ester resin matrix for applications with specific durability requirements. In addition, vinyl esters can also be processed at ambient and elevated temperatures, being widely used as fibre impregnation matrices to manufacture large (and simple) geometry pultruded FRP profiles mainly used in bridge construction [122].

Phenolic resins consist of low-polarity groups, such as aromatic rings, and highly polar groups, such as hydroxyls (Figure 2.11), resulting in favourable interactions with a range of fibre reinforcements. This structural compatibility, coupled with the low viscosity in the temperature range in which FRP composites are usually prepared, allows phenolic resins to wet the reinforcements and crosslink through the reinforcement, contributing to good adhesion at the fibre-matrix interface [106].

Phenolics are traditionally classified in resol- and novolac-type resins by reacting phenols with aldehydes. Typically, novolac is obtained in a strongly acidic medium through the reaction of formaldehyde with a molar excess of phenol; hexamethylenetetramine (HMTA)

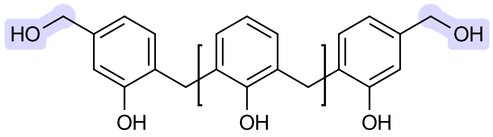

Resol

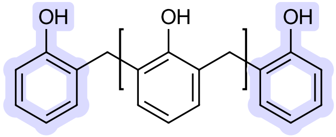

Novolac

Figure 2.11: Types of phenolic resins.

can also be used as a source of formaldehyde for curing novolac-type phenolics, producing formaldehyde and ammonia as by-products [123]. By contrast, resol is obtained by reacting phenol with a molar excess of formaldehyde in an alkaline medium, generating water and formaldehyde as by-products of condensation reactions [124]. These by-products can be released as volatiles during curing, resulting in networks with a substantial voids content that negatively affects the mechanical properties of the cured materials and increases the moisture uptake of composites.

Lower void content can be achieved by replacing water as a diluent with ethylene glycol, which confers low viscosity to the resin and can also act as both a plasticizer and a reactant. In the latter case, ethylene glycol is introduced to the thermoset network through the curing, decreasing the voids content and increasing density, leading to a cured material with improved mechanical properties [125]. In addition, phenolic resins have good dimensional stability, keeping their mechanical properties at relatively high temperatures, and with the advantage of being relatively economical, with a similar cost to polyester.

The main drawbacks are the difficulty in reinforcing and curing phenolic resins, which further present a brownish colour and are difficult to pigment. Phenolic thermosets are also brittle at room temperature; however, they overcome one of the drawbacks associated with the application of organic materials in construction: their high combustibility. Low flammability justifies why phenolic resins are widely used to manufacture FRP composites for applications requiring fire, smoke and toxic fumes production and high-temperature resistance [126], such as interior structural parts, materials used in tunnels, and fire safety components. Furthermore, phenolics-based FRP composites can be produced with complex shapes while maintaining high strength and stiffness, making these materials alternatives to metals in the rail, offshore and construction industries [106].

A more recent phenolic resin type called benzoxazine has been obtained by synthesising diphenolic compounds, aqueous formaldehyde and a primary amine. While typical phenolics are chemically linked through methylene bridges, benzoxazines are linked first by forming a cyclic structure from the phenolic hydroxyl to the ortho position [127]. Consequently, the development of benzoxazine technology presents an alternative to traditional phenolic condensation chemistry, eliminating the problems associated with the volatiles that are generated during the condensation reaction.

Finally, the use of phenolic-based resins can improve fire safety (in terms of mechanical performance) and reduce the costs of FRP composites, especially with carbon fibre reinforcement. In addition, among the main properties that successfully result from the combination of phenolic resin and carbon fibres are the excellent thermal stability of carbon fibres and the low thermal conductivity of phenolic resins.

2.2.2.2 Bio-based thermoset resins

For a renewable product to be commercially competitive, it must be economically viable at an industrial scale and possess properties that match or exceed its existing petroleum-derived analogues. However, few bio-based polymers have overcome this challenge [128] since the properties of a polymer depend on its macromolecular structure, namely, chain-sequence, chain-length, chain-isomerism and chain-topology [129], whether it is produced from petroleum- or bio-derived building blocks.

Bio-based thermoset resins have a wide range of mechanical properties and behaviours, from stiff and fragile to flexible and ductile. However, despite the efforts of producers to develop new resins, currently, most thermosets commercially available for manufacturing composites still have reduced incorporation of sustainable raw materials, approximately 30-35%. In addition, these commercial bio-based thermoset resins are suitable for applications in various products, such as boats, automotive, energy, and sports parts [130–133]. By contrast, although new commercial resins have been recently made available [134], the composites market for structural applications still lacks bio-based thermoset resins with processing characteristics suitable for current manufacturing techniques, such as vacuum infusion and pultrusion, and that present the required mechanical and thermomechanical properties (after curing) for load-bearing composite structures.

Indeed, the development of bio-based thermoset resins for high-performance structural applications is needed to improve the sustainability of FRP composites, and recent commercial alternatives have attested this evidence [135,136]. In addition, current research has shown relevant trends for the synthesis and use of renewable raw materials for the production of new bio-based thermoset resins, namely [109,137,138]: (i) epoxy prepolymer based on vegetable oils; (ii) phenolics containing lignin compounds from liquefied wood; (iii) unsaturated polyesters containing reactants derived from agro-by-products; and (iv) reactive diluents for epoxy, polyester, and vinyl ester derived from biomass [139–141]. These developments are summarised next.

Epoxy bio-resins have been reported in the literature recently, and the main approaches to making them more sustainable are focused on (i) replacing bisphenol-A with aliphatic long-chains or other polyhydroxy bio-compounds [142–144], (ii) replacing epichlorohydrin derived from petroleum with its bio-based counterparts [145], and (iii) using bio-based alternatives to petroleum-derived amines [146].

Although many studies have been reported on epoxidized vegetable oils (from soybean oil, castor oil, linseed oil, and others), it is known that epoxies from these long hydrocarbon chains present lower mechanical and/or thermomechanical properties when compared with their petroleum-derived counterparts [147,148]. By contrast, aromatic groups based on biomass (such as those derived from lignins, tannins and furans) have been shown to provide higher performance to the resulting epoxy resins [149–153].

Epichlorohydrin, the more expensive compound, is obtained by the chlorination of propylene followed by a sequence of reactions, and it confers high reactivity to the epoxy precursor. However, it is classified as carcinogenic, mutagenic, and reprotoxic (CMR) compound of category 1B. Interestingly, ECH is now industrially produced from bio-based glycerol [145], and the conversion of glycerol to the chemical ECH is economically attractive [154,155]. The bio-based weight content of DGEBA is about 25%, when the synthesis is made from bio-based ECH.

Unsaturated polyester bio-resins have been studied under their two primary constituents, namely: the main chain (prepolymer) and the reactive diluent. Regarding the prepolymer, the focus has been on replacing petroleum-derived diacids and diols with bio-based counterparts. In particular, the synthesis of unsaturated polyesters based on long-chain diacids and diols results in a more flexible cured thermoset material [156–158]; however, increasing the crystallinity of the polyester or decreasing amorphous zones around its main chain results in a polymer with good mechanical and thermomechanical properties, but with very high viscosity at room temperature. Consequently, many attempts have failed to balance incorporating as much bio-content as possible and achieving suitable processing properties for different manufacturing techniques of high-performance materials, such as composites.

The replacement of styrene by bio-based vinyl monomers that provide compatible reactivity and solubility with the polyester backbone has also been studied [159]. However, the few alternatives reported are still economically unfeasible compared to styrene, such as those based on acrylic monomers [160]. Furthermore, to promote traditional curing reactions, which use initiators and accelerators based on peroxides and metal salts, respectively, a minimal amount of styrene has still been shown to be necessary [161]. Thus, the production of bio-based unsaturated polyester resins without styrene capable of competing with their counterparts based entirely on petroleum-derived raw materials is still a challenge to be overcome.

Vinyl ester bio-resins have also been reported [140]. However, their development matches the challenges of bio-content incorporation found in both epoxy and unsaturated polyester resins, since the main chain of a conventional vinyl ester resin comprises BPA monomers, also present in epoxy. At the same time, it is diluted in styrene, such as polyesters.

Phenolic bio-resins have been studied and some practical applications have already been implemented [162,163]. The main focus in the development of bio-based phenolics has been the replacement of oil-derived phenol and formaldehyde by bio-based building blocks, especially those derived from biomass [164]. Glyoxal, furans and lignin derivatives are candidates to replace formaldehyde during the synthesis of phenolic resins. By contrast, lignin, tannin and cardanol are alternative raw materials to replace petroleum-based phenol [165–167]. Furthermore, lignin (polyphenolic in composition) has been considered the most promising substitute for phenol in phenol-formaldehyde resins because of its phenolic nature. Moreover, its many functional surface –OH groups and surface modification, have shown an improved reinforcing effect on the performance of biocomposites [102,168].

Finally, the development of high-performance bio-resins is directly linked to the advances and availability of raw materials provided by renewable platforms, which are synthesised to form the bio-based building blocks present in the polymer's molecular structure. Therefore, developing renewable bio-based polymers and materials derived from biosources, such as biomass-derived and by-products feedstocks and natural monomers, has become a focus of intensive research to foster and promote sustainability. However, significant challenges should be well addressed [151], namely:

1. relatively high-cost of certain biomass feedstocks and bio-refinery technologies;
2. processing, physical, mechanical and thermal properties, which are often not competitive with their petroleum-derived counterparts; and
3. the lack of universally accepted quantitative metrics on economic sustainability.

2.2.2.3 Renewable platform

One guiding principle to sustainable development is that the rate of natural resource consumption cannot exceed its regeneration rate if the system is sustainable in the long term [145,169]. This balance has encouraged a focus on renewable resources, including those derived from regenerable biomass, as feedstocks for the next generation of plastics. For bio-derived feedstocks, the rate and time scale of CO_2 sequestration can, in principle, be in balance with the use and release, resulting in an overall "neutral" carbon footprint. This carbon footprint is in contrast with the carbon cycle for petroleum feedstocks, in which the rate and time scale of CO_2 sequestration (millions of years) is much slower than the use and release (1–10 year time frame) [170].

Recent researches suggest that the development of more sustainable thermosets should be based on the use of raw materials that are renewable and/or less toxic to human health and with lower carbon emissions [109,171,172]. In this context, there are two approaches for preparing bio-based polymers [173], in which (1) biomass resources are converted to monomers or key intermediates via large-scale biochemical processes (*i.e.*, they are bio-refined), and (2) biomass resources are directly used as ingredients in polymer synthesis [174,175].

Table 2.5: Bio-based monomers to thermoset applications.

Monomer	**Source**	**Application**
Furfural	Bagasse, corn cobs *etc.*	Phenolics
Soybean oil	Soybean by-products	Polyesters and epoxies
Linseed oil, pine oil *etc.*	Vegetable oils	Epoxies
Lignin and tannin	Biomass	Polyesters, epoxies, *etc.*
Terpenes and rosins	Conifer plants	Thermosets
Citric acid	Citrus fruits by-product	Polyesters
Castor oil	*Ricinus communis*	Polyurethanes
Cardanol	*Anacardium occidentelle*	Thermosets

Natural polymers, such as cellulose, hemicellulose, and lignin, are among the most abundant sources of renewably sourced carbon [176]. The properties of these raw materials can be enhanced by physical or chemical modifications, making them valuable materials for various applications. By contrast, molecules including vegetable oils, terpenes, and CO_2 are also relevant renewable raw materials. These raw materials can be further converted to value-added chemicals in integrated bio-refineries, in analogy with the current petroleum refineries practice. Table 2.5 gives examples of transformation chains of bio-based monomers to thermoset polymer applications.

Bio-refinery products, such as alcohols and glycerol, are also helpful monomers for sustainable polymers. Among the different biomass sources for bio-refinery, the lignocellulosic is attractive because of the availability of feedstock; for example, agro-food wastes, or even paper wastes, are available at competitive prices, and the use of these feedstocks does not compete with the food supply.

According to Zhang [145], as the chemical composition of renewable resources is quite different from those derived from petroleum-based resources, new scientific and technological innovations have been developed from more efficient catalytic strategies to convert these resources into chemical platforms, monomers, polymers, and products that can be produced economically on a sufficiently large scale for commodity materials.

Finally, vegetable biomass is generated from CO_2 and H_2O using sunlight as the energy source, producing O_2 as a subproduct. The primary products formed are cellulose, hemicellulose, and lignin. Besides those components, plants can also elaborate energy storage products, such as lipids, sugars, starches, and other products, such as terpenes (relatively rich in hydrogen and carbon) found in essential oils, which can be transformed into components of resins [177].

2.2.3 Manufacturing techniques

Sustainable composites (or biocomposites), used for structural applications in construction, must be developed to match the best property-sustainability-processing correlation, depending on the target end use application. When manufacturing FRP biocomposites, it should be borne in mind that their suitability to the structural design is mainly influenced by the constituent materials (matrix and fibres), composition and fibre architecture. Different combinations chosen from the range of fibres and matrices can increase the sustainable potential of the product, especially, from raw materials incorporated into the FRP biocomposite (which can be partially or fully derived from renewable resources). Furthermore, hybrid biocomposites containing more than one type of fibre reinforcement or matrix are also currently being developed to provide better properties and also lead to substantial cost savings due to the incorporation of cheaper raw materials [178,179].

Efficiency in manufacturing of structural composites has been addressed, specifically for the aerospace, automotive, marine and energy industries, which require advanced manufacturing technologies in terms of shape, accuracy, lead time, energy consumption and production costs [180]. More recently, technologies are being developed to be applied in the manufacturing of advanced composites [181–183], for example: automated tape layup (ATL), automated fibre placement (AFP), continuous tow shearing (CTS), filament winding (FW), through-thickness reinforcement (TTR), tailored fibre placement (TFP), automated preforming cell (APC) and overmoulding.

Discontinuous-fibre composites have also been studied to provide another alternative to increase the sustainability of composites manufacturing [184,185]. Furthermore, a response that will certainly come over the next few years, specially because of the advent of the end-of-life of FRP components from wind turbines and civil structures, is the beginning of an assembly between conventional and newer manufacturing techniques, focusing on recycling and reusing composite materials [186–190]. However, despite recent efforts to increase sustainability in composites manufacturing process, FRP composites used in structural applications in construction, such as (i) CFRP strips and tendons for structural strengthening and reinforcement; (ii) pultruded GFRP profiles used as structural members; (iii) FRP composite rebars for concrete, and; (iv) FRP composite laminates for sandwich panels, are still largely manufactured by conventional techniques [191–194].

FRP composites used in structural construction applications are typically produced by the following techniques: (1) hand lay-up (or wet lay-up), (2) vacuum infusion, and (3) pultrusion. Composites produced by these techniques usually have less complex geometries when compared with structural shapes applied in airplanes, automobiles and wind turbines. In fact, the increase in sustainability associated to the production of FRP biocomposites must address first existing (conventional) manufacturing processes, due to their larger current consume, in order to become more competitive, to boost and spread its use more quickly in structural applications.

2.2.3.1 Hand lay-up

The manufacturing process known as hand lay-up involves the manual laying down of individual layers (or plies) of reinforcement fibres (which can also be applied in the form of 'prepregs') into an opened mould, and then laminating them with resin [195], using specially designed rollers to ensure that the laminate will be free from gas or air bubbles, see Figure 2.12.

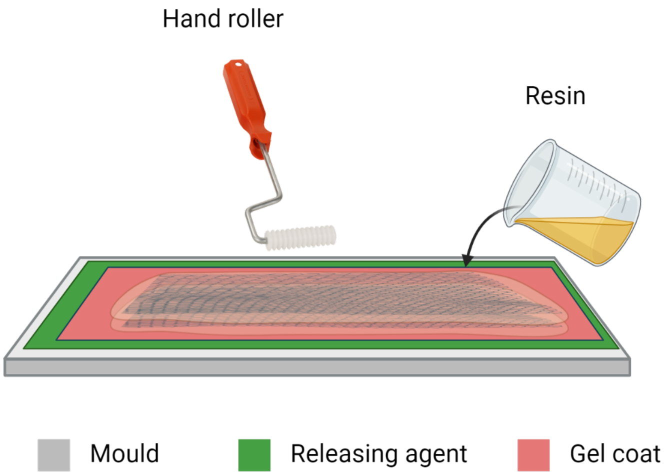

Figure 2.12: Hand lay-up technique.

Hand lay-up can be applied in a plant or on-site, and the composite part will form into the shape and dimensions of the mould or surface in which it was manufactured. When the manufacturing is made in a plant, FRP elements are produced inside a opened or closed mould, being removed after curing. However, on-site manufacturing is often used for construction applications, in which FRP elements are directly applied over the surface of an existing structural element that is intended to be strengthened. Here, the main difficulty or concern consists of guaranteeing an adequate connection between the FRP element and the structural element to be strengthened [191].

Hand lay-up is highly adaptable to new parts and design changes. Its composition variability (such as fibre and resin features, and resin/fibre ratio), latitude in size, shape, and design possibilities (reinforcement direction), enables a manufactured part by lay-up to be tailored to structurally and economically fit its desired function. Furthermore, large parts can be produced with minimum tooling cost and start-up lead time, because semi-skilled workers are needed and are easily trained, and any material that will hold its shape can be used as a mould form [196]. By contrast, product uniformity is difficult to maintain within a single part or from one part to another. This process results in only one finished surface (the reverse surface is usually rough), and parts often have low fibre fraction volume.

The process is also labour-intensive and longer cure times are required, resulting in low production rates. Furthermore, quality is related to the skills of the operator and as with other manual processes, there is also potential for discrepancies between parts caused by human variation [197,198].

Human interference on lay-up features may become more evident when the technique is performed on retrofitting concrete structures, especially, shear and flexural strengthening of I- and T-beams (which has non-obtuse edges) using hand-layup sheets and fabrics of carbon or glass fibres, and reinforced concrete column FRP wrapping. However, despite these drawbacks, the adaptability provided by hand lay-up means it remains a key part of the composites industry, providing one of the most important manufacturing methods for many applications [191,195,199].

The design of FRP composites produced by hand lay-up involves more than determining the dimension and shape of the FRP; it also involves paying attention to what happens to the mix in or on the mould, especially what happens to the fibres in the mix, and which properties can be obtained. The fibre impregnation and curing kinetics of the part involves the choice of the resin system to be used in the hand lay-up process. Further performance properties, processing and handling characteristics, such as gel time, shrinkage, exothermic peak, viscosity, and thixotropy, are also relevant considerations in the definition of the resin to be specified. In addition to the materials used, an execution (manufacturing) plan must be adopted to ensure its suitability for the project. The following are a set of procedures described in the literature for hand lay-up technique [5,191,196, 200]:

- **Mould preparation:** starts with a thorough buffing and polishing of an (unused) mould. For strengthening concrete structures, removing unwanted residues, roughening and cleaning the surface are necessary steps to guarantee the composite-substrate adhesion and plies uniformity;
- **Releasing agent:** after mould preparation, for production in plant, a releasing material (such as polyvinyl alcohol (PVA)) is applied to the mould – usually three or four coats applied in perpendicular directions – avoiding the part from being permanently bond of the mould surface. A proper mould preparation will enable the smooth separation of the FRP part from the mould. If this operation is neglected or if short cuts are taken, product appearance will be jeopardised, and if a part hangs-up in the mould and cannot be removed, both the part and the mould might have to be scrapped. For on-site manufacturing (retrofitting), a releasing agent is not applied on the (concrete) surface to be strengthened;
- **Gel coat:** normally, a polyester, mineral filled, pigmented, non-reinforced layer or coating is applied first to the mould; it will become the outer surface of the laminate when completed. This produces a decorative, high protective, glossy, coloured

surface, which requires little or no subsequent finishing. Furthermore, this layer is useful for protection from external environmental agents and it improves the service life of the product. Usually this gelcoat is about 0.5 mm thick;

- **Lamination of plies:** after gel coating curing, layers of fibres (in the form of mat, woven fabric or roving) are laid and spread manually onto the mould. In this phase, resin and catalyst are either premixed in a bucket, and then the catalysed resin is poured (or applied with a brushed) manually over the previously stretched plies. The operator facilitates the penetration of the resin and removes the air bubbles inside the plies with the hand roller (squeegee), by compacting it against the mould. Cored laminates (where a layer of end-grain balsa, foam, plywood, or another material, is sandwiched between layers of resin-saturated fibre) are attainable with either hand lay-up, and additional layers of woven rovings (or mats) can then be applied until the total design thickness is achieved;
- **Curing time:** subsequently, the process of curing starts thanks to an exothermic reaction between catalyst and resin, hardening the FRP composite, at ambient or elevated temperature (depending of the catalyst system). The degree of curing of the different layers can be improved by means of elevated temperature, pressure and/or vacuum. However, in most civil engineering structural applications, the hand lay-up technique is used without application of external pressure, with the curing process taking place at ambient temperature; and
- **Demoulding:** after curing either at room temperature or at some specific temperature, the produced composite part is taken out and further processed (for example, under post-curing) to obtain improved mechanical and thermophysical properties.

2.2.3.2 Vacuum infusion

Vacuum infusion is a closed mould resin infusion production process that presents similarities with resin transfer moulding (RTM). The most striking difference is that the fully enclosing, two-part rigid moulds used in RTM are replaced with a one-part rigid mould sealed with a vacuum bag. The reinforcement is laid on the rigid mould with a layer of removable flow-enhancement medium, used to reduce fill time, along with peel ply to facilitate disposal. Inlets and outlets are placed, and the vacuum bag is sealed to the rigid mould using sealant tape. Air is extracted from the cavity to compact the reinforcement layers between the vacuum bag and the mould and subject resin to a pressure differential – see Figure 2.13. As a result, the resin flows through the compacted fibre reinforcement layers [201].

When dry reinforcements are placed in an open mould, the fibres' quantity and orientation can also be precisely controlled. However, the vacuum infusion process (closed mould) allows manufacturing parts with low porosity and a final fibres volume typically higher than

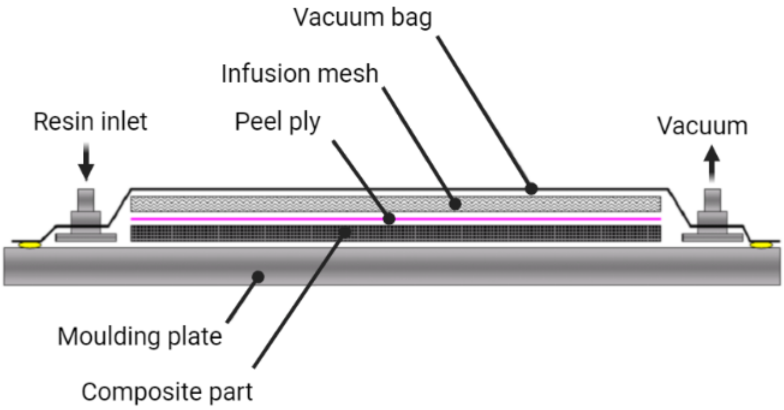

Figure 2.13: Vacuum infusion technique [202].

that obtained using an open mould. Through variations in the processing parameters and construction of moulds, there is a high number of different designations and patents for liquid composite moulding (LCM) processes, which can be classified in four main categories, depending on the mould construction and resin injection system, namely: (1) RTM, (2) compression RTM (CRTM), (3) RTMLight, and (4) resin infusion (also known as vacuum assisted resin transfer moulding (VARTM) or vacuum assisted resin infusion (VARI)). These different systems are adapted to the manufacturing scenario, to provide a cost-effective solution. For large parts or small series, the use of a single-sided mould and vacuum bag allows savings on the tooling cost [192].

Vacuum infusion process also allows to reduce the harmful volatile organic compounds generated by thermoset resins, making them compliant with the stringent new environmental standards put in place in many countries. A typical vacuum set-up with its various elements, and the functions of the different ancillary materials, are described below:

- **Vacuum bag:** the principal element to provide the airtightness needed for evacuating and compacting the lay-up is a plastic film (vacuum foil). This film is used to cover the entire setup, creating the vacuum bag. The film material must be strong enough to resist mechanical wear and must remain sufficiently elastic throughout the manufacturing process to adapt to the component geometry;
- **Sealant tape:** the vacuum foil is sealed at the edges by attaching it to the mould surface with a sealant material. Typical sealants are available as tapes of rubber-like adhesive material. As a rule, the areas of the mould to which the sealant tape is to be applied should be free of release agent; in practice, these areas are often temporarily covered with adhesive tape when applying the release agent. Also, when installing the vacuum bag, sufficient excess foil should be provided to avoid tears at the edges and curvatures of the composite part. This can be obtained by including additional loops of sealant together with a fold in the vacuum foil (sometimes called ‘duck feet’);

- **Vacuum infrastructure:** the evacuation of the vacuum bag is realised by vacuum pumps connected via tubes and hoses to intake valves in the vacuum set-up. The intakes must be positioned either in the vacuum bag, wherein the vacuum foil must be perforated to provide a passage. To further distribute the airflow efficiently, installing additional channels underneath the vacuum bag is usually necessary, *e.g.*, by stacking up several narrow layers of breather fabric;
- **Breather:** typically, the entire setup is covered with a layer of breather fabric, consisting of a perforated fabric or fleece textile, which is sufficiently rigid to resist crushing under pressure, thus maintaining its porous structure to airflow under all process conditions. In addition, the presence of the breather will allow for homogeneous pressure distribution and thereby homogeneous compaction of the layers over the entire surface of the setup; and
- **Release film:** a release film can be inserted between the cured composite part and the ancillary materials in the setup to prevent adhesion between them. Release films are treated such that their surface will not adhere to the resin. Typically, this release film is perforated in order to allow resin bleed to the breather. In addition, a layer of peel-ply is usually laid over the reinforcement, allowing for easy separation of the part from the consumables and providing uniform surface finish of the produced part.

Once the bagging is finished, it is advisable to conduct an airtightness test on the entire setup before curing. Pressure leaks due to damage in the vacuum bag itself (such as cuts, torn-off folds or wrinkles, or perforations), at the vacuum bag sealant tape or at the valves and tubes can usually be repaired prior to curing, if detected in time. However, if not detected, they can lead to substantial defects in the cured component. The airtightness of the vacuum setup can be easily verified. First, the setup is evacuated. Then, the vacuum pump is disconnected. By monitoring the rise in pressure inside the setup, the tightness of the system can be quantified and evaluated. The setup would only be released for cure if the tightness complies with predefined requirements (*e.g.* loss in vacuum not exceeding 50 mbar during a leak test of at least 5 min). As the vacuum bag employed during the process provides minimal rigidity, the preform thickness will vary in relation to the pressure inside the cavity, and so will the reinforcement permeability, which is governed by the local reinforcement architecture.

During manufacture by the vacuum infusion process, the operator typically has little control over the advancement of the flow. The controllable parameters are the placement of the inlets and vents, the positioning and dimensions of the flow channels, injection and vent pressure, and the temperature of the mould (for control of viscosity and cure kinetics of the resin); the type of reinforcement and its orientation is also relevant, but these will most often be decided based on the functional and structural design of the FRP product.

Successful process development by trial and error requires experience and can be long and expensive. Reduction of development costs requires a good understanding of the physics of the process, and the process designer can benefit from developing an accurate simulation tool. While simulation can significantly aid the design process, simulation can also highlight the areas of the mould requiring extra attention or help defining where to place the monitoring equipment to determine the end of filling. Some flow sensing equipment can also monitor the resin's progression in the mould directly and can be used in conjunction with fast process simulation tools to automate injection gate control.

2.2.3.3 Pultrusion

Pultrusion consists of an automated continuous and cost-effective manufacturing process that allows converting directly the resin and the reinforcing fibres into FRP composites with constant cross-section [203]. During manufacturing, FRP pultruded parts are under sufficient tension while they cure. This aligns the fibres well and results in a compact, high fibre content product, allowing to reach a very high strength-to-weight ratio. The process has a low labour content and a high raw material conversion efficiency, where about 80-90% of the cost of pultruded composites comes from the raw materials it uses, since it is a continuous processing technique [204]. The amortised machine cost and the labour to run pultrusion machines correspond only to a small portion of the total factory costs. Together, these features explain, in part, why pultrusion is one of the manufacturing techniques most often used to produce commercial FRP composite parts for structural applications in construction.

The following products are typically manufactured by pultrusion: (i) CFRP strips or laminates; (ii) GFRP profiles of open-form (such as I, H or U shapes) or closed-form (tubular) cross-sections; and (iii) multi-cellular closed-form panels with internal webs [191].

In the traditional pultrusion process, an open bath system filled with resin is used for fibre impregnation before entering the heating die, and the resin in excess is removed when the fibres pass through preforming guides – see Figure X. However, in modern pultrusion machines, the fibres enter dry directly into an injection chamber (an integral part of the die), being impregnated with the resin supplied under pressure. This new resin injection system enables a more accurate control of the fibres position, providing higher material uniformity, and allows for a higher degree of fibre impregnation [205]. Changes in matrix composition can also be introduced more rapidly during the process. Due to the absence of an open bath system, resin injection reduces the evaporation of solvents from the matrix, thereby providing a healthier work environment and reducing pollutant emissions.

Regardless of whether the impregnation process is an open bath or injection system, as the wet reinforcement travels in a short length through the heated metallic die (typically, 0.5 m to 1.0 m), curing of the matrix occurs at high temperatures varying from 90 °C to 180 °C, depending on the matrix system used. As the degree of curing increases, the FRP composite shrinks and separates from the internal walls of the die, exiting the die as a

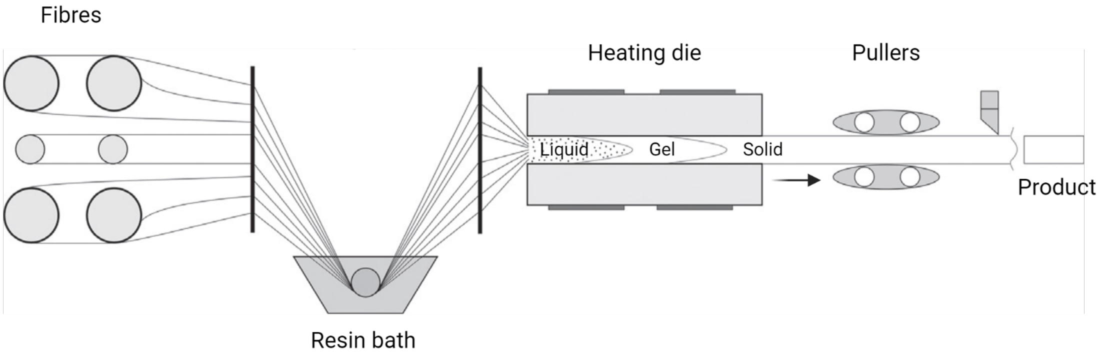

Figure 2.14: Pultrusion technique (open bath system) [206].

finished product. The cured composite is then permanently pulled in the main direction of the reinforcement by reciprocating pullers, synchronised to provide a constant speed. At the end of the assembly line, an automated and moving cut-off saw is used to obtain preset lengths of product (often limited by transportation requirements), without stopping the manufacturing process. The pultrusion rates of production greatly depend on the type of machine used and also on the shape of the cross-section being produced. On average, a current cross-section may be produced at a rate of $2\,\mathrm{m}/\,\mathrm{min}$.

While pultrusion machines vary in design, the process is essentially the same, and it can be divided into three main phases:

- **Fibre impregnation:** the fibre reinforcements in the form of unidirectional rovings (UDs), continuous filament mats (CFMs), and/or surface veils, are held on creel racks and fed continuously through a guiding system, which allows positioning the different reinforcement types according to a pre-established fibre architecture for each of the laminates that will constitute the pultruded part. Subsequently, these reinforcements are impregnated with a low-viscosity matrix system in a resin bath or resin injection chamber. The wetted-out reinforcement pack is then collimated into a preformed shape before entering the heating die;
- **Heating and curing:** polymerisation takes place inside the forming die, in which the part changes its state from liquid to gel and then to solid state, with the help of the heat provided by the heaters. The cured object has the shape of the cross-section to be produced, resulting in a part with predetermined shape and dimensions; and
- **Cutting:** the resin-impregnated fibre reinforcement progresses via a pulling system to the cut-off saw where the polymerised product is cut to its final length.

Pultruded profiles present high tensile, compressive and flexural strengths in the direction of the (pultrusion) axis, along which most of the reinforcing fibres are aligned. However, in transverse directions, the mechanical properties (stiffness and strength) are much lower and this can govern their design; this can be improved through the use of fabrics or non-fabrics with fibres oriented in the transverse direction. In general, industrial pultruded

GFRP parts contain UD rovings and CFM layers impregnated by a thermosetting resin system [206]. By contrast, CFRP laminates, usually comprising fibres in a preferred direction, are produced by pultrusion impregnating unidirectional carbon fibre rovings with epoxy resins without the use of CFM or surface veils.

In spite of recent studies about the possible use of thermoplastics (even recycled) in pultrusion [207–210], the pultrusion process is largely dominated by the use of thermosetting resins, because of their easy adhesion to reinforcements and more efficient impregnation of fibres due to their low viscosity.

Unsaturated polyester and vinylester are some of the most common resins used to manufacture pultruded FRP composites [211]. Phenolic and epoxy resins are also used in structural applications in construction; however, they are more frequently used when there are specific requirements concerning fire behaviour or resistance to aggressive environments, respectively. FRP composites based on epoxy resins are often more expensive compared to other resin matrix systems. All these systems have features, for example, chemical shrinkage and exothermic reactivity, which are crucial for the pultrusion process. The higher chemical polymerisation reactivity presented by polyester resins provides faster curing during processing than epoxy or vinylester, enabling higher pulling speeds to be used for manufacturing of pultruded FRP composites. Moreover, in polyesters the gelation occurs at lower conversion rates or degree of curing values, when compared to epoxies.

2.3 Bio-based composite applications

2.3.1 Strengthening of concrete structures

In structural applications, FRPs composites comprising synthetic fibres in a bio-based matrix can perform similarly to traditional composites. For example, recent studies reported the use of bio-based thermoset FRPs composites for external strengthening of concrete members.

McSwiggan and Fam [212] carried out flexural tests on RC beams strengthened in bending using FRP sheets and comprising two bio-based resin types, namely: (i) an epoxidized pine (EP) oil resin blend, and (ii) a furfuryl alcohol resin based on raw materials derived from corn cobs and sugarcane. The bond tests using small scale notched concrete beams showed that the EP oil resin blend had comparable bond strength to conventional epoxy. Furthermore, the EP oil resin also provided similar results to conventional epoxy in CFRP- and GFRP-strengthened full-scale beams; Figure 2.15 illustrates the failure modes that were observed in those tests. Regarding the furfuryl alcohol resin, the results showed a fragile bond when used for hand lay-up of fibres directly on the tension face of concrete beams (*i.e.*, bond-critical application) due to concrete alkalinity. By contrast, an excellent bond was observed when the furfuryl alcohol resin was used in the prefabrication of cured CFRP sheets, which were then bonded to the concrete surface using conventional epoxy adhesive. Consequently, this investigation showed that further studies on curing and surface treatments are required for furfuryl alcohol resin applications in FRP-concrete hand lay-up.

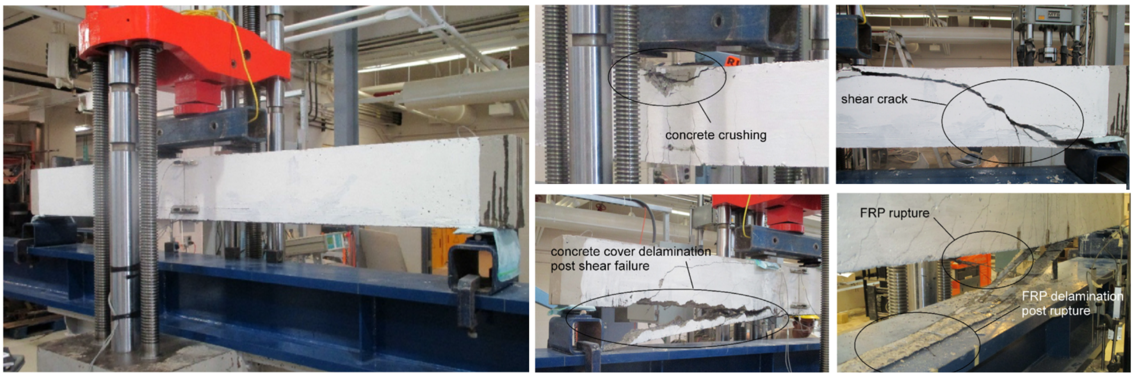

Figure 2.15: Strengthening of RC beams using externally bonded FRP sheets with bio-based matrices [212].

Eldridge and Fam [213] performed environmental tests to assess the durability of concrete cylinders wrapped with conventional epoxy-GFRP compared to bio-based-resin-GFRP (made from FA). Three control groups of concrete cylinders were included for comparison with the bio-based counterparts: (i) unconfined (i.e., without GFRP wraps), (ii) unconditioned bio-based-resin-GFRP-wrapped, and (iii) unconditioned conventional epoxy-GFRP-wrapped cylinders. The specimen configuration was intended to simulate the rehabilitation of circular concrete columns using GFRP circumferential wraps. Furthermore, conditioned specimens were tested under axial compression, at 23, 40, and 50 ℃, after various periods (29, 97, 182 and 300 days) of exposure and compared to counterparts kept at room temperature as well as to unconfined control specimens.

The results showed that unconditioned control epoxy- and bio-based-resin-GFRP had the same confinement (strengthening ratio) to the concrete cylinders, suggesting that glass fibres govern the axial strength increase independently from the type of resin. Conditioned epoxy- and bio-based-resin-GFRP specimens showed a slight difference in strength after 300 days, which was considered statistically significant only at 23 ℃, but not at 40 ℃ and 55 ℃, showing that the strength at higher temperatures over the long-term exposure of the bio-based resin was similar to its epoxy counterpart, which is a significant parameter for structural applications. However, more studies about the possibility of degradation of this bio-based resin due to fungus or rodent attacks were recommended.

Foruzanmehr *et al.* [214] studied the degradation mechanisms of GFRP composites produced from bio-based resins for external rehabilitation of structures. A comparative study was carried out between two types of resins, namely: (i) FA-based resin and (ii) conventional epoxy resin. Mechanical, physical-chemical and environmental degradation tests were carried out. The results showed that FA resins should have chemical formulations compatible with the fibres - those resins have undergone more significant hydrolysis compared to epoxy due to higher porosity, reducing more significantly the mechanical capacity of the produced composites.

2.3.2 Pultruded profiles and FRP laminates

Exploratory studies have also shown the potential of bio-based resins as matrices for manufacturing pultruded FRP laminates. For example, Ma *et al.* [215,216] developed a bio-based resin for pultrusion and studied more suitable processing parameters for processing with bio-based resins. Among the main results, it was found that the short-term mechanical properties of pultruded profiles manufactured with the bio-based resin were comparable to those of conventional pultrusion laminates.

McIsaac and Fam [217] tested three blends of bio-based resins with a conventional epoxy. The bio-content varied from 10 to 41% by weight in the final mixtures of resins, comprising: (i) a product derived from wood and vegetables, (ii) a liquid from cashew nutshell liquid (CNSL), and (iii) a epoxidized linseed oil (ELO). The samples were produced by hand lay-up with glass and carbon reinforcement fibres and were evaluated in relation to their mechanical properties and lap splice length between laminates. The mixture between epoxy and bio-based resin derived from wood and vegetables with 41% bio-content showed the best results, similar to those of conventional FRP-epoxy samples.

2.3.3 Sandwich panels

Bio-based resins have also been studied as matrices for FRP face sheets of sandwich panels. Mak *et al.* [218] evaluated the mechanical properties of sandwich panels with face sheets of bio-based resins derived from pine oil. Figure 2.16 presents the experimental setup for testing the sandwich panel manufactured with the bio-based resin.

The reinforcing fibres were impregnated with epoxy resin by hand application over the foam, and then the system was sealed with a bag typically used for vacuum application. Various failure mechanisms were verified under flexural loading, and the results showed that the flexural strength of bio-resin panels was 23% lower than that of panels with conventional epoxy resin. Such performance values confirm the high potential of bio-based resins; however, the results also indicated the need for improvements in their chemical structures and fibre interaction envisaging their broad applicability.

2.3.4 Construction of bridges

Smits [219] analysed the application of FRP composites in the design of bridges. The author discussed the challenges and opportunities of this relatively new material, for both architecture and engineering, and the survey of recent structural solutions in FRP included

Figure 2.16: Experimental set-up of sandwich panel manufactured from bio-based resin [218].

bio-composites. In this context, a pedestrian bridge was built in Eindhoven from linen fibres, bio-based resins derived from vegetable oils, poly(lactic acid) foam and natural cork, as illustrated in Figure 2.17. Aspects such as the carbon footprint and the treatment of plant fibres were briefly discussed; however, since this was one of the first structures built and tested with bio-composites in civil engineering applications, it is still necessary to deepen the knowledge about the mechanical behaviour and durability of these materials.

2.4 Concluding remarks

The results obtained in recent studies concerning bio-based resins and bio-composites show quite clearly that they have high potential for structural applications in civil engineering. Switching to renewable sources will increase the eco-efficiency of structural composites that are already in use and will provide an innovative and significant response regarding the construction industry's sustainability. However, some aspects of bio-resins and their respective bio-composites require further investigation, such as (i) the mechanical and thermomechanical properties, (ii) the processing, (iii) the performance of the fibre-matrix interface, and (iv) the long-term durability.

As a result, there is still space to increase the eco-efficiency of bio-resins and bio-composites, evaluating: (i) different formulations and blends of existing commercial bio-resins, (ii) the synthesis of new resins based on raw materials derived from renewable sources, capable of competing with petroleum-based products in the coming years, and (iii) the need to adjust bio-resins to conventional processing techniques, such as vacuum infusion and pultrusion, in order to facilitate further manufacturing on an industrial scale and target the main current applications of composites in the construction industry.

Figure 2.17: Bio-composite footbridge in Eindhoven across the river Dommel [219], manufactured from flax fibres, bio-based resin, poly(lactic acid) foam, and natural cork.

2.5 References

[1] Bob Geldermans, Peter Luscuere, Sabine Jansen, and Martin Tenpierik. Beyond Cities: Materialen, producten & circulair bouwen. *TVVL Magazine*, 45(1):22–25, January 2016.

[2] Rijk Blok, Joris Smits, Rafail Gkaidatzis, and Patrick Teuffel. Bio-based composite footbridge: Design, production and in situ monitoring. *Structural Engineering International*, 29(3):453–465, 2019.

[3] J.F. Davalos, P. Qiao, and L. Shan. Advanced fiber-reinforced polymer (FRP) structural composites for use in civil engineering. In Hwai Chung Wu, editor, *Advanced Civil Infrastructure Materials*, Woodhead Publishing Series in Civil and Structural Engineering, chapter 4, pages 118–202. Woodhead Publishing, 2006.

[4] DuPont^{TM}. Technical Guide for Kevlar® Aramid Fiber, 2019.

[5] Lawrence C. Bank. *Composites for Construction: Structural Design with FRP Materials*. John Wiley & Sons, Inc., 1st edition, 2006.

[6] Elizaveta Martynova and Holger Cebulla. Glass fibers. In Boris Mahltig and Yordan Kyosev, editors, *Inorganic and Composite Fibers*, The Textile Institute Book Series, chapter 7, pages 131–163. Woodhead Publishing, 2018.

[7] Brahim Benmokrane, Mathieu Robert, and T. Youssef. Reinforcement of concrete using fibre-reinforced polymer composites. In Vistasp M. Karbhari, editor, *Durability of Composites for Civil Structural Applications*, Woodhead Publishing Series in Civil and Structural Engineering, chapter 11, pages 225–246. Woodhead Publishing, 2007.

[8] James L. Thomason. Glass fibre sizing: A review. *Composites Part A: Applied Science and Manufacturing*, 127:105619, 2019.

[9] E. K. Drown, H. Al Moussawi, and L. T. Drzal. Glass fiber 'sizings' and their role in fiber-matrix adhesion. *Journal of Adhesion Science and Technology*, 5(10):865–881, 1991.

[10] Aref Cevahir. Glass fibers. In M. Özgür Seydibeyoğlu, Amar K. Mohanty, and Manjusri Misra, editors, *Fiber Technology for Fiber-Reinforced Composites*, Woodhead Publishing Series in Composites Science and Engineering, chapter 5, pages 99–121. Woodhead Publishing, 2017.

[11] Ruben D. B. Sevenois, David Garoz Gómez, Erik C. Verboven, Siebe W. F. Spronk, Francisco A. Gilabert, Mathias Kersemans, Lincy Pyl, and Wim Van Paepegem. Multiscale approach for identification of transverse isotropic carbon fibre properties and prediction of woven elastic properties using ultrasonic identification. *Composites Science and Technology*, 168:160–169, 2018.

[12] Zijian Wu, Hongyu Cui, Lei Chen, Dawei Jiang, Ling Weng, Yingyi Ma, Xuejiao Li, Xiaohong Zhang, Hu Liu, Ning Wang, Jiaoxia Zhang, Yong Ma, Mingyan Zhang, Yudong Huang, and Zhanhu Guo. Interfacially reinforced unsaturated polyester carbon fiber composites with a vinyl ester-carbon nanotubes sizing agent. *Composites Science and Technology*, 164:195–203, 2018.

[13] Weiwei Jiao, Yemeng Cai, Wenbo Liu, Fan Yang, Long Jiang, Weicheng Jiao, and Rongguo Wang. Preparation of carbon fiber unsaturated sizing agent for enhancing interfacial strength of carbon fiber/vinyl ester resin composite. *Applied Surface Science*, 439:88–95, 2018.

[14] Weiwei Jiao, Wenbo Liu, Fan Yang, Long Jiang, Weicheng Jiao, and Rongguo Wang. Improving the interfacial strength of carbon fiber/vinyl ester resin composite by self-migration of acrylamide: A molecular dynamics simulation. *Applied Surface Science*, 454:74–81, 2018.

[15] Andrés A. Torres-Acosta. Galvanic Corrosion of Steel in Contact with Carbon-Polymer Composites. I: Experiments in Mortar. *Journal of Composites for Construction*, 6(2):112–115, 2002.

[16] M. N. Alias and Richard Brown. Damage to composites from electrochemical processes. *Corrosion*, 48(5):373–378, 1992.

[17] Yong Bai and Wei-Liang Jin. Marine Composite Materials and Structure. In Yong Bai and Wei-Liang Jin, editors, *Marine Structural Design*, chapter 2, pages 19–37. Butterworth-

Heinemann, Oxford, Second Edition edition, 2016.

[18] Darshil U. Shah, Peter J. Schubel, Peter Licence, and Mike J. Clifford. Hydroxyethylcellulose surface treatment of natural fibres: the new twist in yarn preparation and optimization for composites applicability. *Journal of Materials Science*, 47(6):2700–2711, 2012.

[19] Maya Jacob John and Rajesh D. Anandjiwala. Recent developments in chemical modification and characterization of natural fiber-reinforced composites. *Polymer Composites*, 29(2):187–207, 2008.

[20] Umar Nirmal, Jamil Hashim, and M.M.H. Megat Ahmad. A review on tribological performance of natural fibre polymeric composites. *Tribology International*, 83:77–104, 2015.

[21] Ulrich Riedel and Jörg Nickel. *Applications of Natural Fiber Composites for Constructive Parts in Aerospace, Automobiles, and Other Areas*, chapter 1, page 11. American Cancer Society, 2005.

[22] Sunil Kumar Ramamoorthy, Mikael Skrifvars, and Anders Persson. A Review of Natural Fibers Used in Biocomposites: Plant, Animal and Regenerated Cellulose Fibers. *Polymer Reviews*, 55(1):107–162, 2015.

[23] Azam Ali, Khubab Shaker, Yasir Nawab, Madeha Jabbar, Tanveer Hussain, Jiri Militky, and Vijay Baheti. Hydrophobic treatment of natural fibers and their composites — A review. *Journal of Industrial Textiles*, 47(8):2153–2183, 2018.

[24] Daniel Gay. *Composite materials: design and applications*, volume 1. CRC Press Taylor & Francis Group, Boca Raton, 3 edition, 2014.

[25] Mei-po Ho and Hao Wang and Joong-Hee Lee and Chun-kit Ho and Kin-tak Lau and Jinsong Leng and David Hui. Critical factors on manufacturing processes of natural fibre composites. *Composites Part B: Engineering*, 43(8):3549–3562, 2012.

[26] Mohd. Ramesh. Kenaf (Hibiscus cannabinus L.) fibre based bio-materials: A review on processing and properties. *Progress in Materials Science*, 78-79:1–92, 2016.

[27] Kin tak Lau, Pui yan Hung, Min-Hao Zhu, and David Hui. Properties of natural fibre composites for structural engineering applications. *Composites Part B: Engineering*, 136:222–233, 2018.

[28] M. P. Staiger and N. Tucker. Natural-fibre composites in structural applications. In Kim L. Pickering, editor, *Properties and Performance of Natural-Fibre Composites*, Woodhead Publishing Series in Composites Science and Engineering, chapter 8, pages 269–300. Woodhead Publishing, 1st edition, 2008.

[29] Takashi Nishino, Kiyofumi Takano, Katsuhiko Nakamae, Kiyoshi Saitaka, Shyuichi Itakura, Jun'ichi Azuma, and Keizo Okamura. Elastic modulus of the crystalline regions of cellulose triesters. *Journal of Polymer Science Part B: Polymer Physics*, 33(4):611–618, 1995.

[30] Wei Chen, Gary C. Lickfield, and Charles Q. Yang. Molecular modeling of cellulose in amorphous state part ii: effects of rigid and flexible crosslinks on cellulose. *Polymer*, 45(21):7357–7365, 2004.

[31] Wei Chen, Gary C. Lickfield, and Charles Q. Yang. Molecular modeling of cellulose in amorphous state. Part I: model building and plastic deformation study. *Polymer*, 45(3):1063–1071, 2004.

[32] Alan Howard Cottrell, John Desmond Bernal, Cecil Edwin Henry Bawn, Alan Howard Cottrell, and Frederick Charles Frank. Strong solids. *Proceedings of the Royal Society of London. Series A. Mathematical and Physical Sciences*, 282(1388):2–9, 1964.

[33] Christophe Baley. Analysis of the flax fibres tensile behaviour and analysis of the tensile stiffness increase. *Composites Part A: Applied Science and Manufacturing*, 33(7):939–948, 2002.

[34] Stephen J. Eichhorn, R. J. Young, Richard J. Davies, and Christian Riekel. Characterisation of the microstructure and deformation of high modulus cellulose fibres. *Polymer*, 44(19):5901–5908, 2003. In Honour of Ian Ward's 75th Birthday.

[35] Lorna J. Gibson. The hierarchical structure and mechanics of plant materials. *Journal of The Royal Society Interface*, 9(76):2749–2766, 2012.

[36] Yan Li, Yiu-Wing Mai, and Lin Ye. Sisal fibre and its composites: a review of recent developments. *Composites Science and Technology*, 60(11):2037–2055, 2000.

[37] Luke CoDyre, Kenneth Mak, and Amir Fam. Flexural and axial behaviour of sandwich panels with bio-based flax fibre-reinforced polymer skins and various foam core densities. *Journal of Sandwich Structures & Materials*, 20(5):595–616, 2018.

[38] Kim Louise Pickering, Mohd Ghazali Aruan Efendy, and Tan Minh Le. A review of recent developments in natural fibre composites and their mechanical performance. *Composites Part A: Applied Science and Manufacturing*, 83:98–112, 2016. Special Issue on Biocomposites.

[39] Omar Faruk, Andrzej K. Bledzki, Hans-Peter Fink, and Mohini Sain. Biocomposites reinforced with natural fibers: 2000–2010. *Progress in Polymer Science*, 37(11):1552–1596, 2012. Topical Issue on Polymeric Biomaterials.

[40] Jochen Gassan and Andrzej K. Bledzki. Possibilities for improving the mechanical properties of jute/epoxy composites by alkali treatment of fibres. *Composites Science and Technology*, 59(9):1303–1309, 1999.

[41] Hazizan Md. Akil, Mohd Firdaus Omar, Adlan Akram M. Mazuki, Sahnizam Safiee, Zainal Ariffin M. Ishak, and Azhar Abu Bakar. Kenaf fiber reinforced composites: A review. *Materials & Design*, 32(8):4107–4121, 2011.

[42] Seema Jain, Rakesh Kumar, and U. C. Jindal. Mechanical behaviour of bamboo and bamboo composite. *Journal of Materials Science*, 27(17):4598–4604, 1992.

[43] Stefano Castegnaro, Chiara Gomiero, Cristiano Battisti, Matteo Poli, M. Basile, P. Barucco, U. Pizzarello, Marino Quaresimin, and Andrea Lazzaretto. A bio-composite racing sailboat: Materials selection, design, manufacturing and sailing. *Ocean Engineering*, 133:142–150, 2017.

[44] Mohd. Ramesh, Palanikumar Kayaroganam, and Konireddy Hemachandra C. Reddy. Plant fibre based bio-composites: Sustainable and renewable green materials. *Renewable and Sustainable Energy Reviews*, 79:558–584, 2017.

[45] Alain Bourmaud, Johnny Beaugrand, Darshil U. Shah, Vincent Placet, and Christophe Baley. Towards the design of high-performance plant fibre composites. *Progress in Materials Science*, 97:347–408, 2018.

[46] A. K. Mohanty, M. Misra, and G. Hinrichsen. Biofibres, biodegradable polymers and biocom-

posites: An overview. *Macromolecular Materials and Engineering*, 276-277(1):1–24, 2000.

[47] Dipa Ray and Sunanda Sain. Plant fibre reinforcements. In Dipa Ray, editor, *Biocomposites for High-Performance Applications*, chapter 1, pages 1–21. Woodhead Publishing, 2017.

[48] Paul Wambua, Jan Ivens, and Ignaas Verpoest. Natural fibres: can they replace glass in fibre reinforced plastics? *Composites Science and Technology*, 63(9):1259–1264, 2003.

[49] W. D. Rick Brouwer. Natural Fibre Composites in Structural Components: Alternative Applications for Sisal? In Food and Agriculture Organization of the United Nations (FAO), editor, *Proceedings of a Seminar held by the Food and Agriculture Organization of the UN (FAO) and the Common Fund for Commodities (CFC)*, Rome, 2000. Common Fund for Commodities (CFC).

[50] Kalimuthu Mayandi, Nagarajan Rajini, M. Manojprabhakar, Suchart Siengchin, and Nadir Ayrilmis. Recent studies on durability of natural/synthetic fiber reinforced hybrid polymer composites. In Mohammad Jawaid, Mohamed Thariq, and Naheed Saba, editors, *Durability and Life Prediction in Biocomposites, Fibre-Reinforced Composites and Hybrid Composites*, Woodhead Publishing Series in Composites Science and Engineering, chapter 1, pages 1–13. Woodhead Publishing, 2019.

[51] Ehsan Bari, Jeffrey J. Morrell, and Asghar Sistani. Durability of natural/synthetic/biomass fiber–based polymeric composites: Laboratory and field tests. In Mohammad Jawaid, Mohamed Thariq, and Naheed Saba, editors, *Durability and Life Prediction in Biocomposites, Fibre-Reinforced Composites and Hybrid Composites*, Woodhead Publishing Series in Composites Science and Engineering, chapter 2, pages 15–26. Woodhead Publishing, 2019.

[52] Hom Nath Dhakal, Zhongyi Zhang, and Melvin O. Richardson. Effect of water absorption on the mechanical properties of hemp fibre reinforced unsaturated polyester composites. *Composites Science and Technology*, 67(7):1674–1683, 2007.

[53] Mohammad Mazedul Kabir, Hao Wang, Kin Tak Lau, and Francisco Cardona. Chemical treatments on plant-based natural fibre reinforced polymer composites: An overview. *Composites Part B: Engineering*, 43(7):2883–2892, 2012. Natural Materials in Composites Engineering.

[54] Maurice W. Chai, Simon Bickerton, Debes Bhattacharyya, and Raj Das. Influence of natural fibre reinforcements on the flammability of bio-derived composite materials. *Composites Part B: Engineering*, 43(7):2867–2874, 2012. Natural Materials in Composites Engineering.

[55] Nam K. Kim, Swagata Dutta, and Debes Bhattacharyya. A review of flammability of natural fibre reinforced polymeric composites. *Composites Science and Technology*, 162:64–78, 2018.

[56] James L. Thomason and Jose L. Rudeiros-Fernández. Thermal degradation behaviour of natural fibres at thermoplastic composite processing temperatures. *Polymer Degradation and Stability*, 188:109594, 2021.

[57] Ellen Lackey, James G. Vaughan, Kapil Inamdar, and Brittany Hancock. Statistical characterization of pultruded composites with natural fiber reinforcements – part a: Fabrication. *Journal of Natural Fibers*, 4(4):73–87, 2008.

[58] Naheed Saba, Mohammad Jawaid, M. Tahir Paridah, and Othman Al-Othman. A review on

flammability of epoxy polymer, cellulosic and non-cellulosic fiber reinforced epoxy composites. *Polymers for Advanced Technologies*, 27(5):577–590, 2016.

[59] Michael George, Michael Chae, and David C. Bressler. Composite materials with bast fibres: Structural, technical, and environmental properties. *Progress in Materials Science*, 83:1–23, 2016.

[60] Darshil U. Shah. Natural fibre composites: Comprehensive Ashby-type materials selection charts. *Materials & Design (1980-2015)*, 62:21–31, 2014.

[61] Elisabetta Monaldo, Francesca Nerilli, and Giuseppe Vairo. Basalt-based fiber-reinforced materials and structural applications in civil engineering. *Composite Structures*, 214:246–263, 2019.

[62] A. Richard Horrocks. Technical fibres for heat and flame protection. In A. Richard Horrocks and Subhash C. Anand, editors, *Handbook of Technical Textiles*, chapter 8, pages 237–270. Woodhead Publishing, Second Edition edition, 2016.

[63] Bethany Middleton. Composites: Manufacture and Application. In Vannessa Goodship, Bethany Middleton, and Ruth Cherrington, editors, *Design and Manufacture of Plastic Components for Multifunctionality*, chapter 3, pages 53–101. William Andrew Publishing, Oxford, 2016.

[64] Boris Mahltig. Basalt Fibers. In Boris Mahltig and Yordan Kyosev, editors, *Inorganic and Composite Fibers*, The Textile Institute Book Series, chapter 9, pages 195–217. Woodhead Publishing, 2018.

[65] Zhishen Wu, Xin Wang, Jianxun Liu, and Xingfen Chen. Mineral fibres: basalt. In Ryszard M. Kozłowski and Maria Mackiewicz-Talarczyk, editors, *Handbook of Natural Fibres*, Woodhead Publishing Series in Textiles, chapter 13, pages 433–502. Woodhead Publishing, second edition edition, 2020.

[66] Shibang Group (SBM). Basalt Fiber Manufacturing Process. `https://www.qualitygrinder.com/solution/basalt-fiber-manufacturing-process.html`, accessed January 2021.

[67] Global Basalt Engineering LLC. Basalt Rocks Exploration: High-Quality Basalt Fiber. `https://basalt.engineering/basalt_rocks`, accessed January 2021.

[68] A G Novitskii and M V Efremov. Technological aspects of the suitability of rocks from different deposits for the production of continuous basalt fiber. *Glass and Ceramics*, 69(11):409–412, 2013.

[69] Hetu Sheth. *A Photographic Atlas of Flood Basalt Volcanism*. Springer International Publishing AG, 1st edition, 2018.

[70] Juan Carlos Carracedo and Valentin R. Troll. North-East Atlantic Islands: The Macaronesian Archipelagos. In David Alderton and Scott A. Elias, editors, *Encyclopedia of Geology*, pages 674–699. Academic Press, Oxford, second edition edition, 2021.

[71] Kunal Singha. A Short Review on Basalt Fiber. *International Journal of Textile Science*, 1(4):19–28, 2012.

[72] CEP-FIP. FRP reinforcement in RC structures. Technical Report 40, fib Bulletin, 2007.

[73] Vivek Dhand, Garima Mittal, Kyong Yop Rhee, Soo-Jin Park, and David Hui. A short review

on basalt fiber reinforced polymer composites. *Composites Part B: Engineering*, 73:166–180, 2015.

[74] Mário de Araújo. Natural and man-made fibres: Physical and mechanical properties. In R. Fangueiro, editor, *Fibrous and Composite Materials for Civil Engineering Applications*, Woodhead Publishing Series in Textiles, chapter 1, pages 3–28. Woodhead Publishing, 2011.

[75] Valentina Lopresto, Claudio Leone, and Isabella De Iorio. Mechanical characterisation of basalt fibre reinforced plastic. *Composites Part B: Engineering*, 42(4):717–723, 2011.

[76] Vincenzo Fiore, Tommaso Scalici, Guido Di Bella, and Antonino Valenza. A review on basalt fibre and its composites. *Composites Part B: Engineering*, 74:74–94, 2015.

[77] Hafsa Jamshaid and Rajesh Mishra. A green material from rock: basalt fiber – a review. *The Journal of The Textile Institute*, 107(7):923–937, 2016.

[78] Tamás Deák and Tibor Czigány. Chemical Composition and Mechanical Properties of Basalt and Glass Fibers: A Comparison. *Textile Research Journal*, 79(7):645–651, 2009.

[79] Volkan Acar, Ferit Cakir, Elif Alyamaç, and M.Özgür Seydibeyoğlu. Basalt fibers. In M. Özgür Seydibeyoğlu, Amar K. Mohanty, and Manjusri Misra, editors, *Fiber Technology for Fiber-Reinforced Composites*, Woodhead Publishing Series in Composites Science and Engineering, chapter 8, pages 169–185. Woodhead Publishing, 2017.

[80] Hafsa Jamshaid. Basalt fiber and its applications. *Journal of Textile Engineering & Fashion Technology*, 1(6):254–255, 2017.

[81] Calvin Ralph, Patrick Lemoine, John Summerscales, Edward Archer, and Alistair McIlhagger. Relationships among the chemical, mechanical and geometrical properties of basalt fibers. *Textile Research Journal*, 89(15):3056–3066, 2019.

[82] Sandeep Kumar, Brian G. Falzon, Jeffery Kun, Emma Wilson, Georg Graninger, and Stephen C. Hawkins. High performance multiscale glass fibre epoxy composites integrated with cellulose nanocrystals for advanced structural applications. *Composites Part A: Applied Science and Manufacturing*, 131:105801, 2020.

[83] Abdelghani Hajlane, Hamid Kaddami, and Roberts Joffe. Chemical modification of regenerated cellulose fibres by cellulose nano-crystals: Towards hierarchical structure for structural composites reinforcement. *Industrial Crops and Products*, 100:41–50, 2017.

[84] Darshil U. Shah. Developing plant fibre composites for structural applications by optimising composite parameters: a critical review. *Journal of Materials Science*, 48:6083–6107, 2013.

[85] Darshil U. Shah. *Characterisation and optimisation of the mechanical performance of plant fibre composites for structural applications*. Ph.D Thesis, University of Nottingham, 2013.

[86] Ahu Gumrah Dumanli and Alan H. Windle. Carbon fibres from cellulosic precursors: a review. *Journal of Materials Science*, 47:4236–4250, 2012.

[87] Yelin Deng. *Life Cycle Assessment of Biobased Fibre-Reinforced Polymer Composites*. Phd thesis, KU Leuven, 2014.

[88] John Summerscales, Nilmini Dissanayake, Amandeep Virk, and Wayne Hall. A review of bast fibres and their composites. Part 2 - Composites. *Composites Part A: Applied Science*

and Manufacturing, 41(10):1336–1344, 2010.

[89] Elisabetta Monaldo, Francesca Nerilli, and Giuseppe Vairo. Effectiveness of some technical standards for debonding analysis in FRP-concrete systems. *Composites Part B: Engineering*, 160:254–267, 2019.

[90] P. I. Bashtannik, A. I. Kabak, and Yu. Y. Yakovchuk. The Effect of Adhesion Interaction on the Mechanical Properties of Thermoplastic Basalt Plastics. *Mechanics of Composite Materials*, 39(1):85–88, 2003.

[91] Marianne Inman, Eythor Rafn Thorhallsson, and Kamal Azrague. A Mechanical and Environmental Assessment and Comparison of Basalt Fibre Reinforced Polymer (BFRP) Rebar and Steel Rebar in Concrete Beams. *Energy Procedia*, 111:31–40, 2017. 8th International Conference on Sustainability in Energy and Buildings, SEB-16, 11-13 September 2016, Turin, Italy.

[92] Bin Wei, Hailin Cao, and Shenhua Song. Tensile behavior contrast of basalt and glass fibers after chemical treatment. *Materials & Design*, 31(9):4244–4250, 2010.

[93] Jongsung Sim, Cheolwoo Park, and Do Young Moon. Characteristics of basalt fiber as a strengthening material for concrete structures. *Composites Part B: Engineering*, 36(6):504–512, 2005.

[94] V. Fiore, G. Di Bella, and A. Valenza. Glass–basalt/epoxy hybrid composites for marine applications. *Materials & Design*, 32(4):2091–2099, 2011.

[95] Francesca Nerilli, Michele Marino, and Giuseppe Vairo. A numerical failure analysis of multi-bolted joints in frp laminates based on basalt fibers. *Procedia Engineering*, 109:492–506, 2015. XXIII Italian Group of Fracture Meeting, IGFXXIII.

[96] Francesca Nerilli and Giuseppe Vairo. Strengthening of reinforced concrete beams with basalt-based FRP sheets: An analytical assessment. *AIP Conference Proceedings*, 1738(1):270016, 2016.

[97] Francesca Nerilli and Giuseppe Vairo. Progressive damage in composite bolted joints via a computational micromechanical approach. *Composites Part B: Engineering*, 111:357–371, 2017.

[98] Francesca Nerilli and Giuseppe Vairo. Experimental investigation on the debonding failure mode of basalt-based FRP sheets from concrete. *Composites Part B: Engineering*, 153:205–216, 2018.

[99] Jiawei Shi, Hong Zhu, Zhishen Wu, Rudolf Seracino, and Gang Wu. Bond Behavior between Basalt Fiber–Reinforced Polymer Sheet and Concrete Substrate under the Coupled Effects of Freeze-Thaw Cycling and Sustained Load. *Journal of Composites for Construction*, 17(4):530–542, 2013.

[100] Dejian Shen, Yong Ji, Fenfang Yin, and Jinyang Zhang. Dynamic Bond Stress-Slip Relationship between Basalt FRP Sheet and Concrete under Initial Static Loading. *Journal of Composites for Construction*, 19(6):04015012, 2015.

[101] Smitha Gopinath, A. Ramachandra Murthy, Nagesh R. Iyer, and M. Prabha. Behaviour of reinforced concrete beams strengthened with basalt textile reinforced concrete. *Journal of Industrial Textiles*, 44(6):924–933, 2015.

[102] Amar K. Mohanty, Singaravelu Vivekanandhan, Jean-Mathieu Pin, and Manjusri Misra. Composites from renewable and sustainable resources: Challenges and innovations. *Science*, 362(6414):536–542, 2018.

[103] Yunqing Zhu, Charles Romain, and Charlotte K. Williams. Sustainable polymers from renewable resources. *Nature*, 540(7633):354–362, December 2016.

[104] Amit K Naskar, Jong K Keum, and Raymond G Boeman. Polymer matrix nanocomposites for automotive structural components. *Nature Nanotechnology*, 11(12):1026–1030, 2016.

[105] Ever J. Barbero. *Introduction to Composite Materials Design*. CRC Press, 3rd edition, 2017.

[106] Elisabete Frollini, Cristina G. da Silva, and Elaine C. Ramires. Phenolic resins as a matrix material in advanced fiber-reinforced polymer (FRP) composites. In Jiping Bai, editor, *Advanced Fibre-Reinforced Polymer (FRP) Composites for Structural Applications*, Woodhead Publishing Series in Civil and Structural Engineering, chapter 2, pages 7–43. Woodhead Publishing, 2013.

[107] Norbert Miskolczi. Polyester resins as a matrix material in advanced fibre-reinforced polymer (FRP) composites. In Jiping Bai, editor, *Advanced Fibre-Reinforced Polymer (FRP) Composites for Structural Applications*, Woodhead Publishing Series in Civil and Structural Engineering, chapter 3, pages 44–68. Woodhead Publishing, 2013.

[108] Geoff Gibson. Epoxy resins. In Marianne Gilbert, editor, *Brydson's Plastics Materials (Eighth Edition)*, chapter 27, pages 773–797. Butterworth-Heinemann, eighth edition edition, 2017.

[109] J.-M. Raquez, M. Deleglise, M.-F. Lacrampe, and P. Krawczak. Thermosetting (bio)materials derived from renewable resources: A critical review. *Progress in Polymer Science*, 35(4):487–509, 2010. Topical Issue on Biomaterials.

[110] Bryan Ellis. *Chemistry and Technology of Epoxy Resins*. Springer Netherlands, 1st edition, 1993.

[111] Frank R. Jones. Unsaturated polyester resins. In Marianne Gilbert, editor, *Brydson's Plastics Materials*, chapter 26, pages 743–772. Butterworth-Heinemann, eighth edition edition, 2017.

[112] Mona Malik, Veena Choudhary, and I. K. Varma. Current Status of Unsaturated Polyester Resins. *Journal of Macromolecular Science, Part C*, 40(2-3):139–165, 2000.

[113] Alain Fradet and Patrick Arlaud. Unsaturated polyesters. In Geoffrey Allen and John C. Bevington, editors, *Comprehensive Polymer Science and Supplements*, chapter 19, pages 331 – 344. Pergamon, Amsterdam, 1989.

[114] Nicholas A. Rorrer, Derek R. Vardon, John R. Dorgan, Erica J. Gjersing, and Gregg T. Beckham. Biomass-derived monomers for performance-differentiated fiber reinforced polymer composites. *Green Chemistry*, 19:2812–2825, 2017.

[115] AOC Trusted Solutions. Synolite$^{\text{TM}}$. `https://aocresins.com/en-emea/home/`, accessed February 2021.

[116] Scott Bader. Crystic$^{®}$ Polyester Resin U904LVK.

[117] Polynt Composites. Composites Products.

[118] P. K. Mallik. *Fiber-Reinforced Composites: Materials, Manufacturing, and Design*. CRC Press, 3 edition, 2007.

[119] Andreas Kandelbauer, Gianluca Tondi, Oscar C. Zaske, and Sidney H. Goodman. Unsaturated polyesters and vinyl esters. In Hanna Dodiuk and Sidney H. Goodman, editors, *Handbook of Thermoset Plastics*, chapter 6, pages 111–172. William Andrew Publishing, Boston, 3 edition, 2014.

[120] Matthew B. Launikitis. Vinyl ester resins. In George Lubin, editor, *Handbook of Composites*, chapter 3, pages 38–49. Springer, Boston, 1982.

[121] L.C. Hollaway and P.R. Head. *Advanced Polymer Composites and Polymers in the Civil Infrastructure*. Elsevier Science, 2001.

[122] Fabrizio Sarasini and Carlo Santulli. Vinylester resins as a matrix material in advanced fibre-reinforced polymer (FRP) composites. In Jiping Bai, editor, *Advanced Fibre-Reinforced Polymer (FRP) Composites for Structural Applications*, Woodhead Publishing Series in Civil and Structural Engineering, chapter 4, pages 69–87. Woodhead Publishing, 2013.

[123] Hiroshi Aiba. *Novolak Production*. Springer, Berlin, 2010.

[124] Jürgen Lang and Marc Cornick. *Resole Production*. Springer, Berlin, 2010.

[125] K. P. Singh and G. R. Palmese. Enhancement of phenolic polymer properties by use of ethylene glycol as diluent. *Journal of Applied Polymer Science*, 91(5):3096–3106, 2004.

[126] Christy S. Tyberg, Muthumanickam S. Sankarapandian, K. Bears, Pojen Shih, Alfred C. Loos, David A. Dillard, James E. McGrath, Judy S. Riffle, and Usman A.K. Sorathia. Tough, void-free, flame retardant phenolic matrix materials. *Construction and Building Materials*, 13(6):343–353, 1999.

[127] Arno Gardziella, Louis A. Pilato, and Andre Knop. *Phenolic Resins: Chemistry, Reactions, Mechanism*. Springer, Berlin, 2 edition, 2000.

[128] Mingyong Xiong, Deborah K. Schneiderman, Frank S. Bates, Marc A. Hillmyer, and Kechun Zhang. Scalable production of mechanically tunable block polymers from sugar. *Proceedings of the National Academy of Sciences*, 111(23):8357–8362, 2014.

[129] George John, Subbiah Nagarajan, Praveen Kumar Vemula, Julian R. Silverman, and C.K.S. Pillai. Natural monomers: A mine for functional and sustainable materials – Occurrence, chemical modification and polymerization. *Progress in Polymer Science*, 92:158–209, 2019.

[130] Sicomin Epoxy Systems. Bio-based Epoxy. `https://sicomin.com/products/epoxy-systems/bio-based-epoxy`, accessed September 2021.

[131] INEOS Composites. Envirez™. `https://www.ineos.com/businesses/ineos-enterprises/businesses/ineos-composites/products/unsaturated-polyester-resins/envirez/`, accessed September 2021.

[132] Entropy resins. Super Sap®. `https://entropyresins.com/sustainability/super-sap/`, accessed September 2021.

[133] Easy Composites. IB2 Epoxy Infusion Bio Resin. `https://www.easycomposites.co.uk/IB2-epoxy-laminating-resin`, accessed September 2021.

[134] TFC Biomass biobased chemicals. Biorez™. `https://www.transfurans.be/products`, accessed July 2021.

[135] VIOBOND. Sustainable binder: Upscaling new lignin-phenol-formaldehyde resin produc-

tion with wood-based biorefinery lignin. `https://www.bbi.europa.eu/projects/viobond`, accessed November 2021.

[136] Stora Enso. Lineo™. `https://www.storaenso.com/en/newsroom/news/2019/2/aiming-at-future-with-100-bio-based-resin`, accessed July 2021.

[137] Ana Dotan. Biobased thermosets. In Hanna Dodiuk and Sidney H. Goodman, editors, *Handbook of Thermoset Plastics*, chapter 15, pages 577–622. William Andrew Publishing, Boston, third edition edition, 2014.

[138] Kalsoom Jan, Md. Akiful Haque, Shaoqing Cui, Gregory Reimonn, Ana Dotan, Taofeng Lu, and Wan-Ting Chen. Thermosets from renewable sources. In Hanna Dodiuk, editor, *Handbook of Thermoset Plastics (Fourth Edition)*, Plastics Design Library, chapter 14, pages 679–718. William Andrew Publishing, Boston, fourth edition edition, 2022.

[139] Arvin Z. Yu, Eric M. Serum, Anna C. Renner, Jonas M. Sahouani, Mukund P. Sibi, and Dean C. Webster. Renewable reactive diluents as practical styrene replacements in biobased vinyl ester thermosets. *ACS Sustainable Chemistry & Engineering*, 6(10):12586–12592, 2018.

[140] Santosh K. Yadav, Kevin M. Schmalbach, Emre Kinaci, Joseph F. Stanzione, and Giuseppe R. Palmese. Recent advances in plant-based vinyl ester resins and reactive diluents. *European Polymer Journal*, 98:199–215, 2018.

[141] John H. Vergara, Santosh K. Yadav, Oluwadamilola Bolarin, John J. La Scala, and Giuseppe R. Palmese. Synthesis and characterization of low-viscosity bio-based styrene alternatives for bisphenol a vinyl ester thermosetting resins. *ACS Sustainable Chemistry & Engineering*, 8(46):17234–17244, 2020.

[142] Eric D. Hernandez, Alexander W. Bassett, Joshua M. Sadler, John J. La Scala, and Joseph F. Stanzione. Synthesis and characterization of bio-based epoxy resins derived from vanillyl alcohol. *ACS Sustainable Chemistry & Engineering*, 4(8):4328–4339, 2016.

[143] Fengshuo Hu, John J. La Scala, Joshua M. Sadler, and Giuseppe R. Palmese. Synthesis and characterization of thermosetting furan-based epoxy systems. *Macromolecules*, 47(10):3332–3342, 2014.

[144] Fengshuo Hu, Santosh Kumar Yadav, John J. La Scala, James Throckmorton, and Giuseppe R. Palmese. Epoxidized soybean oil modified using fatty acids as tougheners for thermosetting epoxy resins: Part 1. *Journal of Applied Polymer Science*, 138(24):50570, 2021.

[145] Xiangyi Zhang, Mareva Fevre, Gavin O. Jones, and Robert M. Waymouth. Catalysis as an enabling science for sustainable polymers. *Chemical Reviews*, 118(2):839–885, 2018.

[146] Giuseppe R. Palmese, Santosh K. Yadav, John Vergara, and John J. LaScala. Renewable furan based amine curing agents for epoxy thermoset, 2019. Patent WO 2019/040389 AI.

[147] Sushanta K. Sahoo, Vinay Khandelwal, and Gaurav Manik. Development of completely bio-based epoxy networks derived from epoxidized linseed and castor oil cured with citric acid. *Polymers for Advanced Technologies*, 29(7):2080–2090, 2018.

[148] Andrea Anusic, Yannick Blößl, Gernot Oreski, and Katharina Resch-Fauster. High-performance thermoset with 100% bio-based carbon content. *Polymer Degradation and Stability*, 181:109284, 2020.

[149] Rémi Auvergne, Sylvain Caillol, Ghislain David, Bernard Boutevin, and Jean-Pierre Pascault. Biobased thermosetting epoxy: Present and future. *Chemical Reviews*, 114(2):1082–1115, jan 2014.

[150] Eric Ramon, Carmen Sguazzo, and Pedro M. G. P. Moreira. A review of recent research on bio-based epoxy systems for engineering applications and potentialities in the aviation sector. *Aerospace*, 5(4), 2018.

[151] Jintao Wan, Jianqing Zhao, Xianwei Zhang, Hong Fan, Junhao Zhang, Daodao Hu, Pujun Jin, and De-Yi Wang. Epoxy thermosets and materials derived from bio-based monomeric phenols: Transformations and performances. *Progress in Polymer Science*, 108:101287, 2020.

[152] Feifei Ng, Guillaume Couture, Coralie Philippe, Bernard Boutevin, and Sylvain Caillol. Bio-based aromatic epoxy monomers for thermoset materials. *Molecules*, 22(1):48, 2017.

[153] Jun Deng, Xiaoqing Liu, Chao Li, Yanhua Jiang, and Jin Zhu. Synthesis and properties of a bio-based epoxy resin from 2,5-furandicarboxylic acid (FDCA). *RSC Adv.*, 5:15930–15939, 2015.

[154] Bruce M. Bell, John R. Briggs, Robert M. Campbell, Susanne M. Chambers, Phil D. Gaarenstroom, Jeffrey G. Hippler, Bruce D. Hook, Kenneth Kearns, John M. Kenney, William J. Kruper, D. James Schreck, Curt N. Theriault, and Charles P. Wolfe. Glycerin as a renewable feedstock for epichlorohydrin production. the gte process. *CLEAN – Soil, Air, Water*, 36(8):657–661, 2008.

[155] Chun Hui Zhou, Heng Zhao, Dong Shen Tong, Lin Mei Wu, and Wei Hua Yu. Recent advances in catalytic conversion of glycerol. *Catalysis Reviews*, 55(4):369–453, 2013.

[156] Thomas J. Farmer, Rachael L. Castle, James H. Clark, and Duncan J. Macquarrie. Synthesis of Unsaturated Polyester Resins from Various Bio-Derived Platform Molecules. *International Journal of Molecular Sciences*, 16(7):14912–14932, 2015.

[157] Mohamed Naceur Belgacem and Alessandro Gandini. Materials from Vegetable Oils: Major Sources, Properties and Applications. In Mohamed Naceur Belgacem Gandini and Alessandro, editors, *Monomers, Polymers and Composites from Renewable Resources*, chapter 3, pages 39–66. Elsevier, Amsterdam, 2008.

[158] Bojana Z. Fidanovski, Pavle M. Spasojevic, Vesna V. Panic, Sanja I. Seslija, Jelena P. Spasojevic, and Ivanka G. Popovic. Synthesis and characterization of fully bio-based unsaturated polyester resins. *Journal of Materials Science*, 53(6):4635–4644, 2018.

[159] Ana C. Fonseca, Inês M. Lopes, Jorge F.J. Coelho, and Arménio C. Serra. Synthesis of unsaturated polyesters based on renewable monomers: Structure/properties relationship and crosslinking with 2-hydroxyethyl methacrylate. *Reactive and Functional Polymers*, 97:1–11, 2015.

[160] Kingsley Kema Ajekwene. Properties and Applications of Acrylates. In Ángel Serrano-Aroca and Sanjukta Deb, editors, *Acrylate Polymers for Advanced Applications*, chapter 3. IntechOpen, Rijeka, 2020.

[161] Kun Liang, Marco Dossi, Davide Moscatelli, and Robin A. Hutchinson. An Investigation of Free-Radical Copolymerization Propagation Kinetics of Styrene and 2-Hydroxyethyl

Methacrylate. *Macromolecules*, 42(20):7736–7744, 2009.

[162] Juan Carlos Domínguez, Mercedes Oliet, María Virginia Alonso, Ester Rojo, and Francisco Rodríguez. Structural, thermal and rheological behavior of a bio-based phenolic resin in relation to a commercial resol resin. *Industrial Crops and Products*, 42:308–314, 2013.

[163] Yongsheng Zhang, Zhongshun Yuan, and Chunbao (Charles) Xu. Engineering biomass into formaldehyde-free phenolic resin for composite materials. *AIChE Journal*, 61(4):1275–1283, 2015.

[164] Mahsan Basafa and Kelly Hawboldt. A review on sources and extraction of phenolic compounds as precursors for bio-based phenolic resins. *Biomass Conversion and Biorefinery*, 2021.

[165] Yongsheng Zhang, Zhongshun Yuan, and Chunbao (Charles) Xu. Bio-based resins for fiber-reinforced polymer composites. In Alan Kin tak Lau and Ada Pui-Yan Hung, editors, *Natural Fiber-Reinforced Biodegradable and Bioresorbable Polymer Composites*, chapter 8, pages 137–162. Woodhead Publishing, 2017.

[166] Nguyen Le Huong, Nguyen Huu Nieu, Ton That Minh Tan, and Ullrich J. Griesser. Cardanol-phenol-formaldehyde resins. thermal analysis and characterization. *Die Angewandte Makromolekulare Chemie*, 243(1):77–85, 1996.

[167] Benoit Briou, Sylvain Caillol, Jean-Jacques Robin, and Vincent Lapinte. Cardanol-based and formaldehyde-free flexible phenolic networks. *European Journal of Lipid Science and Technology*, 120(7):1800175, 2018.

[168] Dávid Kun and Béla Pukánszky. Polymer/lignin blends: Interactions, properties, applications. *European Polymer Journal*, 93:618–641, 2017.

[169] Laura Hay, Alex Duffy, and R.I. Whitfield. The sustainability cycle and loop: Models for a more unified understanding of sustainability. *Journal of Environmental Management*, 133:232–257, 2014.

[170] Ramani Narayan. Carbon footprint of bioplastics using biocarbon content analysis and life-cycle assessment. *MRS Bulletin*, 36(9):716–721, 2011.

[171] Joseph F. Stanzione III, Joshua M. Sadler, John J. La Scala, Kaleigh H. Reno, and Richard P. Wool. Vanillin-based resin for use in composite applications. *Green Chemistry*, 14:2346–2352, 2012.

[172] Alessandro Gandini and Talita M. Lacerda. From monomers to polymers from renewable resources: Recent advances. *Progress in Polymer Science*, 48:1–39, 2015. Topical Volume on Polymer Chemistry.

[173] Mitsuhiro Shibata and Masanori Asano. Biobased thermosetting resins composed of terpene and bismaleimide. *Journal of Applied Polymer Science*, 129(1):301–309, 2013.

[174] Michael FitzPatrick, Pascale Champagne, Michael F. Cunningham, and Ralph A. Whitney. A biorefinery processing perspective: Treatment of lignocellulosic materials for the production of value-added products. *Bioresource Technology*, 101(23):8915–8922, 2010.

[175] Francesco Cherubini and Sergio Ulgiati. Crop residues as raw materials for biorefinery systems – A LCA case study. *Applied Energy*, 87(1):47–57, 2010.

[176] Arthur J. Ragauskas, Charlotte K. Williams, Brian H. Davison, George Britovsek, John Cairney, Charles A. Eckert, William J. Frederick, Jason P. Hallett, David J. Leak, Charles L. Liotta, Jonathan R. Mielenz, Richard Murphy, Richard Templer, and Timothy Tschaplinski. The path forward for biofuels and biomaterials. *Science*, 311(5760):484–489, 2006.

[177] Avelino Corma, Sara Iborra, and Alexandra Velty. Chemical routes for the transformation of biomass into chemicals. *Chemical Reviews*, 107(6):2411–2502, 2007. PMID: 17535020.

[178] Vijaykumar Guna, Manikandan Ilangovan, M.G. Ananthaprasad, and Narendra Reddy. Hybrid biocomposites. *Polymer Composites*, 39(S1):E30–E54, 2018.

[179] R. Petrucci, C. Santulli, D. Puglia, E. Nisini, F. Sarasini, J. Tirillò, L. Torre, G. Minak, and J.M. Kenny. Impact and post-impact damage characterisation of hybrid composite laminates based on basalt fibres in combination with flax, hemp and glass fibres manufactured by vacuum infusion. *Composites Part B: Engineering*, 69:507–515, 2015.

[180] Philippe Boisse, editor. *Advances in Composites Manufacturing and Process Design*. Woodhead Publishing, Cambridge, UK, 2015.

[181] National Composites Centre (NCC). `https://www.nccuk.com`. Accessed on January 10, 2021.

[182] Bristol Composites Institute (ACCIS). `http://www.bristol.ac.uk/composites/`. Accessed on January 10, 2021.

[183] Jolie Frketic, Tarik Dickens, and Subramanian Ramakrishnan. Automated manufacturing and processing of fiber-reinforced polymer (FRP) composites: An additive review of contemporary and modern techniques for advanced materials manufacturing. *Additive Manufacturing*, 14:69–86, 2017.

[184] Yizhuo Li, Soraia Pimenta, Jordan Singgih, Stefan Nothdurfter, and Karsten Schuffenhauer. Experimental investigation of randomly-oriented tow-based discontinuous composites and their equivalent laminates. *Composites Part A: Applied Science and Manufacturing*, 102:64–75, 2017.

[185] Hana Yu, Kevin D. Potter, and Michael R. Wisnom. A novel manufacturing method for aligned discontinuous fibre composites (high performance-discontinuous fibre method). *Composites Part A: Applied Science and Manufacturing*, 65:175–185, 2014.

[186] Amanda Conroy, Sue Halliwell, and Tim Reynolds. Composite recycling in the construction industry. *Composites Part A: Applied Science and Manufacturing*, 37(8):1216–1222, 2006. The 2nd International Conference: Advanced Polymer Composites for Structural Applications in Construction.

[187] Stella Job. Recycling glass fibre reinforced composites – history and progress. *Reinforced Plastics*, 57(5):19–23, 2013.

[188] Swati Verma, Bhuvaneshwari Balasubramaniam, and Raju Kumar Gupta. Recycling, reclamation and re-manufacturing of carbon fibres. *Current Opinion in Green and Sustainable Chemistry*, 13:86–90, 2018. Reuse and Recycling / UN SGDs: How can Sustainable Chemistry Contribute? / Green Chemistry in Education.

[189] Shubham Utekar, Suriya V K, Neha More, and Adarsh Rao. Comprehensive study of recycling of thermosetting polymer composites – driving force, challenges and methods.

Composites Part B: Engineering, 207:108596, 2021.

[190] Zhe Liu, Thomas A. Turner, Kok H. Wong, and Stephen J. Pickering. Development of high performance recycled carbon fibre composites with an advanced hydrodynamic fibre alignment process. *Journal of Cleaner Production*, 278:123785, 2021.

[191] João Ramôa Correia. Materials for Construction and Civil Engineering: Science, Processing, and Design. In M. Clara Gonçalves and Fernanda Margarido, editors, *Fibre-Reinforced Polymer (FRP) Composites*, chapter 11, page 56. Springer International Publishing, 2015.

[192] S. Bickerton, Q. Govignon, and P. Kelly. Resin infusion/liquid composite moulding (LCM) of advanced fibre-reinforced polymer (FRP). In Jiping Bai, editor, *Advanced Fibre-Reinforced Polymer (FRP) Composites for Structural Applications*, Woodhead Publishing Series in Civil and Structural Engineering, chapter 7, pages 155–186. Woodhead Publishing, 2013.

[193] Ismet Baran. Pultrusion processes for composite manufacture. In Philippe Boisse, editor, *Advances in Composites Manufacturing and Process Design*, chapter 16, pages 379–414. Woodhead Publishing, 2015.

[194] Rani F. El-Hajjar, Hua Tan, and Krishna M. Pillai. Advanced processing techniques for composite materials for structural applications. In Nasim Uddin, editor, *Developments in Fiber-Reinforced Polymer (FRP) Composites for Civil Engineering*, Woodhead Publishing Series in Civil and Structural Engineering, chapter 3, pages 54–77e. Woodhead Publishing, 2013.

[195] Michael Elkington, Dominic Bloom, Carwyn Ward, Anna Chatzimichali, and Kevin Potter. Hand layup: understanding the manual process. *Advanced Manufacturing: Polymer & Composites Science*, 1(3):138–151, 2015.

[196] Charles Wittman and Gerald D. Shook. Hand lay-up techniques. In George Lubin, editor, *Handbook of Composites*, pages 321–367. Springer, Boston, MA, 1982.

[197] Tetsuo Kikuchi, Yuichiro Tani, Yuka Takai, Akihiko Goto, and Hiroyuki Hamada. Relationships between degree of skill, dimension stability and mechanical properties of composite structure in hand lay-up method. In Sarah Sharples and Steven T. Shorrock, editors, *Contemporary Ergonomics and Human Factors 2014*, pages 101–109. CRC Press, 2014.

[198] Helen V. Jones, Anna P. Chatzimichali, Rox Middleton, Kevin D. Potter, and Carwyn Ward. Exploring the discrete tools used by laminators in composites manufacturing: application of novel concept. *Advanced Manufacturing: Polymer & Composites Science*, 1(4):185–198, 2015.

[199] Perumalsamy Balaguru, Antonio Nanni, and James Giancaspro. *FRP Composites for Reinforced and Prestressed Concrete Structures: A Guide to Fundamentals and Design for Repair and Retrofit*. Taylor & Francis's Structural Engineering: Mechanics and Design series. CRC Press, 1st edition, 2009.

[200] Raghu R. Kuppusamy, Satyajit Rout, and Kaushik Kumar. Advanced manufacturing techniques for composite structures used in aerospace industries. In Kaushik Kumar and J. Paulo Davim, editors, *Modern Manufacturing Processes*, Woodhead Publishing Reviews: Mechanical Engineering Series, chapter 1, pages 3–12. Woodhead Publishing, 2020.

[201] Nuno C. Correia, François Robitaille, Andrew C. Long, Chris D. Rudd, Pavel Šimáček,

and Suresh G. Advani. Analysis of the vacuum infusion moulding process: I. Analytical formulation. *Composites Part A: Applied Science and Manufacturing*, 36(12):1645–1656, 2005.

[202] Kosin Abdurohman and Mabe Siahaan. Effect of mesh-peel ply variation on mechanical properties of e-glass composite by infusion vacuum method. *Journal of Physics: Conference Series*, 1005:012009, apr 2018.

[203] Ismet Baran. *Pultrusion: State-of-the-art Process Models*. Smithers Rapra Technology, 1st edition, 2015.

[204] S.C. Joshi. The pultrusion process for polymer matrix composites. In Suresh G. Advani and Kuang-Ting Hsiao, editors, *Manufacturing Techniques for Polymer Matrix Composites (PMCs)*, Woodhead Publishing Series in Composites Science and Engineering, chapter 12, pages 381–413. Woodhead Publishing, 2012.

[205] João Ramôa Correia. Pultrusion of advanced fibre-reinforced polymer (FRP) composites. In Jiping Bai, editor, *Advanced Fibre-Reinforced Polymer (FRP) Composites for Structural Applications*, Woodhead Publishing Series in Civil and Structural Engineering, chapter 9, pages 207–251. Woodhead Publishing, 2013.

[206] Ismet Baran. Pultrusion processes for composite manufacture. In Philippe Boisse, editor, *Advances in Composites Manufacturing and Process Design*, chapter 16, pages 379–414. Woodhead Publishing, 2015.

[207] Arthur Babeau, Sébastien Comas-Cardona, Christophe Binetruy, and Gilles Orange. Modeling of heat transfer and unsaturated flow in woven fiber reinforcements during direct injection-pultrusion process of thermoplastic composites. *Composites Part A: Applied Science and Manufacturing*, 77:310–318, 2015.

[208] Paulo J. Novo, João F. Silva, João P. Nunes, and Antoínio T. Marques. Pultrusion of fibre reinforced thermoplastic pre-impregnated materials. *Composites Part B: Engineering*, 89:328–339, 2016.

[209] María Asensio, Puria Esfandiari, Karina C. Núñez, João F. Silva, Antoínio T. Marques, Juan C. Merino, and José M. Pastor. Processing of pre-impregnated thermoplastic towpreg reinforced by continuous glass fibre and recycled pet by pultrusion. *Composites Part B: Engineering*, 200:108365, 2020.

[210] Kirill Minchenkov, Alexander Vedernikov, Alexander Safonov, and Iskander Akhatov. Thermoplastic Pultrusion: A Review. *Polymers*, 13(2), 2021.

[211] Ben R. Bogner, Walt V. Breitigam, Mike Woodward, and Kenneth L. Forsdyke. Thermoset resins for pultrusion. In Trevor F. Starr, editor, *Pultrusion for Engineers*, Woodhead Publishing Series in Composites Science and Engineering, chapter 4, pages 97–174. Woodhead Publishing, 2000.

[212] Ciaran McSwiggan and Amir Fam. Bio-based resins for flexural strengthening of reinforced concrete beams with frp sheets. *Construction and Building Materials*, 131:618–629, 2017.

[213] Amanda Eldridge and Amir Fam. Durability of Concrete Cylinders Wrapped with GFRP Made from Furfuryl Alcohol Bioresin. *Journal of Composites for Construction*, 18(6):04014013, 2014.

[214] Mohammadreza Foruzanmehr, Said Elkoun, Amir Fam, and Mathieu Robert. Degradation characteristics of new bio-resin based-fiber-reinforced polymers for external rehabilitation of structures. *Journal of Composite Materials*, 50(9):1227–1239, 2016.

[215] C.C.M Ma, M.S Yn, J.L Han, C.J Chang, and H.D Wu. Pultruded fibre-reinforced furfuryl alcohol resin composites: 1. process feasibility study. *Composites Manufacturing*, 6(1):45–52, 1995.

[216] C.C.M Ma, M.S Yn, J.L Han, C.J Chang, and H.D Wu. Pultruded fibre-reinforced furfuryl alcohol resin composites: 2. static, dynamic mechanical and thermal properties. *Composites Manufacturing*, 6(1):53–58, 1995.

[217] Anne McIsaac and Amir Fam. The effect of bio-based content in resin blends on tensile properties of FRP wet layup systems. *Construction and Building Materials*, 168:328–337, 2018.

[218] Kenneth Mak, Amir Fam, and Colin MacDougall. Flexural Behavior of Sandwich Panels with Bio-FRP Skins Made of Flax Fibers and Epoxidized Pine-Oil Resin. *Journal of Composites for Construction*, 19(6):04015005, 2015.

[219] Joris Smits. Fiber-Reinforced Polymer Bridge Design in the Netherlands: Architectural Challenges toward Innovative, Sustainable, and Durable Bridges. *Engineering*, 2(4):518–527, 2016.

Part II

Resins

Chapter 3

ISO-based unsaturated polyesters

Abstract

This chapter presents the development of unsaturated polyester main chains based on monomers derived from renewable sources, namely, isosorbide, 1,3-propanediol, and fumaric acid, with petroleum-derived phthalic anhydride. The low molecular weight oligoesters achieved a high bio-content of up to 87.1 wt.% and they were incorporated into reactive diluents formulated to be eco-friendlier and less toxic compared to the typical styrene incorporation approach, thus resulting in unsaturated polyester resins with viscosities between 750 and 950 cP. These resins are suitable for use in fibre reinforced polymer production, having the benefit of presenting over 50 wt.% of bio-content in some formulations. Moreover, the crosslinked polyesters exhibit comparable mechanical and thermomechanical behaviour to their oil-based counterparts, with modulus of elasticity and tensile strength of up to 3.9 GPa and 62.1 MPa, respectively, and glass transition temperatures of up to 106 ℃. Figure 3.1 presents a graphical abstract summarising this chapter.

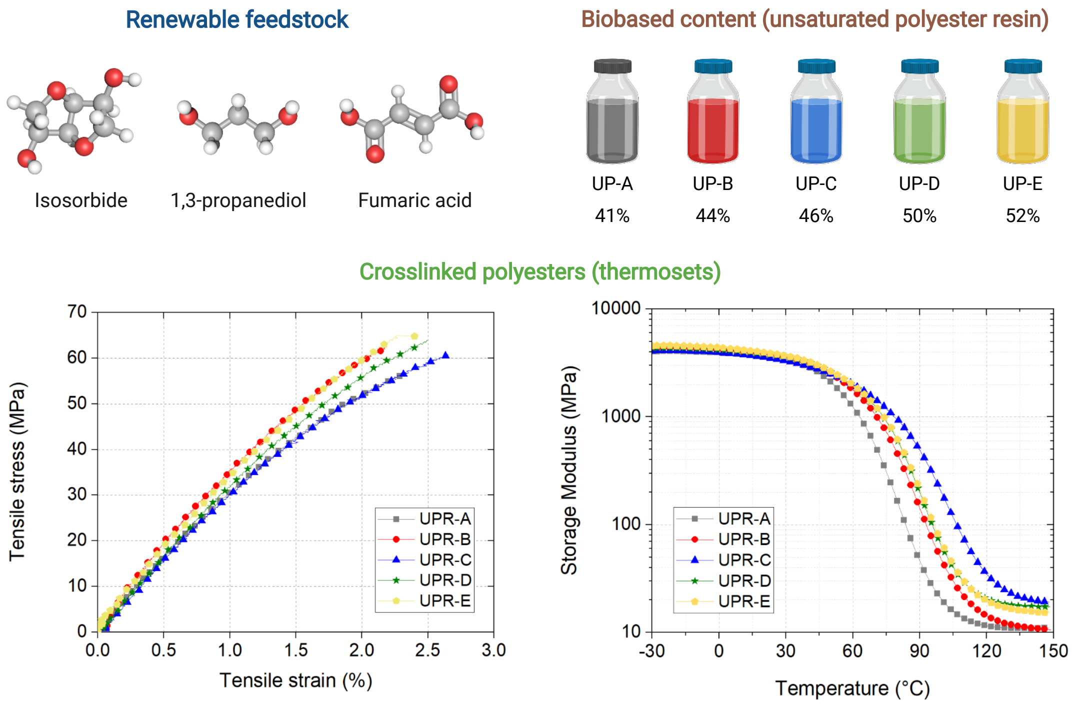

Figure 3.1: Graphical abstract of the bio-based unsaturated polyesters.

3.1 Introductory remarks

The vast majority of thermoset polyesters are fully produced using raw materials derived from petrochemical sources, and very few studies reported thermoset polyesters produced from renewable feedstock. The current lower cost and wide availability of crude oil are the main reasons for the slow progress in the development of greener thermoset polyesters. However, a growing societal awareness of the need to shift towards environmentally sustainable materials and processes together with the foreseeable limitations in the long-term supply of petroleum are accelerating the development of more sustainable routes for the production of thermoset polyesters [1,2].

Bio-based thermoplastic polyesters recently reported in the literature [3] can provide a basis for developing thermosets, especially regarding the characteristics of the raw materials used in the main chain. Those thermoplastic polyesters are typically synthesised from bio-based saturated acids and diols and used primarily in packaging. However, they often have unsuitable processing, mechanical, and thermomechanical properties for higher performance applications, such as those required by FRP composites.

Bio-based unsaturated polyesters based on vegetable oils-derived fatty acids have been reported in the literature [4–6]. Several product segments use these polyesters, especially paints. However, fatty acids are undesirable for high-performance applications due to their flexibility arising from their relatively long chains. Furan-based building blocks, such as 2,5-furandicarboxylic acid (FDCA), have also been used for polyester synthesis since they are stiffer and result in polyesters with excellent thermomechanical properties [7–9]. Nevertheless, furan-based raw materials are not yet commercially competitive because of their high production cost and low availability.

Although other bio-based saturated diacids that can be used to synthesise polyesters have emerged, such as itaconic, adipic, and succinic, petroleum-derived phthalic anhydride (PA) is still essential to produce general-purpose polyester (orthophthalic) because of its aromatic structure, which confers higher strength and stiffness to the crosslinked resin. PA also has a lower cost than its bio-based counterparts. Thus, the production of high-performance bio-based thermoset polyesters benefits from keeping PA as a saturated acid, even if this reduces the final bio-based content. However, it is worth referring that while PA is nowadays derived from benzene, toluene, and xylene fraction of the crude mixture, it can be produced from the aromatic fraction of coal tar and it is expected that most of the coal will be in the future obtained from wood, and therefore renewable [10].

Renewable production of PA from other renewable sources (such as corn straw) has also been recently investigated, and the life cycle greenhouse gas (GHG) emissions appear promising compared to the traditional process for its production. However, there is still a high dependence on fossils, in particular in the combined heat and power section, and solvent consumption during the bio-refining process [11].

Regarding the unsaturations present in the polyester main chain, an alternative way to synthesise unsaturated blocks while maintaining the functionality for crosslinking is through the replacement of petroleum-derived maleic anhydride by a bio-based diacid capable of providing double bonds to the chain. Fumaric acid (FA) is the prominent diacid with such characteristics; this unsaturated dicarboxylic acid is non-toxic and is naturally formed in minor amounts or can be obtained from agriculture by-products, for instance, through the fermentation of sugarcane bagasse [12–14]. Thus, using bio-based FA to synthesise part of an unsaturated block of the polymer main chain makes it possible to increase the renewable content of polyester. In addition, the fumarate double bond is more reactive than the maleate one, due to lower steric hindrance, resulting in a more complete radical polymerisation and a lower need for post-cure treatment [15].

Glycols are also an essential part of the building blocks, along with diacids. As diols, glycols or short chain diols promote linear polyesters and determine toughness, stiffness, and even thermomechanical properties. In addition, the use of bio-based diols to replace petroleum-derived ones, such as ethylene glycol (EG) and propylene glycol (PG), can represent about one-third of the bio-content by weight of a thermoset polyester. Herein, 1,3-propanediol (PDO) and isosorbide (ISO) diols are considered as potential replacements for petroleum-derived diols. PDO is a renewable aliphatic diol derived from corn sugar fermentation [16–18], which has low viscosity (liquid at room temperature) and is compatible with polyesters of aromatic or rigid cyclic morphology. Conversely, ISO can provide additional stiffness to the main polyester chain because it consists of a rigid cyclic structure, resulting in a polymer with higher thermomechanical properties than those of polyesters based on conventional aliphatic diols [19–23].

Thermoset polyesters also use vinyl monomers as a reactive diluent because they simultaneously reduce the viscosity of the reactive resin and are responsible for radical polymerisation with the main chain double bonds for the 3D network formation, usually styrene. The reactive diluent can represent up to half of the weight of the thermoset polyester, but very often 30 to 40 wt.%. Hence, the development of thermoset polyesters must also include more sustainable and preferably less toxic reactive diluents. Additionally, those diluents must be compatible with the main chain, and after their incorporation, thermoset polyesters must have similar processing characteristics to conventional ones.

In general, acrylate-type monomers are well known for the mechanical and physical properties of the respective polymers, such as toughness, elasticity, strength at break, and quite good oil and heat resistance [24]. For example, 2-hydroxyethyl methacrylate (HEMA) is a possible replacement for styrene (at least partially) since it contains polymerizable double bonds, which provide propagating radicals with similar reactivity as styrene; with the advantage of a lower environmentally impact [25]. However, HEMA behaves like rubber at room temperature, which can pose some difficulties in its processing. Therefore, a blend between HEMA and styrene can be a more sustainable alternative as a reactive diluent for thermoset polyesters while maintaining high-performance properties [26].

Although the previously mentioned raw materials are the basis for developing less petroleum-dependent thermoset polyesters, the adequate formulation and macromolecular structural design of the main chain as well as its compatibility with reactive diluents are essential to make bio-based thermoset polyesters suitable for high-performance applications. The bio-based thermoset polyesters must present a macromolecular structure capable of matching or even improving the resulting mechanical and thermomechanical properties relative to their conventional counterparts, beyond ensuring high bio-content, competitive cost, and industrial scalability.

In this context, this chapter presents five different bio-based unsaturated polyester formulations with mechanical, thermomechanical, and processing performance that is competitive with typical petroleum-derived alternatives. This is achieved using monomers derived from renewable resources specifically selected to confer adequate characteristics to the polymer main chain. These building blocks, synthesised from diacids with diols, vary according to the tested formulations, providing high strength, stiffness, and increased glass transition temperatures. The resulting oligoesters are assessed by their polycondensation kinetics, distribution, and molecular structure. The viscosity, mechanical properties, and thermomechanical properties of the thermoset polyester resins obtained by incorporating the main chain with reactive diluents of lower toxicity are also presented.

3.2 Experimental

3.2.1 Materials

ISO ($>$98%, Roquette) and PDO (Susterra™ propanediol, DuPont Tate & Lyle) were used herein as diols for synthesising the bio-based polyester prepolymers, with ISO being a monomer capable of providing additional stiffness to the thermoset polyester resin upon free radical curing. EG ($>$99%, Sigma-Aldrich) was also used as a diol in three of the formulations presented herein. PA (99%, Sigma-Aldrich) was used as a saturated aromatic diacid also to provide additional stiffness to the thermoset upon curing. FA ($>$98%, Sigma-Aldrich) was used in all formulations to provide unsaturations (double bonds) for the main chain, which could undergo free radical curing.

Styrene (Omnova Solutions) and HEMA (97%, Sigma-Aldrich) were blended to obtain a reactive diluent with lower styrene content to be incorporated with the bio-based unsaturated polyester main chain. Furthermore, imidazole, hydroquinone, and toluhydroquinone were obtained from Sigma-Aldrich. Methyl ethyl ketone peroxide (MEKP) and cobalt octoate 1 wt.% (in diisodecyl phthalate) were obtained from EcoCompositos S.A. All the chemicals were used as received.

3.2.2 Prepolymer formulations

In general, the main chain (prepolymer consisting of diacids and diols) represents most of the weight of thermoset polyesters. Herein, the prepolymer formulations aim to design polyesters that simultaneously present a high bio-content, match, or exceed the mechanical, thermomechanical, and processing properties of comparable conventional non-bio-based polyesters and are commercially competitive with those.

Table 3.1 shows the formulations investigated herein, consisting of unsaturations (FA), aromatic rings (PA), aliphatic (PDO and/or EG), and cyclic (ISO) structures. The presence of building blocks along the main chain is designed to provide: (i) a high crosslink density, which results in higher thermomechanical properties; (ii) strength, stiffness, and elongation capacity, which would not limit the use in various high-performance applications as matrix of fibre-polymer composites; and (iii) has suitable viscosity after incorporation with reactive diluents, to be used as a casting or fibre impregnating resin.

Table 3.1: Prepolymer formulations.

Prepolymer			Monomer (mol)				
Group	**Sample**	**S:U**[a]	**PA**	**FA**	**PDO**	**ISO**	**EG**
I	UP-A	1:2	2.145	4.289	2.383	2.383	2.383
	UP-B	1:3	1.627	4.880	2.410	2.410	2.410
	UP-C	1:4	1.310	5.241	2.426	2.426	2.426
II	UP-D	1:3	1.591	4.772	4.713	2.357	-
	UP-E	1:4	1.281	4.745	4.745	2.372	-

[a] S:U represents the molar fraction between saturated (S) and unsaturated (U) acids

Although achieving a fully bio-based polyester is ideal, some petrochemical monomers are still essential for the polymer to achieve similar performance and commercial competitiveness compared to conventional polyesters. Therefore, partially bio-based polyester main chains were divided into two groups and pursued according to the following characteristics:

i) UP-A, UP-B, and UP-C belong to the group (I) formulations containing PA and EG as saturated diacid and aliphatic diol, respectively. Even though PA is petroleum-derived, its aromatic structure provides a higher stiffness to the polyester than those synthesised from long-chain diacids, such as fatty acids. The replacement of PA by furan-based diacids would also be an alternative option; however, furan-based diacids have a significantly higher cost, making them incompatible with the lower-cost requirement set for the polymer;

ii) UP-D and UP-E belong to the group (II) formulations. The main feature is the total replacement of EG by other eco-friendlier glycols, mainly to produce polyester with higher bio-based content without reducing its mechanical and thermomechanical properties. Herein, the balance between ISO (33 mol%) and PDO (67 mol%) was designed to produce main chains with higher stiffness and similar viscosities with respect to their fully petroleum-derived counterparts; and

iii) both groups (I) and (II) have the presence of bio-based FA to replace its petroleum-derived cis isomer, derived from maleic anhydride.

3.2.3 Synthesis

The prepolymers were prepared by catalysed bulk polycondensation. In a typical experiment, PA (240.9 g, 1.627 mol), FA (570.3 g, 4.880 mol), PDO (183.4 g, 2.410 mol), ISO (352.2 g, 2.410 mol), and EG (149.6 g, 2.410 mol) were added to a 2 litres four-neck reactor (with bottom drain valve) equipped with an anchor blade mechanical stirrer, a heating mantle controlled by a thermocouple configured to a set-point temperature at 206 ℃ (ranging between 202 ℃ and 210 ℃), a submerged nitrogen inlet and a condenser attached to a dean-stark adaptor to collect the water formed from the reaction and also the one used for raw material solubilisation. No vacuum was applied during the synthesis.

Imidazole (2.99 g, 0.044 mol) was used as the catalyst. In addition, hydroquinone (0.30 g, 2.72 mmol) and 2-methyl hydroquinone (0.30 g, 2.41 mmol) were added as the free radical polymerisation inhibitor to prevent gelation. All reactants were added at room temperature. The mixture was then stirred, and the acid terminal groups and samples removed from the reactor were periodically titrated with potassium hydroxide (KOH, 0.1M) and phenolphthalein as titrant solution and indicator, respectively, to determine their concentration as the reaction progressed (see Appendix A.1).

Acid number (AN) titration and viscosity measurements (at 125 ℃ in a Cone & Plate ICI viscosimeter) were verified each hour, and the first sample was taken after three hours from the beginning of the reaction. Then, the reaction was allowed to proceed until the acid number reached a constant value (consistently below 50 mgKOH/g) combined with a maximum viscosity of 2000 cP, which required 8 hours.

3.2.4 Bio-based content

The procedures specified in part 4 Annex B (B1 and B2) of the ISO 16620 [27] standard were used to determine the bio-based carbon and mass content for each reactant. Tables A.6, A.9, and A.10 (in Appendix A.4) show the calculation procedures.

3.2.5 Kinetics

During synthesis progress, the concentration of acid that had not yet been esterified was measured by titration to determine the AN. Consequently, the conversion or extent of reaction (p) was estimated as follows,

$$p = 1 - \frac{\mathrm{AN}}{\mathrm{AN}_0} \tag{3.1}$$

where AN$_0$ is the initial acid number. AN$_0$ for the prepolymers ranged from 477 to 491 mgKOH/g. Herein, the synthesis' goal was an extent of reaction of about 90% ($p = 0.90$), corresponding to an oligomeric molecular weight of approximately 2.5 kDa.

As the reaction progressed, it was possible to estimate the degree of polymerisation (X_n) from p. Nonetheless, the concentration of the components had a stoichiometric imbalance ($r = N_{COOH}/N_{OH} < 1$). Thus, the modified Carothers equation for the X_n was considered as follows,

$$X_n = \frac{1 + r}{1 + r - 2rp} \tag{3.2}$$

The number average molecular weight (M_n) was determined by assuming the typical hypotheses around the degree of polymerisation and neglecting the weight of the OH group present in the terminal groups. Thus,

$$M_n = X_n M_0 \tag{3.3}$$

where M_0 is the molecular weight of the repeating unit. M_0 was calculated from the weighted average of the components (diacids and diols) for each prepolymer formulation [22], which can be accessed in Table A.3 from Appendix A.2.2. Then, the extent of reaction (or conversion) and Equation 3.3 were combined as follows,

$$M_w = X_n M_0 (1 + p) \tag{3.4}$$

where M_w is the weight average molecular weight. The theoretical results from Equations 3.3 and 3.4 were compared with the molecular weights determined by GPC.

3.2.6 Blending process

Polyester prepolymers were cooled to a temperature between 140 °C and 150 °C after AN and viscosity achieved their respective target ranges. Then, prepolymers were diluted, without any previous purification step, using a blend of styrene and HEMA (in equal parts) as a reactive diluent. An incorporation temperature ranging between 75 °C and 85 °C was used during dilution to obtain the unsaturated polyester resins, which were cooled to room temperature as soon as they became homogeneous. The resin systems were blended to make their composition 60% prepolymer and 40% reactive diluent, both by weight.

3.2.7 Crosslinking

The 2 wt.% MEKP was used to initiate the free radical polymerisation of each resin and 1 wt.% cobalt octoate was added as a promoter. Resins were cured for 24 hours in a glass mould at 23 °C, post-cured at 100 °C for 4 hours, and allowed to stabilise at room temperature before any analysis was conducted.

3.2.8 Prepolymer characterisation

GPC tests were performed to determine the M_n, M_w, and dispersity ($Đ$) of the polyester main chain samples using THF as eluent, according to ISO 13885 [28] part 1, in a concentration of 1 mg/ml. The samples were filtered and injected into a column set consisting of one precolumn (8 × 50 mm) PSS SDV, and columns (8 × 300 mm) PSS SDV analytical linear S, both with a 3 µm particle size, and filled with polystyrene crosslinked with divinylbenzene (gel). The columns were equilibrated at 40 ℃ before elution with purged THF at a 1 ml/ min rate. The eluent was monitored using dual detectors; the first was a UV/Visible detector (model JASCO UV-4075) set to 254 nm, and the second was a Refractive Index Detector (model JASCO RI-4030), both held at 40 ℃. The molecular weights were calculated based on the retention time from a conventional calibration with narrow polystyrene standards (M_n of 266–59300 Da); see more details in Appendix A.3. The viscosity tests were performed on a Cone & Plate ICI viscometer from REL (Research Equipment London Ltd.), according to ISO 2884 [29] part 2. The viscosity was taken at 125 ℃ as the average value of three measurements.

3.2.9 Crosslinked thermoset characterisation

Tensile test specimens were prepared according to the geometry type 1A defined in ISO 527 [30] part 2 (see Appendix B.1.2). In general, five specimens were prepared for each type of resin and tested under laboratory conditions at 23 ± 2 ℃ and 58 ± 2% relative humidity.

DMA was performed to obtain thermomechanical properties using a dynamic mechanical analyser from TA Instruments, model DMA Q800. Specimens with dimensions 60 mm × 10 mm × 4 ± 0.5 mm were manufactured according to ASTM E1640 [31] and tested in a 35 mm dual cantilever configuration. The specimens were subjected to a constant strain amplitude of 15 µm at a constant oscillation frequency of 1 Hz while submitted to a temperature sweep at a constant heating rate of 2 ℃/ min, starting at –30 ℃ and ending at 150 ℃ (see Appendix B.2). The T_g was determined (i) based on the onset of the storage modulus decay and (ii) from the tan δ peak.

The crosslink density (ν_e) was determined based on the kinetic theory of rubber elasticity by using the following equation [32]:

$$\nu_e = \frac{G'}{\mathrm{RT}} = \frac{E'}{3\mathrm{RT}} \tag{3.5}$$

where R is the gas constant (8.314 J K/mol), T is the absolute temperature in K, and E' is the flexural storage modulus obtained in the rubbery plateau. Herein, the beginning of the rubbery state region of the storage modulus was taken to estimate the crosslink density.

The kinetic theory of rubber elasticity assumes that the network is ideal and all chains are effective in elastic deformation [33].

3.3 Results and discussion

The syntheses for all bio-based unsaturated polyester formulations were performed successfully. The main results for the prepolymer and thermoset polyesters obtained are presented below.

3.3.1 Bio-based mass and carbon content

Except for PA and EG, all other monomers are derived from renewable resources, resulting in prepolymer and thermoset polyesters with high bio-based carbon (x_B) and mass (m_B) contents, as shown in Table 3.2.

The high bio-based contents presented by polyesters fulfil one of the principles of green chemistry according to the procedure outlined in Annex B of ISO 16620 [34] part 1, with some unsaturated polyester resins reaching more than 50 wt.% of bio-based content. The results also show a higher bio-content as the FA ratio increases in the main chain, since FA is bio-based and was used to increase the crosslink density of the polymer and, in turn, decrease the amount of FA. Furthermore, as expected, the replacement of EG by PDO and ISO also increases the polyester's bio-content.

Table 3.2: Bio-based carbon (x_B) and mass (m_B) contents of the prepolymers and their respective thermoset resins, determined according to the procedure outlined in Annex B of ISO 16620 [27] part 4.

Sample	x_B	m_B
	(%)	**(%)**
UP-A (UPR-A)	63.7 (38.2)	68.7 (41.2)
UP-B (UPR-B)	69.7 (41.8)	73.7 (44.2)
UP-C (UPR-C)	80.1 (48.1)	76.8 (46.1)
UP-D (UPR-D)	78.6 (47.2)	84.1 (50.4)
UP-E (UPR-E)	82.5 (49.5)	87.1 (52.3)

Although x_B and m_B have decreased after incorporation of the prepolymers with the reactive diluents because these are not fully derived from renewable resources, the partial replacement of styrene by HEMA also allowed to obtain UPRs with a lower styrene content, benefiting from lower toxicity of HEMA relative to styrene. Moreover, bio-based reagents used in the proportions stipulated herein provided thermoset polyesters with a bio-content higher than 50%. Therefore, this study shows that the most recent advances achieved by synthesising thermoplastic polyesters based on renewable raw materials such as ISO can be expanded to produce unsaturated polyester resins, notably by introducing bio-based FA unsaturation into the polyester main chain. Herein, the use of PDO proves to be essential to maintain a high bio-based content and ensure that these polyesters have viscosities comparable to their conventional (petroleum-based) counterparts.

3.3.2 Prepolymer characterisation

3.3.2.1 Kinetics and molecular weight distribution

All formulations had ANs equal to or below 50 mgKOH/g (see Table 3.3), which is similar to the typical ANs of conventional unsaturated polyester prepolymers [35]. Regarding the group (I) formulations with EG, increasing amounts of FA decreased the AN. However, the same was not observed for group (II) formulations, containing PDO and ISO, where the ANs were equal for both prepolymers. In addition, the higher reactivity presented by the UP-B and UP-C formulations resulted in a higher conversion of the prepolymer main chain and, consequently, higher degrees of polymerisation, as discussed ahead.

Table 3.3: Prepolymer composition analysis.

Sample	**Time**	**AN**	**Theoretical**		**GPC analysis**				
			p	X_n	M_n	M_w	$Đ$	p	X_n
	(min)	**(mgKOH/g)**	**(%)**	**(a.u)**	**(kDa)**	**(kDa)**	**(-)**	**(%)**	**(a.u)**
UP-A (UPR-A)	480	50	90	6.6	1.42	4.00	2.81	91	7.4
UP-B (UPR-B)	480	45	91	7.1	1.46	2.76	1.89	92	7.8
UP-C (UPR-C)	360	38	92	7.9	1.56	2.77	1.77	93	8.5
UP-D (UPR-D)	480	47	90	6.8	1.45	3.59	2.47	91	7.1
UP-E (UPR-E)	480	47	90	6.9	1.24	2.59	2.09	88	6.2

Kinetic plots of X_n, calculated from Equation 3.2, as a function of time are illustrated in Figure 3.2 for the last 20% of the polyesterification, occurring after 180 min, when the reaction medium has few pure reagents, and the ester product no longer acts as a solvent. Deviation below 80% conversion also occurs for the simple esterification that results when a monocarboxylic acid replaces dicarboxylic acid [36].

The results show very similar reaction rates (k_2, slope of the degree of polymerisation *vs.* time) among formulations, except for UP-C, which presented much higher conversion for a shorter reaction time compared with the other formulations, achieving the highest theoretical degree of polymerisation. The higher fumaric acid concentration can explain this phenomenon in UP-C. In fact, as the formulation had a higher fumaric acid concentration, higher conversions were achieved for both groups I and II.

Figure 3.3 present the signal as a function of retention time results obtained from the gel permeation chromatography tests.

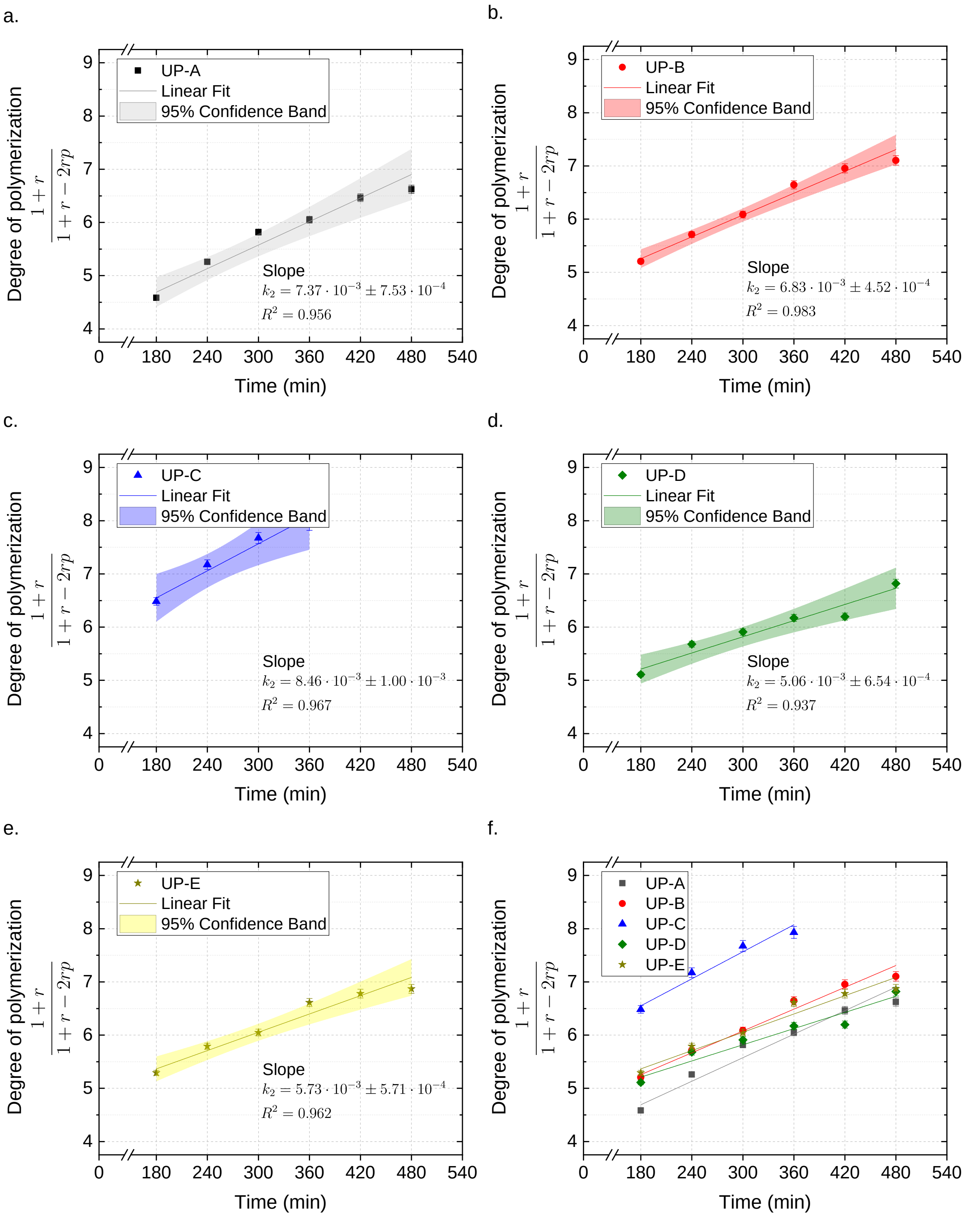

Figure 3.2: Kinetics of polyesterification reaction for the polyester prepolymers: a. UP-A; b. UP-B; c. UP-C; d. UP-D; e. UP-E; and f. overlapping of various formulations.

The results show that the prepolymers of both groups (I) and (II) behaved as low molecular weight macromolecules (oligoesters), with M_n varying between 1.2 kDa and 1.5 kDa, which falls within the range referred in the literature for unsaturated polyesters [37,38], with a degree of polymerisation lower than 10 for all samples. These oligoesters with low degree of polymerisation resulted in resins with low working viscosities when dissolved with the reactive diluent. Limiting the prepolymer viscosity resulted in cutting the reaction at lower conversions than those observed in thermoplastic polyesters. However, the degrees of polymerisation obtained herein agree with those reported in the literature for thermoset polyesters, which range between 6 and 15 [39,40].

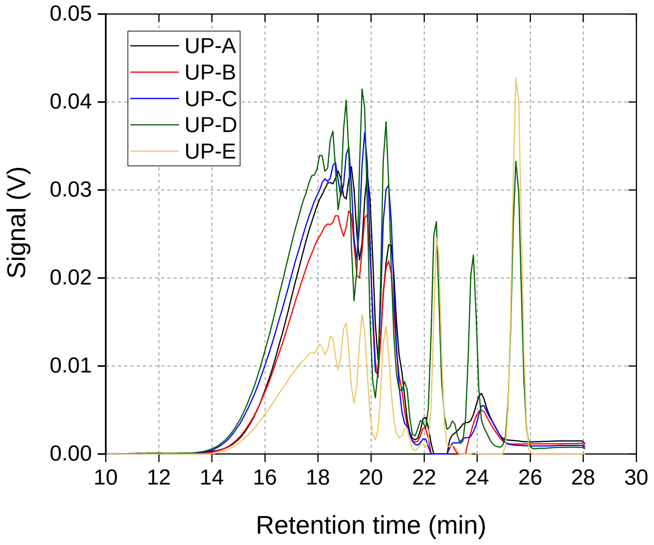

Figure 3.3: GPC curves for all formulations.

Furthermore, it is observed that increasing the FA content for the group (I) formulations with EG resulted in polyester prepolymers with longer chain lengths and lower dispersity. By contrast, the results obtained for group (II) formulations show that the total replacement of EG by the other bio-based diols (PDO and ISO) results in lower M_n and higher dispersity when compared to formulations from the group (I) with the same FA content, namely UP-B and UP-C. The higher ISO concentration can explain this behaviour, since the steric hindrance from their secondary alcohols results in lower conversion for the same reaction time during synthesis of the polyester prepolymer, where macromolecules with lower chain lengths are produced. Finally, EG has primary alcohol groups that are more reactive with the diacid/anhydride monomers than ISO, and a more homogeneous material is obtained.

3.3.2.2 Prepolymer viscosity

Monitoring viscosity during synthesis allowed ensuring that all polyester prepolymers had viscosities at 125 ℃ below 2000 cP, as shown in Figure 3.4. This criterion enabled the production of unsaturated polyester prepolymers with suitable viscosity for subsequent incorporation with a percentage of reactive diluent of 40 wt.%. Furthermore, low viscosity polyesters promote better cure performance due to the higher mobility of the polymeric chains, aligning with the industry standards regarding conventional resins for impregnating synthetic or natural fibres used in FRP composites.

In this study, increasing viscosity is among the main factors that limited reaction progress to higher conversions. ISO is known to contribute to a more significant increase in

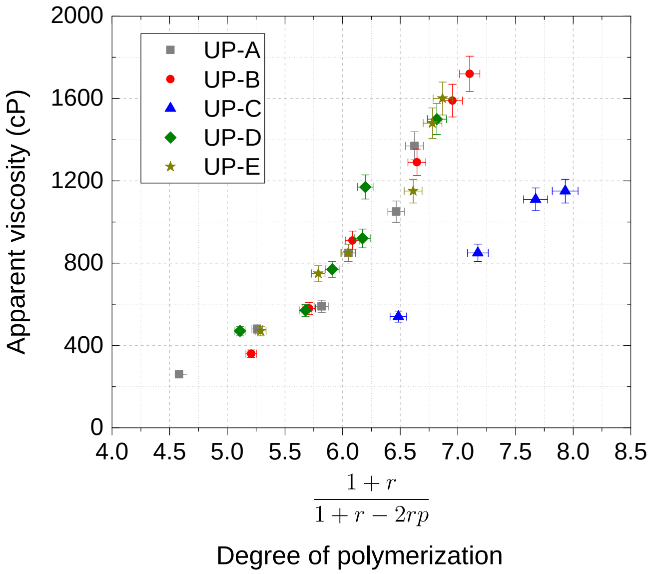

Figure 3.4: Viscosity of the prepolymers measured at 125 ℃.

prepolymer viscosity compared to other aliphatic diols due to its intrinsic characteristics of steric hindrance [41] and *Ordelt* saturation (branched formation) with FA. Even if branching takes place at a low level, without further crosslinking and gelling, the obtained prepolymers are generally unsuitable for preparing UPR due to their high viscosity. Furthermore, an unsaturated polyester prepolymer synthesised exclusively from ISO would likely not be miscible with styrene [42]. The curing process would also result in inhomogeneous network formation with poor mechanical properties. Herein, all formulations contain a maximum of 33 mol% ISO concerning the total amount of glycol, limiting the excessive increase in viscosity due to ISO. In addition, inhibitors (hydroquinone and toluhydroquinone) were added to minimise *Ordelt* saturation and mitigate gelling. Finally, the deviation of the UP-C formulation compared to the other ones agrees with the previously shown higher degree of polymerisation obtained with the former formulation.

3.3.3 Resin characterisation

3.3.3.1 Resin viscosity

The viscosity of the UPRs was measured under the same procedures performed for the prepolymer but at 25 ℃. The results from Table 3.4 also show that the unsaturated polyester resins developed herein are suitable for different processing techniques used in composites, such as hand layup, vacuum infusion, and pultrusion. In addition, these resins have the additional advantage of having a lower styrene concentration than typical (conventional) thermoset polyesters, this reduction being of 50% of the total amount of styrene used compared to a styrene-only reactive diluent.

Table 3.4: Viscosity of the unsaturated polyester resins.

Sample	Incorporation ratio			Viscosity at 25 ℃
	Prepolymer (%)	Styrene (%)	HEMA (%)	(cP)
UPR-A	60	20	20	780
UPR-B	60	20	20	950
UPR-C	60	20	20	750
UPR-D	60	20	20	800
UPR-E	60	20	20	820

3.3.3.2 Tensile properties

Tensile stress-strain nominal curves are analysed herein to assess the effects of the different building blocks on the mechanical properties of the bio-based thermoset polyesters. Figure 3.5 illustrates one representative curve for each thermoset polyester formulation, showing that all formulations presented tensile curves with an initial linear elastic branch, followed by a gradual loss of stiffness for higher strains, resulting in the brittle tensile failure of the specimen, as is typical for conventional thermoset polyesters under tension.

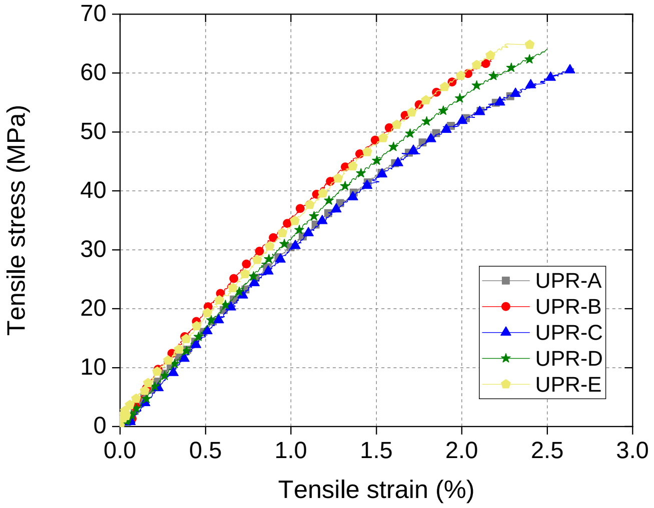

Figure 3.5: Representative tensile stress-strain curves for the biobased thermoset polyesters.

Figure 3.6 presents the tensile strength, modulus of elasticity, and strain at break results obtained for the bio-based thermoset polyester resins. Regarding tensile strength, all resins have very similar results, with mean values ranging from 55 to 62 MPa; however, (i) the mean values are higher for group (II) formulations, synthesised with PDO and ISO, confirming the hypothesis that it is possible to increase the thermoset polyester's bio-content by replacing EG (petroleum-derived) without reducing its strength; (ii) although UPR-A has lower mean tensile strength than UPR-B and UPR-C, the corresponding relative differences are within the standard deviations obtained for these formulations, showing that the increasing ratios of unsaturated to saturated acid adopted here do not significantly affect the tensile strength of the resin; (iii) the same observation may be made for UPR-D and UPR-E, whose results also show no significant differences, and (iv) as a consequence of the previous point, samples with higher FA concentration result in greener thermoset polyesters exhibiting higher thermomechanical properties (as discussed ahead), since higher unsaturated acid content in the main chain potentially results in greater crosslink density, due to the increased availability of double bonds (crosslinkers).

The bio-based thermoset polyesters studied herein exhibited modulus of elasticity that ranged between 3.2 and 3.9 GPa, thus lying within the typical range of values presented by comparable general-purpose commercial products, 2 to 4 GPa [43]. The comparison of the modulus of elasticity results obtained for the different bio-based resins prompts the following comments: (i) UPR-B has the highest mean value among all tested formulations; (ii) as a result, UPR-D, synthesised from bio-based diols in lieu of ethylene glycol, achieved a lower mean value than its counterpart UPR-B of equal crosslink density, thus showing that (iii) for an equal ratio of unsaturated to saturated acid, shorter chains (provided by EG) *versus* longer chains (provided by PDO) resulted in a thermoset with a higher modulus of elasticity, which is therefore more resistant to deformation within the linear elastic stress-strain range; (iv) however, this was not observed for UPR-C and UPR-E, which do not present significant differences between their mean values.

The strains at break of the various thermoset polyesters tested herein, all with high bio-content, have mean values equal to or higher than 2%, thus being compatible with the primary synthetic fibres (glass and carbon) used to manufacture fibre-reinforced polymer composites. Strains at break from group (II) formulations are similar to those of their group (I) counterparts. The following observations are made about the strain at break: (i) UPR-C is the most deformable (flexible) thermoset polyester, since despite having a higher crosslink density, it also has higher X_n and M_n with longer chains than UPR-A and UPR-B, which finally resulted in a more deformable polymer; (ii) UPR-B has a lower mean value than UPR-A, since although both have similar M_n, UPR-B has a higher crosslink density; and (iii) the lower strain at break of UPR-E compared to UPR-D can be partially explained by its higher crosslink density and lower M_n. Therefore, these results show that, for the formulations tested, the strains at break were more influenced by the distribution of molecular weight, chain length, and crosslink density than by the replacement of EG with other glycols from renewable sources.

3.3.3.3 Dynamic mechanical analysis

Dynamic mechanical analysis was used to determine the thermomechanical properties of the cured resins and establish the structural effects of the bio-based constituents on those properties. Figure 3.7 presents the dynamic mechanical analysis curves for the storage modulus (E'), loss modulus (E''), and damping factor (tan δ) of the bio-based resins developed herein, all as function of temperature.

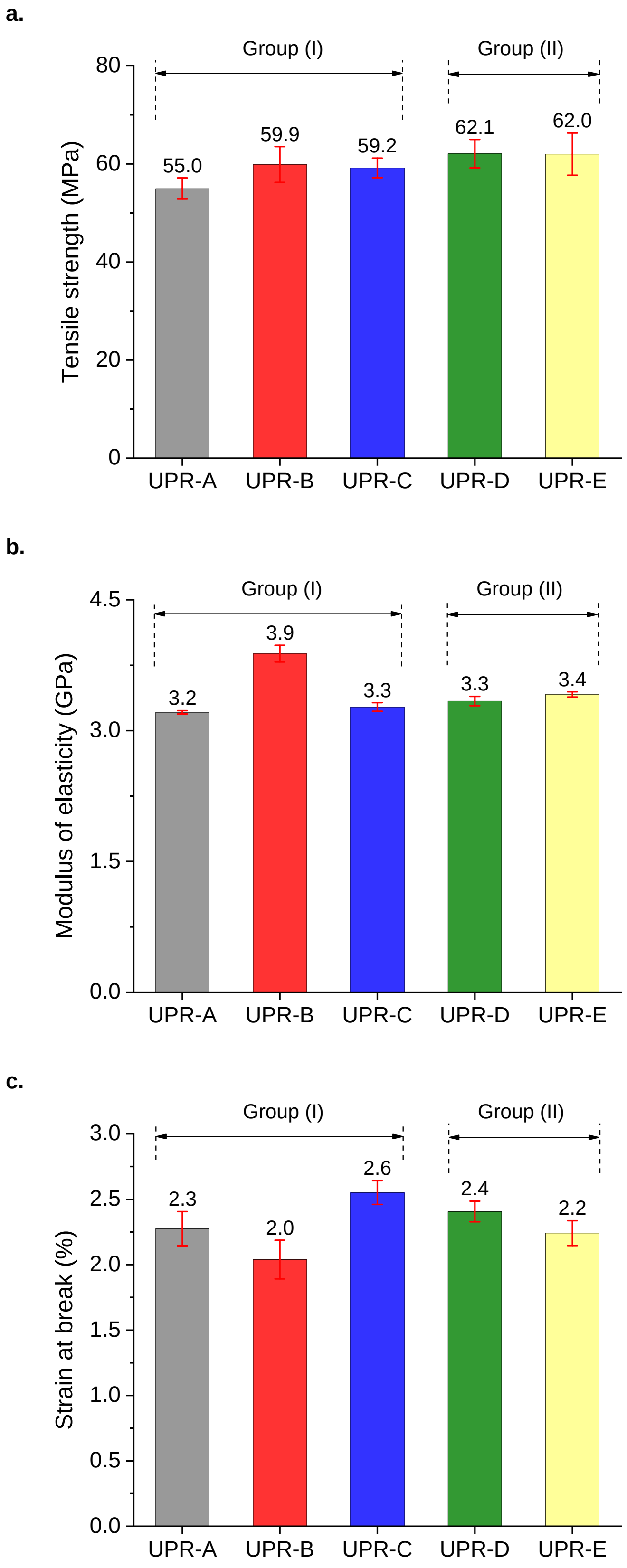

Figure 3.6: Tensile properties of the thermoset polyesters: **a.** tensile strength, **b.** modulus of elasticity, and **c.** strain at break.

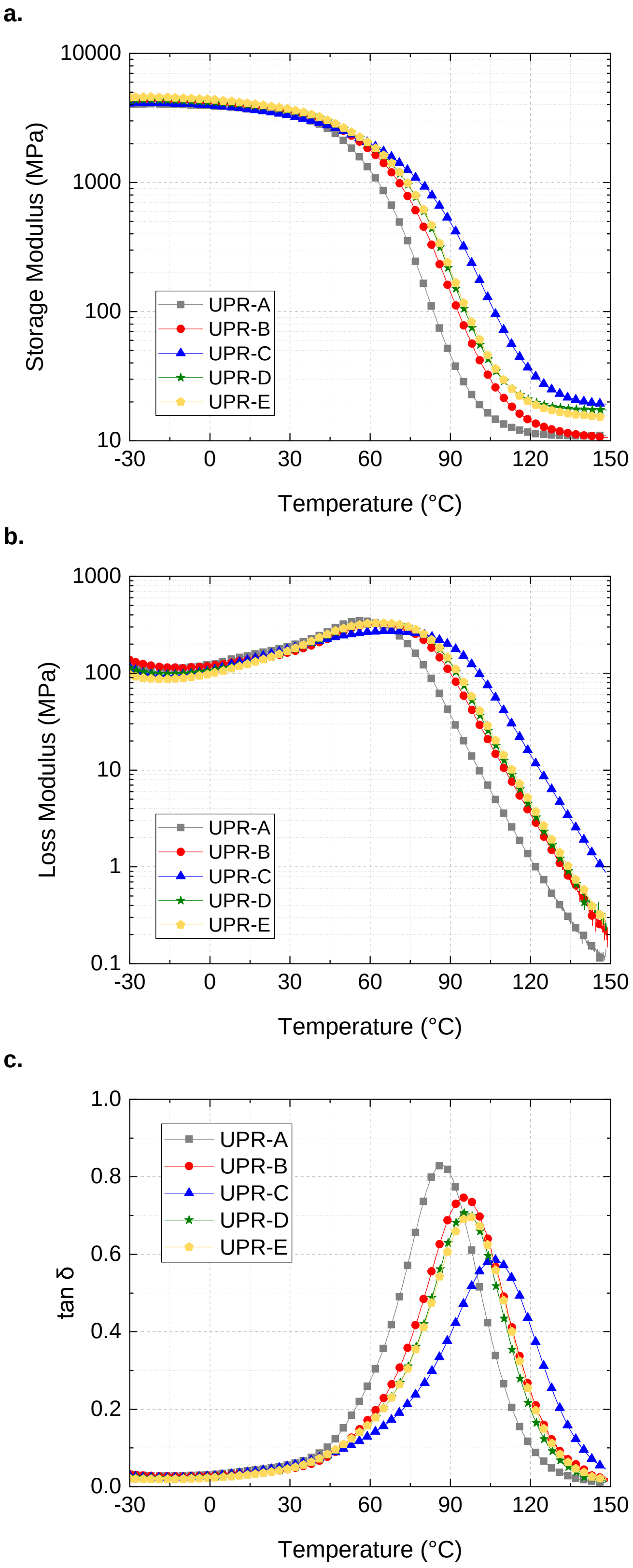

Figure 3.7: Dynamic mechanical analysis curves of the thermoset polyesters: **a.** storage modulus, **b.** loss modulus, and **c.** tan δ.

Regarding the damping factor, for all formulations, the polymeric chain is stable and does not show any movement with temperatures ranging from -30 to $\sim$ 0 °C since its energy dissipation is low. The glass transition stage starts from positive temperatures onwards; however, for all formulations, the chain movement is still very restricted with non-significant values of energy dissipation up to $\sim$ 30 °C. As the temperature increases above 30 °C, the affinity between molecules drops, resulting in a permanent deformation due to the chain movement. The glass transition to a rubbery state starts when the intramolecular interaction has its lowest value, or the highest tan δ value is reached, also known as the alpha transition temperature. The alpha transition temperature occurs when the material is in a leathery state, and a transition from the leathery-to-rubbery to the rubbery state ensues. Figure 3.8 shows an example of these states and transitions as a function of temperature, illustrated for UPR-D.

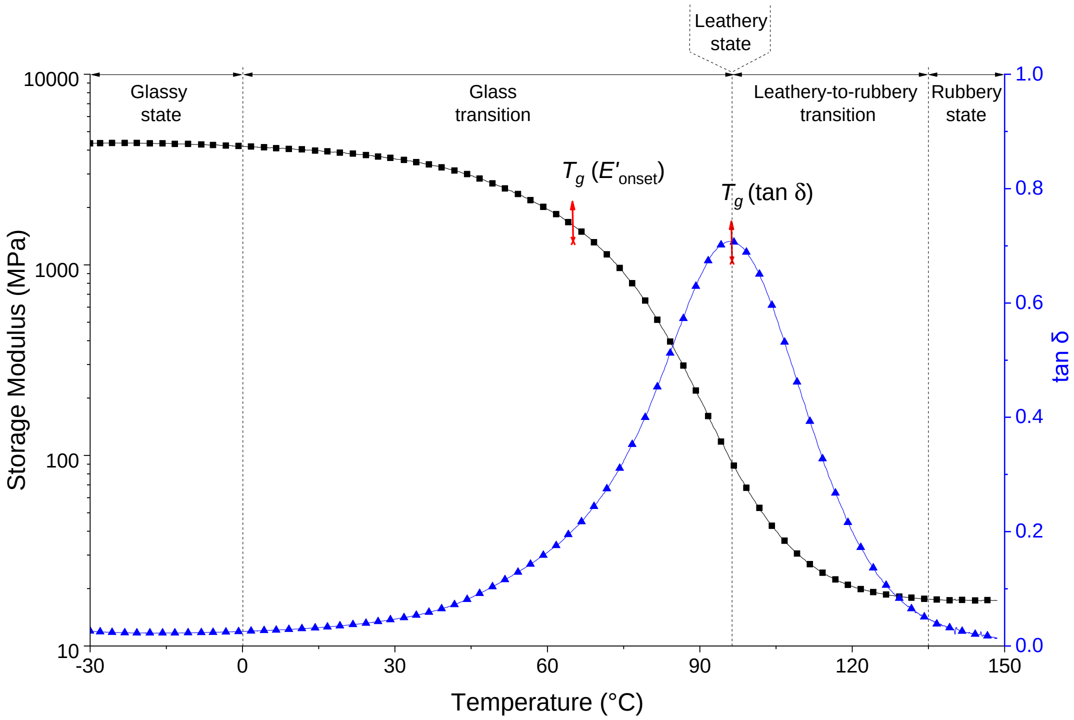

Figure 3.8: Definition of different material states and transitions for the UPR-D thermoset.

In this study, all thermoset formulations have their alpha transition temperatures ranging from 87 to 106 °C, and above this temperature range a gradual drop in tan δ value occurs. UPR-A has the lowest alpha transition temperature value for group (I), probably due to the weak intermolecular chain bonding. In addition, UPR-A has a higher capacity to dissipate energy in the form of heat due to its viscous molecular movements, followed by UPR-B and UPR-C. The higher alpha transition temperature from group (I) is associated to the increasing concentration of FA. Consequently, the higher crosslink density leads to a more cohesive crosslinked network, which translates into higher stiffness (higher E') and into higher amount of energy released when the chains start to move (higher E''). This result may be particularly relevant for several high-performance applications since the energy dissipation capacity is essential for several mechanical properties (*e.g.*, impact strength).

The damping factor peak broadness also increases due to higher crosslink density arising from increased FA concentration. As a result, the deformation in the chain is viscous (in viscoelastic material), which results in a higher loss modulus in the leathery state, leathery-to-rubbery transition, and rubbery state. However, group (II) generated from chain structures (blocks) exclusively based on PDO and isosorbide (without EG) have resulted in equal or lower loss modulus (in the glassy state) for UPR-D and UPR-E against their counterparts with the same FA concentration from group (I).

Figure 3.9 presents the Cole-Cole plot from the loss modulus as a function of the storage modulus, reflecting the viscoelastic behaviour and homogeneity of all formulations. A perfectly semi-circular shape of the curves would define an ideal material with equal storage and loss modulus characteristics. Although the curves shown in Figure 3.9 are not perfect semi-circles, the moduli of all formulations vary similarly. In addition, group (II) formulations have similar behaviour to UPR-C, which is the formulation in group (I) with the highest T_g, with the former exhibiting slightly higher loss modulus in the range between 1 GPa and 3 GPa of storage modulus. This agrees with the hypothesis that the group (II) formulations are slightly more deformable in the glassy state than UPR-C, which is also reflected in the results of the tensile tests.

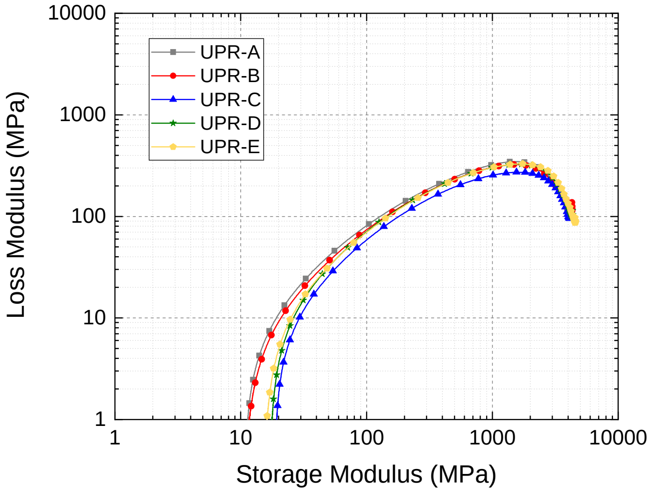

Figure 3.9: Cole-Cole plot.

Table 3.5 shows the thermomechanical and crosslink density results. Two different measurements were used to determine the T_g: (i) the onset of the storage modulus decay, which indicates the temperature at which the storage modulus begins to drop more significantly (lower boundary value or onset), and (ii) the alpha transition temperature from the damping factor, indicating the sample's capacity to dissipate energy since molecular chain mobility is directly proportional to the temperature (upper boundary or tan δ peak). Additionally, this table presents the storage modulus values measured at 25 ℃, 50 ℃, and 135 ℃, as well as the crosslink density determined based on the kinetic theory of rubber elasticity.

Table 3.5: Dynamic mechanical analysis results for the bio-based thermoset polyesters.

Sample	T_g (°C)		E' (MPa)			ν_e
	E'_{onset}	tan δ	25 °C	50 °C	135 °C	(mol/m^3)
UPR-A	56	87	3495	2104	11.2	1.07
UPR-B	62	95	3736	2519	12.8	1.12
UPR-C	71	106	3448	2495	27.4	2.09
UPR-D	66	96	3745	2618	18.9	1.73
UPR-E	65	97	3816	2645	17.8	1.58

As expected, a sharp drop in E' is observed in the glass transition region for all formulations, being most pronounced for UPR-A. In addition, UPR-A and UPR-C have the lowest E' values at the glassy state, resulting in lower stiffness compared with the other formulations throughout this temperature range. However, this trend maintains towards higher temperatures only for UPR-A, including in the rubbery state. Regarding group (I) formulations, the decay of storage modulus occurred for the highest temperature range for UPR-C, and occurred for the lowest temperature range for UPR-A. Among the formulations of group (II), UPR-D and UPR-E did not show significant differences in the decay of their respective storage modulus with temperature.

Comparing the two groups, one can observe that the replacement of EG by PDO and ISO did not have a significant effect on the development of the E' values. The results obtained for UPR-D were very close to those of UPR-B, with the former exhibiting slightly higher T_g and with the advantage that UPR-D has a higher bio-content due to the replacement of EG by PDO and ISO. Additionally, the group (II) formulations presented similar results for all temperature ranges, for all states and all transitions. The observation that the group (II) formulations were able to match or exceed the glass transition temperatures of their counterparts of lower bio-based content is encouraging, as it suggests that it is possible to increase the bio-based content of thermoset polyesters while achieving suitable working temperature ranges for several high-performance applications.

Finally, although the bio-based thermoset polyesters presented herein have been generated from low molecular weight oligomers (which results in a large amount of end groups), this is believed to have been compensated by the reduction of segmental mobility of the polymers around the crosslink junctions. In addition, most of these end groups are consumed during cure, and crosslinks are generated simultaneously [44]. Herein, the design of the main chains (by varying the concentration of bio-based FA) minimised the effect of the low molecular weight of polyesters. Thus, regarding the onset of storage modulus decay, the glass transition temperatures ranged from 56 to 71 °C. These values meet or exceed most of the results reported in the literature for bio-based thermoset polyesters [22,23,25,35,45–50]. Furthermore, they enable the use of the proposed resins in a wide range of high-performance applications, such as FRP composites.

3.4 Concluding remarks

Syntheses of UPRs based on renewable building blocks have been successfully carried out. The synthesised polyester prepolymers are almost entirely based on raw materials derived from renewable sources (reaching 87.1 wt.% bio-content). The high bio-based content of polyester prepolymers, combined with their incorporation in a reactive diluent formed by mixing two reactive monomers (styrene and HEMA), allowed the production of thermoset polyesters that are less reliant on non-renewable resources and are less toxic than their fully petroleum-derived counterparts.

We also found that thermoset polyesters obtained from formulations synthesised exclusively with PDO and ISO as glycols exhibit mechanical and thermomechanical properties that meet or exceed their partially EG-based counterparts also tested herein. Moreover, the processing properties of the UPRs developed here fall within the range of viscosities for many fibre impregnation processing techniques, such as hand layup, vacuum infusion, and pultrusion, with the advantage that some resins have reached more than 50 wt.% of bio-content. Consequently, the properties of these bio-based thermoset polyesters enhance their prospects as successful high-performance green materials, which can be exploited, for example, by the composites industry.

Finally, this study showed that the challenge of expanding the scope and range of application of bio-based UPRs is considerable; however, it is considered that the complex issues surrounding the balance between sustainability, high performance, and processability must take into account the following considerations:

i) the macromolecular structure must be formed from building blocks derived from renewable raw materials that contain unsaturations (provided by unsaturated acid) and rigid structures (provided either by saturated acids or cyclic or aromatic glycols);

ii) the EG typically used in general-purpose UPRs can be entirely replaced by PDO and ISO, both bio-based;

iii) PA is still essential for the synthesis of high-performance unsaturated polyesters due to the stiffness it confers to the polymer and its low cost, but other alternatives to this block must be found to reach fully bio-based and commercially competitive unsaturated polyester chains; and

iv) reactive monomers that can be used as diluents in replacement of styrene must be investigated to produce bio-based unsaturated polyester resins with high mechanical and thermomechanical performance, maintaining low viscosity, while being competitive with their fully petroleum-derived counterparts.

3.5 References

[1] Yunqing Zhu, Charles Romain, and Charlotte K. Williams. Sustainable polymers from renewable resources. *Nature*, 540(7633):354–362, 2016.

[2] Vesna V. Panic, Sanja I. Seslija, Ivanka G. Popovic, Vuk D. Spasojevic, Aleksandar R Popovic, Vladimir B Nikolic, and Pavle M Spasojevic. Simple one-pot synthesis of fully biobased unsaturated polyester resins based on itaconic acid. *Biomacromolecules*, 18(12):3881–3891, 2017.

[3] Amar K. Mohanty, Singaravelu Vivekanandhan, Jean-Mathieu Pin, and Manjusri Misra. Composites from renewable and sustainable resources: Challenges and innovations. *Science*, 362(6414):536–542, 2018.

[4] U. D. Bajpai and Nivedita. Plasticizing polyesters of dimer acids and 1,4-butanediol. In Nicholas P. Cheremisinoff, editor, *Advances in Engineering Fluid Mechanics: Multiphase Reactor and Polymerization System Hydrodynamics*, chapter 22, pages 583–597. Gulf Professional Publishing, Burlington, 1996.

[5] Maike Unverferth. *Fatty acid-derived branched polymer architectures*. PhD thesis, Karlsruhe Institute of Technology (KIT), 2016.

[6] Magdalena Kwiatkowska, Inez Kowalczyk, Konrad Kwiatkowski, Anna Szymczyk, and Zbigniew Rosłaniec. Fully biobased multiblock copolymers of furan-aromatic polyester and dimerized fatty acid: Synthesis and characterization. *Polymer*, 99:503–512, 2016.

[7] George Z. Papageorgiou, Dimitrios G. Papageorgiou, Zoi Terzopoulou, and Dimitrios N. Bikiaris. Production of bio-based 2,5-furan dicarboxylate polyesters: Recent progress and critical aspects in their synthesis and thermal properties. *European Polymer Journal*, 83:202–229, 2016.

[8] Andreia F. Sousa, Carla Vilela, Ana C. Fonseca, Marina Matos, Carmen S. Freire, Gert-Jan M. Gruter, Jorge F. Coelho, and Armando J. Silvestre. Biobased polyesters and other polymers from 2,5-furandicarboxylic acid: a tribute to furan excellency. *Polym. Chem.*, 6(33):5961–5983, 2015.

[9] Min Jiang, Qian Liu, Qiang Zhang, Chong Ye, and Guangyuan Zhou. A series of furan-aromatic polyesters synthesized via direct esterification method based on renewable resources. *Journal of Polymer Science Part A: Polymer Chemistry*, 50(5):1026–1036, 2012.

[10] Andrii Kostyniuk, Miha Grilc, and Blaž Likozar. Catalytic cracking of biomass-derived hydrocarbon tars or model compounds to form biobased benzene, toluene, and xylene isomer mixtures. *Industrial & Engineering Chemistry Research*, 58(19):7690–7705, 2019.

[11] Sara Giarola, Charles Romain, Charlotte K. Williams, Jason P. Hallett, and Nilay Shah. Techno-economic assessment of the production of phthalic anhydride from corn stover. *Chemical Engineering Research and Design*, 107:181–194, 2016. Biorefinery Value Chain Creation.

[12] Fabíola S. Carta, Carlos R. Soccol, Luiz P. Ramos, and José D. Fontana. Production of fumaric acid by fermentation of enzymatic hydrolysates derived from cassava bagasse. *Bioresource Technology*, 68(1):23–28, 1999.

[13] Feng Guo, Min Wu, Zhongxue Dai, Shangjie Zhang, Wenming Zhang, Weiliang Dong, Jie

Zhou, Min Jiang, and Fengxue Xin. Current advances on biological production of fumaric acid. *Biochemical Engineering Journal*, 153:107397, 2020.

[14] Sang Yup Lee, Hyun Uk Kim, Tong Un Chae, Jae Sung Cho, Je Woong Kim, Jae Ho Shin, Dong In Kim, Yoo-Sung Ko, Woo Dae Jang, and Yu-Sin Jang. A comprehensive metabolic map for production of bio-based chemicals. *Nature Catalysis*, 2(1):18–33, 2019.

[15] Hildeberto Nava. Polyesters, Unsaturated. In Herman F. Mark, editor, *Encyclopedia of Polymer Science and Technology*, chapter 11, pages 41–64. John Wiley & Sons, Inc, 3 edition, 2015.

[16] Rajendra K. Saxena, Pinki Anand, Saurabh Saran, and Jasmine Isar. Microbial production of 1,3-propanediol: Recent developments and emerging opportunities. *Biotechnology Advances*, 27(6):895–913, 2009.

[17] Ching Shya Lee and Mohamed K. Aroua and Wan M. Daud and Patrick Cognet and Yolande P. Péres-Lucchese and Paul-Louis Fabre and Olivier Reynes and Laure Latapie. A review: Conversion of bioglycerol into 1,3-propanediol via biological and chemical method. *Renewable and Sustainable Energy Reviews*, 42:963–972, 2015.

[18] Mario Pagliaro. C3-Monomers. In Mario Pagliaro, editor, *Glycerol: The Renewable Platform Chemical*, chapter 2, pages 23–57. Elsevier, 2017.

[19] Dietrich Braun and Matthias Bergmann. 1,4:3,6-Dianhydrohexite als Bausteine fur Polymere. *Journal fur praktische Chemie Chemiker-Zeitung*, 334(4):298–310, jan 1992.

[20] Sebastián Muñoz-Guerra, Cristina Lavilla, Cristina Japua, and Antxon M. Ilarduyaa. Renewable terephthalate polyesters from carbohydrate-based bicyclic monomers. *Green Chemistry*, 16(4):1716–1739, 2014.

[21] Claudio Gioia, Micaela Vannini, Paola Marchese, Alessandro Minesso, Roberto Cavalieri, Martino Colonna, and Annamaria Celli. Sustainable polyesters for powder coating applications from recycled PET, isosorbide and succinic acid. *Green Chemistry*, 16(4):1807–1815, 2014.

[22] Joshua M. Sadler, Faye R. Toulan, Giuseppe R. Palmese, and John J. La Scala. Unsaturated polyester resins for thermoset applications using renewable isosorbide as a component for property improvement. *Journal of Applied Polymer Science*, 132(30), 2015.

[23] Yunsheng Xu, Geng Hua, Minna Hakkarainen, and Karin Odelius. Isosorbide as Core Component for Tailoring Biobased Unsaturated Polyester Thermosets for a Wide Structure–Property Window. *Biomacromolecules*, 19(7):3077–3085, 2018.

[24] Kingsley Kema Ajekwene. Properties and Applications of Acrylates. In Ángel Serrano-Aroca and Sanjukta Deb, editors, *Acrylate Polymers for Advanced Applications*, chapter 3. IntechOpen, 2020.

[25] Ana C. Fonseca, Inês M. Lopes, Jorge F. Coelho, and Arménio C. Serra. Synthesis of unsaturated polyesters based on renewable monomers: Structure/properties relationship and crosslinking with 2-hydroxyethyl methacrylate. *Reactive and Functional Polymers*, 97:1–11, 2015.

[26] Kun Liang, Marco Dossi, Davide Moscatelli, and Robin A. Hutchinson. An Investigation of Free-Radical Copolymerization Propagation Kinetics of Styrene and 2-Hydroxyethyl Methacrylate. *Macromolecules*, 42(20):7736–7744, 2009.

[27] ISO 16620-4. Plastics - Biobased content - Part 4: Determination of biobased mass content.

Technical report, International Organization for Standardization, Geneva, Switzerland, 2016.

[28] ISO 13885. Gel permeation chromatography (GPC) - Part 1: Tetrahydrofuran (THF) as eluent. Technical report, International Organization for Standardization, Geneva, Switzerland, 2008.

[29] ISO 2884. Paints and varnishes - Determination of viscosity using rotatory viscometers - Part 2: Disc or ball viscometer operated at a specified speed. Technical report, International Organization for Standardization, Geneva, Switzerland, 2003.

[30] ISO 527. Plastics - Determination of tensile properties - Part 2: Test conditions for moulding and extrusion plastics. Technical report, International Organization for Standardization, Geneva, Switzerland, 2012.

[31] ASTM E1640. Standard test method for assignment of the glass transition temperature by dynamic mechanical analysis. Technical report, ASTM International, West Conshohocken, Pennsylvania, 2018.

[32] Loren W. Hill. Calculation of crosslink density in short chain networks. *Progress in Organic Coatings*, 31(3):235–243, 1997.

[33] James E. Mark. Experimental Determinations of Crosslink Densities. *Rubber Chemistry and Technology*, 55(3):762–768, jul 1982.

[34] ISO 16620-1. Plastics - Biobased content - Part 1: General principles. Technical report, International Organization for Standardization, Geneva, Switzerland, 2015.

[35] Cátia S. Costa, Ana C. Fonseca, Jorge Moniz, Maria Godinho, Jorge F. Coelho, and Arménio C. Serra. Going greener: Synthesis of fully biobased unsaturated polyesters for styrene crosslinked resins with enhanced thermomechanical properties. *Express Polymer Letters*, 11(11):885–898, 2017.

[36] Harry R. Allcock, Frederick W. Lampe, and James E. Mark, editors. *Contemporary Polymer Chemistry*. Prentice Hall, New Jersey, 3 edition, 2003.

[37] Alain Fradet and Martine Tessier. *Polyesters*, chapter 2, pages 17–134. John Wiley & Sons, Ltd, 2003.

[38] Keith G. Johnson and Lau S. Yang. *Preparation, Properties and Applications of Unsaturated Polyesters*, chapter 21, pages 697–713. John Wiley & Sons, Ltd, 2004.

[39] Earl E. Parker and E. W. Moffett. Physical properties of polyester resin. *Industrial & Engineering Chemistry*, 46(8):1615–1618, 1954.

[40] Frank R. Jones. Unsaturated Polyester Resins. In Marianne Gilbert, editor, *Brydson's Plastics Materials (Eighth Edition)*, chapter 26, pages 743–772. Butterworth-Heinemann, 8th edition, 2017.

[41] Bart A. Noordover, Viola G. van Staalduinen, Robbert Duchateau, Cor E. Koning, van Benthem, Manon Mak, Andreas Heise, August E. Frissen, and Jacco van Haveren. Co- and Terpolyesters Based on Isosorbide and Succinic Acid for Coating Applications: Synthesis and Characterization. *Biomacromolecules*, 7(12):3406–3416, 2006.

[42] Françoise Fenouillot, Alain Rousseau, Gael Colomines, René Saint-Loup, and Jean P. Pascault. Polymers from renewable 1,4:3,6-dianhydrohexitols (isosorbide, isomannide and isoidide): A review. *Progress in Polymer Science*, 35(5):578–622, 2010.

[43] Andreas Kandelbauer, Gianluca Tondi, Oscar C. Zaske, and Sidney H. Goodman. Unsaturated Polyesters and Vinyl Esters. In Hanna Dodiuk and Sidney H B T Handbook of Thermoset Plastics (Third Edition) Goodman, editors, *Handbook of Thermoset Plastics*, chapter 6, pages 111–172. William Andrew Publishing, Boston, 3 edition, 2014.

[44] H. Stutz, K.-H. Illers, and J. Mertes. A generalized theory for the glass transition temperature of crosslinked and uncrosslinked polymers. *Journal of Polymer Science Part B: Polymer Physics*, 28(9):1483–1498, 1990.

[45] Sylvain Cousinet, Ali Ghadban, Etienne Fleury, Frédéric Lortie, Jean-Pierre Pascault, and Daniel Portinha. Toward replacement of styrene by bio-based methacrylates in unsaturated polyester resins. *European Polymer Journal*, 67:539–550, 2015.

[46] Joshua M. Sadler, Faye R. Toulan, Anh-Phuong T. Nguyen, Ronald V. Kayea, Saeed Ziaee, Giuseppe R. Palmese, and John J. La Scala. Isosorbide as the structural component of bio-based unsaturated polyesters for use as thermosetting resins. *Carbohydrate Polymers*, 100:97–106, 2014.

[47] Bojana Z. Fidanovski, Pavle M. Spasojevic, Vesna V. Panic, Sanja I. Seslija, Jelena P. Spasojevic, and Ivanka G. Popovic. Synthesis and characterization of fully bio-based unsaturated polyester resins. *Journal of Materials Science*, 53(6):4635–4644, 2018.

[48] Jinyue Dai, Songqi Ma, Na Teng, Xinyan Dai, Xiaobin Shen, Sheng Wang, Xiaoqing Liu, and Jin Zhu. 2,5-Furandicarboxylic Acid- and Itaconic Acid-Derived Fully Biobased Unsaturated Polyesters and Their Cross-Linked Networks. *Industrial & Engineering Chemistry Research*, 56(10):2650–2657, 2017.

[49] Pratiket B. Bamane, Kunal K. Wadgaonkar, Sachin U. Chambhare, Linchon B. Mehta, and Ramanand N. Jagtap. Replacement of traditional unsaturated acid by bio-based itaconic acid in the preparation of isophthalic acid-based unsaturated polyester resin. *Progress in Organic Coatings*, 147:105743, 2020.

[50] Andreia F. Sousa, Ana C. Fonseca, Arménio C. Serra, Carmen S. Freire, Armando J. Silvestre, and Jorge F. Coelho. New unsaturated copolyesters based on 2,5-furandicarboxylic acid and their crosslinked derivatives. *Polymer Chemistry*, 7(5):1049–1058, 2016.

Chapter 4

DFA-based unsaturated polyester

Abstract

This chapter presents the development of UP and their crosslinked resins (UPRs) based on dimer fatty acid (DFA) and other bio-based building blocks. The original features of these UPs derive from (i) the use of DFA as an aliphatic monomer, partially replacing PA; (ii) the introduction of a DFA-ISO block into the polyester backbone, with the presence of unsaturations provided by bio-based FA; (iii) the use of controlled excess of PDO to control the weight average molecular weight (M_w) and, consequently, the prepolymer viscosity, and (iv) the reduction of styrene content using HEMA. The developed UPRs have similar mechanical and thermomechanical behaviour to the petrochemical ones, presenting high T_g (up to 90 °C), high tensile modulus and strength (up to 2.9 GPa and 40 MPa, respectively) and viscosity of approximately 850 cP, making these resins greener alternatives to fully petroleum-derived UPRs. Figure 4.1 presents a graphical abstract summarising this chapter.

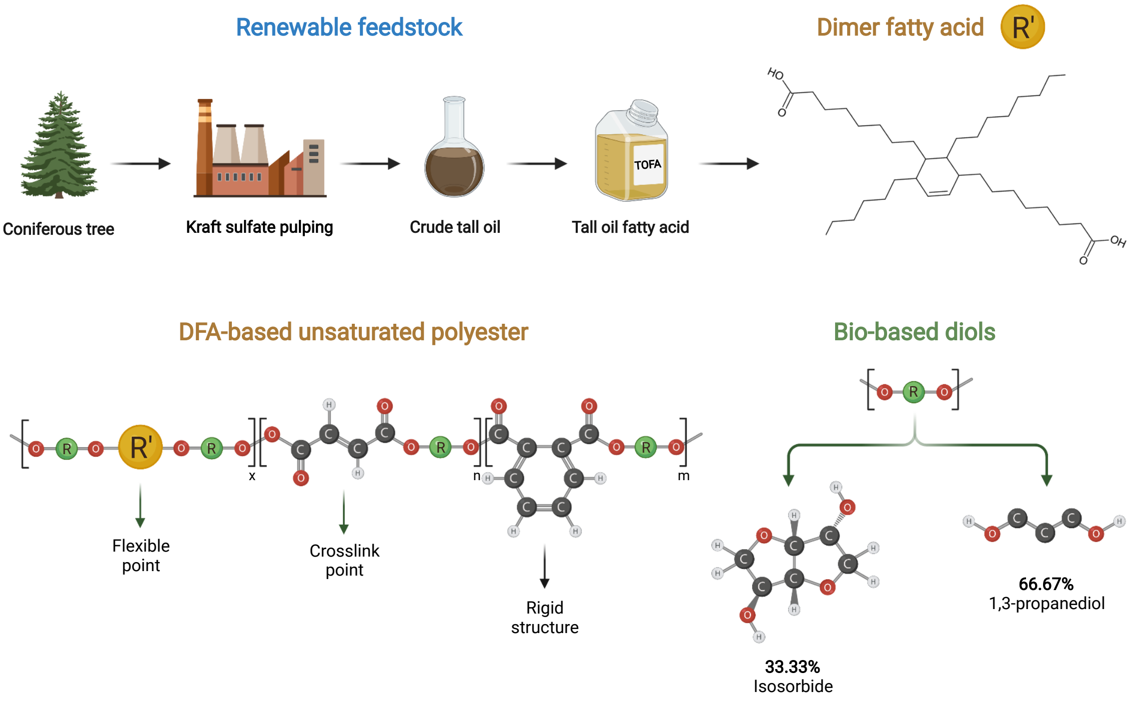

Figure 4.1: Graphical abstract of the DFA-based unsaturated polyesters.

4.1 Introductory remarks

Monomers based on raw materials derived from renewable sources have already been used to synthesise unsaturated polyester resin (UPR), such as dicarboxylic acids [1–4], dihydroxyl alcohols [5–7], and reactive diluents with at least one vinyl group [8–11]. However, although many of these biomass-derived renewable raw materials (such as sugars and starch) are eco-friendly, they have a high cost (due to the complexity of their production), which negatively affects the economic competitiveness of UPRs compared to other thermosets, such as vinyl ester and epoxy resins.

Vegetable-based oils remain the most abundantly used renewable resources for the chemical industry [12]. Fatty acids (mostly obtained from vegetable oils) are prime candidates to replace fossil-based derivates in thermosets due to the following reasons: (i) wide universal availability; (ii) low toxicity; (iii) low costs, and (iv) inherent chemical structures [13,14], which allows them to be efficiently converted into functional renewable building blocks.

The chemical functionalisation of vegetable oils, on either the carboxyl group or the fatty acid chain, can lead to various valuable chemical platforms [15,16]. Consequently, reactants obtained from vegetable oils have been studied and exploited in the syntheses of different types of thermoplastics and thermosetting polyester [17–20]. However, fatty acid-based polymers often do not present stiffness- and strength-properties compatible with mainstream structural applications. As a result, in those cases, it is necessary to design a polymer from long chains with a high-performance oriented structure [21]; for instance, new macromolecular architectures using bio-based building blocks derived from fatty acids, such as dimer fatty acid (DFA), can be produced for those purposes [22,23].

DFAs are the main products of the oligomerisation (dimerization) of C_{18} unsaturated fatty acids, a cyclic dibasic dimer having a total of 36 carbon atoms from tall oil fatty acid (TOFA), see Figure 4.2. DFAs have been used as chain extenders in polyester macromolecular structures since the 1920s, primarily to produce alkyd resins for the coating industry. The availability of DFA is widespread worldwide, and it is expected to grow steadily due to at least three reasons [24]: (i) availability of fatty acids derived from tall oil, a by-product of the paper industry; (ii) increasingly wide range of dimerized fatty acid applications, including adhesives, paints, coatings, lubricants, building blocks, etc., as well as (iii) sustainable economic policies implemented by governments driving the choices of end-use industries towards bio-based products.

When produced from tall oil (see Figure 4.3) [25], DFAs also have the advantage of not depending on the agro-food sector, since tall oil is a readily available by-product of the Kraft pulping process of lignocellulosic biomass and cannot be used for food production [26]. Furthermore, current prices are more competitive compared to other bio-derived monomers, such as those based on furans. DFAs may also contribute to high bio-content

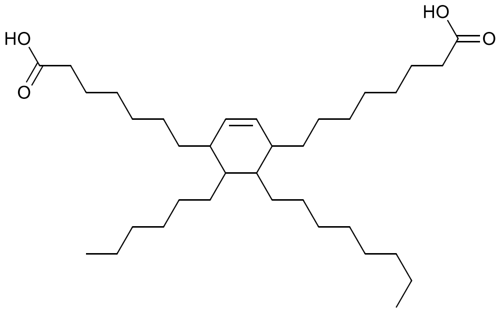

Figure 4.2: Chemical structure of DFA.

incorporation in polyester since they are rich in aliphatic long chains with high molecular weight (∼560 g/mol). Nonetheless, increasing the DFA content in the polyester backbone has been reported to cause a lower glass transition temperature (T_g) due to its amorphous structure and high conformational flexibility of the polymer chains, resulting in polyesters with lower thermomechanical properties [27]. Although in negligible amounts, further to the true dimer fraction, monomeric fatty acid, trimeric and higher polymers are present in these polymerised 'monomers'; this results in a segmented formation with a two- or multi-phase structure, with high deformability. However, the limitations in thermomechanical and mechanical properties of DFA-based polyesters can be overcome by incorporating more rigid building blocks into the backbone.

The esterification reaction of DFA and ISO can result in a less flexible polyester backbone, improving its mechanical and thermomechanical properties, and keep an appropriate sustainably-sourced content since ISO is a building block derived from renewable sources; when used as a monomer, it can provide the polyester with a balance between high performance and sustainability [28–30]. Its cyclic structure is responsible for the increased stiffness of the UP backbone, resulting in polyesters with higher T_g than with conventional aliphatic diols [31,32]. However, when high ISO ratios are incorporated into the polyester backbone, viscosity is also very significantly increased, becoming difficult to dilute it with the reactive solvent, most probably due to the presence of polysaccharides formed during the residence time at the reaction temperature; this may limit its use in the processing of materials that require low viscosities.

The high viscosity presented by UPs based on ISO can be adjusted by using PDO, a renewable aliphatic diol derived from corn sugar fermentation [33–35], which has low viscosity at room temperature, imparting flexibility to the chain of polyesters of aromatic or rigid cyclic morphology. Changing non-renewable aliphatic diols (such as EG and PG) by PDO does not significantly affect the thermomechanical properties of UPRs, especially their T_g [36,37].

High T_g values are typically achieved in densely crosslinked polymers; however, high crosslinking densities can also lead to brittleness. In this respect, to obtain suitable products for each type of application, the prepolymer's crosslinking density can be designed

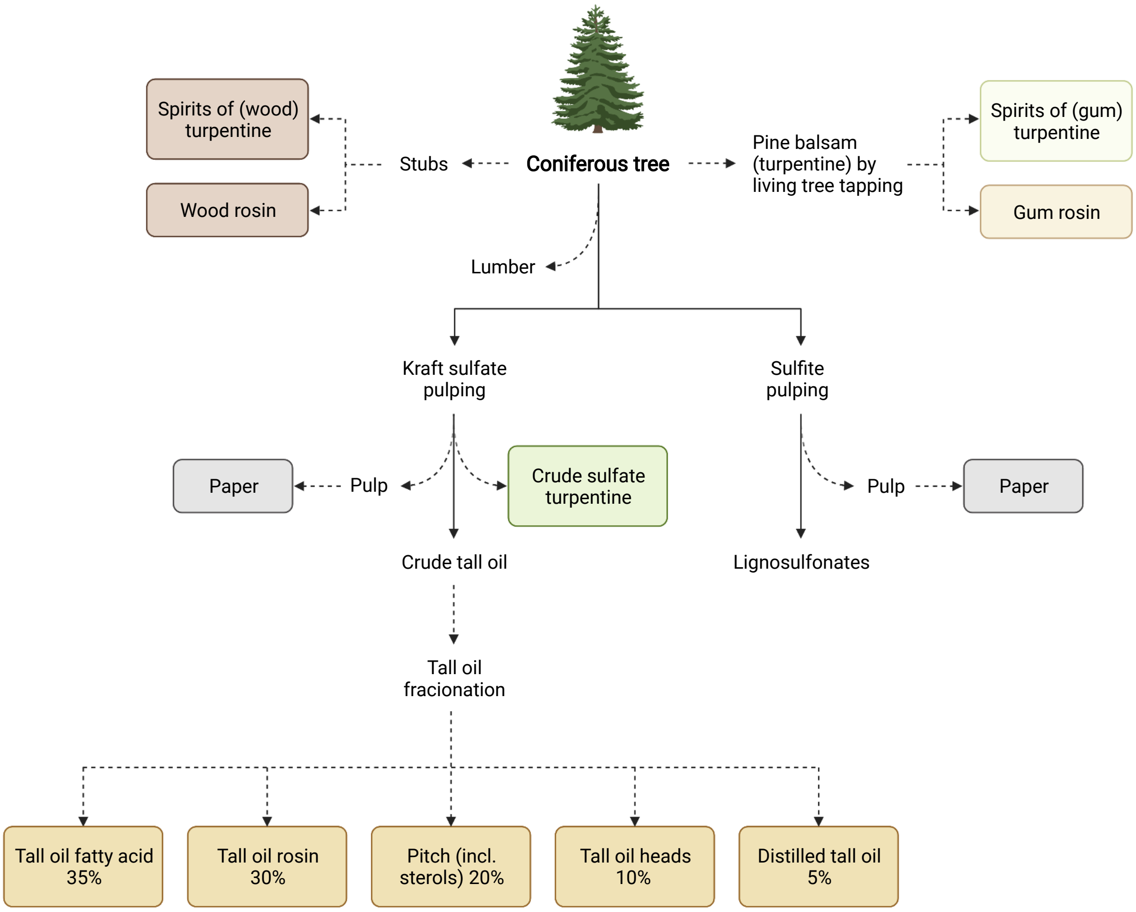

Figure 4.3: The tall oil value chain.

in advance by adjusting the ratio between unsaturated and saturated acids to promote the necessary balance between T_g and toughness. Moreover, increases in both T_g and bio-content can be obtained by replacing maleic anhydride (petroleum-based) with bio-based FA; this is considered a top value added chemical from biomass [38], since it is non-toxic and can be obtained from agroindustry by-products through the fermentation of sugar cane bagasse. Moreover, the fumarate double bond is slightly more reactive than the maleate, resulting in a more complete radical polymerisation and a lower need for post-cure procedures.

The previously discussed bio-based building blocks are widely available and have a high potential for use as raw materials in synthesising UPs (see Figure 4.4). These renewable building blocks can provide competitive mechanical and thermomechanical properties compared with their petroleum-based counterparts. However, the effort to produce UPRs that are more sustainable and less harmful to human health should not be restricted to the development of the UP backbone but should also include the reactive diluents. Reactive diluents must be compatible with the bio-based UP backbone and, after their incorporation, the UPRs must have similar processing characteristics to conventional ones.

High-performance UPRs need some incorporation of styrene (at least ∼10% by weight of

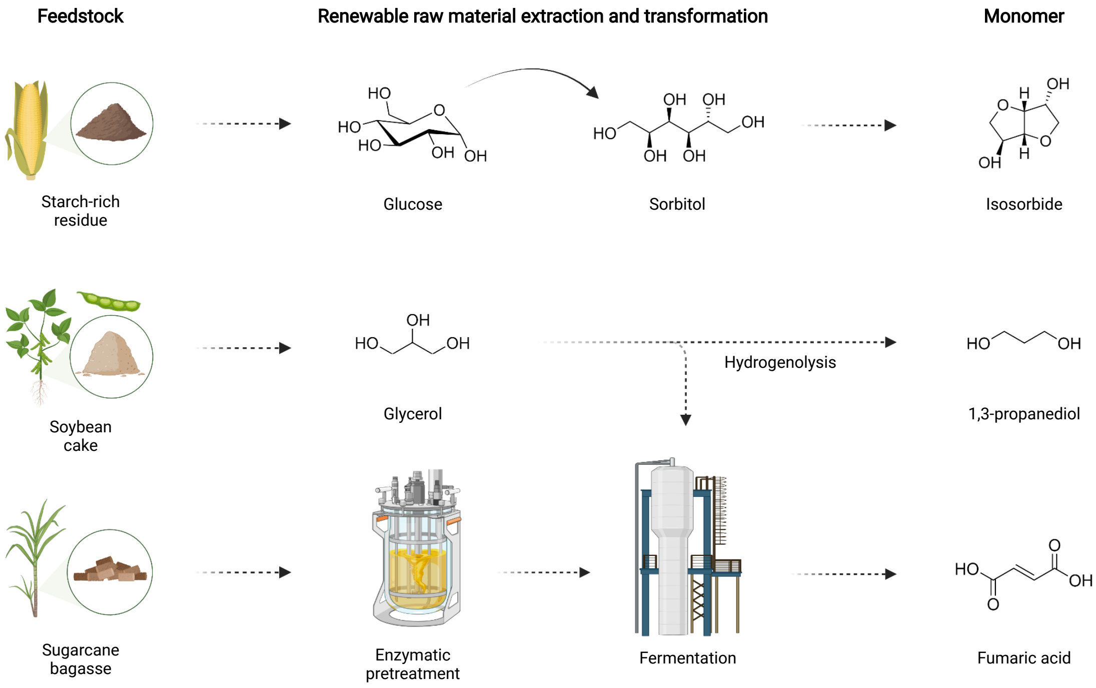

Figure 4.4: Monomers based on renewable raw materials for the UP synthesis.

styrene in the resin composition), especially because the styrene radical plays one very important role in the propagation step. However, styrene oxide is carcinogenic, and styrene is regarded as a hazardous air pollutant (HAP) and a volatile organic compound (VOC), especially problematic under the occurrence of traces of ozone [39]. Furthermore, it is not recommended to use more than 45% by weight of styrene in the resin composition [40], and the molar excess concerning the backbone's double bonds should be lower than 15%. In fact, large amounts of reactive diluent tend to decrease the thermomechanical properties of the cured resin, and non-reacted styrene or excess of other reactive monomers will result in a plasticising effect, lowering the elastic moduli, as well as the long-term performance. This can be a problem in load-bearing structural components, especially those under outdoor exposure or elevated temperatures.

Acrylate-type monomers are an alternative to replace styrene because they generate propagating radicals at the double bonds, with comparable reactivity to styrene and fumaric unsaturations, but are less environmentally damaging. Among these, HEMA has been recently investigated in UPRs [9,41], showing improved mechanical properties, and quite good oil and heat resistance. HEMA is hydrophilic as it contains a hydrophilic pendant group in its structure; in addition, it is a viscous colourless monomer at room temperature and behaves somewhat like rubber [42]. Thus, higher performance can be achieved by a mixture between HEMA and styrene as reactive diluent monomers for UPRs, since good reactivity between HEMA and styrene has been previously reported [43].

In this chapter, the potential of DFA for synthesis with other renewable building blocks, particularly bio-based diols, is investigated towards the development of cured UPRs of high-performance and high renewable content. For this purpose, bio-based UP prepolymers were formulated and prepared using DFA, FA, ISO, PDO and PA. Thus, the main innovation is the development of a novel high-performance UP backbone synthesised from renewable building blocks currently considered as top added value chemical products from biomass. Furthermore, the variations in the formulations have been around the partial replacement of 10% PA by DFA (DFA:PA = 10:90). The results were compared to a reference formulation without the addition of DFA. Furthermore, the 10:90 formulation was tested along with two different bio-based FA concentrations with ratios between saturated and unsaturated acids (S:U) of 1:2.5 and 1:3, respectively. A mixture of styrene and HEMA was used as a reactive diluent, thus resulting in a cured bio-based UPR of high renewable content, containing less VOCs in the liquid resin, compared to conventional petroleum-based ones. The relationships among the bio-based polyester resin's chemical structures, viscosity, mechanical, and thermomechanical properties were investigated.

4.2 Experimental

4.2.1 Materials

ISO (>98%) was obtained from Roquete, Usine de Lestrem (France). PDO was obtained from DuPont Tate & Lyle by the name of Susterra™ propanediol. DFA, Unidyme 18™, was obtained from Kraton Corporation. FA (>98%), PA (99%) and HEMA (97%) were obtained from Sigma-Aldrich. Styrene was obtained from Omnova Solutions. Imidazole, hydroquinone and toluhydroquinone were obtained from Sigma-Aldrich. MEKP and cobalt octoate solution with 1% cobalt content were obtained from EcoCompositos S. A. All the chemicals were used as received.

4.2.2 Prepolymer formulations

Polyesters based on long chains from fatty acids tend to be particularly flexible and deformable, limiting their use for some applications. The five formulations investigated herein (according to Table 4.1) were designed to assess the effect of crosslink density on the thermophysical and mechanical properties of UPs with DFA.

UP-A was synthesised as a reference formulation, without DFA; UP-B, UP-C, UP-D and UP-E were synthesised in the presence of DFA (in partial replacement of 10% and 25% of PA), with two different molar fractions between saturated and unsaturated acids: 1:2.5 and 1:3.0. The insertion of unsaturations into the UP backbone aimed at increasing the crosslink density, resulting in a cured polymer capable of achieving similar modulus of elasticity and T_g to those of their conventional general-purpose counterparts.

The rationale for the slight variation in molar fractions between saturated and unsaturated

Table 4.1: UP prepolymer formulations.

Sample			Mol				
Name	DFA:PA[a]	S:U[b]	PA	DFA	FA	PDO	ISO
UP-A	0:100	1:3.0	1.591	-	4.772	4.713	2.537
UP-B	10:90	1:2.5	1.550	0.172	4.307	4.466	2.233
UP-C	10:90	1:3.0	1.371	0.152	4.570	4.513	2.257
UP-D	25:75	1:2.5	1.205	0.402	4.017	4.166	2.083
UP-E	25:75	1:3.0	1.074	0.358	4.296	4.243	2.122

[a] DFA:PA is the molar percentage in the total moles of saturated acids
[b] S:U is the molar fraction between saturated and unsaturated acids

acids was: (i) to maximise the T_g; but, in parallel, (ii) to avoid a high content of reactive double bonds, which could result in embrittlement of the resin when crosslinked with the reactive diluent (especially styrene); and (iii) to assess the influence of the partial replacement of PA by DFA. Furthermore, to mitigate the flexibility of the backbone provided by DFA and produce stiff polyesters with suitable processability for high-performance applications, the molar fraction between ISO and PDO (about 33 and 67% of the total amount of glycols, respectively) was kept constant in all formulations, ensuring a good relationship between resin viscosity and its hardness after curing.

For the planning of formulations and experiments, it was previously confirmed that polyesterification must be carried out under excess of OH to avoid decarboxylation, and a slight loss of glycol by the air separation system was considered. Consequently, it was found that (i) the amount of COOH groups is slightly less than the content of alcohol groups and that (ii) the backbone's unsaturation content must be very close to that provided by the reactive monomer, particularly when an amount of styrene is used as a reactive monomer, as the copolymerisation is specifically alternated. Thus, an excess of 10 mol% glycol was considered for all formulations.

4.2.3 Synthesis

The prepolymers were prepared by catalysed bulk polycondensation following the formulations shown in Table 4.1. In a typical experiment, PA (229.6 g, 1.550 mol), DFA (97.3 g, 0.172 mol), FA (503.3 g, 4.307 mol), PDO (339.8 g, 4.466 mol) and ISO (326.3 g, 2.233 mol) were added to a two litres four-neck reactor (with bottom drain valve) equipped with an anchor blade mechanical stirrer, a thermocouple to control a heating mantle with a set-point temperature of 206 °C (ranging between 200 °C and 210 °C), a nitrogen inlet and a condenser attached to a dean-stark adaptor to collect the water formed in the reaction and minor amount of the glycol loss. No vacuum was applied during synthesis.

Imidazole (0.2% relative to the total weight of diacids and diols) was used as the polymerisation catalyst. Hydroquinone and 2-methyl hydroquinone (both used at 200 ppm relative to the total weight of diacids and diols) were also added as the free radical polymerisation inhibitor to prevent premature gelation. All reactants were added at room temperature. The mixture was then stirred, and the progress of the reaction was monitored by acid number (AN) titration and by viscosity measurements at 125 ℃ in a Cone & Plate viscosimeter. The reaction was then allowed to proceed until the AN reached a constant value (always below 50 mgKOH/g) combined with a maximum viscosity of 2000 cP, which required around 8 hours.

4.2.4 Biobased content

The biobased carbon and mass content were determined for each reactant according to ISO 16620 [44] part 4 Annex B (B1 and B2). Tables A.7 and A.11 (in Appendix A.4) show the calculation procedures.

4.2.5 Kinetics

To evaluate the reaction kinetics, the same procedures adopted in Chapter 3 were taken into account. The theoretical results from equations 3.3 and 3.4 were compared with the corresponding molecular weights as determined by GPC. M_0 was calculated from the weighted average of the components (diacids and diols) for each UP formulation [31], and it can be accessed from the Appendix A.3.1.

4.2.6 Crosslinking reactions

UPs were cooled to a temperature between 140 ℃ and 150 ℃, after AN and viscosity achieved their respective target values. Then, pristine UPs were diluted, without any previous purification step, using a mixture of styrene and HEMA (in equal parts) as a reactive diluent. This mixture allowed to produce UPRs capable of achieving a better balance among high-performance properties, processing characteristics (for different manufacturing techniques), and friendliness with the environment and human health, since a preliminary assessment showed that this would not be possible using only styrene or HEMA as reactive diluents.

To dilute the UP (prepolymer) with the reactive diluent, an incorporation temperature between 75 ℃ and 80 ℃ was used to obtain the UPRs. All resin samples consisted of a composition with 60% of UP and 40% of reactive diluent, both in weight. The free radical polymerisation of each resin was initiated with 2% methyl ethyl ketone peroxide (MEKP) using 1 wt.% cobalt octoate, added as a promoter. Resins were cured for 24 hours in a glass mould at 23 ℃, post-cured at 100 ℃ for 4 hours and allowed to stabilise at room temperature before any mechanical analyses were conducted.

4.2.7 Prepolymer characterisation

GPC tests were performed to determine the M_n and M_w of the polyester backbone samples using THF as eluent, according to ISO 13885 [45] part 1, in a concentration of 1 mg/ml. The samples were filtered and injected into a column set consisting of one precolumn (8 × 50 mm) PSS SDV, and columns (8 × 300 mm) PSS SDV analytical linear S, both with a 3 µm particle size, and filled with polystyrene crosslinked with divinylbenzene (gel). The columns were equilibrated at 40 ℃ before elution with purged THF at a rate of 1 ml/ min. The eluent was monitored using dual detectors; the first was a UV/Visible detector (model JASCO UV-4075) set to 254 nm and the second was a Refractive Index Detector (model JASCO RI-4030) both held at 40 ℃.

The molecular weights were calculated based on the retention time from a conventional calibration with narrow polystyrene standards (M_n of 266–59300 Da), see Figure A.2 in Appendix A.3.

NMR spectra were recorded on Bruker Advance 500 MHz at ambient temperature, see Figure A.7. ^{1}H chemical shifts (δ) are expressed in ppm relative to Me_4Si (δ = 0) and are reported relative to the solvent peak (^{1}H NMR).

UP-A (500 MHz, acetone-d_6, 298 K): δ = 7.84-7.65 (C-H (phthalate), overlapping multiplets), 6.86-6.74 (C-H (FA), overlapping multiplets), 5.48-3.36 (CH+CH_2 (ISO) and O-CH_2 (PDO), overlapping multiplets), 2.35-2.08 and 1.97-1.82 (-OCH_2CH_2CH_2O- from PDO, overlapping multiplets).

UP-B and UP-C (500 MHz, acetone-d_6, 298 K): δ = 7.84-7.65 (C-H (phthalate), overlapping multiplets), 6.86-6.74 (C-H (FA), overlapping multiplets), 5.47-3.31 (CH+CH_2 (ISO), O-CH_2 (PDO) and CH=CH (DFA), overlapping multiplets), 2.35-2.08 and 1.97-1.82 (-OCH_2CH_2CH_2O- from PDO), and 1.64-0.79 (CH_2 and CH_3 from DFA, broad singlets).

The viscosity tests were performed on a Cone & Plate ICI viscometer from REL (Research Equipment London Ltd.), according to ISO 2884 [46] part 2, see Figure A.10. The viscosity was taken at 125 ℃ as the average value of three measurements.

4.2.8 UPR characterisation

Tensile test specimens were prepared according to the type 1A defined in ISO 527 [47] part 2 (see Appendix B.1.2). The specimens were tested under laboratory conditions at 23 ± 2 ℃ and 55 ± 3% relative humidity. In general, five specimens were prepared for each type of resin.

DMA experiments were performed to obtain thermomechanical properties using a dynamic mechanical analyser from TA Instruments, model DMA Q800. Specimens with dimensions 60 mm × 10 mm × 4 ± 0.5 mm were manufactured according to ASTM E1640 [48] and tested in a 35 mm dual cantilever configuration, see Appendix B.2. The specimens were subjected to a constant strain amplitude of 15 µm at a constant oscillation frequency of 1 Hz while submitted to a temperature sweep at a constant heating rate of 2 ℃/ min, starting at −30 ℃ and ending at 150 ℃.

The crosslink density (ν_e) was determined based on the kinetic theory of rubber elasticity by using the following equation [49]:

$$\nu_e = \frac{G'}{\mathrm{RT}} = \frac{E'}{3\mathrm{RT}} \tag{4.1}$$

where R is the gas constant (8.314 J K/mol), T is the absolute temperature in K, and the shear storage modulus (G') and the flexural storage modulus (E') are obtained in the rubbery plateau. Herein, the rubbery plateau region of the storage modulus, defined based on the DMA tests, was taken to estimate ν_e. The kinetic theory of rubber elasticity assumes that the network is ideal, and all chains are effective in elastic deformation [50].

DMA and tensile tests were also performed on specimens moulded from a commercial orthophthalic UPR (see Appendix B.3), cured and characterised under the same conditions and procedures as the bio-based UPRs developed here. The mechanical and thermomechanical properties obtained from this commercial UPR were considered a benchmark for comparison.

4.3 Results and discussion

4.3.1 Preliminary remarks

As mentioned, the developed UPs are based on a selection of building blocks derived from renewable resources, namely DFA, FA, PDO and ISO. In addition, macromolecular formulations were designed for the development of high-performance polyesters. These new materials have stiff aromatic-like units introduced by cyclic structures; and soft aliphatic moieties, DFA and PDO, which were incorporated to modulate the properties of the ensuing cured polymers, especially in terms of thermal and mechanical behaviour.

It is important to mention that an uncontrolled reaction was observed during the first hours of the synthesis of formulations with 25% DFA (UP-D and UP-E, respectively), resulting in (i) considerable increase in the volume of the reaction product, (ii) formation of a material with a multi-phase aspect (honey-foam-rubber type), and (iii) the reactor breakage during the synthesis of UP-E. Attempts were made to dissolve the UP-D and UP-E samples in acetone and tetrahydrofuran, but the material was found to be insoluble/precipitated for these solvents. The presence of a catalyst and the high temperature associated with the higher viscosity of the dimer fatty acid may have favoured these unwanted phenomena [51]. Consequently, the UP-D and UP-E formulations were discarded from the analysis, as it was not possible to proceed with their synthesis and characterisation. Thus, only the characterisations of UP-A, UP-B and UP-C are addressed in the following sections.

4.3.2 Biobased content

UP prepolymers were synthesised via catalysed direct melt polycondensation with negligible VOC emissions. Except for PA, all other monomers were derived from renewable resources, resulting in the synthesis of UPs with high bio-based carbon (x_B) and mass (m_B) contents, see Table 4.2. The high bio-based contents obtained allow fulfilling one of the principles (use of renewable feedstocks) of green chemistry, according to ISO 16620 [52] part 1.

Table 4.2: Bio-based carbon (x_B) and mass(m_B) contents of UPs and UPRs, according to ISO 16620 [44] part 4.

Sample	x_B (%)	m_B (%)
UP-A (UPR-A)	78.6 (47.2)	84.1 (50.4)
UP-B (UPR-B)	78.2 (46.9)	84.5 (50.7)
UP-C (UPR-C)	80.7 (48.4)	86.2 (51.7)

Bio-based carbon and mass contents decreased after incorporation of UPs with the reactive diluents since these were not fully derived from renewable resources. However, the partial replacement of styrene by HEMA allowed to obtain UPRs with a lower styrene content, benefiting from lower toxicity of HEMA relative to styrene. Furthermore, the use of DFA (in substitution of PA) in the proportions defined in this study, provided UPRs with bio-based mass contents higher than 50%.

4.3.3 Characterisation

4.3.3.1 Kinetic and molecular weight

UP-A, UP-B and UP-C presented ANs of 47, 44 and 43 mgKOH/g, respectively (see Table 4.3). Similar results have been obtained for commercial UPs, which often present ANs ranging from 25 to 50 mgKOH/g [1].

Table 4.3: Composition analysis of the UPs.

Sample	Time (h)	AN (mgKOH/g)	p (%)	GPC analysis M_n (kDa)	M_w (kDa)	$Đ$ (a.u)	p (%)
UP-A	8	47	0.90	1.45	3.6	2.48	0.9
UP-B	8	44	0.90	1.69	7.15	4.23	0.9
UP-C	8	43	0.91	1.55	3.49	2.25	0.91

Kinetic plots of X_n as a function of time are illustrated in Figure 4.5 for the last 20% of the polyesterification, occurring after 180 min, since conversion for the first 80% of the esterification of -COOH and -OH groups do not follow the behaviour of Equation 3.2 for the degree of polymerisation. This deviation below 80% conversion is not unique for polyesterification, being also observed for the simple esterification that results when the dicarboxylic acid is replaced by a monocarboxylic acid [53]. Moreover, the reaction medium is initially changing from one of the pure reactants to one in which the ester product is dominant in the reaction media.

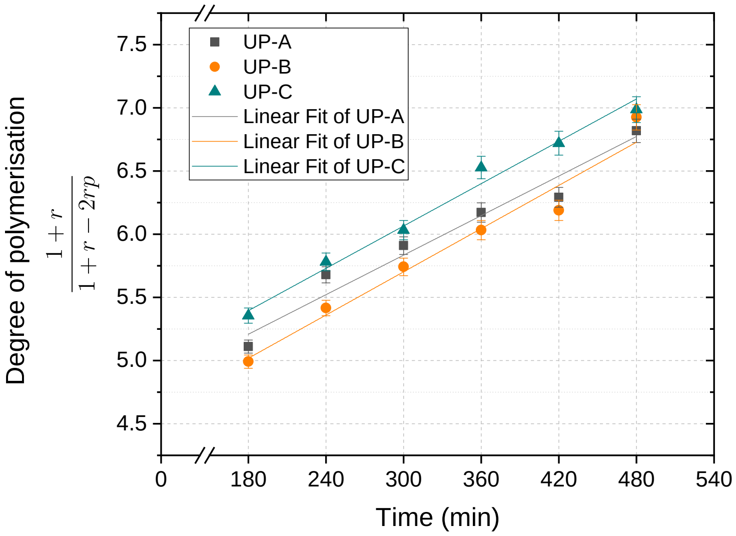

Figure 4.5: Kinetics of polyesterification reaction of UPs.

Beyond that period, chain growth to produce high molar mass material becomes increasingly difficult as the reaction proceeds, especially because (i) of the difficulty in ensuring the precise equivalence of the reactive groups in the starting materials, since diacids and diols with different reactivity were used; (ii) the decreasing concentration of functional groups and the second-order kinetics slows down the progress as their concentration diminishes; and (iii) the increasing likelihood of interference from side reactions (even with the use of inhibitors).

The results obtained show also that the reaction rates (k_2) are very similar among formulations, and a slightly higher conversion was observed when PA was partially replaced by DFA (p = 91% for UP-C against p = 90% for UP-A and UP-B). As a result, the average degrees of polymerisation obtained for UP-A, UP-B, and UPC-C were 6.8, 6.9 and 7.0, respectively. Thus, both the DFA-based prepolymers (UP-B and UP-C) and that without DFA (UP-A) behaved as low molecular weight macromolecules (oligoesters).

Figure 4.5 also shows that the kinetics had a well-defined trend, where the error bars around the conversion represent the experimental error (one standard deviation) resulting from an average obtained from three titrations, which resulted in low standard deviations for all formulations.

The molecular weights determined by GPC (see Figure 4.6) followed a Gaussian distribution (see Figure A.4 in Appendix A.3). The replacement of PA by DFA resulted in higher M_n

when comparing UP-B and UP-C with UP-A (see Table 4.3), which is consistent with the slightly lower AN (and a slightly higher conversion) obtained from DFA-based oligomeric macromolecules. In addition, the higher DFA concentration into the UP-B backbone can also explain its higher M_n when compared with UP-A and UP-C; this is mainly due to its long-chain with an intrinsic high molecular weight that resulted in oligomeric polyester backbones with more different lengths and, consequently, a higher dispersity $Đ$. By contrast, for high-performance purpose, higher M_n is desired to enable higher crosslink density, which provides a higher number of unsaturated sites per macromolecule without the need to increase the concentration of FA. This improves thermal and mechanical properties since it does not sacrifice stiffness and strength by removing the saturated dicarboxylic acid, herein the PA. By contrast, results obtained for UP-B show that the partial replacement of PA by DFA in UP-B reflects a higher dispersity $Đ$ when compared to the other formulations, which can be explained by the higher DFA content in the UP-B backbone.

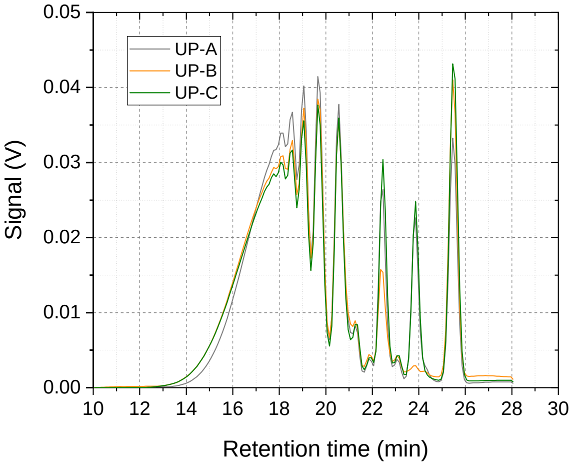

Figure 4.6: Signal as a function of retention time traces from GPC data for the UPRs.

The molecular structure results show also that the UP properties are very much dependent on the characteristics of the raw materials used and the formulation adopted. The UPs developed here presented relatively low molecular weight (M_w of 3.6, 7.1 and 3.5 kDa for UP-A, UP-B and UP-C, respectively), since the polycondensation reactions were controlled to achieve low working viscosities when dissolved in reactive diluent. This resulted in oligomers with a degree of polymerisation lower than 10 for all samples, which is in accordance with the literature for the formation of unsaturated polyesters, for which degrees of polymerisation between 6 and 15 are typically reported [54,55].

4.3.3.2 ^{1}H NMR study

NMR is a convenient tool to estimate the relative proportion of the different monomers present in the polymers. We exemplify here the results for UP-B. This polymer was obtained as a mixture of PA, DFA, FA, PDO, and ISO. We can assign different regions of the spectra with different types of protons as exemplified in the section A.7. While PA and FA appear separated, the CH_2 inner protons of the PDO moiety appear partially superimposed with the solvent protons (acetone). We can nonetheless integrate the CH_2 signals with some level of confidence, although we expect to have a larger error than for the signals that appear isolated.

We can also estimate the amount of fatty acid by integration of the signals that appear between 1.64 and 0.79 ppm that are assigned to CH_2 and CH_3 protons of the DFAs.

Given the amount of the PDO and DFA detected, we can calculate the amount of isosorbide by deducting the integration of the -CH_2O- protons of PDO and CH=CH of the FA that overlap with the isosorbide protons in the 5.47-3.31 ppm region. We arrive thus at the molar fraction PA:DFA:FA:PDO:ISO of 1.00:0.10:1.95:3.24:1.93. The same analysis procedure was performed for UP-C. Table 4.4 presents the molar percentages based on the ^{1}H NMR calculations of the molar fractions.

Some points can be highlighted based on the results obtained for the final structure characterised by ^{1}H NMR and the one initially designed: (i) UP-A, UP-B and UP-C present lower S:U ratios than the fed ones, with FA retention percentages of 91%, 93%, and 91%, respectively; however, (ii) similar FA retention percentages are found for UP-A and UP-B, (iii) a higher unsaturation content (originated from FA) is presented for UP-C when compared with UP-B, and as a consequence, a higher ν_e can be achieved, which partly explains the higher T_g of the respective UPR-C against UP-B; (iv) A:G ratios from ^{1}H NMR show a higher excess of glycol for all UPs, 17%, 15% and 15% higher for UP-A, UP-B and UP-C, respectively, when compared to the fed ratios; (v) a lower structures amount originating from both acids (namely, the aromatic ring from PA, the long carboxylic chain of DFA and the unsaturations from FA) is presented in the final structure of the respective UPRs, with UP-A, UP-B and UP-C retaining 81%, 83% and 83%, respectively, in relation to the fed quantities; (vi) a higher presence of ISO and a lower PDO content in relation to the total of glycols is verified for all UPs, which can be partly explained by the laboratory set up (distillation column, nitrogen flow) that drags more glycol than that used industrially, mainly PDO, which is more susceptible to carryover than ISO; and (vii) the final structure of the UP-B has a DFA:PA ratio very close to that initially fed, however, UP-C has a DFA amount 40% higher in relation to the total saturated acids in the final structure.

4.3.3.3 Viscosity

The control of viscosity during synthesis ensured that all linear thermoplastic UP samples had viscosities at 125 ℃ below 2000 cP, as shown in Figure 4.7 - the error bars represent the standard experimental error (standard deviation) around the three apparent viscosity measurements and the three titration measurements for calculating the degree of polymerisation, both from each reaction time for a same batch. This criterion allowed producing UPs with suitable viscosity for subsequent incorporation with a percentage of

Table 4.4: Comparison between ^{1}H NMR results and predicted structure of the UPs.

Monomer	Feed (%) UP-A	Feed (%) UP-B	Feed (%) UP-C	1H NMR (%) UP-A	1H NMR (%) UP-B	1H NMR (%) UP-C
PA	11.84	12.18	10.66	12.47	12.96	10.83
DFA	-	1.35	1.18	-	1.52	1.78
FA	35.53	33.83	35.53	26.49	25.26	27.24
PDO	35.09	35.09	35.09	35.41	35.2	37.58
ISO	17.54	17.54	17.54	25.64	25.05	22.56
S:U[a]	25:75	29:71	25:75	32:68	34:66	32:68
A:G[b]	48:52	48:52	48:52	39:61	40:60	40:60
PDO:ISO[c]	67:33	67:33	67:33	58:42	58:42	62:38
DFA:PA[d]	-	10:90	10:90	-	11:89	14:86

[a] S:U is the molar percentage between saturated and unsaturated acid
[b] A:G is the molar percentage between acids and glycols
[c] PDO:ISO is the molar percentage between PDO and ISO
[d] DFA:PA is the molar percentage between DFA and PA

reactive diluent of 40% (see Table 4.5). This value is in line with the industry standards regarding conventional resins for the impregnation of synthetic or natural fibres used in FRP composites. Further, the relatively low viscosities have the additional benefit of promoting better cure performance due to the higher mobility of the polymeric chains.

As mentioned, DFA increases polyester viscosity; however, other factors can also limit the extent of reaction due to reaching excessive viscosity; for instance, the presence of ISO can be highlighted. This monomer contributes to a greater increase in the viscosity of UP with relation to other aliphatic diols due to its intrinsic features of steric hindrance and *Ordelt* saturation (branching formation) with fumaric acid. Additionally, a UP produced exclusively from an ISO-based glycol would probably not be miscible in styrene. Even if branching occurs at a low level without additional crosslinking and gelation, the prepolymers obtained are generally unsuitable for UPR preparation due to their very high viscosity. The curing process for this resin would also result in forming a non-homogeneous network with low mechanical properties. To minimise the excessive increase in viscosity due to ISO, the UP-A, UP-B and UP-C were formulated to contain a maximum of 33% in mol of ISO regarding the total amount of glycol. In addition, inhibitors (hydroquinone and toluhydroquinone) were used to minimise *Ordelt* saturation and mitigate gelation. However, it was found that gelation can occur at lower ANs (below 40) when performing polycondensation at elevated temperatures (about 206 °C) due to the long residence time and lower efficiency of the radical inhibitors in the absence of oxygen.

Furthermore, while high DFA content increases the viscosity in UPRs, such as reported in Example 10 from Fekete *et al.* [56], the results obtained here show that the developed UPR formulations can be applied in different processing techniques used in the composites industry, for example, hand layup, vacuum infusion and pultrusion. These resins have the

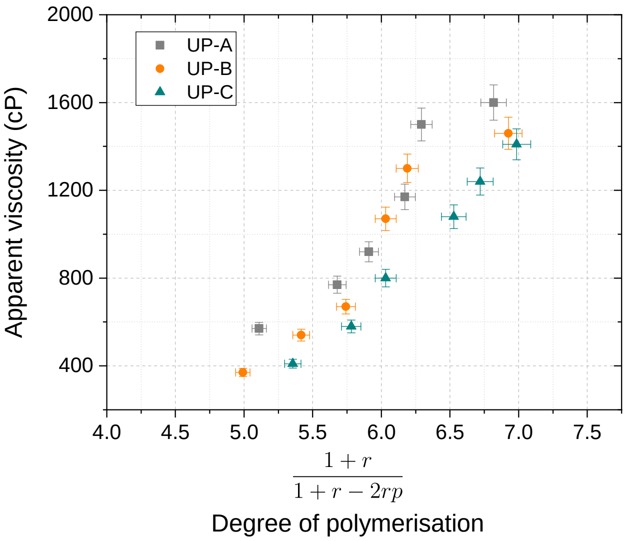

Figure 4.7: Viscosity of the UPs measured at 125 ℃.

Table 4.5: Viscosity of the UPRs measured at 25 ℃.

Sample	Incorporation ratio in wt. (%)			Viscosity
	Prepolymer	HEMA	Styrene	(cP)
UPR-A	60	20	20	800
UPR-B	60	20	20	820
UPR-C	60	20	20	860

additional advantage of having a lower styrene concentration than typical (conventional) UPRs, with this reduction reaching up to 50% of the total amount of styrene used.

4.3.3.4 Tensile properties

Figure 4.8 presents the tensile stress-strain nominal curves of the UPRs. The results show a highly consistent behaviour for UPR-A, UPR-B and UPR-C resins. All curves present an initial elastic linear branch, followed by a gradual loss of stiffness preceding a brittle failure. This behaviour is typical of conventional UPRs under tension. The fully crosslinked structure of UPRs reduces the mobility of the molecules hindering the polymer network's ability to rearrange and accommodate the increasing strains. As a result, internal cracks can form and quickly propagate, thus inducing a brittle failure.

Figure 4.9 presents the tensile strength, modulus of elasticity and strain at break, respectively, for the three resins. Although the DFA-based UPR formulations presented lower modulus of elasticity (-15% and -12% for UPR-B and UPR-C, respectively) when compared with UPR-A (without DFA), their performance was very similar that of commercial petrochemical counterpart tested herein (see Table B.1 in Appendix B.3), as well as that of other conventional formulations well established in the literature [40,57].

Additionally, segmented formulations with aromatic and aliphatic dicarboxylic acid moieties

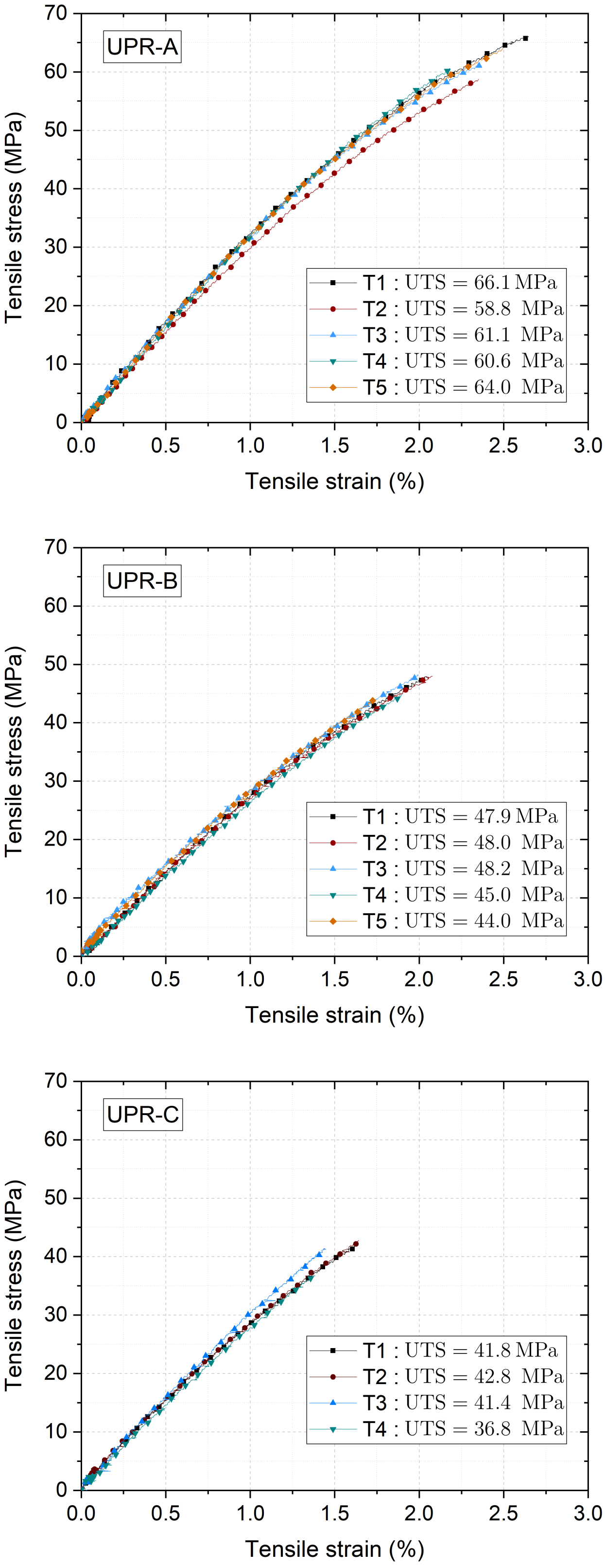

Figure 4.8: Tensile stress-strain curves of the UPRs.

used herein allowed to obtain UPRs with a higher modulus of elasticity when compared to those based on wholly saturated aliphatic dicarboxylic acids, such as succinic and adipic acid, which have been reported in the literature [58]. Some other factors can also explain the higher modulus of elasticity of UPR-A, such as (i) the fact that ISO represents one-third of total glycols, and promoted higher stiffness in the backbone compared to aliphatic diols; (ii) high double bonds content with 1:3 in mol% S:U dicarboxylic acid ratio provided high crosslinking density, which resulted in hard and inflexible cured UPRs; and (iii) the maintenance of a segmented rigid structure in the backbone (from PA) provided chains with lower flexibility when compared with polyesters wholly based on DFA.

The results obtained also show that the partial replacement of PA by DFA (UPR-B and UPR-C) provided lower tensile strength (-16% and -37%, respectively) and strain at break (-37%) when compared to UPR-A. Regardless of this comparison between the three different formulations tested in this study, DFA shows good potential as a partial replacement monomer for PA in the production of UPRs. The results of tensile strength, modulus of elasticity and strain at break obtained for all tested formulations also show that it is possible to reduce the styrene content in UPRs by partially replacing it with HEMA.

Thus, despite the lower mechanical properties presented by UPR-B and UPR-C compared to UPR-A, the DFA-based UPs developed herein have the potential to compete with conventional ones. These formulations may be particularly interesting for non-structural components, for example those made using lightweight natural fibres (*e.g.*, jute, flax, hemp and kenaf), which have typical tensile strains at break compatible with (well below) those exhibited by UPR-B and UPR-C [59–62]. In addition, this study suggests that the synthesis of DFA-based UPs can be designed to incorporate bio-based FA, to provide double bonds capable of crosslinking with reactive diluents, resulting in eco-friendlier UPRs. Herein, PDO and ISO (both derived from renewable sources) were also essential to maintain high bio-based content and to adjust the viscosity and stiffness of these polyesters considering those of conventional counterparts (petroleum-based).

4.3.3.5 Thermomechanical properties

DMA was used to determine the thermomechanical properties of the cured UPRs and to assess the effect of increasing DFA concentration in those properties. Figure 4.10 presents the DMA curves for storage modulus (E'), loss modulus (E'') and tan δ as a function of temperature for the UPRs.

The T_g results are presented in Table 4.6 from the onset of the storage modulus decay and the peak of the tan δ curve; the values of E' at 25 ℃, 50 ℃ and 150 ℃ are also shown. All the cured UPRs displayed T_g values ranging from 60 to 65 ℃ and from 91 to 95 ℃, from the onset of the storage modulus decay and the tan δ peak, respectively. These values enable the use of the proposed resins in a wide range of applications, such as in FRP

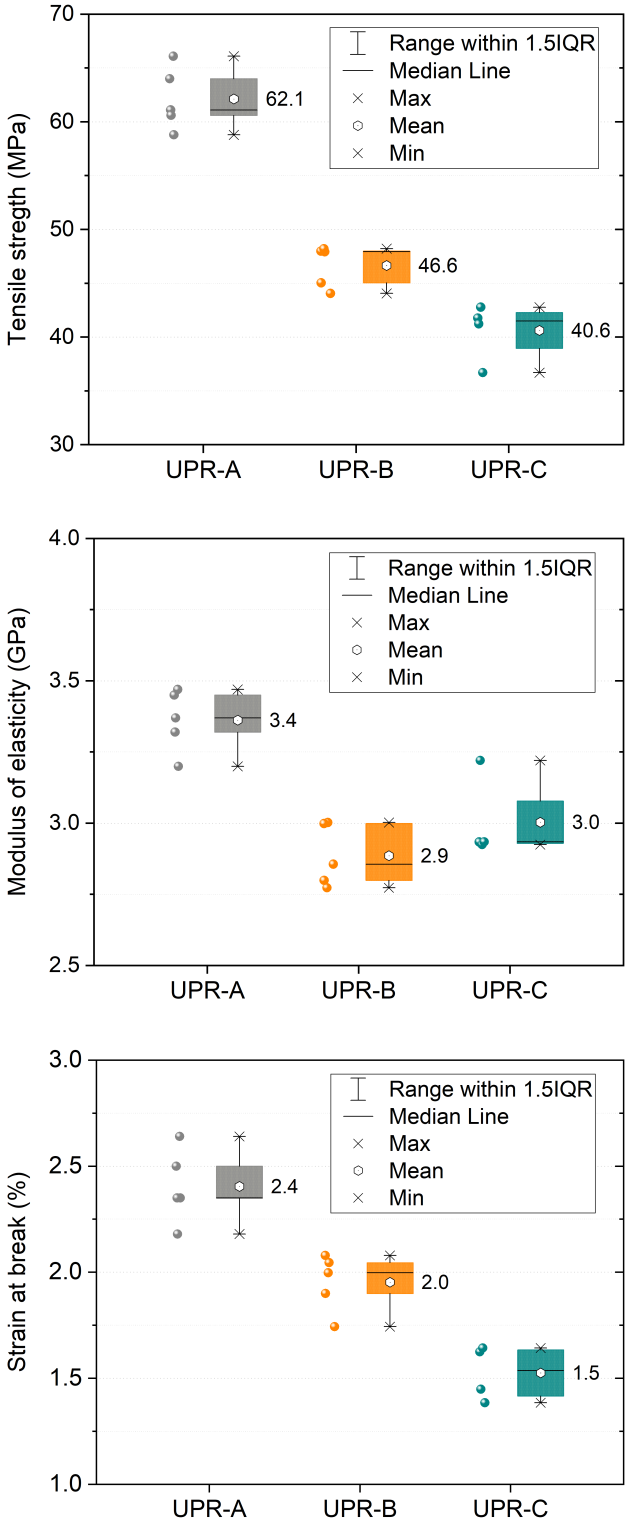

Figure 4.9: Scatter plots from the tensile strength, modulus of elasticity, and strain at break results of the UPRs.

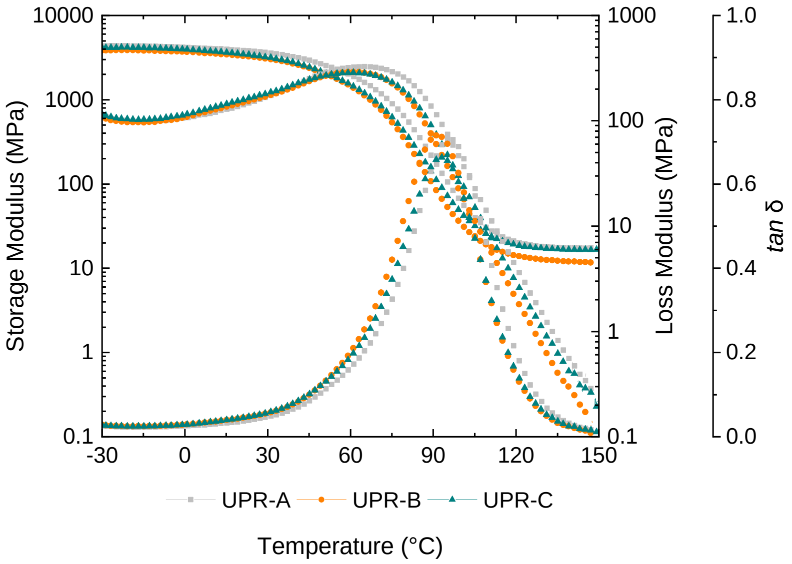

Figure 4.10: DMA curves for the UPRs.

composites, since these results are similar to those found for the commercial UPR tested herein (see Table B.1 in Appendix B.3).

Table 4.6: DMA properties of the UPRs.

Sample	T_g (℃)		E' (MPa)			ν_e
	E'_{onset}	tan δ	25 ℃	50 ℃	125 ℃	(mol/m^3)
UPR-A	65.5	95.5	3745	2618	19	1.9×10^{-3}
UPR-B	60.9	91.4	3207	2082	13	1.3×10^{-3}
UPR-C	61.2	92.9	3365	2129	17	1.7×10^{-3}

The T_g values of the crosslinked thermoset UPRs relate not only to the crosslink density but also to the inherent flexibility of the chain segments, wherein DFA introduces particularly flexible segments when compared to those consisting of PA. Thus, the resin formulations developed in this study overcame the thermomechanical limitations of UPRs based on long- and flexible chains reported in the literature [63], by incorporating relatively small amounts of DFA into the polymer backbone. While resulting in a slight decrease in crosslinking density, this addition did not cause a significant loss of stiffness.

Meanwhile, the E' at 25 ℃ of the cured UPR-A is higher than that for the UPR-B and UPR-C. This result, which is consistent with the tensile results mentioned above (higher modulus of elasticity of UPR-A), is attributed to the lower crosslinking density and overall flexibility provided by the addition of DFA. At higher temperatures, namely at 50 ℃, DFA-based UPRs promoted a lower E' retention (64.9% and 63.3% for UPR-B and UPR-C, respectively, against 69.9% for UPR-A). In addition, incorporating HEMA as a reactive diluent in substitution of 50% wt. of styrene also proved to be a successful strategy regarding the resulting thermomechanical properties of the cured resins.

4.4 Concluding remarks

Syntheses of UPRs based on DFA and other renewable building blocks have been successfully carried out, resulting in unsaturated polyester prepolymers with high bio-based mass content, up to 86.2 wt.%. The high renewable content of the UPs combined with their dilution in a reactive diluent formed by the mixture of two reactive monomers, namely styrene and HEMA, allowed to produce more environmentally friendly – and with a lower styrene content – UPRs when compared to conventional petroleum-based alternatives.

While the DFA-based UPRs developed herein presented lower tensile strength and modulus of elasticity compared to the baseline formulation (containing only PA as saturated acid), their properties are still compatible with several mainstream applications of UPRs. In addition, the UPRs developed in this study presented viscosities that are feasible for various fibre impregnation processing techniques (such as hand-layup, infusion and pultrusion). The thermomechanical properties of the DFA-based UPRs were not significantly different from the baseline formulation due to the balance between PA and DFA ratios, as well as the previously designed crosslink density. These properties of the synthesised DFA-based UPRs attest their potential as greener materials to produce bio-based composites.

The challenge of widening the scope and range of application of sustainable UPRs is considerable; further research is needed to solve issues that involve a balance between sustainability, high performance, and material processability, namely in order to develop (i) stiff renewable building blocks to replace phthalic anhydride, which are compatible with dimer fatty acids; (ii) reactive monomers to be used as diluents, which can fully replace styrene while ensuring high mechanical, thermomechanical and processing performance, and (iii) bio-based catalysts (initiators and accelerators) to achieve fully bio-based UPRs.

4.5 References

[1] Cátia S. M. F. Costa, Ana C. Fonseca, Jorge Moniz, Maria Godinho, Jorge F. J. Coelho, and Arménio C. Serra. Going greener: Synthesis of fully biobased unsaturated polyesters for styrene crosslinked resins with enhanced thermomechanical properties. *Express Polymer Letters*, 11(11):885–898, 2017.

[2] Nicholas A. Rorrerc, Derek R. Vardon, John R. Dorgan, Erica J. Gjersing, and Gregg T. Beckham. Biomass-derived monomers for performance-differentiated fiber reinforced polymer composites. *Green Chemistry*, 19(12):2812–2825, 2017.

[3] Joseph J. Bozell and Gene R. Petersen. Technology development for the production of biobased products from biorefinery carbohydrates—the US Department of Energy's "Top 10" revisited. *Green Chemistry*, 12(4):539–554, 2010.

[4] Andreia F. Sousa, Ana C. Fonseca, Arménio Coimbra Serra, Carmen S. R. Freire, Armando J. D. Silvestre, and Jorge Coelho. New unsaturated copolyesters based

on 2,5-furandicarboxylic acid and their crosslinked derivatives. *Polymer Chemistry*, 7(5):1049–1058, 2016.

[5] Oliver Goerz and Helmut Ritter. Polymers with shape memory effect from renewable resources: crosslinking of polyesters based on isosorbide, itaconic acid and succinic acid. *Polymer International*, 62(5):709–712, 2013.

[6] Paulien F. H. Harmsen, Martijn M. Hackmann, and Harriëtte L. Bos. Green building blocks for bio-based plastics. *Biofuels, Bioproducts and Biorefining*, 8(3):306–324, 2014.

[7] Lidia Jasinska and Cor E Koning. Unsaturated, biobased polyesters and their cross-linking via radical copolymerization. *Journal of Polymer Science Part A: Polymer Chemistry*, 48(13):2885–2895, 2010.

[8] Yupei Su, Shuting Zhang, Xiaohua Zhou, Zhuohong Yang, and Teng Yuan. A novel multi-functional bio-based reactive diluent derived from cardanol for high bio-content UV-curable coatings application. *Progress in Organic Coatings*, 148:105880, 2020.

[9] Linchon B. Mehta, Kunal K. Wadgaonkar, and Ramanand N. Jagtap. Synthesis and characterization of high bio-based content unsaturated polyester resin for wood coating from itaconic acid: Effect of various reactive diluents as an alternative to styrene. *Journal of Dispersion Science and Technology*, 40(5):756–765, may 2019.

[10] Yuehong Zhang, Yuzhan Li, Vijay Kumar Thakur, Liwei Wang, Jiyou Gu, Zhenhua Gao, Bo Fan, Qiong Wu, and Michael R Kessler. Bio-based reactive diluents as sustainable replacements for styrene in MAESO resin. *RSC Advances*, 8(25):13780–13788, 2018.

[11] ZengHui Dai, Qing Li, ZhiWei Chen, Rashidul Kabir Shawon, YiYuan Zhu, HongFen Lv, FeiYa Fu, YaoFeng Zhu, YaQin Fu, and XiangDong Liu. Reactive Diluent Derived from Ferulic Acid for the Preparation of a Fully Biobased Unsaturated Polyester Resin. *ACS Sustainable Chemistry & Engineering*, 8(47):17379–17386, nov 2020.

[12] Ursula Biermann, Uwe Bornscheuer, Michael A. R. Meier, Jrgen O. Metzger, and Hans J. Schfer. Oils and Fats as Renewable Raw Materials in Chemistry. *Angewandte Chemie International Edition*, 50(17):3854–3871, April 2011.

[13] Lucas Montero de Espinosa and Michael A.R. Meier. Plant oils: The perfect renewable resource for polymer science?! *European Polymer Journal*, 47(5):837–852, 2011.

[14] Juan Carlos Ronda, Gerard Lligadas, Marina Galià, and Virginia Cadiz. Vegetable oils as platform chemicals for polymer synthesis. *European Journal of Lipid Science and Technology*, 113(1):46–58, 2011.

[15] Arno Behr and Jessica Pérez Gomes. The refinement of renewable resources: New important derivatives of fatty acids and glycerol. *European Journal of Lipid Science and Technology*, 112(1):31–50, jan 2010.

[16] Swechchha Pandey, Bhausaheb S Rajput, and Samir H Chikkali. Refining plant oils and sugars to platform chemicals, monomers, and polymers. *Green Chemistry*, 23(12):4255–4295, 2021.

[17] Florian Stempfle, Benjamin S. Ritter, Rolf Mülhaupt, and Stefan Mecking. Long-chain aliphatic polyesters from plant oils for injection molding, film extrusion and electrospinning. *Green Chemistry*, 16(4):2008–2014, 2014.

[18] John J. La Scala, James M. Sands, Joshua A. Orlicki, E. Jason Robinette, and Giuseppe R. Palmese. Fatty acid-based monomers as styrene replacements for liquid molding resins. *Polymer*, 45(22):7729–7737, 2004.

[19] Maëlle Gobin, Patrick Loulergue, Jean-Luc Audic, and Loïc Lemiègre. Synthesis and characterisation of bio-based polyester materials from vegetable oil and short to long chain dicarboxylic acids. *Industrial Crops and Products*, 70:213–220, 2015.

[20] Hiroaki Miyagawa, Amar K. Mohanty, Rigoberto Burgueño, Lawrence T. Drzal, and Manjusri Misra. Development of Biobased Unsaturated Polyester Containing Functionalized Linseed Oil. *Industrial & Engineering Chemistry Research*, 45(3):1014–1018, February 2006.

[21] Uday Konwar and Niranjan Karak. Hyperbranched polyether core containing vegetable oil-modified polyester and its clay nanocomposites. *Polymer Journal*, 43(6):565–576, 2011.

[22] Magdalena Kwiatkowska, Inez Kowalczyk, Konrad Kwiatkowski, Anna Szymczyk, and Zbigniew Rosłanieca. Fully biobased multiblock copolymers of furan-aromatic polyester and dimerized fatty acid: Synthesis and characterization. *Polymer*, 99:503–512, 2016.

[23] Maike Unverferth. *Fatty acid-derived branched polymer architectures*. PhD thesis, Karlsruhe Institute of Technology (KIT), 2016.

[24] Khantutta-Kim Tremblay-Parrado, Clara García-Astrain, and Luc Avérous. Click chemistry for the synthesis of biobased polymers and networks derived from vegetable oils. *Green Chemistry*, 23(12):4296–4327, 2021.

[25] Tim Abraham and Rainer Höfer. Lipid-Based Polymer Building Blocks and Polymers. In Krzysztof Matyjaszewski and Martin Möller, editors, *Polymer Science: A Comprehensive Reference*, chapter 10.03, pages 15–58. Elsevier, Amsterdam, 2012.

[26] Goswinus H. M. de Kruijff, Thorsten Goschler, Lukasz Derwich, Nicole Beiser, Oliver M. Türk, and Siegfried R. Waldvogel. Biobased Epoxy Resin by Electrochemical Modification of Tall Oil Fatty Acids. *ACS Sustainable Chemistry & Engineering*, 7(12):10855–10864, jun 2019.

[27] U. D. N. Bajpai and Nivedita. Plasticizing polyesters of dimer acids and 1,4-butanediol. In Nicholas P. Cheremisinoff, editor, *Advances in Engineering Fluid Mechanics:*

Multiphase Reactor and Polymerization System Hydrodynamics, chapter 22, pages 583–597. Gulf Professional Publishing, Burlington, 1996.

[28] Sebastián Muñoz-Guerra, Cristina Lavilla, Cristina Japu, and Antxon Martínez de Ilarduya. Renewable terephthalate polyesters from carbohydrate-based bicyclic monomers. *Green Chemistry*, 16(4):1716–1739, 2014.

[29] Dietrich Braun and Matthias Bergmann. 1,4:3,6-Dianhydrohexite als Bausteine fur Polymere. *Journal fur praktische Chemie Chemiker-Zeitung*, 334(4):298–310, jan 1992.

[30] Claudio Gioia, Micaela Vannini, Paola Marchese, Alessandro Minesso, Roberto Cavalieri, Martino Colonna, and Annamaria Celli. Sustainable polyesters for powder coating applications from recycled PET, isosorbide and succinic acid. *Green Chemistry*, 16(4):1807–1815, 2014.

[31] Joshua M. Sadler, Faye R. Toulan, Giuseppe R. Palmese, and John J. La Scala. Unsaturated polyester resins for thermoset applications using renewable isosorbide as a component for property improvement. *Journal of Applied Polymer Science*, 132(30):1–11, 2015.

[32] Yunsheng Xu, Geng Hua, Minna Hakkarainen, and Karin Odelius. Isosorbide as Core Component for Tailoring Biobased Unsaturated Polyester Thermosets for a Wide Structure–Property Window. *Biomacromolecules*, 19(7):3077–3085, 2018.

[33] Mario Pagliaro. C3-Monomers. In Mario Pagliaro, editor, *Glycerol: The Renewable Platform Chemical*, chapter 2, pages 23–57. Elsevier, 2017.

[34] R. K. Saxena, Pinki Anand, Saurabh Saran, and Jasmine Isar. Microbial production of 1,3-propanediol: Recent developments and emerging opportunities. *Biotechnology Advances*, 27(6):895–913, 2009.

[35] Ching Shya Lee and Mohamed Kheireddine Aroua and Wan Mohd Ashri Wan Daud and Patrick Cognet and Y. Péres-Lucchese and Paul-Louis Fabre and O. Reynes and Laure Latapie. A review: Conversion of bioglycerol into 1,3-propanediol via biological and chemical method. *Renewable and Sustainable Energy Reviews*, 42:963–972, 2015.

[36] Matthew Arthur Page, Hari Babu Sunkara, and Judith Johanna Van Gorp. Unsaturated polyester resin compositions comprising 1,3-propanediol, 2009.

[37] Marian Henryk Szkudlarek and Johan Franz Gradus Antonius Jansen. Unsaturated polyester resin, 2012.

[38] T Werpy and G Petersen. Top Value Added Chemicals from Biomass: Volume I – Results of Screening for Potential Candidates from Sugars and Synthesis Gas. Technical report, United States, 2004.

[39] Ken Sexton, John L. Adgate, Gurumurthy Ramachandran, Gregory C. Pratt, Steven J. Mongin, Thomas H. Stock, and Maria T. Morandi. Comparison of Personal, Indoor, and Outdoor Exposures to Hazardous Air Pollutants in Three Urban Communities. *Environmental Science & Technology*, 38(2):423–430, 2004.

[40] Hildeberto Nava. Polyesters, Unsaturated. In Herman F Mark, editor, *Encyclopedia of Polymer Science and Technology*, chapter 11, pages 41–64. John Wiley & Sons, Inc, 3 edition, 2015.

[41] Ana C. Fonseca, Inês M. Lopes, Jorge F. J. Coelho, and Arménio C. Serra. Synthesis of unsaturated polyesters based on renewable monomers: Structure/properties relationship and crosslinking with 2-hydroxyethyl methacrylate. *Reactive and Functional Polymers*, 97:1–11, 2015.

[42] Kingsley Kema Ajekwene. Properties and Applications of Acrylates. In Ángel Serrano-Aroca and Sanjukta Deb, editors, *Acrylate Polymers for Advanced Applications*, chapter 3. IntechOpen, 2020.

[43] Kun Liang, Marco Dossi, Davide Moscatelli, and Robin A. Hutchinson. An Investigation of Free-Radical Copolymerization Propagation Kinetics of Styrene and 2-Hydroxyethyl Methacrylate. *Macromolecules*, 42(20):7736–7744, 2009.

[44] ISO 16620-4. Plastics - Biobased content - Part 4: Determination of biobased mass content. Technical report, International Organization for Standardization, Geneva, Switzerland, 2016.

[45] ISO 13885. Gel permeation chromatography (GPC) - Part 1: Tetrahydrofuran (THF) as eluent. Technical report, International Organization for Standardization, Geneva, Switzerland, 2008.

[46] ISO 2884. Paints and varnishes - Determination of viscosity using rotatory viscometers - Part 2: Disc or ball viscometer operated at a specified speed. Technical report, International Organization for Standardization, Geneva, Switzerland, 2003.

[47] ISO 527. Plastics - Determination of tensile properties - Part 2: Test conditions for moulding and extrusion plastics. Technical report, International Organization for Standardization, Geneva, Switzerland, 2012.

[48] ASTM E1640. Standard test method for assignment of the glass transition temperature by dynamic mechanical analysis. Technical report, ASTM International, West Conshohocken, Pennsylvania, 2018.

[49] Loren W. Hill. Calculation of crosslink density in short chain networks. *Progress in Organic Coatings*, 31(3):235–243, 1997.

[50] J E Mark. Experimental Determinations of Crosslink Densities. *Rubber Chemistry and Technology*, 55(3):762–768, jul 1982.

[51] U. D. N. Bajpai and Ms. Nivedita. Synthesis of plasticizing polyesters of dimer acid and propane–diol. *Journal of Applied Polymer Science*, 50(4):693–697, oct 1993.

[52] ISO 16620-1. Plastics - Biobased content - Part 1: General principles. Technical report, International Organization for Standardization, Geneva, Switzerland, 2015.

[53] Harry R Allcock, Frederick W Lampe, and James E Mark, editors. *Contemporary Polymer Chemistry*. Prentice Hall, New Jersey, 3 edition, 2003.

[54] Frank R. Jones. Unsaturated polyester resins. In Marianne Gilbert, editor, *Brydson's Plastics Materials*, chapter 26, pages 743–772. Butterworth-Heinemann, eighth edition edition, 2017.

[55] Earl E Parker and E W Moffett. Physical Properties of Polyester Resin. *Industrial & Engineering Chemistry*, 46(8):1615–1618, 1954.

[56] Frank Fekete and John S. Mcnally. Unsaturated polyesters, 1972.

[57] Benny Cherian and Eby Thomas Thachil. Synthesis of unsaturated polyester resin – Effect of choice of reactants and their relative proportions. *International Journal of Polymeric Materials and Polymeric Biomaterials*, 53(10):829–845, oct 2004.

[58] Bojana Z Fidanovski, Pavle M Spasojevic, Vesna V Panic, Sanja I Seslija, Jelena P Spasojevic, and Ivanka G Popovic. Synthesis and characterization of fully bio-based unsaturated polyester resins. *Journal of Materials Science*, 53(6):4635–4644, 2018.

[59] H M Akil, M F Omar, A A M Mazuki, S Safiee, Z A M Ishak, and A Abu Bakar. Kenaf fiber reinforced composites: A review. *Materials & Design*, 32(8):4107–4121, 2011.

[60] Omar Faruk, Andrzej K Bledzki, Hans-Peter Fink, and Mohini Sain. Biocomposites reinforced with natural fibers: 2000–2010. *Progress in Polymer Science*, 37(11):1552–1596, 2012.

[61] K L Pickering, M G Aruan Efendy, and T M Le. A review of recent developments in natural fibre composites and their mechanical performance. *Composites Part A: Applied Science and Manufacturing*, 83:98–112, 2016.

[62] Christophe Baley. Analysis of the flax fibres tensile behaviour and analysis of the tensile stiffness increase. *Composites Part A: Applied Science and Manufacturing*, 33(7):939–948, 2002.

[63] Chengguo Liu, Jun Li, Wen Lei, and Yonghong Zhou. Development of biobased unsaturated polyester resin containing highly functionalized castor oil. *Industrial Crops and Products*, 52:329–337, 2014.

Chapter 5

FDCA-based unsaturated polyester

Abstract

This chapter presents the development of unsaturated polyester (UP) main chains and their crosslinked resins (UPRs) based on 2,5-furandicarboxylic acid (FDCA) and other bio-based building blocks. The original features of these UPs derive from (i) the use of FDCA as an aromatic monomer replacing phthalic anhydride (PA), (ii) the introduction of a FDCA-isosorbide block into the polyester backbone with the presence of unsaturations provided by bio-based fumaric acid (FA), (iii) the use of isosorbide (ISO) and 1,3-propanediol (PDO) instead of ethylene glycol and 1,2 propylene glycol, and (iv) the reduction of styrene content using 2-hydroxyethyl methacrylate (HEMA). The developed UPR have similar thermal and mechanical behaviour to the petrochemical ones, presenting T_g up to 102 ℃, tensile modulus and strength up to 3.9 GPa and 63.3 MPa, respectively, and viscosity between 800 and 1250 cP, making these resins greener alternatives to fully petroleum-derived UPR for high-performance applications. Figure 5.1 presents a graphical abstract about this chapter.

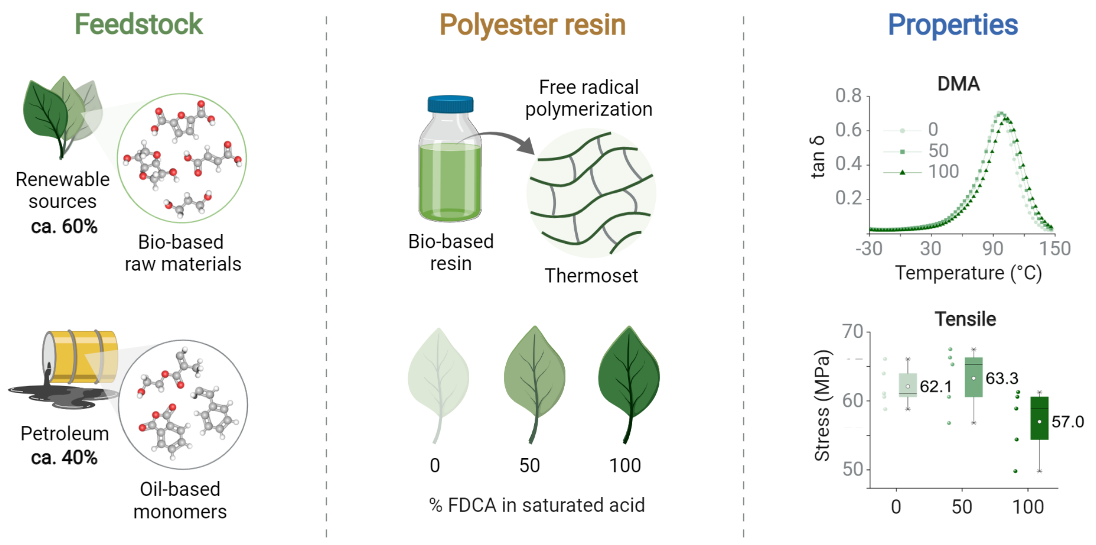

Figure 5.1: FDCA-based unsaturated polyester graphical abstract.

5.1 Introductory remarks

Most research on polymers for industrial applications has focused on thermoplastics, particularly for packaging [1]. However, compared with the rapid progress on bio-based thermoplastics, research on bio-based thermoset resins has been overlooked [2]. Thermoset resins are often used in the production of fibre reinforced polymer (FRP) for several industries, such as construction, automobile, aerospace, marine and wind turbines, reflecting their potential for the development of eco-friendly high-performance products.

The previous research efforts on bio-based thermoset resins focused on formulations that aimed at increasing the bio-content of the unsaturated polyester (UP) backbone [3–6] and at decreasing the styrene-content by reactive diluents derived from bio- or less toxic counterparts [7]. Thus, a more sustainable performance of these plastics must involve incorporating the bio-based polyester backbone diluted in greener vinyl reactive monomers to produce eco- or human health-friendlier UPRs [8]. Among such approaches, monomers considered as renewable building blocks have already been used for synthesis of UPRs, particularly, dicarboxylic acids [9–12], dihydroxyl alcohols [13–15] and reactive diluents with at least one vinyl group [16–19].

It is known that to maintain or improve the mechanical properties of bio-based UPs, when compared to conventional ones, a balance between aliphatic and aromatic or cyclic compounds must be kept within the polyester backbone; for example, FDCA (Figure 5.2), is a potential replacement monomer for oil-derived diacids or anhydrides, such as PA, iso and orthophthalic acid, since it often provides higher mechanical strength and T_g when compared to the above-mentioned aromatic diacids or even to terephthalic acid. Furthermore, FDCA-based polyesters exhibit a semi crystalline structure, but crystallise at a slower rate than polyesters containing an aromatic ring, resulting in much improved barrier properties against oxygen, carbon dioxide, and water vapour, which could be beneficial for high-performance applications, such as in more aggressive environments. The complete replacement of PA by FDCA, at the industrial scale, is still economically not feasible due to relatively high market prices of the latter monomer; however, prices have been decreasing substantially in recent years due to the increased production of that renewable furan building block with increasing usage for plastics production [20–23].

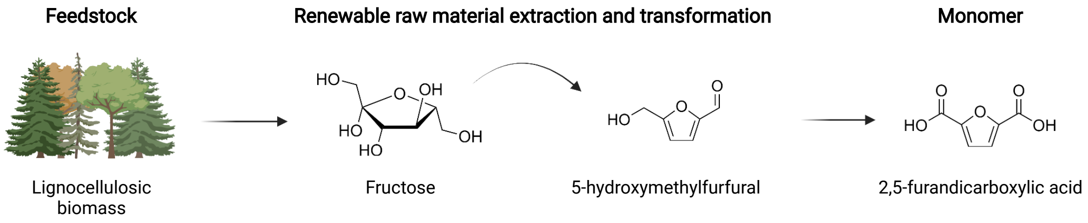

Figure 5.2: From lignocellulosic biomass to FDCA monomer production.

Recently, research has also focused on ISO to provide stiffness to the UP backbone structure, resulting in polyesters with higher T_g than with conventional aliphatic diols [24,25]. By contrast, there is a lack of information about the T_g of UPRs synthesised from FDCA-ISO, which limits its range of applicability, for example concerning its use as a matrix for manufacturing FRP composites for structural applications, where the T_g has significant influence on the maximum service temperature that may be considered in the design of structural component, namely used outdoors.

FDCA and ISO have also been shown in the literature to provide UPRs with higher viscosities [26]. In such cases, viscosity can be adjusted with PDO [27–29], which has low viscosity (liquid at room temperature) and is compatible with polyester of aromatic or rigid cyclic morphology. In addition, the sustainability of UP can be further increased by replacing maleic anhydride (petroleum-based) with bio-based FA [30–32]. The use of FA derived from renewable resources as an unsaturated monomer in the UP backbone allows increasing the bio-content of the polyester and, moreover, due to lower steric hindrance the fumarate double bond is more reactive than the maleate, resulting in a more complete radical polymerisation and a lower need for post-cure treatment.

The balance between T_g and toughness is determined, among other parameters, by the crosslinking density in the UP backbone. Generally, the higher the crosslinking density, the higher the T_g. However, with increasing crosslinking density, the toughness decreases requiring a balance between strength and ductility for each type of application. The crosslinking density of the linear polyester prepolymer can be designed in advance by adjusting the ratio between unsaturated and saturated dicarboxylic acids in the polyester backbone to promote a good balance between T_g and toughness.

Finally, resins for FRP composites should have adequate viscosity and gel time to guarantee the complete impregnation of the reinforcing fibres. Therefore, different variations of the resin composition must be available to allow adjusting it for manufacturing processes with diverse requirements, such as hand layup, vacuum infusion, or pultrusion. Typically, such processes require relatively low viscosity resins (100-2000 cP).

In addition to the previously described strategy of incorporating PDO in the polymer backbone, excessive resin viscosity can be overcome in other ways; for instance, by increasing the styrene content to decrease the target viscosity of the UPR. However, styrene is regarded as a HAP and a VOC, and specially under the occurrence of traces of Ozone the styrene oxide can be formed [33], which is a recognised carcinogen.

Large amounts of reactive diluent tend to decrease the thermophysical properties of the cured resin – it is not recommended to use more than 45% by weight of styrene in the resin composition [34] – and the excess molar in relation with the double bonds in the backbone should be lower than 15%. Non-reacted styrene or excess of any other reactive monomer will result in a plasticising effect, lowering the elastic moduli as well as the long-term performance. This can be a problem in load-bearing structural components, especially those under outdoor exposure to elevated temperatures and/or moisture.

Recently, research has been dedicated to finding ways to eliminate or at least reduce the use of these highly hazardous reactive diluents. For example, methacrylate was reported as an alternative to replacing styrene [35], since methacrylate contains polymerizable radicals through double bonds, which provide similar reactivity as styrene but are less environmentally damaging. An acrylate that has been recently investigated is the HEMA. At room temperature, HEMA is a viscous colourless monomer [36]. HEMA is hydrophilic as it contains a hydrophilic pendant group in its structure. In general, acrylate monomers are well known for the physical properties they impart to the respective polymers, such as elasticity, strength to breakage, and quite good oil and heat resistance. Several studies have shown that HEMA is a suitable alternative to styrene [16,37]. Moreover, HEMA has been used together with styrene as diluent monomer with the UPR, as reactivity between HEMA and styrene has been reported [38].

In this chapter, the application of monomers derived from renewable resources in UPRs is hence considered for structural applications in various areas/fields, namely towards the development of cured UPR of high performance and with high bio-based content via an industrially scalable and eco-friendly approach. For this, bio-based UP backbones were formulated and prepared using FDCA, FA, ISO, PDO and phthalic anhydride (PA), via melt polycondensation. Therefore, the main innovation is the development of a novel high-performance polyester backbone synthesised from renewable building blocks currently considered as top value-added chemical products from biomass [39,40]. However, the variations in the formulations have been around the different concentrations of FDCA, and its incorporation was carried out in three different replacement ratios: 0%, 50%, and 100%. Further, a mixture of styrene and HEMA was used as a reactive diluent, resulting in a cured bio-based polyester resin which is more environmentally sustainable and contains fewer VOCs than conventional petroleum-based ones. The relationships between chemical structures, viscosity, mechanical, and thermomechanical properties were investigated.

5.2 Experimental

5.2.1 Materials

ISO (>98%) was obtained from Roquette, Usine de Lestrem (France). PDO was obtained from DuPont and Tate & Lyle by the name of Susterra™propanediol. FDCA (98%) was obtained from Ambeed, Inc. FA (>98%), PA (99%) and HEMA (97%), imidazole, hydroquinone and toluhydroquinone were obtained from Sigma-Aldrich. Styrene was obtained from Omnova Solutions. MEKP and cobalt octoate 1% were obtained from EcoCompositos S.A. All the chemicals were used as received.

5.2.2 Synthesis

The prepolymers were prepared by catalysed bulk polycondensation following the formulations shown in Table 5.1 and illustrated in Figure 5.3. In a typical experiment, PA (0.792 mol), FDCA (0.792 mol), FA (4.732 mol), PDO (4.694 mol) and ISO (2.347 mol) were added to a 2 litres four-neck reactor (with bottom drain valve) equipped with an anchor blade mechanical stirrer, a thermocouple to control a heating mantle with a set-point temperature at 206 ℃ (ranging between 202 ℃ and 210 ℃), a nitrogen inlet and a condenser attached to a dean-stark adaptor to collect the water (formed in the reaction and raw material solubilization). No vacuum was applied during synthesis.

Herein, imidazole (0.2% relative to the total weight of diacids and diols) was used as the polymerisation catalyst. Hydroquinone and 2-methyl hydroquinone (both used at 200 ppm relative to the total weight of diacids and diols) were also added as the free radical polymerisation inhibitor to prevent premature gelation. All reactants were added at room temperature. The mixture was then stirred, and the progress of the reaction was monitored by acid number (AN) titration and by viscosity measurements at 125 ℃ in a Cone & Plate ICI viscosimeter, see Appendices A.1 and A.6. The reaction was then allowed to proceed until the AN reached a constant value (always below 50 mgKOH/g) combined with a maximum viscosity of 3000 cP, which required approximately 7 to 8 h.

For the planning of formulations and experiments, it was previously confirmed that polyesterification must be carried out under excess of OH to avoid decarboxylation and consider a slight loss of glycol by the air separation system. Consequently, it was found that the amount of carboxylic acid groups is slightly less than the content of alcohol groups. Furthermore, the backbone's unsaturation content must be very close to those provided by the reactive monomer, particularly when an amount of styrene is used as a reactive monomer, as the copolymerisation is specifically alternated.

Table 5.1: UP prepolymer formulations.

Sample				Mol				
Name	**FDCA:PA**	**S:U**[a]	**A:G**[b]	**PA**	**FDCA**	**FA**	**ISO**	**PDO**
UP0	0:100	1:3	1:1.1	1.591	–	4.732	4.713	2.357
UP50	50:50	1:3	1:1.1	0.792	0.792	4.732	4.694	2.347
UP100	100:0	1:3	1:1.1	–	1.591	4.732	4.694	2.337

[a] S:U represents the molar fraction between saturated and unsaturated acid
[a] A:G represents the total molar fraction between acids and glycols

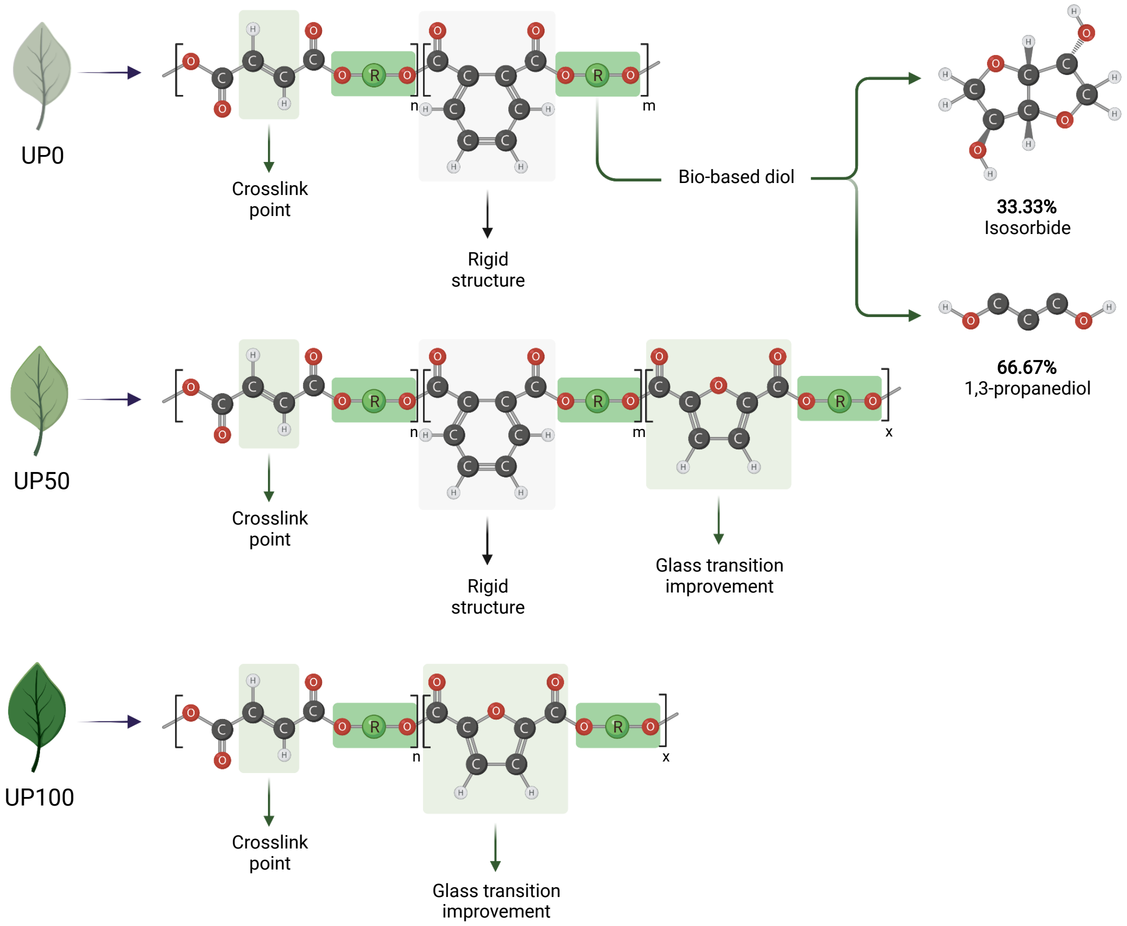

Figure 5.3: Chemical segment structures of the synthesised UPs.

5.2.3 Bio-based content

The bio-based carbon and mass content was determined for each reactant according to ISO 16620 [41] part 4, Annex B (B1 and B2). Tables A.8 and A.11 (from the Appendix A.4) show the calculation procedures.

5.2.4 Kinetics

To evaluate the reaction kinetics, the same procedures adopted in Chapter 3 were taken into account. The theoretical results from equations 3.3 and 3.4 were compared with the corresponding molecular weights as determined by GPC. M_0 was calculated from the weighted average of the components (diacids and diols) for each UP formulation [24], and it can be accessed in Table A.5 from Appendix A.2.2.

5.2.5 Crosslinking reactions

UPs were cooled to a temperature between 140 ℃ and 150 ℃, after AN and viscosity achieved their respective target values. Then, pristine UPs were diluted, without any previous purification step, using a mixture of styrene and HEMA (in equal parts) as a reactive diluent. This mixture aimed at producing UPRs capable of achieving a better balance among high-performance properties, processing characteristics (for different manufacturing techniques), and friendliness with the environment and human health.

To dilute the UP (prepolymer) with reactive diluent, an incorporation temperature between 75 ℃ and 85 ℃ was used to obtain the UPRs. All resin samples consisted of a composition with 60% of UP and 40% of reactive diluent, both in weight, as illustrated in Figure 5.4. After shelf-life confirmation, where the resin samples were stable after storage at room temperature for at least three weeks, the free radical polymerisation of each resin was initiated with 2% MEKP using 1% cobalt octoate (wt.) added as a promoter. Resins were cured for 24 h in a glass mold at 23 ℃, post-cured at 100℃ for 4 h and allowed to stabilise at room temperature before any analyses were conducted.

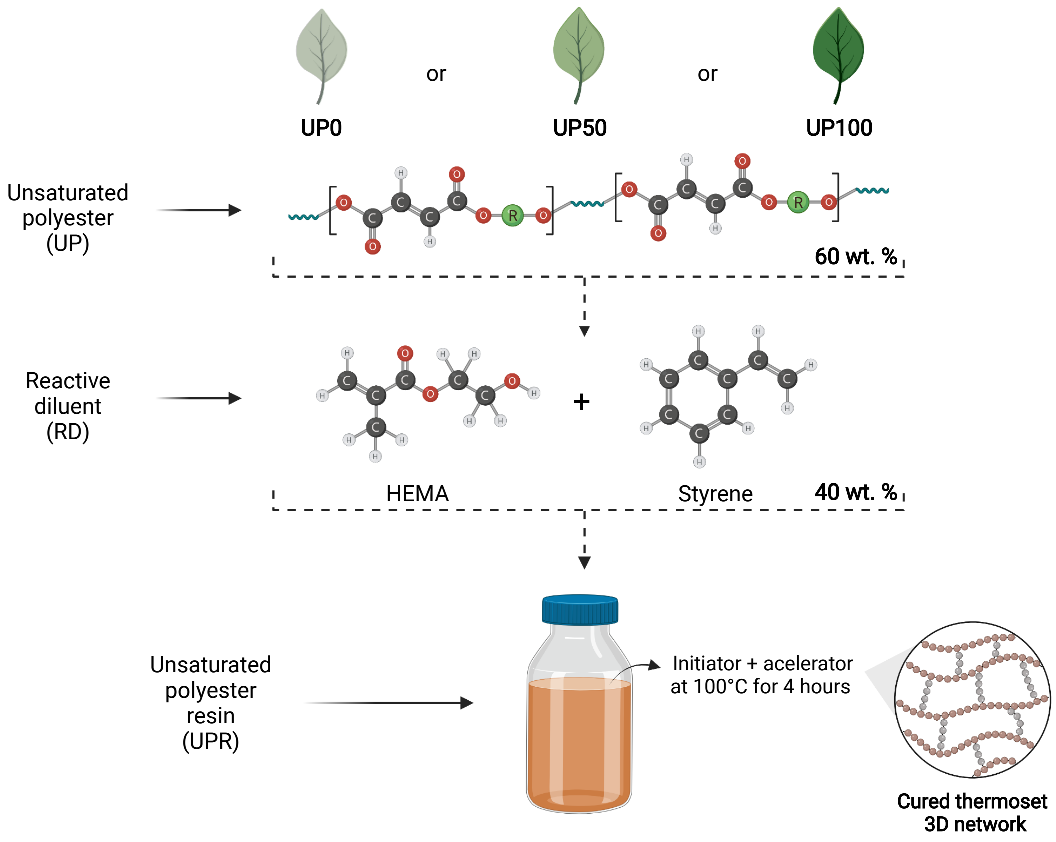

Figure 5.4: Chemical structures of the synthesised UPRs.

5.2.6 Prepolymer characterisation

5.2.6.1 Gel permeation chromatography

GPC tests were performed to determine the number average molecular weight M_n and weigth average molecular weight M_w of the polyester backbone samples using tetrahydrofuran (THF) as eluent, according to ISO 13885-1 [42], in a concentration of 1 mg/mL. The samples were filtered and injected into a column set consisting of one precolumn (8

× 50 mm) PSS SDV, and columns (8 × 300 mm) PSS SDV analytical linear S, both with a 3 µm particle size, and filled with polystyrene crosslinked with divinylbenzene (gel). The columns were equilibrated at 40 ℃ before elution with purged THF at a rate of 1 mL/ min. The eluent was monitored using dual detectors; the first was a UV/Visible detector (model JASCO UV-4075) set to 254 nm and the second was a Refractive Index Detector (model JASCO RI-4030). The molecular weights were calculated based on the retention time from a conventional calibration with narrow polystyrene standards (M_n of 266-59300 Da), see Appendix A.3.

5.2.6.2 Nuclear magnetic resonance

NMR spectra were recorded on Bruker Advance 500 MHz at ambient temperature, see Appendix A.5. ^{1}H chemical shifts (δ) are expressed in ppm relative to Me_4Si (δ = *0*) and are reported relative to the solvent peak (^{1}H NMR).

UP0 (500 MHz, acetone-d_6, 298 K): δ = 7.84-7.65 (C-*H* (phthalate), overlapping multiplets), 6.86-6.74 (C-*H* (FA), overlapping multiplets), 5.48-3.36 (C*H*+CH_2 (ISO) and O-CH_2 (PDO), overlapping multiplets), 2.28-2.07 and 1.97-1.82 (-OCH_2CH_2CH_2O- from PDO, overlapping multiplets).

UP50 (500 MHz, acetone-d_6, 298 K): δ = 7.84-7.65 (C-*H* (phthalate), overlapping multiplets), 7.36-7.29 (C-*H* (furan), overlapping multiplets), 6.86-6.74 (C-*H* (FA), overlapping multiplets), 5.48-3.36 (C*H*+CH_2 (ISO) and O-CH_2 (PDO), overlapping multiplets), 2.28-2.07 and 1.97-1.82 (-OCH_2CH_2CH_2O- from PDO, overlapping multiplets).

UP100 (500 MHz, acetone-d_6, 298 K): δ = 7.36-7.29 (C-*H* (furan), overlapping multiplets), 6.86-6.74 (C-*H* (FA), overlapping multiplets), 5.48-3.36 (C*H*+CH_2 (ISO) and O-CH_2 (PDO), overlapping multiplets), 2.28-2.07 and 1.97-1.82 (-OCH_2CH_2CH_2O- from PDO, overlapping multiplets).

5.2.6.3 Viscosity

The viscosity tests were performed on a Cone & Plate ICI viscometer instrument from REL (Research Equipment London Ltd.), Figures A.10, according to ISO 2884 part 2 [43]. The viscosity was taken as the average value of three measurements.

5.2.7 UPR characterisation

5.2.7.1 Barcol hardness

Barcol hardness tests were performed using a Barber & Colman Barcol impressor (Appendix B.1.1), according to ASTM D2583 [44]. Twenty-five tests were conducted on each specimen. After the tests, the mean obtained was taken as the Barcol hardness.

5.2.7.2 Tensile properties

Tensile test specimens were prepared according to ISO 527 part 2 [45] and were manufactured according to the type 1A specified in that standard (see Appendix B.1.2). The specimens were tested under laboratory conditions with room temperature of 23 ± 2 ℃ and 55 ± 3% relative humidity. For all specimens, width and thickness were measured with a digital micrometer at three points along the length to check tolerances and minimum area for axial stress calculation.

5.2.7.3 Dynamic mechanical analysis

DMA experiments were performed to obtain the thermomechanical properties of the resins using a dynamic mechanical analyser from TA Instruments, model DMA Q800, see Figure B.4. Specimens with dimensions 60 mm × 10 mm × 4 ± 0.5 mm were fabricated according to ASTM E1640 [46] and tested in a 35 mm dual cantilever clamp configuration. Specimens were subjected to a constant strain amplitude of 15 µm at a constant oscillation frequency of 1 Hz while submitted to a temperature sweep at a constant heating rate of 2 ℃/min, starting at –30 ℃ and ending at 150 ℃. The T_g was determined (i) based on the onset values of the storage modulus decay and (ii) from the tan δ peak.

The experimental crosslink density (ν_e) was determined based on the kinetic theory of rubber elasticity from the rubbery modulus using the following equation [47]:

$$\nu_e = \frac{G'}{\mathrm{RT}} = \frac{E'}{3\mathrm{RT}} \tag{5.1}$$

where R is the gas constant (8.314 J K/mol), and T is the absolute temperature in K, and G' is the shear storage modulus. The flexural storage modulus (E') was obtained in the rubbery plateau. Herein, the rubbery plateau region of the storage modulus, defined based on the DMA tests, was taken to estimate ν_e. The kinetic theory of rubber elasticity assumes that the network is ideal and all chains are effective in elastic deformation [48].

For comparison, both tensile and DMA tests were performed on specimens moulded from a commercial resin (see section B.2 in Appendix B), cured and characterised under the same conditions as the bio-based UPRs herein developed.

5.3 Results and discussion

5.3.1 Prepolymers

The molar fraction between saturated and unsaturated acids (S:U = 1:3) aimed to balance the thermophysical and mechanical properties to reach a similar performance to their general purpose petroleum-derived counterparts. Setting this ratio for all formulations intended: (i) to promote a crosslinking density in the backbone able to achieve a high T_g;

(ii) to avoid a high content of reactive double bonds, responsible for the embrittlement of the resin when crosslinked with the reactive diluent (especially styrene) and (iii) to allow the direct evaluation of the influence of replacing PA by FDCA. Furthermore, the molar fraction between ISO and PDO (about 33% and 67% of the total amount of glycols, respectively) were intended to produce stiff polyesters with suitable processability for applications in FRP composites, ensuring a good relationship between the resin viscosity and its hardness after curing. An excess of 10 mol% glycol was used to compensate for its distillation loss during the polycondensation reaction.

5.3.2 Bio-based content

UP prepolymers were synthesised from diacids and diols via the catalysed direct melt polycondensation with negligible VOC emissions. Except for PA, all other monomers were obtained from renewable resources, resulting in the synthesis of UPs with almost wholly bio-based carbon (x_B) and mass (m_B) contents, of respectively 99.7% and 99.8% for the UP100 prepolymer (see Table 5.2). Meanwhile, non-bio-based catalyst and inhibitors used during synthesis, even if in a very small percentage, prevented the UP backbone from being produced with 100% renewable content. Despite this, the high level of bio-based content presented in all UPs fulfil a relevant principle of green chemistry, since according to ISO 16620-1 [49], bio-based plastics are those that contain materials, wholly or partially of biogenic origin, where the concept of bio-based content for plastics refers to '*the amount of bio-based carbon, the amount of the content of synthetic bio-based polymer or the amount of the bio-based mass content only*'.

Table 5.2: Bio-based carbon and mass content of UPs and UPRs, according to ISO 16620-4 [41].

Sample	x_B (%)	m_B (%)
UP0 (UPR0)	78.6 (47.2)	84.1 (50.4)
UP50 (UPR50)	88.8 (53.3)	91.9 (55.2)
UP100 (UPR100)	99.7 (59.8)	99.8 (59.9)

Bio-based carbon and mass contents decreased after incorporation of UPs with the reactive diluent since these diluents are not fully derived from renewable resources. However, the partial replacement of styrene by HEMA allowed to obtain UPRs with a lower concentration of toxic monomers when compared to conventional ones (wholly styrene-based), resulting in materials with a lower harmful potential to human health [37,50]. In addition, the use of FDCA (in replacement of PA) in the proportions stipulated in this study provided UPR resins with bio-based content reaching approximately 60%. Thus, this study shows that the most recent advances obtained by the synthesis of thermoplastic UPs based on FDCA and ISO, can be expanded to the production of UPRs, particularly, by introducing unsaturation with bio-based FA into the polyester backbone. Herein, PDO was also essential to maintain high bio-based content and to adjust the viscosity of these polyesters comparatively to that of conventional counterparts (petroleum-based).

5.3.3 Kinetics

The progress of the polyesterification reaction was monitored using AN titration (see Table A.2) and viscosity measurements to calculate the extent of the reaction and the processing ability of the samples, which allowed to produce prepolymers with similar molecular weights and with viscosities suitable for incorporation in reactive solvents. UPs used in the preparation of commercial UPRs often present AN values ranging from 25 to 50 mgKOH/g [11], which were fulfilled in this study with the bio-based UPRs.

Plotting values of $1 + r/(1 + r - 2rp)$ as a function of time typically shows that equation 3.2 is not obeyed from $p = 0$ up to about $p = 0.80$ (*i.e.*, for the first 80% of the esterification of COOH and OH groups). The deviation below 80% conversion is not unique for polyesterification, since it is also observed for the simple esterification that results when the dicarboxylic acid is replaced by a monocarboxylic acid. Apparently, the major reason for the non-adherence to equation 3.2 below about 80% conversion is that the reaction medium is changing from one of pure reactants initially to one in which the ester product is the solvent. It is often considered that the kinetics of condensation polymerisation are relevant only for the last 20% of the reaction when the reaction medium has become essentially invariant [51].

Second-order plots are shown in Figure 5.5 for the last 20% of the polyesterification, after 180 min of reaction. Beyond that period, chain growth to produce high molar mass material becomes increasingly difficult as the reaction proceeds. This is due to several reasons, such as: (i) the difficulty in ensuring the precise equivalence of the reactive groups in the starting materials, since more than two monomers were used, (ii) the decreasing frequency of functional groups meeting and reacting as their concentration diminishes, and (iii) the increasing likelihood of interference from side reactions (even with the use of inhibitors). Thus, it was preferred to avoid the production of high molar mass to avoid gelation, even with conversions above 90%. However, the higher conversion was observed when PA was replaced by FDCA, since for the same reaction time, a lower AN was obtained for the fully FDCA-based backbone (see Table A.2 in Appendix A.2.1).

Figure 5.5 also shows that the kinetics had a well-defined trend, where the error bars around the conversion represent the standard deviation resulting from three titrations; for all formulations, the standard deviation was low.

5.3.4 Molecular weight

The molecular weights determined by GPC followed a Gaussian distribution (see Figure A.4 in Appendix A.3), with M_n varying between 1.4 kDa and 2.0 kDa, which falls within the

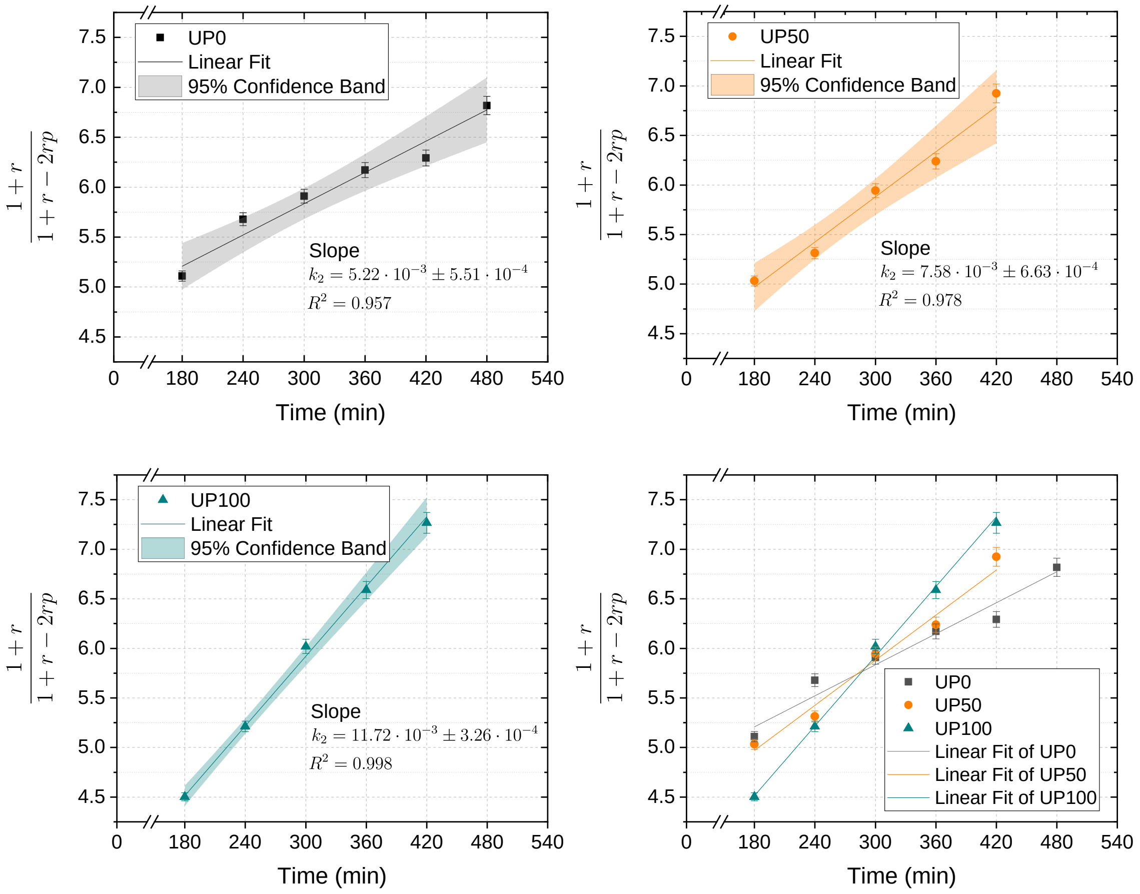

Figure 5.5: Kinetics of polyesterification reaction of UPs.

range referred in the literature [52,53]. The replacement of PA by FDCA resulted in higher M_n and lower dispersity when comparing UP0 to UP100, since a lower AN was achieved by the UP100, and for the same OH–COOH ratio, resulted in higher conversion and with more similar chain lengths (see Table 5.3), which is consistent with the higher degree of polymerisation obtained from oligomeric macromolecules wholly based on FDCA. Higher M_n is desired to enable higher crosslink density, which provides a higher number of unsaturated sites per macromolecule without the need to increase the concentration of FA. This improves thermal and mechanical properties since it does not sacrifice stiffness and strength by removing the saturated dicarboxylic acid. By contrast, UP50 shows that the partial replacement of PA by FDCA reflects a higher dispersity *Đ* and lower M_n when compared to the other formulations, which can be explained by the greater number of reactants in its composition, *i.e.*, herein diols compete to react not only with FA and just one more saturated dicarboxylic acid, but they also participate in the reaction with two other saturated acids, namely PA and FDCA. Furthermore, the presence of low molecular weight fractions in UP0 and UP50 samples was observed, which is typical in orthophthalic polyesters.

When compared with similar formulations reported in the literature, *e.g.*, PPIF25 from Dai *et al.* [54], UP02 from Suriano *et at.* [55], MSIB1322 from Xu *et al.* [25], polyester 4 from

Table 5.3: Composition analysis of the UPs.

Sample	AN	Theoretical			GPC analysis			
	(mgKOH/g)	p^a (%)	M_n (kDa)	M_w (kDa)	M_n (kDa)	M_w (kDa)	$Đ$ (a.u)	p^b (%)
UP0	47	0.90	1.47	2.80	1.45	3.60	2.48	0.90
UP50	47	0.90	1.53	2.91	1.40	5.60	4.00	0.89
UP100	43	0.91	1.53	2.93	2.00	3.20	1.60	0.94

[a] Conversion obtained from titration, according to Equation 3.1.

[b] Conversion obtained from GPC tests.

Jasinska and Koning [14], which take into account ratios of saturated to unsaturated acid that are close to that presented here, UP100 presents higher M_n and lower $Đ$. UP100 from the present study also has higher M_n when compared to UPs based on itaconic acid, such as those synthesized by Panic *et al.* [56], and those based on oxalic, succinic and adipic acid prepared by Fidanovski *et al.* [8] Although the example UP4 from Sousa *et al.* [9] presents higher M_n than those studied here in UP0, UP50 and UP100, no viscosity data corresponding to M_n is available in that study (this information would be relevant, since high molecular weight often results in higher viscosity and more difficult processing).

The UP properties are very much dependent on the characteristics of the raw materials used and the formulation adopted. The UPs developed here presented relatively low molecular weight since the polycondensation reactions were controlled to achieve low working viscosities when dissolved in reactive diluent. This resulted in oligomers with a degree of polymerisation lower than 10 for all samples, which is in accordance with the literature for the formation of unsaturated polyesters, for which degrees of polymerisation between 6 and 15 are typically reported [57,58].

5.3.5 ^{1}H NMR study

NMR is a convenient tool to estimate the relative proportion of the different monomers present in the polymers. We exemplify here for UP50, the most complicated case. This polymer was obtained as a mixture of FDCA, PA, FA, PDO and ISO. We can assign different regions of the spectra with different types of protons, as exemplified in Figure A.9 and Table A.13 (included in Appendix A.5). While FDCA, PA and FA appear separated, the CH_2 inner protons of the PDO moiety appear partially superimposed with the solvent protons (acetone). We can nonetheless integrate CH_2 signals with some level of confidence, although we expect to have a larger error than for the signals that appear isolated. Given the amount of the PDO detected, we can calculate the amount of isosorbide by deducting the integration of the -CH_2O- protons that overlap with the isosorbide protons in the 5.48-3.36 ppm region. We arrive thus at the molar fraction PA:FDCA:FA:PDO:ISO of 1.16:1.00:5.06:6.33:6.31. The same analysis procedure was performed for UP0 and UP100. Table 5.4 presents the molar percentages based on the ^{1}H NMR calculations of the molar fractions mentioned above.

Table 5.4: Comparison between ^{1}H NMR results and predicted structure of the UPs.

Monomer	Feed (mol %)			^{1}H NMR (mol %)		
	UP0	UP50	UP100	UP0	UP50	UP100
PA	11.84	5.92	-	12.48	5.69	-
FDCA	-	5.92	11.84	-	4.91	10.72
FA	35.53	35.53	35.53	26.51	27.41	29.47
PDO	35.09	35.09	35.09	35.44	31.04	34.98
ISO	17.54	17.54	17.54	25.57	30.95	24.83
S:U[a]	25:75	25:75	25:75	32:68	28:72	27:73
A:G[b]	48:52	48:52	48:52	39:61	38:62	40:60
PDO:ISO[c]	67:33	67:33	67:33	58:42	50:50	58:42

[a] S:U represents the molar percentage between saturated and unsaturated acid
[b] A:G represents the molar percentage between acids and glycols
[c] PDO:ISO represents the molar percentage between PDO and ISO

Some points can be highlighted from the results shown in Table 5.4 between the structure characterised by ^{1}H NMR and the initially fed: (i) UP50 and UP100 have similar S:U ratios with the fed ones, with a lower retention percentage of FA, 96% and 97%, respectively; (ii) the lowest retention percentage of FA is found in UP0, around 90%; (iii) as a consequence of the higher FA amount in the final structure of the UP100, a higher ν_e can be achieved, which partly explains the higher T_g of the respective UPR100, which will be discussed later; (iv) A:G ratios from ^{1}H NMR show a higher excess of glycol for all UPs, with 17%, 19% and 15% higher for UP0, UP50 and UP100, respectively, when compared to the fed ratios; (v) a lower acid amount is presented in the final structure of the respective UPRs, with UP0, UP50 and UP100 retaining 81%, 79% and 83%, respectively, in relation to the fed quantities, and; (vi) a higher presence of ISO and a lower PDO content in relation to the total of glycols is verified for all UPs, which can be explained by the laboratory set up (distillation column, nitrogen flow) that drags more glycol than that used industrially, mainly PDO, which is more susceptible to carryover than ISO.

5.3.6 Viscosity

The control of viscosity during synthesis ensured that all linear thermoplastic UP samples had viscosities at 125 ℃ below 3000 cP, as shown in Figure 5.6 where the error bars represent one standard deviation around the average values of the three apparent viscosity measurements and the three titration measurements for calculating the degree of polymerisation, both from each reaction time for a same batch. This criterion allowed producing UPs with suitable viscosity for subsequent incorporation with a percentage of reactive diluent of 40%, see Table 5.5. This value is in line with the industry standards regarding conventional thermoset polyester resins. Furthermore, the relatively low viscosities have the added benefit of promoting better cure performances due to the higher mobility of the polymeric chains.

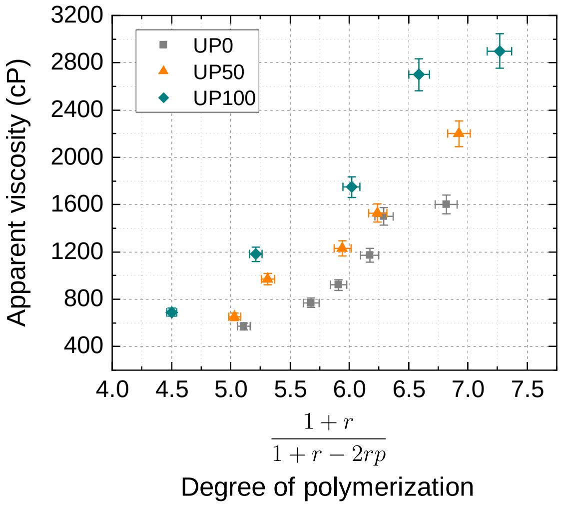

Figure 5.6: Viscosity of the UPs measured at 125 ℃.

Among the main factors that limited the extent of reaction due to excessive viscosity being reached, the presence of ISO can be highlighted. This monomer contributes to a higher increase in the viscosity of UP in relation to other aliphatic diols due to its intrinsic features of steric hindrance [59] and *Ordelt* saturation (branching formation) with FA. Additionally, a UP produced exclusively from an ISO-based glycol would probably not be miscible in styrene [60]. Even if branching occurs at a low level, without additional crosslinking and gelation, the prepolymers obtained are generally unsuitable for UPR preparation due to their high viscosity. The curing process for this resin would also result in the formation of a non-homogeneous network with poor mechanical properties. To minimise the excessive increase in viscosity due to ISO, all UPs were formulated to contain a maximum of 33 mol% of ISO regarding the total glycol amount. Moreover, inhibitors (hydroquinone and toluhydroquinone) were used to minimise *Ordelt* saturation and mitigate gelation. However, it was found that gelation can occur at lower acid numbers (AN below 40) when performing polycondensation at elevated temperatures (about 206 ℃).

Table 5.5: Viscosity of the UPRs.

Sample	Incorporation ratio in wt. (%)			Viscosity
	Prepolymer	HEMA	Styrene	(cP)
UPR0	60	20	20	800
UPR50	60	20	20	1290
UPR100	60	20	20	1250

Furthermore, while FDCA also increases the viscosity in UPRs, the results obtained show that the UPR formulations developed here can be applied for different processing techniques used in the composites industry, for example, hand layup, vacuum infusion and pultrusion. These resins have the additional advantage of having a lower concentration of styrene than typical (conventional) UPRs, with this reduction reaching up to 50% of the total amount of styrene used.

5.3.7 Hardness

Barcol hardness average values increased from 30 ± 1 (UPR0) to 32 ± 1 (UPR100) as PA was replaced by FDCA into the UP backbone. This (slight) difference can be explained by the fact that UPR100 presents greater-formed 3D network, since a higher degree of polymerisation was obtained from UP100 macromolecule (having more crosslinkable sites) and, consequently this lead to a higher crosslinking density. The higher crosslinking density potentially achieved after incorporation with reactive diluents should result in stronger interactions between atoms or molecules, and thus in harder thermosets. By contrast, UPR50 had Barcol hardness of 30 ± 2, showing similar hardness compared to UPR0, but a higher scatter of results because of a higher *Đ* of the polymer molecular structure, as seen previously in Table 5.3.

The overall differences between UPR0, UPR50 and UPR100 in terms of Barcol hardness were very limited. This shows that the hardness of UPR specimens based on FDCA building blocks used herein has not been negatively influenced compared to that of UPR specimens based on petrochemical PA. More specifically, the Barcol hardness values measured for the bio-based resins compare relatively well with those of the commercial (petrochemical) counterpart tested herein, which presents a Barcol hardness of 40.

5.3.8 Tensile behaviour

The tensile stress-strain nominal curves of the UPRs are presented in Figure 5.7. The results show a highly consistent behaviour of the curves for UPR0 and UPR50 and the highest scatter for UPR100. The high variability in the tensile strength results of UPR100, also reflected in the scatter of its strain at break (whose mean value is also lower), should be attributed to its higher brightness compared to its UPR0 and UPR50 counterparts. However, all formulations present tensile curves with an initial elastic linear branch, a gradual loss of stiffness for higher strains, and hard and brittle stress-strain behaviour, reflecting a typical constitutive behaviour of conventional UPR under tension. The fully crosslinked structure of the UPRs obstructs the mobility of the molecules, and the network chains cannot easily align in the tensile direction, which is one of the sources of ductility. This barrier may form an internal crack, and initiate crack propagation, making a ductile thermoset polymer become brittle [61].

Figure 5.8 presents the statistical values for tensile strength, modulus of elasticity, and strain at break, respectively. The UPR0, UPR50, and UPR100 formulations presented modulus of elasticity of 3.4 GPa, 3.4 GPa and 3.9 GPa, respectively, matching or exceeding their general-purpose commercial counterparts, which vary on average from 2 to 4 GPa

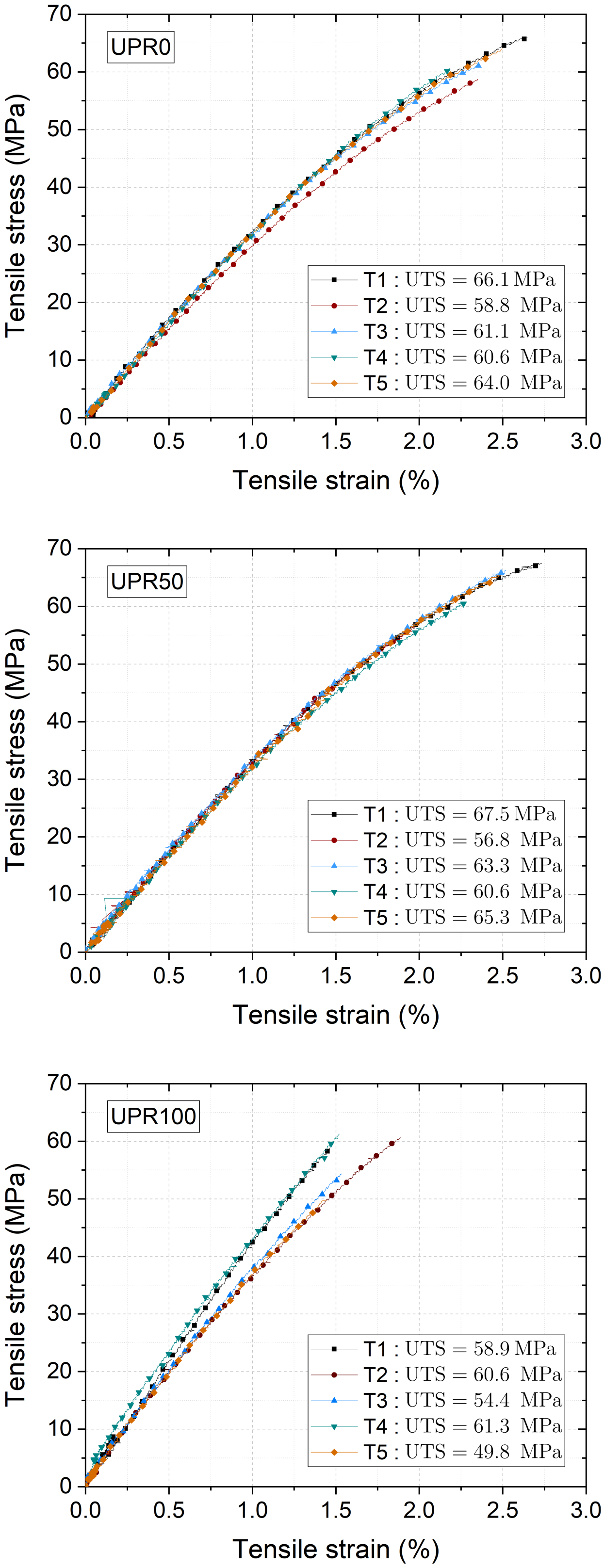

Figure 5.7: Tensile stress-strain curves of the FDCA-based UPRs.

[62], as well as other conventional formulations well established in the literature [34,63]. Formulations with aromatic and furan dicarboxylic acids used herein also allowed to obtain UPRs with a higher modulus of elasticity when compared to those UPRs based on saturated aliphatic dicarboxylic acids, such as, succinic, itaconic, and adipic acid, which have been addressed in the literature [8,56]. Some other factors can also explain the higher modulus of elasticity, namely (i) high double bonds content with 1:3 in mol% S:U dicarboxylic acid ratio in all formulations, providing high crosslinking density, which results in hard and inflexible cured UPRs; (ii) prepolymer synthesised from rigid structure saturated acids (PA and FDCA), which provides chains with lower flexibility when compared with polyesters based on diacids derived from natural oils; and (iii) the fact that one-third of total glycols have been ISO, also responsible for promoting greater rigidity in the backbone compared to aliphatic diols.

The results presented here also evidenced that the total replacement of PA by FDCA (UPR100) provided the highest modulus of elasticity. By contrast, the UPR100 polyester resins showed lower tensile strength (-8%) and strain at break (-37%) when compared to the UPR0. The outlier shown in Figure 5.8c was disregarded for calculating the mean of the UPR100 strains. Thus, the mean strain at break was 1.5%. Considering that strength is not just an intrinsic polymer property but also depends on the concentration and dimensions of defects in the casting and curing of UPRs which present volume shrinkage on curing of (about 8 to 12%), tensile strength results are generally lower than the real polymer capacity. Regardless of this comparison between the three different formulations tested in this study, FDCA shows good potential as a replacement monomer to PA in the production of UPRs. In fact, the tensile strength results obtained for the bio-based UPRs developed herein were higher when compared to those of the conventional petroleum-derived resin that was also tested herein as a commercial reference (see Table B.1 from the Appendix B.3), and which is widely used as a high-performance thermoset polyester matrix, with the additional advantage of the proposed UPR0, UPR50, and UPR100 formulations having a high bio-based content.

The results of tensile strength, modulus of elasticity and strain at break obtained for all tested formulations also show that it is possible to reduce the styrene content in UPRs by its partial replacement by HEMA. Namely, it was found that the mechanical properties were not negatively affected when compared to a commercial unsaturated polyester resin tested herein, which uses exclusively styrene as a reactive diluent.

5.3.9 Dynamic mechanical analysis

DMA was used to determine the thermomechanical properties of the cured UPRs and to assess, mainly, the effect of increasing the FDCA concentration. Figure 5.9 presents the DMA curves for the storage modulus (E'), loss modulus (E'') and tan δ as a function of temperature for the UPRs. The T_g results are presented in Table 5.6 based on the onset

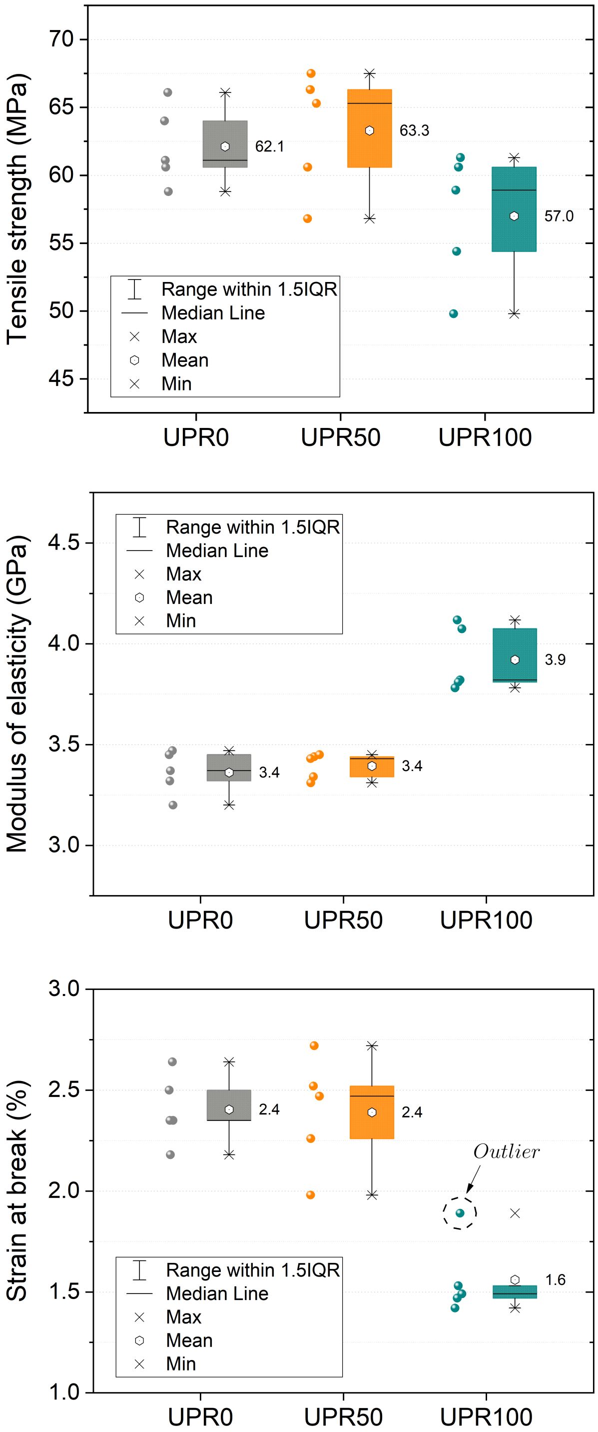

Figure 5.8: Scatter plots of UPRs tensile results: **a.** tensile strength; **b.** modulus of elasticity; and **c.** strain at break.

value of the storage modulus decay and the peak of the tan δ curve; the values of E' at 25 ℃, 50 ℃ and 150 ℃ are also presented.

All the cured UPRs displayed T_g values ranging from 65 to 70 ℃ and from 95 to 102 ℃, based on the onset of the storage modulus decay and tan δ peak, respectively. These values enable the use of the proposed resins in a wide range of high-performance applications, such as FRP composites.

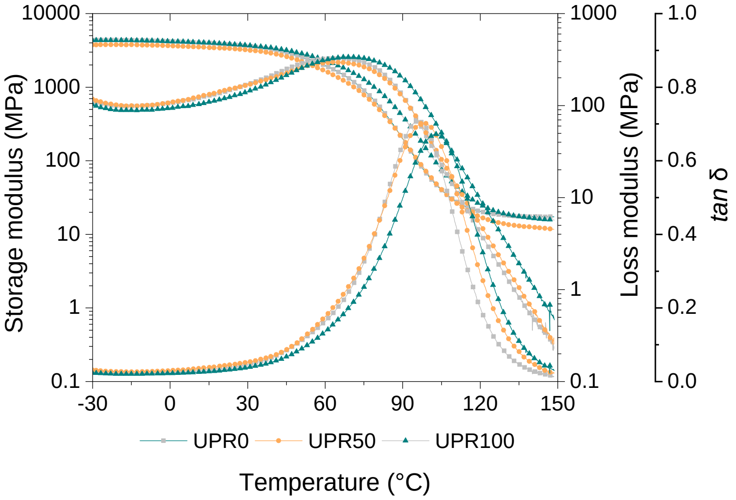

Figure 5.9: Overlapping DMA curves of all UPRs.

Despite the high ν_e presented by the UPRs, as shown in Table 5.6, the T_g values of the crosslinked thermosets relate to the crosslink density and the rigidity of the chain segments [64]. This explains the higher T_g for formulations with FDCA (particularly, UPR50 and UPR100), since the furan ring of FDCA contributed with greater rigidity and intermolecular force in the molecular chains and, consequently, promoted a decreased mobility of chain segments of the cured UPRs.

Table 5.6: DMA properties of the UPRs.

Sample	T_g (℃)		E' (MPa)			ν_e
	E'_{onset}	tan δ	25 ℃	50 ℃	125 ℃	(mol/m^3)
UPR0	65	96	3745	2618	19	1.9×10^{-3}
UPR50	65	98	3305	2289	15	1.5×10^{-3}
UPR100	70	102	3810	2916	21	2.1×10^{-3}

Meanwhile, it is quite clear that the E' at 25 ℃ of the cured UPR100 was higher than for the UPR0, due to the above mentioned reasons. The backbone of the UPR50 comprises two different types of saturated acid monomer blocks, namely, FDCA- and PA-blocks, unlike UPR0 and UPR100, which have either only-FDCA- or only-PA-blocks in their backbones. This larger number of reagents (with different reactivities) used in the backbone synthesis of the UPR50 resulted in the lowest p and the lowest M_n compared to the other formulations. In addition, the highest $Đ$ was observed for the backbone of the UPR50. Thus, the presence of macromolecules with different chain lengths (but with high M_w) resulted in a more heterogeneous material and in a thermoset with lower capacity to store (or higher capacity to dissipate) elastic energy under loading.

At higher temperatures, namely at 50 °C, FDCA promoted retention of approximately 76.5% of the storage modulus for the UPR100 against 69.9% for the UPR0 consisting of saturated acid exclusively based on phthalic anhydride. The E' retention values corresponding to the T_g (onset) of the UPR0, UPR50 and UPR100 were 43%, 40%, and 52%, respectively. Thus, the full replacement of phthalic anhydride by FDCA in the prepolymer backbone improved the thermomechanical properties of the resulting cured thermosets, which is desirable for many high-performance applications.

The incorporation of HEMA, as a reactive diluent for the UPRs proved to be successful also regarding thermomechanical properties. Conversely, thermoset FDCA-polyesters incorporated without a minimum styrene content typically present low storage modulus [9,54], thus not being suitable for several high-performance applications. It is possible to highlight the following observations when comparing the thermomechanical results obtained for the bio-based UPRs developed herein with those for their commercial counterpart (entirely petroleum-derived): (i) all bio-based formulations presented T_g's equal to or very close to that of the commercial UPR, showing that the formulations and syntheses of the bio-based blocks resulted in novel and promising bio-based thermoset polyesters, suitable for use in high-performance applications at relatively high temperatures; (ii) UPR100 allowed producing thermoset polyesters capable of achieving thermomechanical properties that are competitive with those of commercial UPR (entirely replacing PA by FDCA); (iii) at room temperature, the storage modulus of all bio-based formulations matched or exceeded those of the commercial counterpart; and (iv) at 50 °C, the UPR100 storage modulus was higher than its commercial counterpart – this shows that, together with FDCA, the other chosen bio-based monomers, namely the ISO and PDO diols, as well as the concentration of FA used in the formulations tested herein, resulted in a thermoset polyester capable of storing more energy when loaded at high temperatures. This property can be relevant for several engineering applications, especially for high-performance products, such as composites.

5.4 Concluding remarks

Syntheses of UPRs based on FDCA and other renewable building blocks have been successfully carried out. The linear UPs synthesised are almost entirely based on renewables (reaching 99.8 wt.%). The high bio-based content of the UPs combined with their dilution in a diluent formed by the mixture of two reactive monomers, namely, styrene and HEMA, allowed to produce more environmentally and health-friendly UPRs than conventional ones. In addition, it was shown (UPR100) that FDCA can replace its petrochemical counterpart

(PA) with improved mechanical and thermomechanical properties. Together with their chemical composition (bio-based) and processing properties, which fall within the range of viscosities of various fibre impregnation processing techniques (such as pultrusion), these properties of the synthesised UPRs increase their prospects as successful greener high-performance materials, which can be exploited, for example, by the composites industry.

5.5 References

[1] Amar K Mohanty, Singaravelu Vivekanandhan, Jean-Mathieu Pin, and Manjusri Misra. Composites from renewable and sustainable resources: Challenges and innovations. *Science*, 362(6414):536–542, 2018.

[2] Jinyue Dai, Songqi Ma, Yonggang Wu, Lijing Han, Lisheng Zhang, Jin Zhu, and Xiaoqing Liu. Polyesters derived from itaconic acid for the properties and bio-based content enhancement of soybean oil-based thermosets. *Green Chemistry*, 17(4):2383–2392, 2015.

[3] Thomas J Farmer, Rachael L Castle, James H Clark, and Duncan J Macquarrie. Synthesis of Unsaturated Polyester Resins from Various Bio-Derived Platform Molecules. *International Journal of Molecular Sciences*, 16(7):14912–14932, 2015.

[4] Alessandro Gandini and Talita M Lacerda. From monomers to polymers from renewable resources: Recent advances. *Progress in Polymer Science*, 48:1–39, 2015.

[5] Mohamed Naceur Belgacem and Alessandro Gandini. Materials from Vegetable Oils: Major Sources, Properties and Applications. In Mohamed Naceur Belgacem Gandini and Alessandro, editors, *Monomers, Polymers and Composites from Renewable Resources*, chapter 3, pages 39–66. Elsevier, Amsterdam, 2008.

[6] Carla Vilela, Andreia F Sousa, Ana C Fonseca, Arménio C Serra, Jorge F J Coelho, Carmen S R Freire, and Armando J D Silvestre. The quest for sustainable polyesters – insights into the future. *Polym. Chem.*, 5(9):3119–3141, 2014.

[7] Sylvain Cousinet, Ali Ghadban, Etienne Fleury, Frédéric Lortie, Jean-Pierre Pascault, and Daniel Portinha. Toward replacement of styrene by bio-based methacrylates in unsaturated polyester resins. 67:539–550, 2015.

[8] Bojana Z Fidanovski, Pavle M Spasojevic, Vesna V Panic, Sanja I Seslija, Jelena P Spasojevic, and Ivanka G Popovic. Synthesis and characterization of fully bio-based unsaturated polyester resins. *Journal of Materials Science*, 53(6):4635–4644, 2018.

[9] New unsaturated copolyesters based on 2,5-furandicarboxylic acid and their crosslinked derivatives. *Polymer Chemistry*, 7(5):1049–1058, 2016.

[10] Biomass-derived monomers for performance-differentiated fiber reinforced polymer composites. *Green Chemistry*, 19(12):2812–2825, 2017.

[11] Cátia S. M. F. Costa, Ana C. Fonseca, Jorge Moniz, Maria Godinho, Jorge F. J. Coelho, and Arménio C. Serra. Going greener: Synthesis of fully biobased unsaturated polyesters for styrene crosslinked resins with enhanced thermomechanical properties. *Express Polymer Letters*, 11(11):885–898, 2017.

[12] Joseph J Bozell and Gene R Petersen. Technology development for the production of biobased products from biorefinery carbohydrates—the US Department of Energy's "Top 10" revisited. *Green Chemistry*, 12(4):539–554, 2010.

[13] Oliver Goerz and Helmut Ritter. Polymers with shape memory effect from renewable resources: crosslinking of polyesters based on isosorbide, itaconic acid and succinic acid. *Polymer International*, 62(5):709–712, 2013.

[14] Lidia Jasinska and Cor E Koning. Unsaturated, biobased polyesters and their cross-linking via radical copolymerization. *Journal of Polymer Science Part A: Polymer Chemistry*, 48(13):2885–2895, 2010.

[15] Paulien F H Harmsen, Martijn M Hackmann, and Harriëtte L Bos. Green building blocks for bio-based plastics. *Biofuels, Bioproducts and Biorefining*, 8(3):306–324, 2014.

[16] Linchon B Mehta, Kunal K Wadgaonkar, and Ramanand N Jagtap. Synthesis and characterization of high bio-based content unsaturated polyester resin for wood coating from itaconic acid: Effect of various reactive diluents as an alternative to styrene. *Journal of Dispersion Science and Technology*, 40(5):756–765, may 2019.

[17] ZengHui Dai, Qing Li, ZhiWei Chen, Rashidul Kabir Shawon, YiYuan Zhu, HongFen Lv, FeiYa Fu, YaoFeng Zhu, YaQin Fu, and XiangDong Liu. Reactive Diluent Derived from Ferulic Acid for the Preparation of a Fully Biobased Unsaturated Polyester Resin. *ACS Sustainable Chemistry & Engineering*, 8(47):17379–17386, nov 2020.

[18] Yupei Su, Shuting Zhang, Xiaohua Zhou, Zhuohong Yang, and Teng Yuan. A novel multifunctional bio-based reactive diluent derived from cardanol for high bio-content UV-curable coatings application. *Progress in Organic Coatings*, 148:105880, 2020.

[19] Yuehong Zhang, Yuzhan Li, Vijay Kumar Thakur, Liwei Wang, Jiyou Gu, Zhenhua Gao, Bo Fan, Qiong Wu, and Michael R Kessler. Bio-based reactive diluents as sustainable replacements for styrene in MAESO resin. *RSC Advances*, 8(25):13780–13788, 2018.

[20] Andreia F Sousa, Carla Vilela, Ana C Fonseca, Marina Matos, Carmen S R Freire, Gert-Jan M Gruter, Jorge F J Coelho, title ="Biobased polyesters Silvestre Armando J. D., and 5-furandicarboxylic acid: a tribute to furan excellency other polymers from 2. Biobased polyesters and other polymers from 2,5-furandicarboxylic acid: a tribute to furan excellency. *Polym. Chem.*, 6(33):5961–5983, 2015.

[21] Min Jiang, Qian Liu, Qiang Zhang, Chong Ye, and Guangyuan Zhou. A series of furan-aromatic polyesters synthesized via direct esterification method based on renewable resources. *Journal of Polymer Science Part A: Polymer Chemistry*, 50(5):1026–1036, 2012.

[22] George Z Papageorgiou, Dimitrios G Papageorgiou, Zoi Terzopoulou, and Dimitrios N Bikiaris. Production of bio-based 2,5-furan dicarboxylate polyesters: Recent progress and critical aspects in their synthesis and thermal properties. *European Polymer Journal*, 83:202–229, 2016.

[23] Alessandro Gandini. The behaviour of furan derivatives in polymerization reactions. In M. Gordon, editor, *Polymer Chemistry. Advances in Polymer Science*, pages 47–96. Springer Berlin Heidelberg, Berlin, Heidelberg, 1 edition, 1977.

[24] Joshua M Sadler, Faye R Toulan, Giuseppe R Palmese, and John J La Scala. Unsaturated

polyester resins for thermoset applications using renewable isosorbide as a component for property improvement. *Journal of Applied Polymer Science*, 132(30), 2015.

[25] Yunsheng Xu, Geng Hua, Minna Hakkarainen, and Karin Odelius. Isosorbide as Core Component for Tailoring Biobased Unsaturated Polyester Thermosets for a Wide Structure–Property Window. *Biomacromolecules*, 19(7):3077–3085, 2018.

[26] Mónica Lomelí-Rodríguez, José R Corpas-Martínez, Susan Willis, Robert Mulholland, and Jose A Lopez-Sanchez. Synthesis and Characterization of Renewable Polyester Coil Coatings from Biomass-Derived Isosorbide, FDCA, 1,5-Pentanediol, Succinic Acid, and 1,3-Propanediol. *Polymers*, 10(6), 2018.

[27] R K Saxena, Pinki Anand, Saurabh Saran, and Jasmine Isar. Microbial production of 1,3-propanediol: Recent developments and emerging opportunities. *Biotechnology Advances*, 27(6):895–913, 2009.

[28] C S Lee, M K Aroua, W.M.A.W. Daud, P Cognet, Y Pérès-Lucchese, P-L Fabre, O Reynes, and L Latapie. A review: Conversion of bioglycerol into 1,3-propanediol via biological and chemical method. *Renewable and Sustainable Energy Reviews*, 42:963–972, 2015.

[29] Mario Pagliaro. C3-Monomers. In Mario Pagliaro, editor, *Glycerol*, chapter 2, pages 23–57. Elsevier, 2017.

[30] Sang Yup Lee, Hyun Uk Kim, Tong Un Chae, Jae Sung Cho, Je Woong Kim, Jae Ho Shin, Dong In Kim, Yoo-Sung Ko, Woo Dae Jang, and Yu-Sin Jang. A comprehensive metabolic map for production of bio-based chemicals. *Nature Catalysis*, 2(1):18–33, 2019.

[31] F. S. Carta, C. R. Soccol, L. P. Ramos, and J D Fontana. Production of fumaric acid by fermentation of enzymatic hydrolysates derived from cassava bagasse. *Bioresource Technology*, 68(1):23–28, 1999.

[32] Current advances on biological production of fumaric acid. *Biochemical Engineering Journal*, 153:107397, 2020.

[33] Ken Sexton, John L Adgate, Gurumurthy Ramachandran, Gregory C Pratt, Steven J Mongin, Thomas H Stock, and Maria T Morandi. Comparison of Personal, Indoor, and Outdoor Exposures to Hazardous Air Pollutants in Three Urban Communities. *Environmental Science & Technology*, 38(2):423–430, 2004.

[34] Hildeberto Nava. Polyesters, Unsaturated. In Herman F Mark, editor, *Encyclopedia of Polymer Science and Technology*, chapter 11, pages 41–64. John Wiley & Sons, Inc, 3 edition, 2015.

[35] Giuseppe R. Palmese, John Joseph La Scala, Joshua Matthew Sadler, and Anh-Phuong Thy Lam. Renewable bio-based (meth)acrylated monomers as vinyl ester cross-linkers, 2017.

[36] Kingsley Kema Ajekwene. Properties and Applications of Acrylates. In Ángel Serrano-Aroca Deb and Sanjukta, editors, *Acrylate Polymers for Advanced Applications*, chapter 3. IntechOpen, 2020.

[37] Ana C Fonseca, Inês M Lopes, Jorge F J Coelho, and Arménio C Serra. Synthesis of unsaturated polyesters based on renewable monomers: Structure/properties relationship and crosslinking with 2-hydroxyethyl methacrylate. *Reactive and Functional Polymers*, 97:1–11, 2015.

[38] Kun Liang, Marco Dossi, Davide Moscatelli, and Robin A Hutchinson. An Investigation of Free-

Radical Copolymerization Propagation Kinetics of Styrene and 2-Hydroxyethyl Methacrylate. *Macromolecules*, 42(20):7736–7744, 2009.

[39] Lauren Winstel. Top Value Added Chemicals: The Biobased Economy 12 Years Later, 2017.

[40] T. Werpy and G. Petersen. Top Value Added Chemicals from Biomass. Volume I: Results of Screening for Potential Candidates from Sugars and Synthesis Gas. Technical report, U.S. Department of Energy, U.S. Department of Energy, 2004.

[41] ISO 16620-4. Plastics - Biobased content - Part 4: Determination of biobased mass content. Technical report, International Organization for Standardization, Geneva, Switzerland, 2016.

[42] ISO 13885. Gel permeation chromatography (GPC) - Part 1: Tetrahydrofuran (THF) as eluent. Technical report, International Organization for Standardization, Geneva, Switzerland, 2008.

[43] ISO 2884. Paints and varnishes - Determination of viscosity using rotatory viscometers - Part 2: Disc or ball viscometer operated at a specified speed, 2003.

[44] ASTM D2583. Standard Test Method for Indentation Hardness of Rigid Plastics by Means of a Barcol Impressor. Technical report, ASTM International, West Conshohocken, PA, 2013.

[45] ISO 527. Plastics - Determination of tensile properties - Part 2: Test conditions for moulding and extrusion plastics. Technical report, International Organization for Standardization, Geneva, Switzerland, 2012.

[46] ASTM E1640. Standard test method for assignment of the glass transition temperature by dynamic mechanical analysis. Technical report, ASTM International, West Conshohocken, Pennsylvania, 2018.

[47] Loren W Hill. Calculation of crosslink density in short chain networks. *Progress in Organic Coatings*, 31(3):235–243, 1997.

[48] J E Mark. Experimental Determinations of Crosslink Densities. *Rubber Chemistry and Technology*, 55(3):762–768, jul 1982.

[49] ISO 16620-1. Plastics - Biobased content - Part 1: General principles. Technical report, International Organization for Standardization, Geneva, Switzerland, 2015.

[50] Yuchao Wu, Mingen Fei, Renhui Qiu, Wendi Liu, and Jianhui Qiu. A review on styrene substitutes in thermosets and their composites. *Polymers*, 11(11), 2019.

[51] Harry R Allcock, Frederick W Lampe, and James E Mark, editors. *Contemporary Polymer Chemistry*. Prentice Hall, New Jersey, 3 edition, 2003.

[52] Alain Fradet and Martine Tessier. *Polyesters*, chapter 2, pages 17–134. John Wiley & Sons, Ltd, 2003.

[53] K. G. Johnson and L. S. Yang. *Preparation, Properties and Applications of Unsaturated Polyesters*, chapter 21, pages 697–713. John Wiley & Sons, Ltd, 2004.

[54] Jinyue Dai, Songqi Ma, Na Teng, Xinyan Dai, Xiaobin Shen, Sheng Wang, Xiaoqing Liu, and Jin Zhu. 2,5-furandicarboxylic acid- and itaconic acid-derived fully biobased unsaturated polyesters and their cross-linked networks. *Industrial & Engineering Chemistry Research*, 56(10):2650–2657, 2017.

[55] Raffaella Suriano, Maria Nelly Garcia Gonzalez, and Stefano Turri. Environmental Profile and Technological Validation of New High-Tg Unsaturated Polyesters from Fully Bio-Based

Monomers and Reactive Diluents. *Journal of Polymers and the Environment*, 29(4):1122–1133, 2021.

[56] Vesna V Panic, Sanja I Seslija, Ivanka G Popovic, Vuk D Spasojevic, Aleksandar R Popovic, Vladimir B Nikolic, and Pavle M Spasojevic. Simple One-Pot Synthesis of Fully Biobased Unsaturated Polyester Resins Based on Itaconic Acid. *Biomacromolecules*, 18(12):3881–3891, 2017.

[57] Frank R Jones. Unsaturated Polyester Resins. In Marianne Gilbert, editor, *Brydson's Plastics Materials (Eighth Edition)*, chapter 26, pages 743–772. Butterworth-Heinemann, 8th edition, 2017.

[58] Earl E Parker and E W Moffett. Physical Properties of Polyester Resin. *Industrial & Engineering Chemistry*, 46(8):1615–1618, 1954.

[59] Bart A. J. Noordover, Viola G. van Staalduinen, Robbert Duchateau, Cor E. Koning, van Benthem, Manon Mak, Andreas Heise, August E. Frissen, and Jacco van Haveren. Co- and Terpolyesters Based on Isosorbide and Succinic Acid for Coating Applications: Synthesis and Characterization. *Biomacromolecules*, 7(12):3406–3416, 2006.

[60] F. Fenouillot, A. Rousseau, G. Colomines, R. Saint-Loup, and J.-P. Pascault. Polymers from renewable 1,4:3,6-dianhydrohexitols (isosorbide, isomannide and isoidide): A review. *Progress in Polymer Science*, 35(5):578–622, 2010.

[61] D.W. van Krevelen and Klaas te Nijenhuis. *Properties of Polymers: Their Correlation With Chemical Structure; their Numerical Estimation and Prediction from Additive Group Contributions*. Elsevier Science, 4 edition, 2009.

[62] Andreas Kandelbauer, Gianluca Tondi, Oscar C Zaske, and Sidney H Goodman. Unsaturated Polyesters and Vinyl Esters. In Hanna Dodiuk and Sidney H B T Handbook of Thermoset Plastics (Third Edition) Goodman, editors, *Handbook of Thermoset Plastics*, chapter 6, pages 111–172. William Andrew Publishing, Boston, 3 edition, 2014.

[63] Benny Cherian and Eby Thomas Thachil. Synthesis of unsaturated polyester resin – Effect of choice of reactants and their relative proportions. *International Journal of Polymeric Materials and Polymeric Biomaterials*, 53(10):829–845, oct 2004.

[64] Songqi Ma, Dean C. Webster, and Farukh Jabeen. Hard and flexible, degradable thermosets from renewable bioresources with the assistance of water and ethanol. *Macromolecules*, 49(10):3780–3788, 2016.

Part III

Composites

Chapter 6

Bio-based GFRP composites

Abstract

This chapter presents the manufacturing and mechanical and thermomechanical characterisation of a bio-based GFRP composite, produced by vacuum infusion, using a high-performance bio-based unsaturated polyester resin; this resin was developed in-house and more than 50 wt.% of its content is derived from renewable raw materials. Bio-based GFRP specimens, with a mass fibre content of 60%, comprising uni- and bi-directional mats, were successfully produced, and their mechanical and thermomechanical behaviour was assessed and compared to an equivalent GFRP composite produced with conventional petroleum-based unsaturated polyester resin and the same fibre architecture. The bio-based GFRP composite presented (i) 538 MPa, 210 MPa, and 52 MPa of tensile, compressive, and shear strengths, (ii) 20 GPa, 24 GPa, and 2.5 GPa of tensile, compressive, and shear moduli, and (iii) 3.0%, 0.8%, and 14.8% of tensile, compressive, and shear strain at failure. These figures meet or exceed the mechanical properties of the equivalent GFRP composite produced with conventional petroleum-derived resin, evaluated under the same conditions. Furthermore, the bio-based GFRP composite presented a T_g of 64 ℃ (defined from the onset of the storage modulus decay), enabling its use in outdoor applications. These figures highlight the potential of the bio-based GFRP composite developed herein for structural applications, which offers a key advantage in terms of sustainability. Figure 6.1 presents a graphical abstract about this chapter.

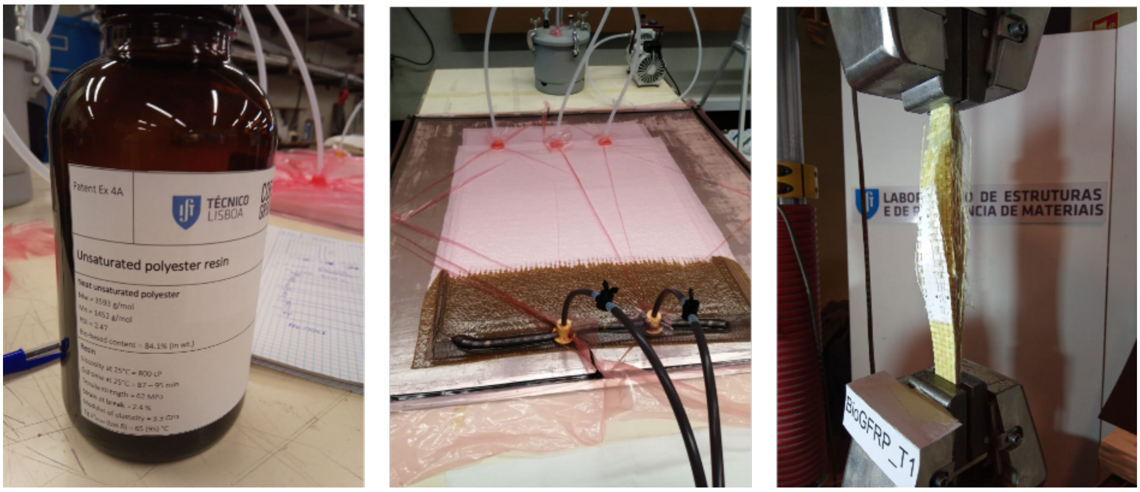

Figure 6.1: Bio-based GFRP laminate graphical abstract.

6.1 Introductory remarks

Sustainability is becoming especially relevant for the fibre-polymer composites industry, given its extensive use of non-renewable materials; in recent years, research efforts have been heavily invested in developing more circular and sustainable polymers and composites [1,2]. Particular focus has been given, for example, to: (i) developing bio-based thermoplastics [3–5], (ii) achieving recyclability of thermosets [6–8], such as epoxy- or polyesters-type vitrimers [9–12], namely through the use of dynamic hardeners/agents [13–16] or by chemical depolymerisation [17,18], and (iii) replacing synthetic fibres with natural (mainly vegetable) ones [19–22] to manufacture greener (or closed-loop) composites for different industries, such as automotive, naval, and wind energy. Despite such efforts, one of today's biggest challenges is the introduction of sustainable composites in products that require high mechanical, thermomechanical, processing and durability performance, namely those used in civil engineering structural applications.

Composite parts used in the new construction or strengthening of civil engineering structures located outdoors (*e.g.*, bridges, viaducts, platforms, piers, docks, tunnels, buildings, and others) require high-mechanical performance, durability, and cost effectiveness. In this respect, performance and processing limitations and insufficient durability data are restricting the use of (more) sustainable composites developed to date in civil structural applications [23–28]. For instance, bio-based thermoplastics typically have high viscosity and require heat and pressure during moulding [29,30], which precludes their use as a fibre impregnation matrix in typical large-scale FRP production techniques, such as pultrusion or vacuum infusion. In addition, when alternative high-performance matrices present mechanical, thermomechanical, and processing properties suitable for high-performance applications, they are expensive, which limits the commercial prospect of their use in mainstream composite products [31–36].

Although recyclable thermoset composites are seen as a potential solution to increase the circularity of the composites industry, their durability is yet to be comprehensively characterised, namely under long-term exposure to external weathering degradation agents likely to be found in civil engineering structures, such as moisture, saline environments, thermal effects, ultraviolet radiation, among others [37,38].

The use of natural fibres, particularly vegetable ones, also entails some critical drawbacks, which still need to be overcome, such as: (i) biodegradability, including the risk of microbial contamination [39,40]; (ii) hydrophilicity (whereas thermoset resins are hydrophobic), associated with significant potential moisture absorption of composites reinforced by natural fibres (up to 8% or 10%), also causing the subsequent degradation of fibres and reduction in material performance over time; (iii) flammability – these fibres are not resistant to high temperatures – generally, they lose their stiffness at around 160 ℃ and thermally degrade at a temperature of approximately 200 ℃ [41–45], preventing their use with some matrices and manufacturing techniques, such as pultrusion; and (iv) their tensile strength is lower when compared to conventional man-made fibres; thus, they are best suited to produce parts that do not require particularly high strength [46,47].

In this context, a quicker and more competitive way to improve the sustainability of the fibre-polymer composites industry should involve replacing petroleum-derived matrices with bio-based counterparts, since thermoset matrices can represent 30-70% of the fibre-polymer composite weight. Among thermoset matrices, unsaturated polyesters are the most often used, due to their lower cost when compared to epoxies and vinylester [48]. Although unsaturated polyesters are most suited for structural applications subjected to less aggressive exposure conditions, they are versatile and their processing, mechanical and thermomechanical properties are suitable to produce glass fibre reinforced polymer (GFRP) profiles, laminates, strips, and other composite structural parts [49]. Unsaturated polyesters are typically used to impregnate glass fibre reinforcement [50]; however, they are also compatible with several other types of reinforcing fibres, such as basalt and (although less commonly) carbon [51–54]. Thus, the use of high-performance thermoset polyester matrices derived from renewable raw materials for the manufacturing of FRP composites can be considered as a significant advancement towards a more sustainable composites industry; indeed, this approach entails a potential reduction of the environmental impacts of FRP composites [55–58].

Previous efforts in this respect were made by Rorrer *et al.* [59], who developed a GFRP composite from a muconic acid-based unsaturated polyester resin. The glass fibre impregnation was carried out by soaking the fibres with the bio-based resin between two sheets of Teflon on a plate heated to 80 ℃ and allowed to react for 4 hours. Although the authors reported the shear modulus[1], other relevant mechanical and processing properties, such as tensile strength and viscosity, were not presented. Later, Rorrer *et al.* [60] also tested muconate-containing unsaturated polyester resins diluted in mixtures of styrene, methacrylic acid, and cinnaminic acid, as a matrix for impregnating double-ply woven glass fibre mat; the same manufacturing procedures used in the previous study were applied and, subsequently, the composite was placed in a vacuum oven for 48 hours. The bio-based composite had a sustainable potential, but no information was provided about the resin viscosity. The T_g of the composite was determined by differential scanning calorimetry (DSC), varying between 90 ℃ and 100 ℃.

Dai *et al.* [61] developed fully bio-based composites with itaconic acid-based unsaturated polyester diluted in dimethyl itaconate and reinforced with cotton fabrics. Due to the constituent materials used, the composites presented low tensile strength (34 MPa), thus not being competitive for structural applications. Skrifvars *et al.* [62] investigated the potential of using a low cost, randomly oriented non-woven viscose fabric impregnated with a bio-based unsaturated polyester resin in structural composites. However, the mechanical

---

[1] The value reported by the authors, $\sim$32 GPa is unusually high, being most likely incorrect.

properties obtained were too low for structural applications; and, moreover, the thermo-mechanical properties (which are relevant for design, namely for outdoor applications) were not presented and the bio-based resin derived from soybean oil derivatives had a low bio-content of only 13%.

Wu *et al.* [63] produced a series of thermosets based on palm oil and isosorbide with a bio-based content of 60%. They used a variety of fibre mats for reinforcement, ranging from natural bamboo and kenaf fibres to synthetic fibres, such as glass and carbon fibres. The fibres were stacked and wetted with resin and then pressed into a hot compression mould. Although this is not a typical technique used in the large-scale fabrication of composites for civil structural applications, the material produced presented high glass transition temperature (∼136 °C to 193 °C). Hosseini *et al.* [32] tested a bio-based methacrylate epoxidized sucrose soyate diluted in styrene as a matrix for unidirectional E-glass composites, manufactured by compression moulding. The mechanical properties were similar to those of a conventional vinyl ester resin, which was used for comparison.

Other recent studies have also focused on the use of FRP composites comprising synthetic fibres in a bio-based thermoset polymeric matrix for external strengthening applications, such as those previously mentioned in the literature review by McSwiggan and Fam [64], showing potential of bio-based furfural alcohol resins for FRP composites used in construction rehabilitation. In addition, bio-based resins have also been studied as matrices for FRP face sheets of sandwich panels; the results obtained by Mak *et al.* [65] confirmed the high potential of the bio-based resins used; however, the authors also indicated the need for improvements in terms of their chemical structures and of the fibre interaction envisaging their broad applicability.

It is worth referring the work by Smits [66] who presented a survey about the application of FRP composites in bridges, including bio-based composites. He reported the construction of a pedestrian bridge in Eindhoven, produced with (i) linen fibres and (ii) bio-based resins derived from vegetable oils, poly(lactic acid) foam and natural cork. This was one of the first footbridges with bio-based composites to be built and tested. Aspects such as the carbon footprint and the treatment of plant fibres were briefly discussed. Despite its innovation, this project shows that additional research and development is necessary to improve the performance of bio-based composites for civil structural applications.

Despite the efforts to develop new bio-based resins, currently, most thermosets commercially available for manufacturing composites [2] still have reduced incorporation of sustainable raw materials, approximately 30-35% [67–69]. It is also worth referring that although new commercial resins have recently been made available [70], the composites market for structural applications still lacks bio-based thermoset resins with processing characteristics suitable for current manufacturing techniques, such as vacuum infusion and

---

[2] These commercial bio-based thermoset resins are suitable for applications in various products, such as boats, automotive, energy, and sports parts.

pultrusion, and that present the required mechanical and thermomechanical properties (after curing) for load-bearing composite structures.

In this context, there are challenges to be overcome for the development of more sustainable unsaturated polyester resins with a potential to achieve, at the same time: (i) mechanical and thermomechanical behaviour suitable for structural applications in construction, (ii) processing properties compatible with typical techniques used to manufacture large-scale FRP parts, such as vacuum infusion and pultrusion, and (iii) having a high bio-content from raw materials derived from renewable sources. In addition, the characterisation of relevant mechanical and thermomechanical properties of bio-based composites developed to date is still scarce, namely in what concerns the compressive, interlaminar shear and in-plane shear properties, and the glass transition temperature from DMA tests; this last information is essential for the structural design of bio-based GFRP composites, since the T_g determination by DMA is more relevant to determine the stiffness reduction of the composite caused by the increase in temperature – this method is required in the future European Technical Specification for the "*Design of Fibre-Polymer Composite Structures*" [71].

This chapter presents the manufacturing and mechanical characterisation of a bio-based GFRP composite, manufactured by vacuum infusion, combining glass fibres and a high-performance bio-based unsaturated polyester resin recently developed in-house [72–74], which was synthesised using monomers (diacids and diols) derived from renewable sources. The cured bio-based resin has a renewable content of more than 50% by weight, while containing less volatile organic compounds in the liquid resin compared to typical conventional petroleum-based alternatives. Thus, the main goal and innovation of the study presented herein is the development of a bio-based GFRP composite with (i) high bio-based content that meets or exceeds the previously referenced works, and (ii) mechanical and thermomechanical properties capable of competing with those of its conventional counterpart, manufactured with petroleum-derived unsaturated polyester resins. For this purpose, an experimental campaign was conducted towards the manufacturing and subsequent mechanical and thermomechanical characterisation of bio- and conventional-based GFRP, which were produced and tested under the same conditions.

6.2 Experiments

6.2.1 Materials

Bio-based unsaturated polyester resin (Resin-B) was used as a polymer matrix for glass fibre impregnation during the production of a bio-based GFRP composite (GFRP-B). Resin-B was produced by synthesising monomers (diacids and diols) derived from renewable raw materials. The bio-based unsaturated main chain (prepolymer) obtained from the polycondensation reaction was subsequently incorporated using a mixture of styrene and

HEMA (in equal parts) as a reactive diluent [72–74], according illustrated in Figure 5.4 in the chapter 5.

The following main features of the bio-based resin can be highlighted: (i) the replacement of maleic anhydride and ethylene glycol (both petroleum-derived) by fumaric acid, isosorbide and 1,3-propanediol (renewable sources-derived), respectively, which allowed the bio-based resin to achieve more than 50% in weight of bio content; (ii) suitable viscosity (750cP at 23 ℃) for the vacuum infusion technique; and (iii) mechanical and thermomechanical properties that match or exceed those of its petroleum-derived counterparts.

In this study, a conventional petroleum-derived unsaturated polyester resin (Resin-C) with viscosity of 300 cP at 23 ℃, obtained from Scott Bader, under the commercial designation of Crystic U 904 LV^{TM}, was also used for glass fibre impregnation to produce a conventional GFRP (GFRP-C). This commercial resin was used as a reference for comparison with Resin-B. Thus, the mechanical and thermomechanical characterisation was performed for both Resin-C and Resin-B under identical conditions. Both resins were post-cured at 100 ℃ for 4 hours. Table 1 shows the mechanical and thermomechanical properties obtained for the cured resins, namely the mean values of: strength ($\sigma_{t,max}$ and $\sigma_{c,max}$), modulus of elasticity (E_t and E_c) and strain at break ($\epsilon_{t,max}$ and $\epsilon_{c,max}$) in tension (t) and compression (c); shear strength (τ_{max}), shear modulus (G) and distortion at failure (γ_{max}); and (T_g), based on the onset value of the storage modulus decay.

Table 6.1: Mean values of mechanical and thermomechanical properties of Resin-C and Resin-B specimens.

Specimen	$\sigma_{t,max}$ **(MPa)**	E_t **(GPa)**	$\epsilon_{t,max}$ **(%)**	$\sigma_{c,max}$ **(MPa)**	E_c **(GPa)**	$\epsilon_{c,max}$ **(%)**	τ_{max} **(MPa)**	G **(GPa)**	γ_{max} **(%)**	T_g[a] **(℃)**	T_g[b] **(℃)**
Resin-C	60.7	3.0	1.9	131.5	4.5	5.2	58.4	1.4	5.2	75	102
Resin-B	62.1	3.4	2.4	119.4	3.8	5.3	64.9	1.5	5.4	65	96

[a] T_g from onset of storage modulus decay
[b] T_g from tan δ peak

The glass reinforcement comprised: (i) unidirectional fiberglass mats (WR-500) with 500 g/m^2, obtained from Castro Composites (Spain); and (ii) bidirectional (0°/90°) fiberglass mats (G-Sheet E 90/10, Type A) with 440 g/m^2, obtained from S&P Clever Reinforcement Ibérica. Figure 6.2 presents the detailed layup of the glass fibre reinforcement layers, which were stacked in a symmetric and balanced configuration.

6.2.2 Manufacturing

GFRP-C and GFRP-B composite laminates were produced by vacuum infusion. The vacuum equipment and consumables[3] were obtained from Easy Composites (United

---

[3] Vacuum pump, resin trap, vacuum bagging film, peel ply, breather cloth, infusion mesh, PVC vacuum hoses, straight and tee vacuum hose connectors, resin infusion connector, sealant tape, and auxiliary elements for infusion.

Kingdom) and Castro Composites (Spain).

Figure 6.2 illustrates the manufacturing setup, which is also depicted in Figure 6.3 for the infusion of the GFRP-B composite laminate (the same procedure was adopted to manufacture the GFRP-C composite laminate). Before starting the infusion, vacuum was applied for 24 hours to ensure adequate pressure and confirm the absence of leaks. Afterwards, the resin was transferred with vacuum, which was kept for additional 24 hours, achieving a homogeneous percolation of the resin along the laminate, namely in-between the various layers, thus improving the potential adhesion between each constituent.

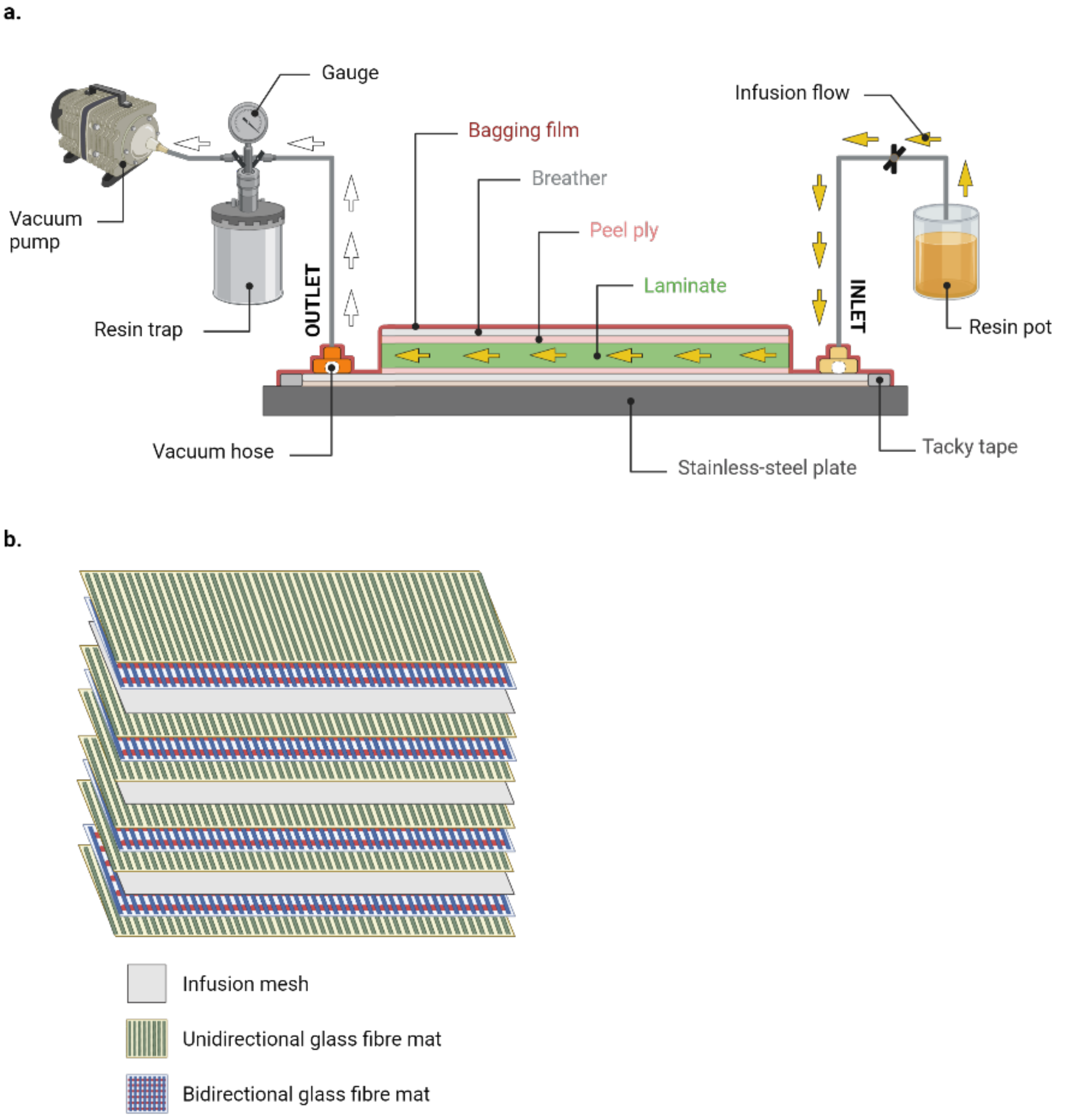

Figure 6.2: GFRP manufacturing procedures: **a.** setup, **b.** fibre layup.

The manufacturing of the GFRP composite laminates was prepared with the following components: (i) 4 bidirectional glass fibre mats and six unidirectional glass fibre mats, with approximate dimensions of 1.03 m in length and 0.70 m in width; (ii) two sheets of

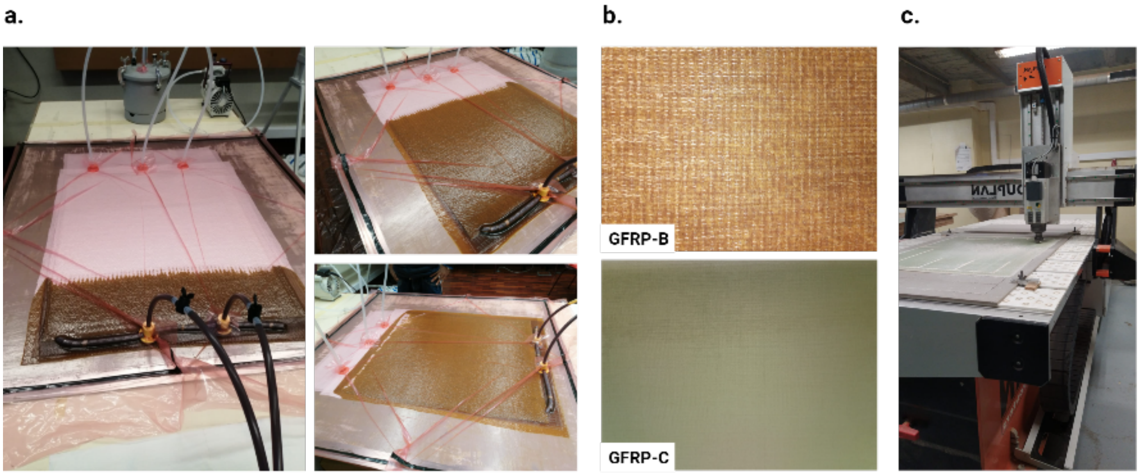

Figure 6.3: Manufacturing of the GFRP plates: **a.** Infusion process for manufacturing of composites (representation for GFRP-B plate); **b.** produced plates; and **c.** cutting plates to obtain specimens for mechanical and thermomechanical characterisation.

breather fabric; (iii) two sheets of peel ply fabric; (iv) three sheets of infusion mesh; and (v) a plastic film about 1.5 m in length and 1.5 m in width.

The unidirectional glass fibre mats and the infusion mesh mats were positioned according to the percolation direction of the resin to allow a better impregnation between fibrous layers. The conventional Resin-C was prepared with 100 parts of resin to 0.7 parts of MEKP initiator. For the Resin-B, 100 parts of bio-based resin were mixed with 2 parts of MEKP initiator and 0.8 parts of cobalt octoate accelerator. During the manufacturing process, both GFRP composite laminates - with conventional (GFRP-C) and bio-based (GFRP-B) resins - were infused at room temperature (23 °C), and the laminate temperatures were monitored during the process, never exceeding 30 °C.

After demoulding, both GFRP-C and GFRP-B composite laminates had thicknesses of approximately 5 mm (Figure 36.2b). The GFRP laminates were then cut using a computer numeric control (CNC) machine (Figure 6.2c) to obtain the specimens required for the various characterisation tests – mechanical and thermomechanical – with dimensions according to each test standard (*cf.* section 6.2.4). Before testing, the GFRP specimens were subjected to an initial curing of 24 hours at 20 °C and, subsequently, to a post-curing cycle of 4 hours at 100 °C.

6.2.3 Mechanical characterisation tests

The mechanical behaviour of both types of GFRP composites, produced with the bio-based and the conventional resins, was assessed in the direction with higher reinforcement ratio by means of the following tests: (i) tension, (ii) compression, (iii) in-plane shear, and (iv) interlaminar shear.

The mechanical characterisation tests were performed using an Instron 8800D universal test machine, and a video-extensometer (high-definition Sony$^{\text{TM}}$ video camera, model XCG 5005E, Fujinon - Fujifilm HF50SA-1 lens) to measure material deformations.

The tensile tests were carried out according to ISO 527-4 [75], under displacement control, at a loading rate of 2 mm/ min. The compressive tests were performed according to ASTM 6641/D6641M[76], using a combined loading compression (CLC) test fixture – the tests were conducted under displacement control, at a loading rate of 1.3 mm/ min. The in-plane shear tests were performed according to ASTM D5379/D5379M-5 [77] (Iosipescu or V-notched beam method) - the axial loading of the two independent modules (which apply in-plane shear stresses) was applied under displacement control, at a rate of 2 mm/ min. Interlaminar shear tests were carried out according to ISO 14130 [78] by the short-beam method in rectangular test specimens, loaded in a 23 mm span. Tests were carried out at a loading rate of 1 mm/ min.

For all types of tests, a total of 5 specimens were used for each type of resin. For all specimens, the width and thickness were measured with a digital micrometre to check tolerances and to compute the (minimum) area for axial and shear stress calculation; these measurements were made at three points along the gauge length of specimens used in tensile, compressive and interlaminar shear tests, and in the notched section of specimens used in shear tests.

The specimens were tested under laboratory conditions with room temperature of 23±2 °C and 55±3% of relative humidity. The fibre mass fraction of the GFRP composites from calcination tests according ISO 1172 [79].

6.2.4 Thermomechanical characterisation tests

DMA experiments were performed to assess the thermomechanical behaviour of the GFRP composites produced with the bio-based and the conventional resins. Tests were carried out in a dynamic mechanical analyser from TA Instruments, model DMA Q800, according to ASTM E1640-09 [80] in a 35 mm dual cantilever clamp configuration. Specimens were subjected to a constant strain amplitude of 15 µm at a constant oscillation frequency of 1 Hz, while submitted to a temperature sweep at a constant heating rate of 2 °C/ min, starting at –30 °C and ending at 150 °C. The T_g was defined from (i) the onset value of the storage modulus decay, and (ii) the peak of the tan δ.

6.3 Results and discussion

6.3.1 Tensile and compressive behaviour

Figure 6.4 shows the nominal tensile stress-strain curves for GFRP-C and GFRP-B specimens, which were very consistent within each group. For both types of specimens, the curves present the typical tensile behaviour of fibre-polymer composites, with an initial linear branch, followed by a gradual loss of stiffness for higher strains, until the occurrence of brittle tensile failure. The failure mode of both types of specimens was also typical of fibre-polymer composites, involving the generalised delamination of reinforcing layers and the rupture of glass fibres, as shown in Figure 6.5.

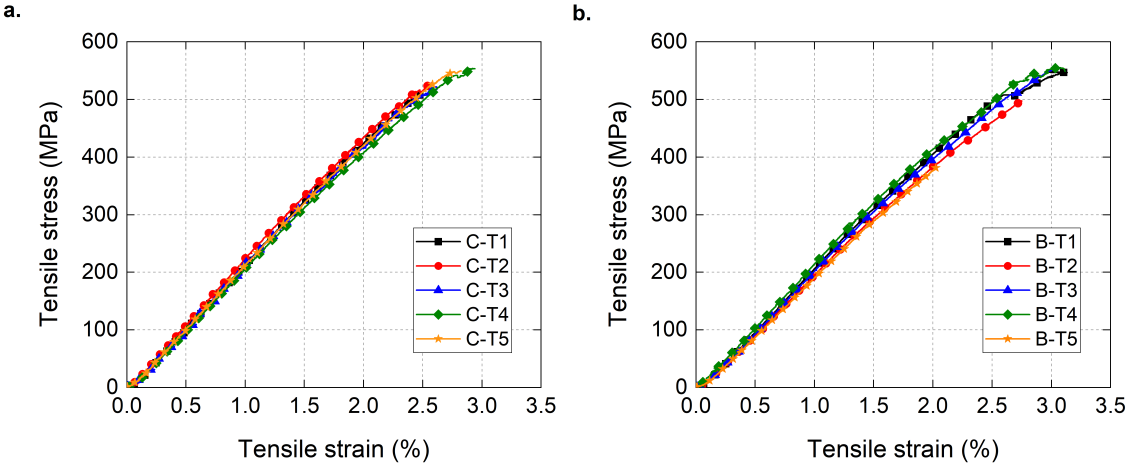

Figure 6.4: Nominal tensile stress-strain curves: **a.** GFRP-C, and **b.** GFRP-B.

Table 6.2 summarises the resulting mechanical properties in tension (and compression, presented ahead) of both GFRP-C and GFRP-B specimens. Overall, the tensile properties obtained for both types of GFRP composites are very similar: (i) the modulus of elasticity in tension of GFRP-B (20.6±0.7 GPa) was about 6% lower compared to that of GFRP-C (21.9±0.9 GPa); (ii) the tensile strengths virtually matched, being 538.1±23.6 MPa and 533.0±16.5 MPa, respectively for GFRP-B and GFRP-C; and (iii) the strain at break in tension of GFRP-B (3.0±0.1%) was about 10% higher compared with that of GFRP-C (2.7±%). Although a direct comparison is not possible (due to differences in fibre content and architecture), these results match or exceed, those found in the literature (for example, by Hosseini *et al.* [31]).

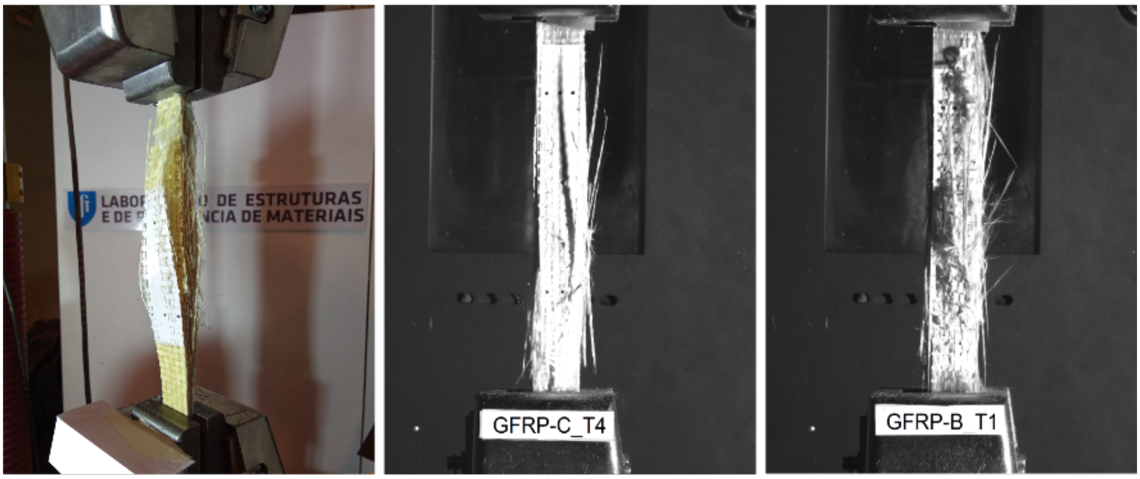

Figure 6.5: Tensile failure modes of representative GFRP-C and GFRP-B specimens.

Table 6.2: Mechanical properties in tension and compression of GFRP specimens (mean ± standard deviation).

Specimen	$\sigma_{t,max}$ (MPa)	E_t (GPa)	$\epsilon_{t,max}$ (%)	$\sigma_{c,max}$ (MPa)	E_c (GPa)	$\epsilon_{c,max}$ (%)
GFRP-C	533.0±16.5	21.9±0.9	2.7±0.2	169.6±10.8	25.1±0.3	0.7±0.1
GFRP-B	538.1±38.6	20.6±0.7	3.0±0.1	210.4±27.8	24.9±2.2	0.8±0.1

The above-mentioned figures, as well as the curves depicted in Figure 6.4 show that no significant differences were observed between the tensile behaviour of the GFRP-B and GFRP-C composites. This attests the mechanical potential of the GFRP-B composite compared to its petroleum-derived counterpart as regards the mechanical behaviour in tension, as well as the effectiveness of the bio-based Resin-B in distributing stresses among glass fibres, the main role of the polymer matrix of composites subject to tension.

Figure 6.6 shows the nominal compression stress-strain curves for GFRP-B and GFRP-C specimens. For both types of composites, the behaviour was approximately linear up to failure, which also occurred in a brittle way. However, compared to the results obtained in tension, the stress-strain curves in compression are less “linear” and there is higher scatter within each series, which is partly attributed to the test setup, namely to the smaller gauge length (which also affects the precision of the video-extensometer).

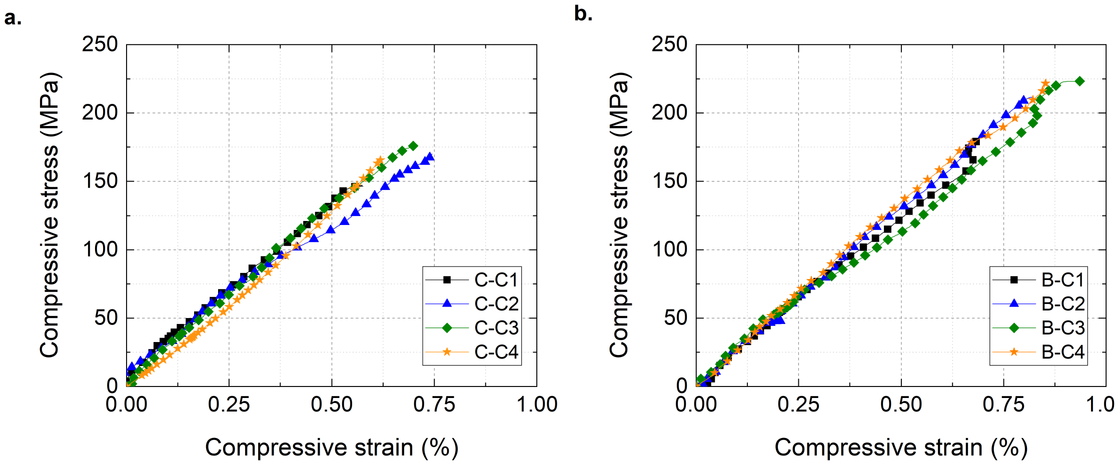

Figure 6.6: Nominal compressive stress-strain curves: **a.** GFRP-C and **b.** GFRP-B. (a premature failure was observed in one of the GFRP-B specimens, and therefore, only the curves of 4 specimens were presented. The same happened for GFRP-C.)

The compressive properties obtained in these tests, which are summarised in Table 6.2, prompt the following comments: (i) the modulus of elasticity in compression of GFRP-B (24.9±2.2 GPa) matched that of GFRP-C (25.1±0.3 GPa); (ii) the compressive strength of GFRP-B (210.4±27.8 MPa) was 24% higher compared to GFRP-C (169.6±10.8 MPa); and, accordingly, (iii) the strain at break in compression of GFRP-B (0.8±0.1%) was also 14% higher than that of GFRP-C (0.7±0.1%).

Figure 6.7 shows the failure modes of representative specimens of GFRP-B and GFRP-C composites. All specimens exhibited delamination of the reinforcing layers and fibre kinking, which is a typical failure mode of fibre-polymer composites loaded in compression, considered "*acceptable*" according to ASTM 6641/6641M [76].

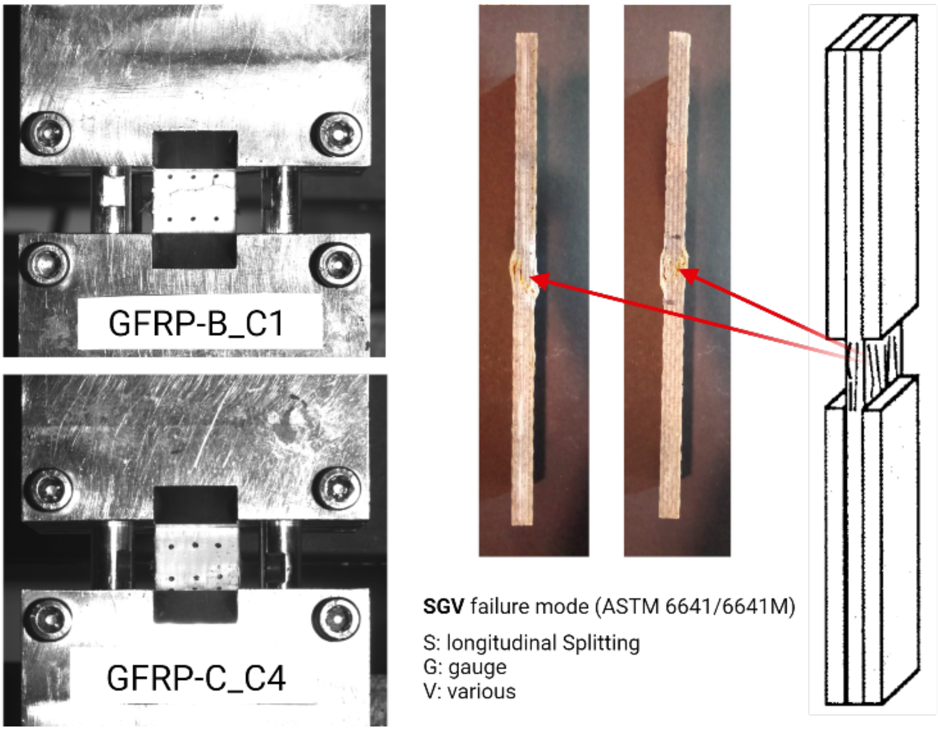

Figure 6.7: Compressive failure modes of representative GFRP-C and GFRP-B specimens.

Figure 6.8 presents representative stress-strain curves that allow comparing the axial behaviour of GFRP-B and GFRP-C composites under tensile and compressive stresses; this figure also includes, as a reference, representative stress-strain curves of the corresponding resins Resin-C and Resin-B, obtained in [72–74].

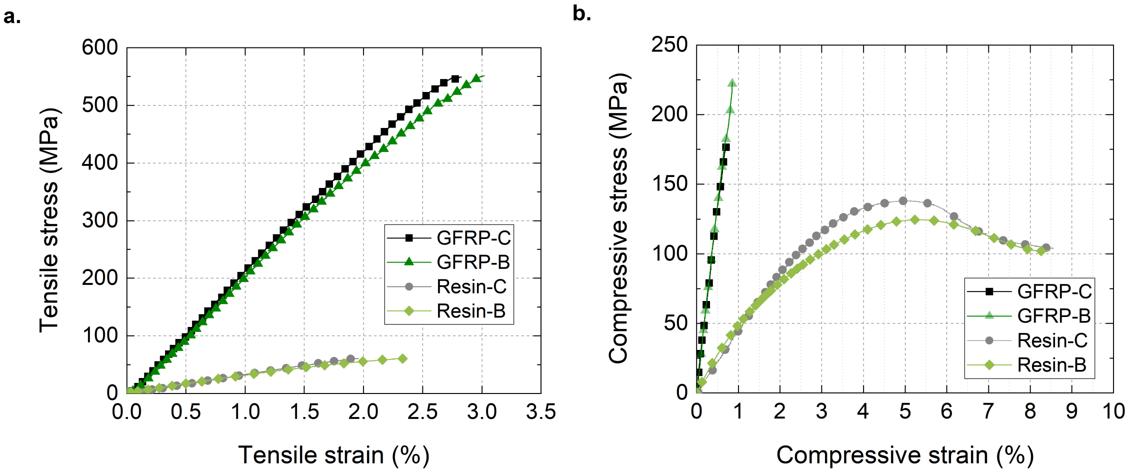

Figure 6.8: Representative nominal axial stress-strain curves of GFRP and resin specimens: **a.** tensile and **b.** compressive.

Figure 6.9 complements the previous figure, by presenting representative axial stress-strain curves for GFRP-C and GFRP-B composites and their respective resins – these curves illustrate in a single plot the full axial behaviour of those materials, allowing to compare the magnitude of their tensile and compressive strengths and strains at failure.

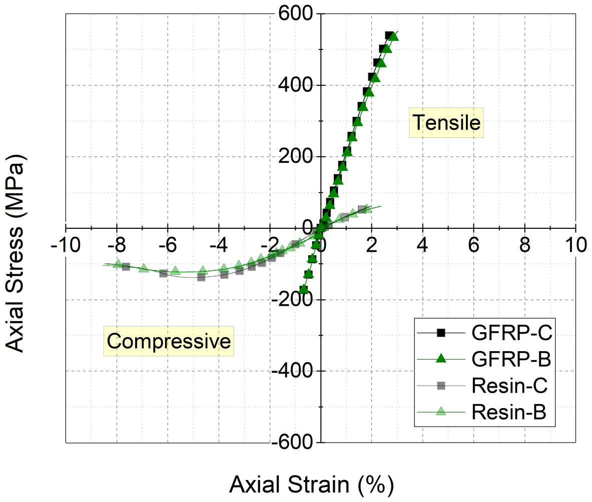

Figure 6.9: Representative nominal axial stress-strain curves in tension and compression of GFRP and resin specimens.

It is shown that while the values of the tensile strain at break of resins and corresponding composites are relatively similar, that is not the case for the values of the compressive strain at break, which are much lower in GFRP composites than in their corresponding resins. Under tensile stresses, the highest strain at break of Resin-B resulted in the highest strain at break of the GFRP-B composite. In contrast, although Resin-B presented lower compressive strength compared with Resin-C, the GFRP-B composite achieved significantly higher compressive strength than the GFRP-C composite.

The magnitude of the relative differences between the average values of compressive strength of both types of composites is somewhat unexpected (in spite of the relatively high scatter of this property, *e.g.* coefficient of variation (CoV) of 13% for GFRP-B). Although it is not possible to establish a direct relationship between the strength of the resins and the strength of their respective composites, the higher performance of GFRP-B in terms of compressive strength may be due to the better performance of its resin under tensile (in terms of strain at break) and shear (in terms of strength) loading - in both cases, 11% higher. In fact, the relatively complex failure of composites in compression involved delamination and fibre kinking (as expected). Delamination is typically due to transverse tensile stresses that develop as a result of the Poisson effect and, therefore, are resisted by the tensile strength of the matrix - such strength was similar for both composites, but the strain at break was higher in Resin-B. On the other hand, fibre kinking depends on the shear strength of the polymer matrix, which was higher in Resin-B. This may (at least partly) explain the higher compressive strength of GFRP-B.

6.3.2 Shear behaviour

Figure 6.10 shows the nominal shear stress-distortion curves for GFRP-B and GFRP-C specimens subjected to in-plane shear loading. Both series of GFRP-C and GFRP-B specimens presented very similar shear stress-distortion curves, with an initial linear stage up to approximately 20% of the maximum shear stress, followed by a non-linear branch with progressive stiffness reduction. Most specimens attained a shear stress peak for very large distortion values (ranging from 10% and 20%); in a limited number of specimens, when the distortion of 20% (set as limit for these tests) was attained, the shear stress had reached a plateau or was still slightly increasing. The in-plane shear strength was taken as the highest value between the maximum shear stress reached in the shear stress-distortion curve and the shear stress corresponding to the limit distortion of 20%.

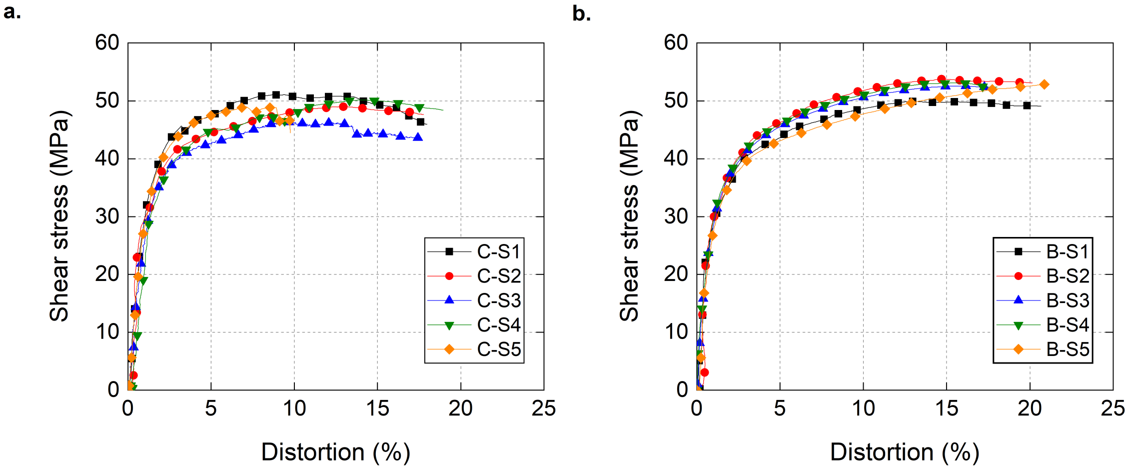

Figure 6.10: Nominal shear stress-distortion curves of GFRP-C and GFRP-B specimens.

Despite the overall similarity in the shear stress *vs.* distortion responses, the pre-peak stiffness reduction and the post-rupture shear stress reduction were both more pronounced in the GFRP-C composite than in the GFRP-B one, with the latter presenting a more extensive plateau region after reaching the maximum stress, as can be observed in Figure 6.11.

Figure 6.12 presents the failure modes of representative GFRP specimens tested under in-plane shear. Failure occurred in a similar way for both types of composites, due to shear stresses in the notched section. The specimens presented a vertical crack (delaminated region) in this central section, which is a typical and “acceptable” failure mode according to ASTM D5379/D5379M [77].

Table 6.3 presents a summary of the in-plane shear properties of the GFRP-B and GFRP-C composites: (i) the shear modulus of GFRP-B (1.0±0.2 GPa) was about 17% lower compared to GFRP-C (1.2±0.2 GPa), however, this difference is within the same order of magnitude as the CoV for this property in both series was quite high (16-20%); (ii) the in-plane shear strength for GFRP-B (52.5±1.4 MPa) was about 7% higher compared to

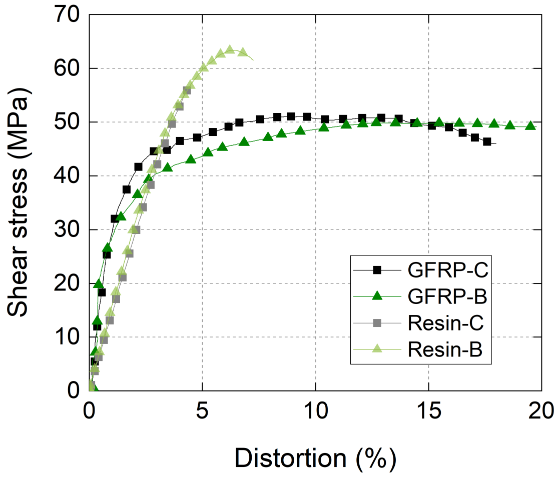

Figure 6.11: Representative shear stress-distortion curves of GFRP and resins specimens.

GFRP-C (49.1±1.6 MPa); (iii) and the distortion at maximum shear stress of GFRP-B (1.56±0.19%) was ∼30% higher than that of GFRP-C (1.07±0.16%). The higher shear strength of composite GFRP-B can be due to the same reasons put forward to explain its higher compressive strength.

The plot provided in Figure 6.11, showing the shear stress *vs.* distortion curves for the bio-based and conventional resins and the corresponding composites, prompts the following comments: (i) as expected, the shear moduli of the GFRP-B and GFRP-C composites was higher than that of the corresponding Resin-B and Resin-C, which is naturally due to the contribution of the fibre reinforcement (that includes uni- and bidirectional fibres); (ii) the shear strength of Resin-B and Resin-C was about 20% higher than that of the corresponding GFRP-B and GFRP-C composites - this indicates that the fibre reinforcement (which did not include fibres oriented at directions other than 0°and 90°) was the limiting constituent material in attaining higher shear stress levels.

Table 6.3: Mechanical properties in in-plane and interlaminar shear of GFRP specimens (mean ± standard deviation).

Specimens	τ_{max} **(MPa)**	G **(GPa)**	γ_{max} **(%)**	τ_{ILSS} **(MPa)**
GFRP-C	49.1±1.6	2.9±0.1	10.6±2.6	21.0±0.6
GFRP-B	52.5±1.4	2.5±0.5	14.8±1.1	21.1±2.2

Table 6.3 also presents the interlaminar shear strength of both types of GFRP composites. Despite the relatively high standard deviation obtained for GFRP-B, the interlaminar shear strength of the bio-based composite (21.1±2.2 MPa) matched that of the conventional one (21.0±0.6 MPa) - this result suggests that the fibre-matrix adhesion obtained with the bio-based resin is adequate, matching that of the conventional resin. Figure 6.13 shows the failure modes (top view) of representative specimens, where the lighter regions correspond to areas where delamination has occurred. As for the previous mechanical

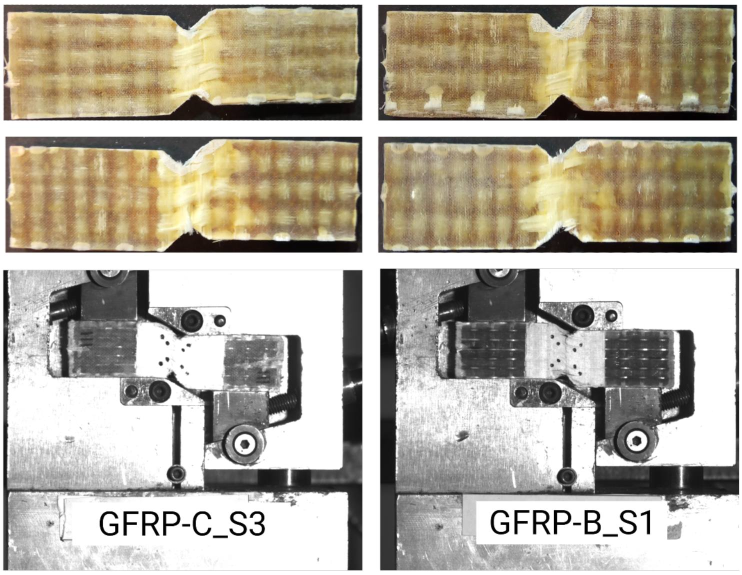

Figure 6.12: V-Notched beam shear test failure modes of representative GFRP-C and GFRP-B specimens.

tests, all specimens tested for interlaminar shear showed a similar failure mode.

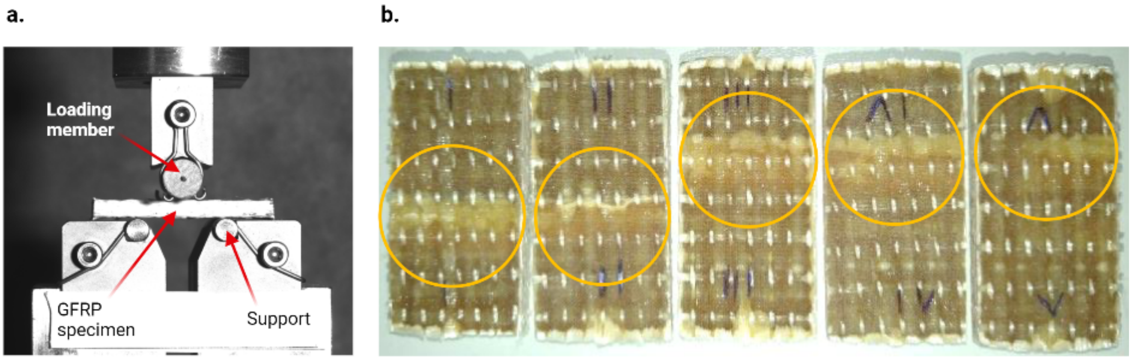

Figure 6.13: Interlaminar shear tests: **a.** loading configuration (short-beam method), and **b.** failure modes of representative GFRP specimens.

6.3.3 Thermomechanical behaviour

Dynamic mechanical analysis was used to determine the thermomechanical properties of the composites and, together with the mechanical tests, to establish the potential use of the bio-based composite (GFRP-B) to replace its petroleum-derived counterpart (GFRP-C) in high-performance civil engineering applications, namely those located outdoors, where the temperature-dependence of mechanical properties is quite relevant. The T_g is a common indicator of such performance.

Figure 6.14 presents the results of DMA tests, namely the storage modulus (E'), the loss modulus (E''), and the damping factor (tan δ) as a function of temperature, for the GFRP-C and GFRP-B composites and their corresponding resins.

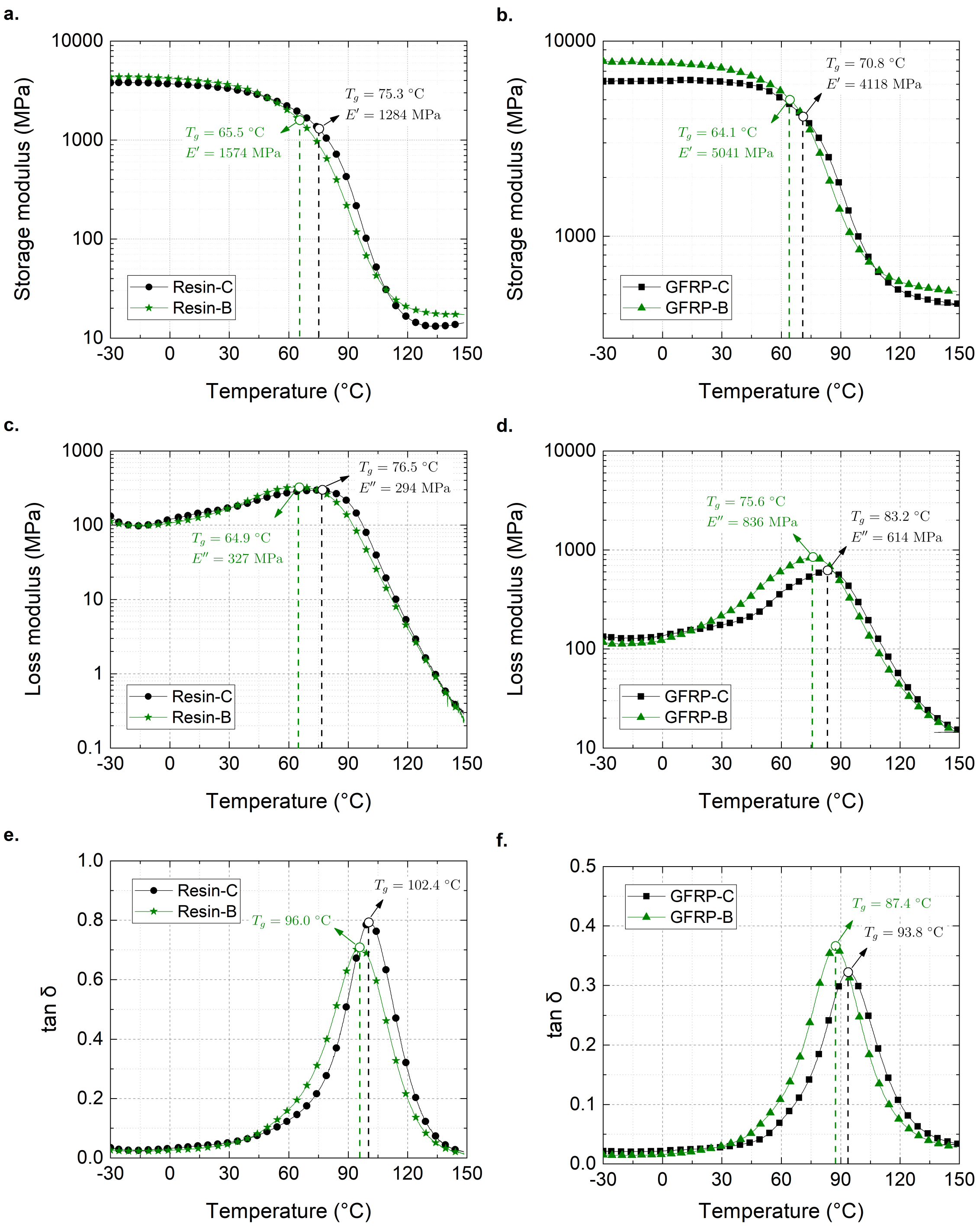

Figure 6.14: Thermomechanical properties of GFRP and resin specimens.

The storage modulus curves of both types of resins and their composites present a well-defined and sharp drop with temperature increase across the glass transition region. The storage modulus of both “pairs” of curves (composite-resin) are quite consistent and so are the resulting estimates of T_g obtained from the onset value of the storage modulus decay - the results obtained prompt the following comments: (i) the storage modulus reduction of the bio-based Resin-B is very similar to that of the conventional Resin-C; however, for the former resin, the reduction is steeper and occurs for slightly lower temperatures, resulting in T_g estimates of 66 ℃ and 75 ℃ for Resin-B and Resin-C, respectively; (ii) the same is observed for the corresponding composites, with GFRP-C presenting slightly (10%) higher T_g (71 ℃) than GFRP-B (64 ℃).

The loss modulus curves show no significant differences between GFRP-B and GFRP-C composites regarding their capacity to dissipate energy for temperatures around 15 ℃ and 25 ℃. However, as the temperature increases towards the glass transition, the energy dissipation is higher for GFRP-B (836 MPa) than for GFRP-C (614 MPa). Composite GFRP-C included a slightly higher fibre mass fraction (64 wt.%) than GFRP-B (60 wt.%), which may explain this result, as higher fibre fractions result in increased internal friction with the polymer matrix, thus promoting energy dissipation [81]. In addition, for both types of composites, the loss modulus curves present a wider shape and a higher peak than for the corresponding resins. The higher peak value of loss modulus for GFRP-B compared to GFRP-C should be partially due to the higher polymer fraction of the former composite.

The tan δ curves of both types of resins and composites also present a typical development, with a well-defined peak in the glass transition, showing no signs of secondary relaxations, which attest the high curing degree of the materials. The results of the tan δ curves are also quite consistent among resin-composite pairs, with slightly lower T_g estimates obtained for the resins. Moreover, the results obtained for the bio-based resin and composite are quite similar to those of the conventional counterparts, with slightly lower (6-7%) T_g estimates: for the resins, the T_gs were 96 ℃ and 102 ℃ for Resin-B and Resin-C, respectively, while for the composites those figures were 87 ℃ and 94 ℃ for GFRP-C and GFRP-B, respectively.

Overall, the results obtained in the DMA tests show that the thermomechanical behaviour of the bio-based composite GFRP-B is quite similar to that of the conventional GFRP-C, which is consistent with the similarity of the thermomechanical behaviour of their resins. Although the T_g presented by GFRP-B is slightly lower than that of GFRP-C, it is still considered suitable for civil structural applications, with the environmental advantage of having a high bio-based content. In this respect, it is worth referring that the recent European Technical Specification for the "*Design of Fibre-Polymer Composite Structures*" [71] recommends a minimum T_g of 60 ℃ (as defined from the onset value of the storage modulus decay plotted in logarithmic scale).

6.4 Concluding remarks

This chapter presented the development, manufacturing, and mechanical and thermo-mechanical characterisation of a GFRPcomposite produced by vacuum infusion using a novel high-performance bio-based unsaturated polyester resin, which was developed in-house with raw materials derived from renewable sources. The mechanical and thermo-mechanical properties of the bio-based GFRP composite were compared with those of its conventional GFRP counterpart, manufactured from a conventional petroleum-derived orthophthalic polyester resin. The main driver of this study was to assess the prospects of using the innovative bio-based resin in the manufacturing of high-performance GFRP composites for civil engineering structural applications, as an alternative to its petroleum-derived counterparts.

The GFRP composites were successfully manufactured, and a suitable impregnation of the glass fibres was observed for both conventional and bio-based unsaturated resins. Thus, the bio-based resin proved to have potential to be applied in the vacuum infusion technique, which is very often used to manufacture large-scale structural composite components, namely bridge decks.

The results of mechanical characterisation tests showed that the mechanical properties in tension, compression, in-plane shear and interlaminar shear of the bio-based GFRP composite meet or even exceed those of its petroleum-derived counterpart, attesting the ability of the bio-based resin to impregnate glass fibre reinforcement and to achieve adequate fibre-matrix adhesion in the cured product. In what concerns the thermomechanical behaviour, although the glass transition temperature of the bio-based GFRP composite was slightly lower than of its conventional counterpart (about 10%), it still exceeded the threshold of 60 ℃, which enables its use in civil structural applications.

The overall results presented in this chapter show the feasibility of using the in-house bio-based GFRP composite developed in this study in high-performance structural applications, providing a more sustainable alternative to GFRP composites currently based on non-renewable resources. Future studies should address different aspects of the bio-based GFRP composite, namely its creep, fatigue and fracture performance, as well as its long-term durability.

6.5 References

[1] Ecoxy. Bio-based recyclable, reshapable and repairable (3R) fibre-reinforced EpOXY composites for automotive and construction sectors. Technical report, European Commission, 2020.

[2] SSUCHY. Sustainable structural and multifunctional biocomposites from hybrid natural fibres and bio-based polymers. Technical report, European Commission, 2022.

[3] Paulien F H Harmsen, Martijn M Hackmann, and Harriëtte L Bos. Green building blocks for bio-based plastics. *Biofuels, Bioproducts and Biorefining*, 8(3):306–324, 2014.

[4] Alessandro Gandini and Talita M Lacerda. From monomers to polymers from renewable resources: Recent advances. *Progress in Polymer Science*, 48:1–39, 2015.

[5] Jan-Georg Rosenboom, Robert Langer, and Giovanni Traverso. Bioplastics for a circular economy. *Nature Reviews Materials*, 2022.

[6] Peyton Shieh, Wenxu Zhang, Keith E. Husted, Samantha L. Kristufek, Boya Xiong, David J. Lundberg, Jet Lem, David Veysset, Yuchen Sun, Keith A. Nelson, Desiree L. Plata, and

Jeremiah A. Johnson. Cleavable comonomers enable degradable, recyclable thermoset plastics. *Nature*, 583(7817):542–547, 2020.

[7] Baolong Wang, Xinyu Wang, Ningdi Xu, Yibo Shen, Fei Lu, Yingying Liu, Yudong Huang, and Zhen Hu. Recycling of carbon fibers from unsaturated polyester composites via a hydrolysis-oxidation synergistic catalytic strategy. *Composites Science and Technology*, 203:108589, 2021.

[8] Chiara Di Mauro, Aratz Genua, Monica Rymarczyk, Caroline Dobbels, Samuel Malburet, Alain Graillot, and Alice Mija. Chemical and mechanical reprocessed resins and bio-composites based on five epoxidized vegetable oils thermosets reinforced with flax fibers or PLA woven. *Composites Science and Technology*, 205:108678, 2021.

[9] Yang Yang, Yanshuang Xu, Yan Ji, and Yen Wei. Functional epoxy vitrimers and composites. *Progress in Materials Science*, 120:100710, 2021.

[10] Jie Zheng, Zhuang Mao Png, Shi Hoe Ng, Guo Xiong Tham, Enyi Ye, Shermin S Goh, Xian Jun Loh, and Zibiao Li. Vitrimers: Current research trends and their emerging applications. *Materials Today*, 51:586–625, 2021.

[11] Balaji Krishnakumar, Andrea Pucci, Prakash P. Wadgaonkar, Indresh Kumar, Wolfgang H Binder, and Sravendra Rana. Vitrimers based on bio-derived chemicals: Overview and future prospects. *Chemical Engineering Journal*, page 133261, 2021.

[12] Matteo Andrea Lucherelli, Antoine Duval, and Luc Avérous. Biobased vitrimers: Towards sustainable and adaptable performing polymer materials. *Progress in Polymer Science*, 127:101515, 2022.

[13] Hafeezullah Memon, Yi Wei, and Chengyan Zhu. Recyclable and reformable epoxy resins based on dynamic covalent bonds – Present, past, and future. *Polymer Testing*, 105:107420, 2022.

[14] Ibon Aranberri, Maite Landa, Edurne Elorza, Asier M Salaberria, and Alaitz Rekondo. Thermoformable and recyclable CFRP pultruded profile manufactured from an epoxy vitrimer. *Polymer Testing*, 93:106931, 2021.

[15] Mikihiro Hayashi. Versatile functionalization of polymeric soft materials by implanting various types of dynamic cross-links. *Polymer Journal*, 53(7):779–788, 2021.

[16] Xinxin Yang, Lizhen Guo, Xu Xu, Shibin Shang, and He Liu. A fully bio-based epoxy vitrimer: Self-healing, triple-shape memory and reprocessing triggered by dynamic covalent bond exchange. *Materials & Design*, 186:108248, 2020.

[17] Carlos A. Navarro, Yijia Ma, Katelyn H. Michael, Hanna M. Breunig, Steven R. Nutt, and Travis J. Williams. Catalytic, aerobic depolymerization of epoxy thermoset composites. *Green Chemistry*, 23(17):6356–6360, 2021.

[18] Doo Hun Kim, Ayeong Yu, and Munju Goh. Oxidative chemical depolymerization of thermoset epoxy resin for green recycling. *Journal of Industrial and Engineering Chemistry*, 96:76–81, 2021.

[19] Omar Faruk, Andrzej K. Bledzki, Hans-Peter Fink, and Mohini Sain. Biocomposites reinforced with natural fibers: 2000–2010. *Progress in Polymer Science*, 37(11):1552–1596, 2012.

[20] M P Staiger and N Tucher. Natural-fibre composites in structural applications. In Kim Louise

Pickering, editor, *Woodhead Publishing Series in Composites Science and Engineering*, chapter 8, pages 269–300. Woodhead Publishing, 1st edition, 2008.

[21] Kin-tak Lau, Pui-yan Hung, Min-Hao Zhu, and David Hui. Properties of natural fibre composites for structural engineering applications. *Composites Part B: Engineering*, 136:222–233, 2018.

[22] Paul Wambua, Jan Ivens, and Ignaas Verpoest. Natural fibres: can they replace glass in fibre reinforced plastics? *Composites Science and Technology*, 63(9):1259–1264, 2003.

[23] Hess Kristen, Hinchcliffe Sean, and Srubar Wil V. Biobased FRPs for Retrofit and Rehabilitation of Civil Infrastructure, 2022.

[24] Aaron T. Michel and Sarah L. Billington. Nonlinear Constitutive Model for Anisotropic Biobased Composite Materials. *Journal of Engineering Mechanics*, 140(11):4014083, 2014.

[25] J Jefferson Andrew and H N Dhakal. Sustainable biobased composites for advanced applications: recent trends and future opportunities – A critical review. *Composites Part C: Open Access*, 7:100220, 2022.

[26] Sripathi Dev Sharma Kopparthy and Anil N Netravali. Review: Green composites for structural applications. *Composites Part C: Open Access*, 6:100169, 2021.

[27] Boon Peng Chang, Amar K Mohanty, and Manjusri Misra. Studies on durability of sustainable biobased composites: a review. *RSC Advances*, 10(31):17955–17999, 2020.

[28] Michael P. Dicker, Peter F. Duckworth, Anna B. Baker, Guillaume Francois, Mark K. Hazzard, and Paul M. Weaver. Green composites: A review of material attributes and complementary applications. *Composites Part A: Applied Science and Manufacturing*, 56:280–289, 2014.

[29] Winifred Obande, Conchúr M. Brádaigh, and Dipa Ray. Continuous fibre-reinforced thermoplastic acrylic-matrix composites prepared by liquid resin infusion – A review. *Composites Part B: Engineering*, 215:108771, 2021.

[30] U K Vaidya and K K Chawla. Processing of fibre reinforced thermoplastic composites. *International Materials Reviews*, 53(4):185–218, 2008.

[31] Nassibeh Hosseini, Dean C. Webster, and Chad Ulven. Advanced biocomposite from highly functional methacrylated epoxidized sucrose soyate (MAESS) resin derived from vegetable oil and fiberglass fabric for composite applications. *European Polymer Journal*, 79:63–71, 2016.

[32] Rui Zhang, Tianyun Li, Houbo Zhou, Huahua Huang, and Yongming Chen. Biobased transparent polyimides with excellent solubility and mechanical properties using myo-inositol derived diamines. *Reactive and Functional Polymers*, 128:91–96, 2018.

[33] Aniruddha Nag, Mohammad Asif Ali, Makoto Watanabe, Maninder Singh, Kittima Amornwachirabodee, Shunsuke Kato, Tetsu Mitsumata, Kenji Takada, and Tatsuo Kaneko. High-performance poly(benzoxazole/benzimidazole) bio-based plastics with ultra-low dielectric constant from 3-amino-4-hydroxybenzoic acid. *Polymer Degradation and Stability*, 162:29–35, 2019.

[34] Kreisler S Y Lau. High-Performance Polyimides and High Temperature Resistant Polymers. In Hanna Dodiuk and Sidney H B T Handbook of Thermoset Plastics (Third Edition) Goodman, editors, *Handbook of Thermoset Plastics*, chapter 10, pages 297–424. William Andrew Publishing, Boston, 3 edition, 2014.

[35] Jacek Andrzejewski, Amar K Mohanty, and Manjusri Misra. Development of hybrid composites reinforced with biocarbon/carbon fiber system. The comparative study for PC, ABS and PC/ABS based materials. *Composites Part B: Engineering*, 200:108319, 2020.

[36] Noureddine Ramdani, Hamza Zaimeche, and Mehdi Derradji. Biobased thermally-stable aromatic cyanate ester thermosets: A review. *Reactive and Functional Polymers*, 168:105037, 2021.

[37] Wouter Post, Arijana Susa, Rolf Blaauw, Karin Molenveld, and Rutger J I Knoop. A Review on the Potential and Limitations of Recyclable Thermosets for Structural Applications. *Polymer Reviews*, 60(2):359–388, apr 2020.

[38] Yu-Yao Liu, Gan-Lin Liu, Yi-Dong Li, Yunxuan Weng, and Jian-Bing Zeng. Biobased High-Performance Epoxy Vitrimer with UV Shielding for Recyclable Carbon Fiber Reinforced Composites. *ACS Sustainable Chemistry & Engineering*, 9(12):4638–4647, March 2021.

[39] Ehsan Bari, Jeffrey J. Morrell, and Asghar Sistani. Durability of natural/synthetic/biomass fiber–based polymeric composites: Laboratory and field tests. In Mohammad Jawaid, Mohamed Thariq, and Naheed Saba, editors, *Durability and Life Prediction in Biocomposites, Fibre-Reinforced Composites and Hybrid Composites*, chapter 2, pages 15–26. Woodhead Publishing Series in Composites Science and Engineering, 2019.

[40] K Mayandi, N Rajini, M Manojprabhakar, Suchart Siengchin, and Nadir Ayrilmis. Recent studies on durability of natural/synthetic fiber reinforced hybrid polymer composites. In Mohammad Jawaid, Mohamed Thariq, and Naheed Saba, editors, *Durability and Life Prediction in Biocomposites, Fibre-Reinforced Composites and Hybrid Composites*, chapter 1, pages 1–13. Woodhead Publishing Series in Composites Science and Engineering, 2019.

[41] N Saba, M Jawaid, M T Paridah, and O Y Al-othman. A review on flammability of epoxy polymer, cellulosic and non-cellulosic fiber reinforced epoxy composites. *Polymers for Advanced Technologies*, 27(5):577–590, 2016.

[42] Ellen Lackey, James G Vaughan, Kapil Inamdar, and Brittany Hancock. Statistical Characterization of Pultruded Composites with Natural Fiber Reinforcements – Part A: Fabrication. *Journal of Natural Fibers*, 4(4):73–87, 2008.

[43] James L Thomason and Jose L Rudeiros-Fernández. Thermal degradation behaviour of natural fibres at thermoplastic composite processing temperatures. *Polymer Degradation and Stability*, 188:109594, 2021.

[44] N K Kim, S Dutta, and D Bhattacharyya. A review of flammability of natural fibre reinforced polymeric composites. *Composites Science and Technology*, 162:64–78, 2018.

[45] M. W. Chai, S. Bickerton, D. Bhattacharyya, and R. Das. Influence of natural fibre reinforcements on the flammability of bio-derived composite materials. *Composites Part B: Engineering*, 43(7):2867–2874, 2012.

[46] Darshil U. Shah. Natural fibre composites: Comprehensive Ashby-type materials selection charts. *Materials & Design*, 62:21–31, 2014.

[47] Michael George, Michael Chae, and David C. Bressler. Composite materials with bast fibres: Structural, technical, and environmental properties. *Progress in Materials Science*, 83:1–23, 2016.

[48] M. H. Irfan. *Chemistry and Technology of Thermosetting Polymers in Construction Applications*. Springer Science+Business Media, Dordrecht, 1 edition, 1998.

[49] João Ramôa Correia. Fibre-Reinforced Polymer (FRP) Composites. In M Clara Gonçalves and Fernanda Margarido, editors, *Materials for Construction and Civil Engineering*, chapter 11, pages 501–556. Springer International Publishing, Cham, 2015.

[50] Frank R. Jones. Unsaturated Polyester Resins. In Marianne Gilbert, editor, *Brydson's Plastics Materials*, chapter 26, pages 743–772. Butterworth-Heinemann, 8 edition, 2017.

[51] V Fiore, T Scalici, G Di Bella, and A Valenza. A review on basalt fibre and its composites. *Composites Part B: Engineering*, 74:74–94, 2015.

[52] V Manikandan, J T Winowlin Jappes, S M Suresh Kumar, and P Amuthakkannan. Investigation of the effect of surface modifications on the mechanical properties of basalt fibre reinforced polymer composites. *Composites Part B: Engineering*, 43(2):812–818, 2012.

[53] Rotich K Gideon, Hangjun Hu, Paul Wambua, and Bohong Gu. Characterizations of basalt unsaturated polyester laminates under static three-point bending and low-velocity impact loadings. *Polymer Composites*, 35(11):2203–2213, 2014.

[54] E. K. Gamstedt, M. Skrifvars, T. K. Jacobsen, and R. Pyrz. Synthesis of unsaturated polyesters for improved interfacial strength in carbon fibre composites. *Composites Part A: Applied Science and Manufacturing*, 33(9):1239–1252, 2002.

[55] Juan P. Correa, Juan M. Montalvo-Navarrete, and Miguel A. Hidalgo-Salazar. Carbon footprint considerations for biocomposite materials for sustainable products: A review. *Journal of Cleaner Production*, 208:785–794, 2019.

[56] Angela Daniela La Rosa, Giuseppe Recca, John Summerscales, Alberta Latteri, Gulia Cozzo, and Gianluca Cicala. Bio-based versus traditional polymer composites. A life cycle assessment perspective. *Journal of Cleaner Production*, 74:135–144, 2014.

[57] Amy Fitzgerald, Will Proud, Ali Kandemir, Richard J Murphy, David A Jesson, Richard S Trask, Ian Hamerton, and Marco L Longana. A Life Cycle Engineering Perspective on Biocomposites as a Solution for a Sustainable Recovery. *Sustainability*, 13(3), 2021.

[58] David Ayre. Technology advancing polymers and polymer composites towards sustainability: A review. *Current Opinion in Green and Sustainable Chemistry*, 13:108–112, 2018.

[59] Nicholas A Rorrer, John R Dorgan, Derek R Vardon, Chelsea R Martinez, Yuan Yang, and Gregg T Beckham. Renewable Unsaturated Polyesters from Muconic Acid. *ACS Sustainable Chemistry & Engineering*, 4(12):6867–6876, 2016.

[60] Nicholas A. Rorrer, Derek R. Vardon, John R. Dorgan, Erica J. Gjersing, and Gregg T. Beckham. Biomass-derived monomers for performance-differentiated fiber reinforced polymer composites. *Green Chemistry*, 19(12):2812–2825, 2017.

[61] ZengHui Dai, ZeWen Yang, ZhiWei Chen, ZhongXiang Zhao, YongJian Lou, YanYan Zhang, TianXing Liu, FeiYa Fu, YaQin Fu, and XiangDong Liu. Fully Biobased Composites of an Itaconic Acid Derived Unsaturated Polyester Reinforced with Cotton Fabrics. *ACS Sustainable Chemistry & Engineering*, 6(11):15056–15063, November 2018.

[62] Mikael Skrifvars, Hom Dhakal, Zhongyi Zhang, Joseph Gentilcore, and Dan Åkesson. Study on the mechanical properties of unsaturated polyester sandwich biocomposites composed of

uniaxial warp-knitted and non-woven viscose fabrics. *Composites Part A: Applied Science and Manufacturing*, 121:196–206, 2019.

[63] Yuchao Wu, Mingen Fei, Tingting Chen, Renhui Qiu, and Wendi Liu. Fabrication of degradable and high glass-transition temperature thermosets from palm oil and isosorbide for fiber-reinforced composites. *Industrial Crops and Products*, 170:113744, 2021.

[64] Ciaran McSwiggan and Amir Fam. Bio-based resins for flexural strengthening of reinforced concrete beams with FRP sheets. *Construction and Building Materials*, 131:618–629, 2017.

[65] Mak Kenneth, Fam Amir, and MacDougall Colin. Flexural Behavior of Sandwich Panels with Bio-FRP Skins Made of Flax Fibers and Epoxidized Pine-Oil Resin. *Journal of Composites for Construction*, 19(6):4015005, December 2015.

[66] Joris Smits. Fiber-Reinforced Polymer Bridge Design in the Netherlands: Architectural Challenges toward Innovative, Sustainable, and Durable Bridges. *Engineering*, 2(4):518–527, 2016.

[67] Easy Composites. LB2 Epoxy Laminating Bio Resin, 2022.

[68] INEOS Composites. Envirez™, 2021.

[69] Sicomin Epoxy Resin. Bio-based epoxy, 2018.

[70] TFC Biomass biobased chemicals. Biorez, 2022.

[71] prEN 19101:2021. Design of Fibre-Polymer Composite Structures. Technical report, Technical Committee 250 (TC250), 2020.

[72] Mateus A. Hofmann, Abu T. Shahid, Mário A. Garrido, Maria J. Ferreira, João R. Correia, and João C. Bordado. Bio-based thermosetting polyester resin for high-performance applications. *ACS Sustainable Chemistry & Engineering*, Accepted(Manuscript ID: sc-2021-069697.R1), 2022.

[73] Mateus A. Hofmann and Abu T. Shahid and Mário A. Garrido and Maria J. Ferreira and João R. Correia and João C. Bordado. Development of biobased thermosetting polyester resins from dimer fatty acids. *Green Chemistry*, Submitted(Manuscript ID: GC-ART-01-2022-000192), 2022.

[74] Mateus A. Hofmann, Mário Garrido, João R. Correia, and João C. Bordado. Development of high-performance biobased thermoset polyester using renewable building blocks from isosorbide, 1,3-propanediol, and fumaric acid. *Journal of Applied Polymer Science*, Submitted(Manuscript ID: app.20220135), 2022.

[75] ISO 527. Plastics - Determination of tensile properties - Part 4: Test conditions for isotropic and orthotropic fibre-reinforced plastic composites, 2021.

[76] ASTM 6641/D6641M. Standard Test Method for Compressive Properties of Polymer Matrix Composite Materials Using a Combined Loading Compression (CLC) Test Fixture. Technical report, ASTM International, 2021.

[77] ASTM D5379/D5379M. Standard Test Method for Shear Properties of Composite Materials by V-Notched Beam Method. Technical report, ASTM International, 2012.

[78] ISO 14130. Fibre-reinforced plastic composites - Determination of apparent interlaminar shear strength by short-beam method, 1998.

[79] ISO 1172. Textile-glass-reinforced plastics - Prepregs, moulding compounds and laminates - Determination of the textile-glass and mineral-filler content - Calcination methods, 1996.

[80] ASTM E1640-09. Standard Test Method For Assignment Of The Glass Transition Temperature By Dynamic Mechanical Analysis. Technical report, ASTM International, 2009.

[81] Heitor Luiz Ornaghi Jr., Alexandre Sonaglio Bolner, Rudinei Fiorio, Ademir Jose Zattera, and Sandro Campos Amico. Mechanical and dynamic mechanical analysis of hybrid composites molded by resin transfer molding. *Journal of Applied Polymer Science*, 118(2):887–896, October 2010.

Chapter 7

Bio-based CFRP composite strips

Abstract

The development of high-performance carbon fibre (CF) reinforced polymer (CFRP) composites based on raw materials derived from renewable sources can promote the reduction of the dependence of these advanced materials on petroleum. This chapter presents the manufacturing – at an industrial environment – of a novel and innovative pultruded CFRP strip prototype produced with a high-performance unsaturated polyester (UP) resin developed in-house, having more than 50 wt.% of its content derived from renewable raw materials. Bio-based CF/UP strips, with a mass fibre content of 66% comprising unidirectional CF strands, were successfully produced, and their mechanical and thermomechanical behaviour was assessed and compared to an equivalent carbon fibre reinforced vinyl ester (CF/VE) strip produced with conventional petroleum-based vinyl ester and the same fibre architecture. The bio-based CF/UP composite strip presented 2095 MPa, 167 GPa, and 1.4% of tensile strength, modulus of elasticity, and strain at failure, respectively. These figures meet or exceed the mechanical properties of the equivalent CFRP composite strip produced with conventional petroleum-derived resin, produced, and tested under the same conditions. Furthermore, the bio-based CF/UP composite strip presented a glass transition temperature of 78 ℃ (defined from the onset of the storage modulus decay), enabling a maximum service temperature of ∼60 ℃, which will not likely be exceeded in most climates. These figures highlight the potential of the bio-based CFRP composite strip developed herein for structural strengthening applications, offering a key advantage in terms of sustainability. Figure 7.1 presents a graphical abstract about this chapter.

Figure 7.1: Bio-based CFRP strip graphical abstract.

7.1 Introductory remarks

CFRP composites are being increasingly used to strengthen civil engineering structures located outdoors (*e.g.*, bridges, viaducts, stadiums, platforms, piers, tunnels, buildings). In these applications, CFRP composites require high mechanical and thermomechanical performance, durability, and cost-effectiveness [1]. Figure 7.2 shows recent strengthening applications of CFRP composites in construction, used in reinforced concrete or masonry members to increase their bending and/or shear capacity, or their serviceability performance. For these applications, CFRPs are typically produced from a fine selection of synthetic raw materials, particularly carbon fibres and petroleum-derived polymer resin matrices, such as epoxy, vinyl ester and, less frequently, unsaturated polyester [2].

Figure 7.2: CFRP strengthening applications of civil engineering structures [3,4]: **a.** Access ramps of A9 Viaduct Riddes, Switzerland; **b.** Maracanã Stadium, Rio de Janeiro, Brazil; **c.** Aabachbrücke railway bridge, Lachen, Switzerland; and **d.** Cultural Centre of São Lázaro, Lisbon, Portugal (fire damaged structure).

In the above-mentioned strengthening applications, the CFRP composites can either be manufactured *in situ* by hand layup, or prefabricated, generally by pultrusion. In the first case, dry fibre mats are applied over (or around) the member that needs to be strengthened, being impregnated with resin that also bonds the composite to the substate. In the second case, prefabricated (pultruded) strips, rods or laminates, typically with fibre volume fraction above 68% [3,4], are adhesively bonded (with epoxy) to the member that requires strengthening – Figure 7.3 illustrates various strengthening applications in buildings and bridges, where CFRP strips are applied either as externally bonded reinforcemente (EBR) or near surface (NSM); in both cases, the strips can be simply bonded as passive reinforcement or pre-stressed.

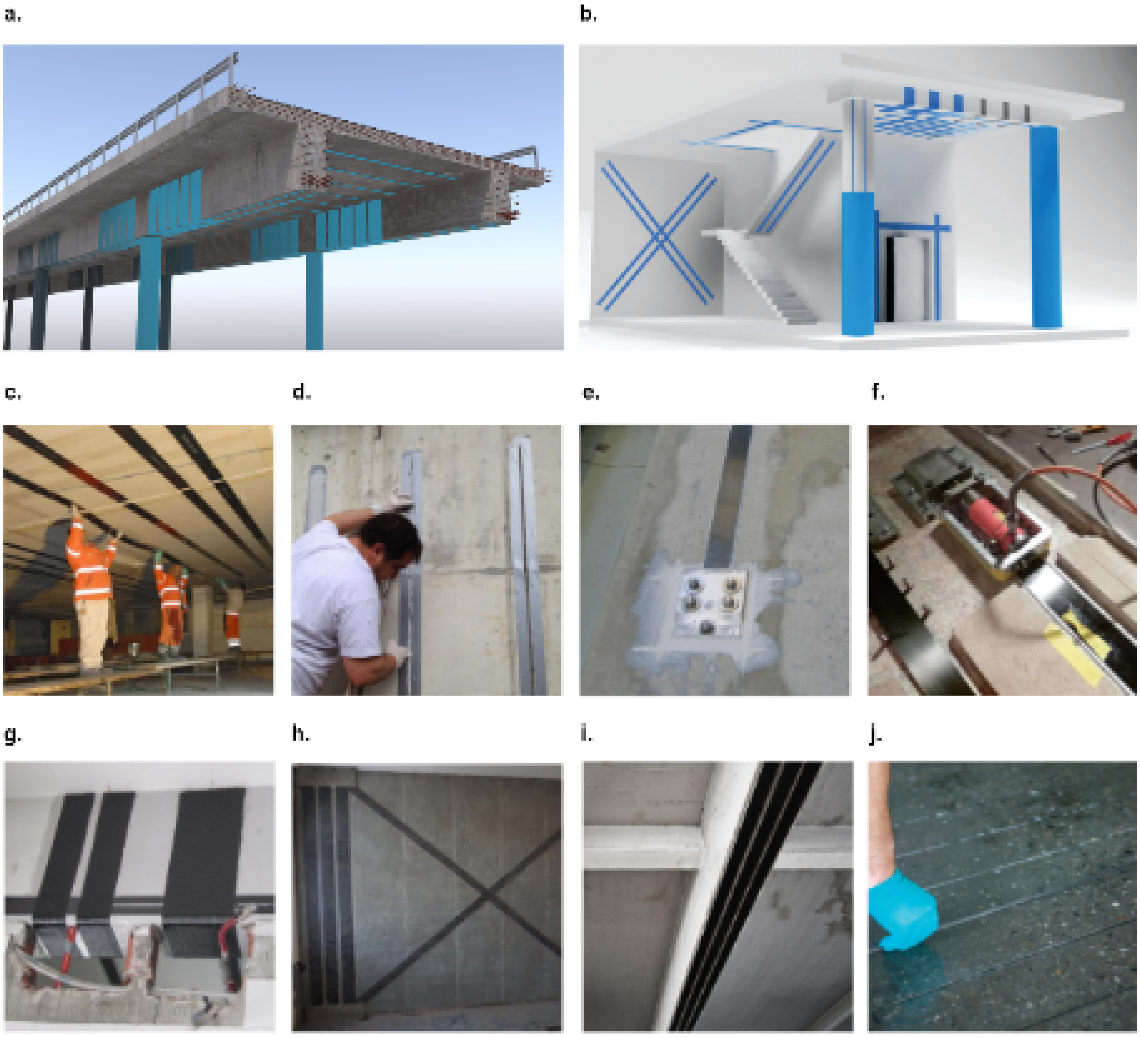

Figure 7.3: CFRP composites used for strengthening reinforced concrete and masonry building and bridge structures [4]: **a.** and **b.** application of strips and mats in bridges and buildings, respectively, **c.** strips applied in slab, **d.** strips applied in wall, **e.** strip with anchoring plate, **f.** pre-stressed strips, **g.** strips and sheets in beam, **h.** strips in masonry for seismic strengthening, **i.** strips in bottom surface of beam, and **j.** strips in top surface of slab.

Because the pultrusion process allows achieving a high fibre volume fraction (higher compared to hand layup or vacuum infusion), the thermoset matrix represents around

30% of the volume of the pultruded CFRP composite. In any case, this figure is still quite relevant and therefore there is plenty of room to increase the sustainability of these non-renewable CFRP composites, and namely of their polymeric matrix. This is particularly relevant considering the increasingly severe level of depletion of natural resources, making it urgent to search for renewable alternatives that allow overcoming the current dependence on petroleum.

The development of more sustainable fibre-polymer composites for high-performance applications has mainly followed two distinct approaches: (I) the search for alternative renewable raw materials for replacing those with higher environmental impact [5–9]; and (II) the development of recyclable composites [10–13]. Despite such efforts, to date the performance and processing limitations as well as the insufficient durability data about such (more) sustainable composites are restricting their use as mainstream products for civil engineering applications [14–19].

Regarding approach (I), one of today's biggest challenges is to develop eco-friendlier fibre reinforcements and polymer matrices suitable for large-scale production methods, such as pultrusion, having comparable mechanical performance and durability to conventional pultruded CFRPs used in civil engineering structures. In this respect, the following main approaches have been pursued: (i) the development of bio-based precursors to produce carbon fibres, able to replace the current petroleum-derived polyacrylonitrile (PAN) fibres [20]; (ii) the replacement of thermoset resins with thermoplastic ones [21–27]; and (iii) the development of bio-based resins derived from renewable resources [28,29].

The development of bio-based precursors for producing carbon fibres faces the current challenge of transforming renewable raw materials (such as cellulose, lignin, or hemicellulose) into fibres that are almost exclusively made up of carbon; to obtain bio-based carbon fibres with comparable mechanical properties to their petroleum-derived counterparts, it is therefore necessary to use higher processing temperatures (∼2900 ℃), which leads to higher energy consumption compared to conventional processes [30]. It is also worth mentioning that the current efforts to replace synthetic fibres with natural counterparts, especially vegetable ones, still do not allow fulfilling the requirements set by mainstream structural applications. In fact, vegetable fibres entail critical drawbacks, which still need to be overcome, such as: (i) flammability and susceptibility to moderately elevated temperatures (160 ℃ to 200 ℃) [31–35], preventing their use in pultrusion; (ii) hydrophilicity, which can induce the subsequent degradation of the fibres; (iii) biodegradability [36,37]; and (iv) lower tensile strength compared to typical synthetic fibres. Due to these limitations, which are yet to be overcome, natural fibres seem to be best suited to produce composite parts that do not require particularly high strength [38,39], *i.e.*, for non-structural applications or secondary members.

It is also worth referring that despite the increasing use of bio-based thermoplastics in the packing industry and other household consumer products [40–42], the properties achieved so far still limit their use in pultrusion. For instance, bio-based thermoplastics typically have high viscosity and require heat and pressure during moulding [43,44], which precludes their use as a fibre impregnation matrix in large scale production processes, such as pultrusion or vacuum infusion. In addition, when alternative high-performance matrices present mechanical, thermomechanical, and processing properties suitable for high-performance applications, they are expensive, which limits the prospect of their use in mainstream composite products [45–50].

Based on the alternatives described above, a quicker and more competitive way to increase the sustainability of CFRPs in the composites industry seems to be replacing conventional petroleum-derived (thermoset) matrices with bio-based counterparts. Among thermoset matrices, unsaturated polyesters have a lower cost when compared to epoxies and vinyl ester [51], being versatile and having processing, mechanical and thermomechanical properties that are suitable to produce pultruded structural parts. Unsaturated polyesters are most often used to impregnate glass fibres [52]. However, it is also possible to obtain good compatibility and improved adhesion with carbon fibres - for this purpose, if necessary, composition modifications in the resin or surface treatments in the fibres can be used [53–55]. In this context, the development of high-performance unsaturated polyesters based on raw materials derived from renewable resources is a possible route towards a (more) sustainable composites industry; in particular, this approach has the potential to reduce the environmental impacts of pultruded CFRP composites [56–59].

Meanwhile, very limited data were reported concerning the development and characterisation of pultruded CFRPs with bio-based (thermosetting) matrices. Ma *et al.* [60,61] made previous efforts in this respect by developing carbon fibre reinforced furfural alcohol prepolymers (with viscosity ranging from 500 and 2000 cP) catalysed with *p*-toluene sulfonic acid for free radical polymerisation during the pultrusion process. In this pioneering study, the characterisation of the CFRPs produced was rather limited; for example, data about the bio-content achieved and the thermomechanical properties of the composite (such as the glass transition temperature) were not presented. In addition, the authors applied a post-curing treatment at very high temperatures ($\sim$200 ℃), which would be unfeasible (or at least not competitive) for large-scale production. Despite the potential of bio-based thermosetting polymers to be used as matrices for impregnating carbon fibres in high-performance pultruded CFRPs, besides the work by Ma *et al.* [60,61], no further studies were found in the literature.

Regarding approach (II), research efforts have been made to develop more circular composites, which focused in particular on their recyclability (reprocessing) [62,63]. In this respect, it has been shown that it is feasible to recover carbon fibres while reprocessing CFRP composites and obtain high-performance products in a closed-loop. As examples of this approach, the following reprocessing methods have been tested on pultruded CFRPs: (i) epoxy- or polyester-type vitrimers [64–67]; (ii) the use of dynamic hardeners/agents

[68–71]; or (iii) chemical depolymerisation [72,73]. Although these methods are seen as a potential solution to increase the circularity of the composites industry, the durability of the resulting products is yet to be comprehensively characterised, namely when subjected to long-term exposure to external weathering degradation agents likely to be found in civil engineering structures, such as moisture, saline environments, thermal effects, ultraviolet radiation, among others [74,75]. In addition, it is also worth referring that the current techniques capable of reclaiming carbon fibres from thermoset CFRPs are not suitable for the pultrusion process, as the resulting reinforcement is discontinuous and of lower grade [76].

This chapter reports a research that follows approach (I), namely focusing on the production and mechanical characterisation of innovative CFRP strengthening strips manufactured by pultrusion, combining unidirectional carbon fibres and a high-performance bio-based unsaturated polyester resin, recently developed in-house [77,78], by synthesising monomers (diacids and diols) derived from renewable sources. The cured bio-based resin has a renewable content of more than 50% by weight while containing less volatile organic compounds in the liquid resin compared to typical conventional petroleum-based alternatives. Thus, the main goal and innovation of the study presented herein is the development, in an industrial setting, of a bio-based CFRP composite strengthening strip with: (i) high bio-based content, meeting or exceeding that of previous studies available in the literature, and (ii) mechanical and thermomechanical properties compatible with the requirements of civil engineering strengthening applications, and comparable to those of conventional CFRP strips manufactured with petroleum-derived vinyl ester resin. For this purpose, an experimental campaign was conducted towards the manufacturing in an industrial pultrusion line, and subsequent mechanical and thermomechanical characterisation, of bio-based and conventional CFRP strengthening strips, which were produced and tested under the same conditions.

7.2 Experiments

7.2.1 Materials

In this study, a bio-based unsaturated polyester (UP) resin – previously developed by the authors [77,78] – was used as a high-performance thermoset matrix in the manufacturing, by pultrusion, of carbon fibre reinforced unsaturated polyester (CF/UP) strengthening strips for civil engineering applications. The bio-based UP resin was developed taking into account the following requirements that resin systems used in pultrusion must fulfil [61]: (i) suitable viscosity (typically between $\sim$500 up to 2000 cP); (ii) high reactivity at high temperatures that are found inside the pultrusion die (typically with a short length, of about $\sim$100 cm); and (iii) good fibre wetting ability.

Taking those requirements into account, the bio-based UP prepolymer was produced by synthesising monomers derived from renewable raw materials, which are illustrated in Figure 7.4. In this respect, the bio-based unsaturated main chain (prepolymer) obtained from the polycondensation reaction was subsequently incorporated using a mixture of styrene and 2-hydroxyethyl methacrylate (HEMA) (in equal parts) as a reactive diluent – Figure 7.5 presents the main steps taken to obtain the bio-based UP resin used in this study; more details are available in [77,78].

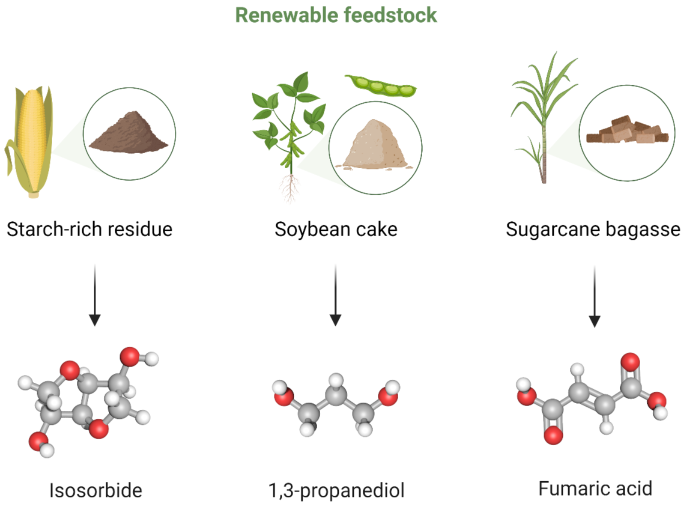

Figure 7.4: From renewable feedstock to the bio-based monomers used in this study.

The replacement of maleic anhydride and ethylene glycol (both petroleum-derived) by fumaric acid, isosorbide and 1,3-propanediol (derived from renewable sources), respectively, together with the use of lower styrene content (compared with conventional resins), allowed the bio-based UP resin to achieve over 50 wt.% of bio-content. In addition, the mechanical and thermomechanical properties of the bio-based resin matched or exceeded those of its petroleum-derived counterparts [77,78].

As a benchmark conventional resin, the petroleum-based vinyl ester (VE) resin currently used as a fibre impregnation matrix for manufacturing pultruded carbon fibre reinforced vinyl ester (CF/VE) strips by S&P Clever Reinforcement Ibérica was also characterised under identical conditions.

For comparison purposes, mechanical and thermomechanical tests were performed for both conventional (VE) and bio-based (UP) neat resins. The VE specimens were prepared using Trigonox (1.3 wt.%) and Perkadox (1 wt.%), as initiator and accelerator, respectively; for UP specimens, methyl ethyl ketone peroxide and cobalt octoate (in the same wt.% concentration) were used as initiator and accelerator, respectively.

Then, VE and UP resin specimens were submitted to a post-curing at 100 ℃ for 4 hours. Five specimens for each resin were subjected to tensile and DMA tests. The results obtained for the cured UP and VE resins are presented in Table 7.1, namely the mean values of strength ($\sigma_{t,max}$), modulus of elasticity (E_t) and strain at failure ($\epsilon_{t,max}$) in tension;

and glass transition temperature (T_g), based on the onset value of the storage modulus decay retrieved by DMA.

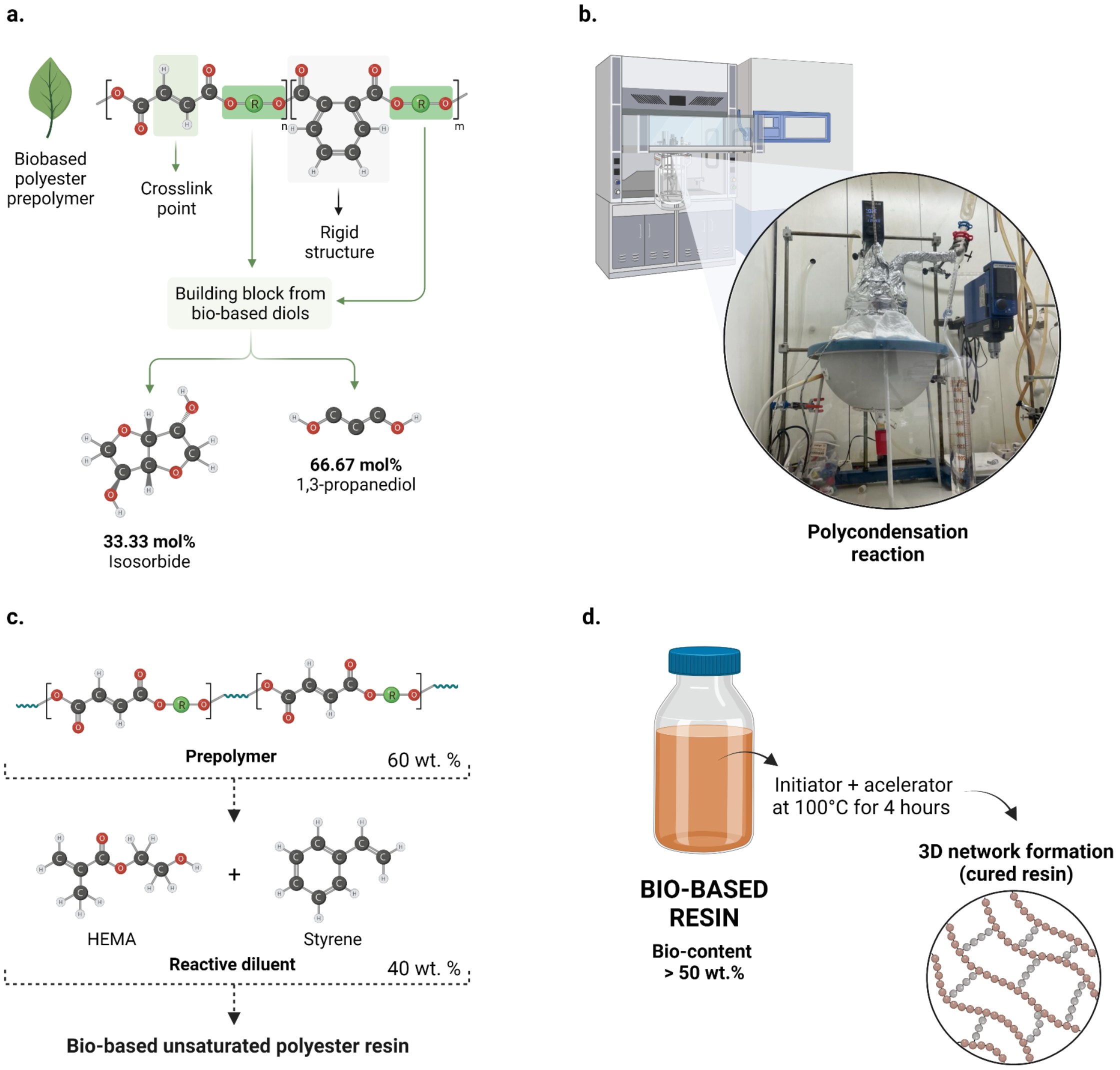

Figure 7.5: Main steps to obtain the bio-based UP resin used in this study: **a.** polyester prepolymer, **b.** polycondensation reaction, **c.** prepolymer incorporation with reactive diluents, and **d.** UP resin and performing the cured resin (more details can be found in [77,78]).

The continuous carbon fibre rovings used in this research, Tenax®-E STS40 F13, were supplied by Teijin. This unidirectional fibre reinforcement has 24000 filaments with a diameter of 7 µm and nominal linear density of 1600 tex, density of 1.78 g/cm^3, tensile strength of 4300 MPa, modulus of elasticity of 240 GPa and strain at break of 1.8%. Each CFRP strip comprised 22 strands of these carbon fibre rovings.

7.2.2 Pultrusion equipment

Figure 7.6 illustrates the pultrusion line of S&P Clever Reinforcement Ibérica, which comprises a Pultrex pultrusion machine where the manufacturing was carried out. Firstly, the continuous carbon fibre rovings, grouped in various creels, were positioned in preforming

Table 7.1: Mean values of tensile properties and T_g of UP and VE resin specimens.

Specimen	$\sigma_{t,max}$ **(MPa)**	E_t **(GPa)**	$\epsilon_{t,max}$ **(%)**	T_g **(℃)**
VE	74.9±4.7	3.4±0.1	3.2±0.7	75
UP	62.1±2.6	3.3±0.1	2.4±0.2	65

guides (Figure 7.7). Then, the fibres were immersed in an impregnation resin bath inside a stainless steel tank (Figure 7.8). Before reaching the heating die, the fibre strands passed through a series of seven clamps with different openings, allowing: (i) to remove the excess of resin, (ii) to expel any air bubbles that may have been incorporated during the resin and additives mixing process; and (iii) to ensure uniform fibre wetting.

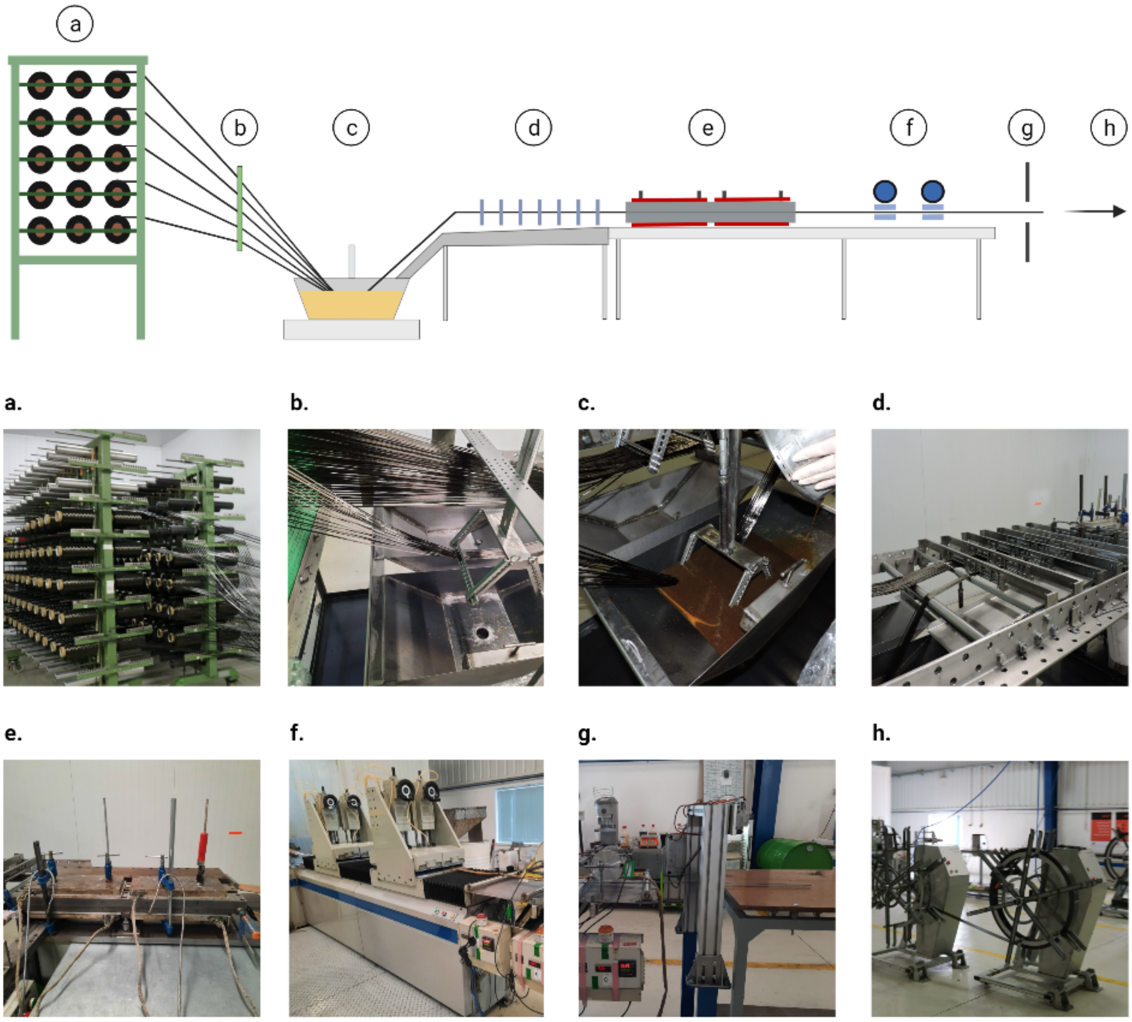

Figure 7.6: Overview of pultrusion process.

The heating die, with chrome plating treatment, has internal dimensions of 20 × 1.4 × 1000 mm. The die has two heating zones (controlled by two heating plates) along the pultrusion direction to guarantee the polymerisation of the matrix. The first heating zone (first half of the pultrusion die) was kept at a temperature setpoint of 150 ℃, while the second zone (second half of the die) was kept at a temperature setpoint of 175 ℃. The pulling rate was fixed at 0.30 m/min to balance manufacturing economy and the (desirably high) degree of cure of the resulting CFRP strips. The pultrusion of both types of CFRP strips was carried out under the same conditions. Figure 7.9 shows the die parameters for the pultrusion process adopted in this study.

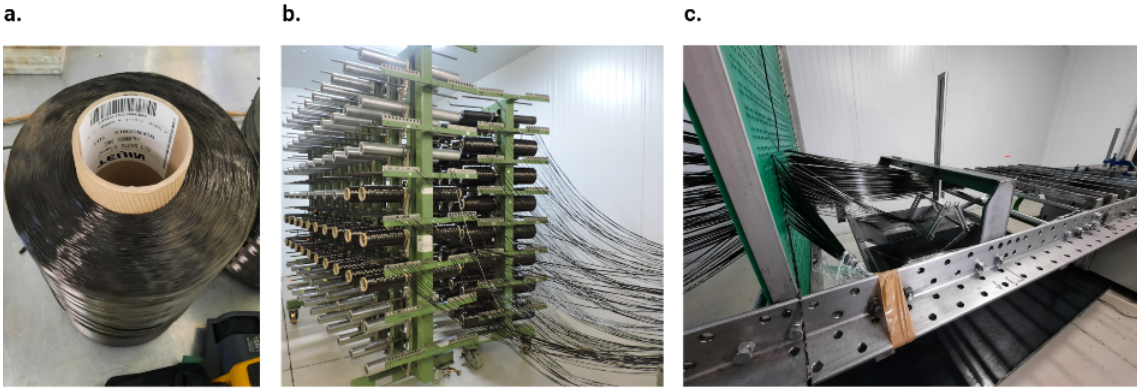

Figure 7.7: Continuous carbon fibre roving – Tenax® filament yarn: **a.** fibre roving, **b.** fibre roving creels, and **c.** preforming guides.

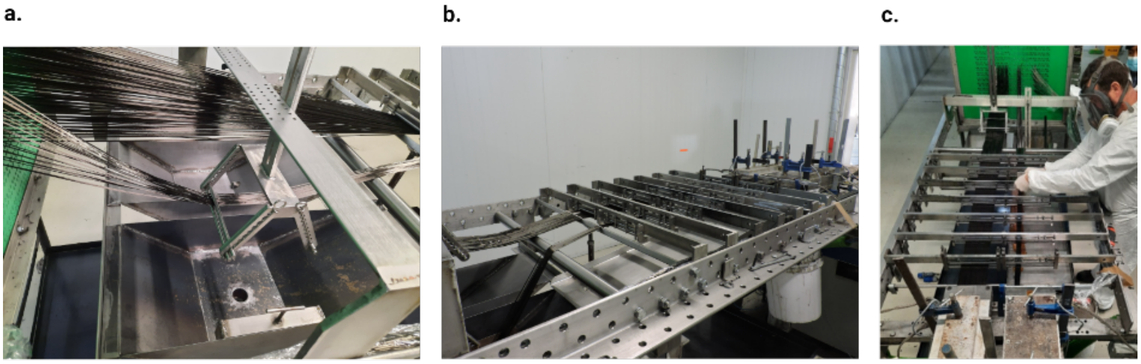

Figure 7.8: Preparation for pultrusion process: **a.** metallic tank for resin bath impregnation; **b.** clamps for uniform impregnation; and **c.** clamp opening adjustments.

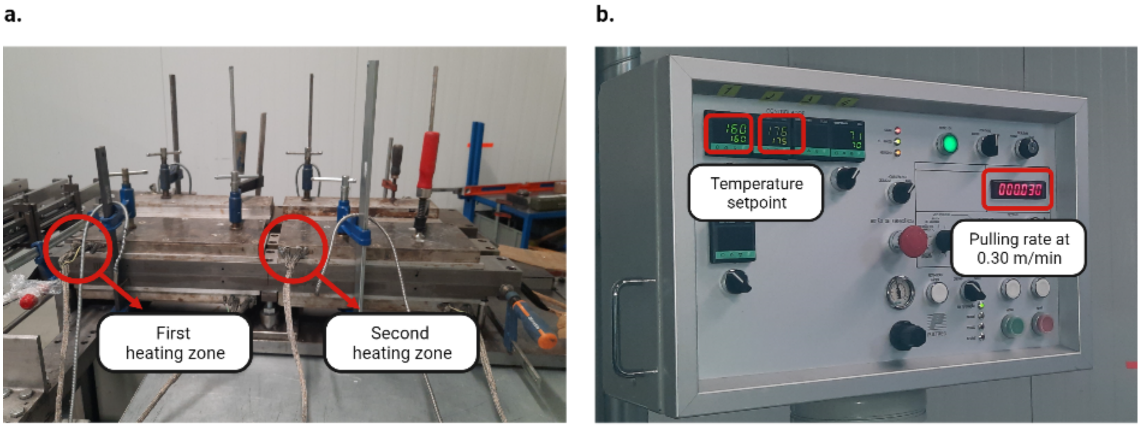

Figure 7.9: Equipment for pultrusion process: a. two heating zones of the die, and b. temperature and pulling rate controllers.

The pullers of the machine's pulling system were fitted with "spacers" to control the out-of-plane stresses applied to the laminates during the pull and consequently to minimise the development of longitudinal cracks in the CFRP composite strips after polymerisation by the impregnation matrix – see Figure 7.10. At the end of the pultrusion line, the pultruded CFRP strips were continuously winded into coils, as typically done for commercialisation purposes (Figure 7.11).

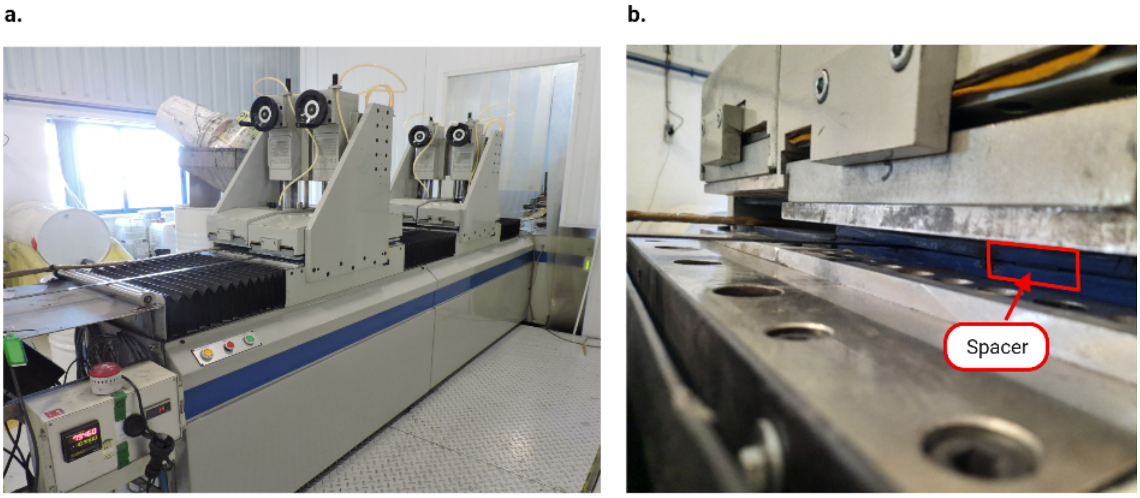

Figure 7.10: Pulling system of pultrusion machine: **a.** reciprocating pullers, and **b.** spacers used to control out-of-plane (bearing) stresses applied to the composite strips.

Figure 7.11: Winders for coiling pultruded strips.

7.2.3 Test methods

7.2.3.1 Overview

In a first stage, prior to manufacturing, the processability of the bio-based and conventional resins used to produce the CFRP strips was investigated, namely, to assess their viscosity, wettability, and gel times.

In a second stage, after manufacturing, the CFRP strips were subjected to different types of physical and mechanical tests, to determine their fibre fraction, Barcol hardness, tensile properties, and thermomechanical behaviour. In addition, the bio-based UP resin and the conventional VE resin were also tested for Barcol hardness, tensile properties, and thermomechanical behaviour, as a reference. The resins were tested after curing at 100 °C for 4 hours, while the pultruded CFRP strips were not subjected to any post-curing. It is worth referring that the same procedures were used in the assessment of both types of resins, as well of the bio-based CF/UP strip specimens and conventional CF/VE ones.

7.2.3.2 Processing parameters

Viscosity tests were performed on the UP and VE resins using a Cone & Plate ICI viscometer from REL (Research Equipment London Ltd.), according to ISO 2884-2 [79]. The viscosity was taken at 23 °C, from the average value of three measurements, obtained by placing two drops of resin into a plate surface, then approached by a rotating cone (constant speed).

Gel time was used as a parameter to monitor reactivity/time to gelation. In this respect, resin samples (12 g) were placed into glass tubes (160 mm in length and 16 mm in diameter), and the tests were performed on a Gelnorm® gel timer instrument at 180 °C.

7.2.3.3 Calcination tests

CF/UP and CF/VE samples produced by pultrusion were subjected to calcination tests to determine the fibre-matrix fraction of the pultruded CFRP strips, following test procedures indicated in ISO 1172 [79]. The samples (3 for each type of resin) were heated in a muffle furnace up to 700 °C, and the weight of the residual fibres (no inorganic filler was added to the resin matrix) was used to calculate the fibre mass fraction (w_f), as follows,

$$w_f = \frac{m_3 - m_1}{m_2 - m_1} \times 100 \tag{7.1}$$

where

- m_1 is the initial mass, in grams, of the dry crucible;
- m_2 is the initial mass, in grams, of the dry crucible plus the dried sample;
- m_3 is the final mass, in grams, of the crucible plus the residue after burning.

Based on the fibre mass fraction, the fibre volume fraction (v_f) was determined as follows,

$$v_f = \frac{w_f}{\frac{\rho_c}{\rho_f}} \tag{7.2}$$

where

- ρ_c is the density of the CFRP composite;
- ρ_f is the density of the carbon fibres.

7.2.3.4 Hardness

Hardness tests were performed on the CFRP composites using a Barber & Colman Barcol impressor, according to ASTM D2583-13 [80]. Ten measurements were taken at different random but evenly distributed locations on each sample. After the tests, the average value obtained was taken as the Barcol hardness. The specimens were tested under laboratory conditions with temperature of 23±2 ℃ and 55±3% relative humidity.

7.2.3.5 Tensile tests

Tensile tests were performed on both types of CFRP composite strips under the above-mentioned laboratory conditions using an Instron 5982 universal test machine, and a video-extensometer (high-definition SonyTM video camera, model XCG 5005E, Fujinon – Fujifilm HF50SA-1 lens) to measure material deformations. The tensile tests were carried out according to ISO 527-5 [81], under displacement control, at a loading rate of 2 mm/min. Five replicate specimens were tested for each type of composite strip.

7.2.3.6 Thermomechanical tests

DMA tests were performed to assess the thermomechanical behaviour of both types of resins – bio-based UP and conventional VE – and of the resulting CFRP composite strips. Tests were carried out in a dynamic mechanical analyser from TA Instruments, model DMA Q800, according to ASTM E1640-09 [82], in a 35 mm dual cantilever clamp configuration. Specimens were subjected to a constant strain amplitude of 15 µm at a constant oscillation frequency of 1 Hz, while submitted to a temperature sweep at a constant heating rate of 2 ℃/ min, starting at –30 ℃ and ending at 150 ℃. The T_g was defined from (i) the onset value of the storage modulus decay, and (ii) the peak of the tan δ. For each type of resin and composite, two replicate specimens were tested.

7.3 Results and discussion

7.3.1 Manufacturing

The bio-based UP resin presented viscosity (at 23 ℃) of 800 cP, fulfilling the requirements for pultrusion. It was prepared in a rotary mixer (Figure 7.12), allowing the addition of the free radical polymerisation catalysts shown in Table 7.2. Gel times were determined for the two resins at 180 ℃ considering two different concentrations of catalysts, as shown in Table 7.2. The results highlighted the high reactivity of the bio-based UP resin, which presented shorter gel times than the petroleum-based VE resin for the same catalyst concentrations. As a result of these tests, the catalyst concentrations for production were set as 1.3% for Trigonox and 1.0% for Perkadox (wt.%), for which the gel time of the bio-based UP resin was 1 min and 11 s (*vs.* 1 min and 19 s for the VE). In addition, Moulex (1 wt.%) and BYK (1 wt.%) were also added as release agent and dispersant additive, respectively, according to the company's production standard. After its preparation, the resin was transferred to the resin tank of the pultrusion line used for the carbon fibre impregnation.

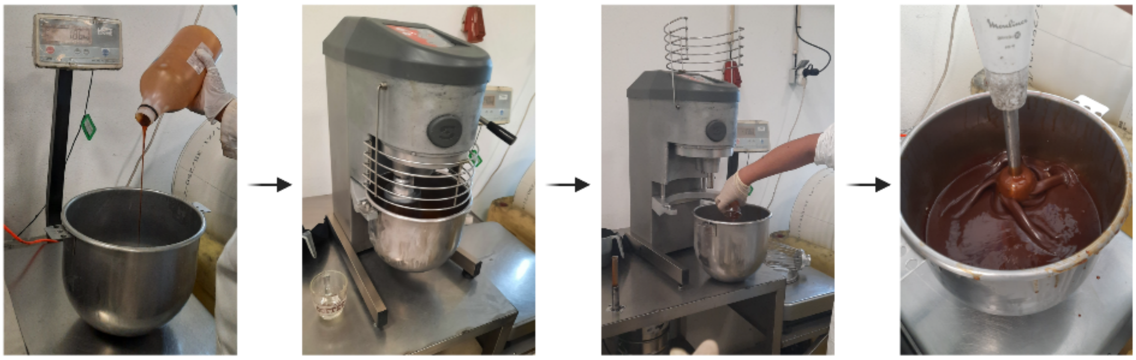

Figure 7.12: Resin preparation.

Table 7.2: Gel time of conventional and bio-based resins (at 180 ℃).

Catalyst	**VE**		**UP**	
Trigonox (wt.%)	1.0	1.3	1.0	1.3
Trigonox (wt.%)	0.5	1.0	0.5	1.0
Gel time (min:sec)	02:00	01:19	01:42	01:11

It is worth referring that the bio-based UP resin used in this study was prepared about three months before the production of the CFRP strips – this period was due to technical scheduling issues, given the need to have the complete production line available for testing. Thus, the bio-based UP resin was tested at the limit of its shelf-life. As a result, an increase in viscosity was observed (visually) compared to the viscosity measured in the same week of its production (in the laboratory), which can be partially explained by the partial volatilization of styrene during this period.

Considering the high viscosity of the bio-based UP resin, preliminary impregnation and pultrusion tests were carried out to evaluate possible adjustments to be made. During the preliminary production tests, the following aspects were observed: (i) deficiency in the wetting of the fibres by the resin, resulting in the formation of ”veins” in the composite strips; and (ii) the apparently insufficient fibre-resin adhesion. For this reason, it was decided to increase the concentration of styrene to reduce the resin's viscosity, thus improving fibre impregnation. Thus, 10% of styrene relative to the total weight of the bio-based UP resin was added. After additional styrene incorporation, the viscosity of the bio-based resin (containing the catalysts) remained stable during the fibre impregnation at 23 ℃ (*i.e.*, impregnation tank temperature), which indicates that the bio-based UP resin fulfilled the (pot-life) requirements for pultrusion.

As a result of the viscosity adjustment, the bio-based UP resin showed very similar wettability to its VE counterpart, as illustrated in Figure 7.13. Adequate wettability is essential to achieve good impregnation of the carbon fibres and to avoid interfacial defects that act as stress concentrators and consequently limit the strength of the resulting composite. The excess of resin during the fibre wetting stage was controlled by a series of preforming plates of increasingly tighter tolerance, as depicted in Figure 7.14.

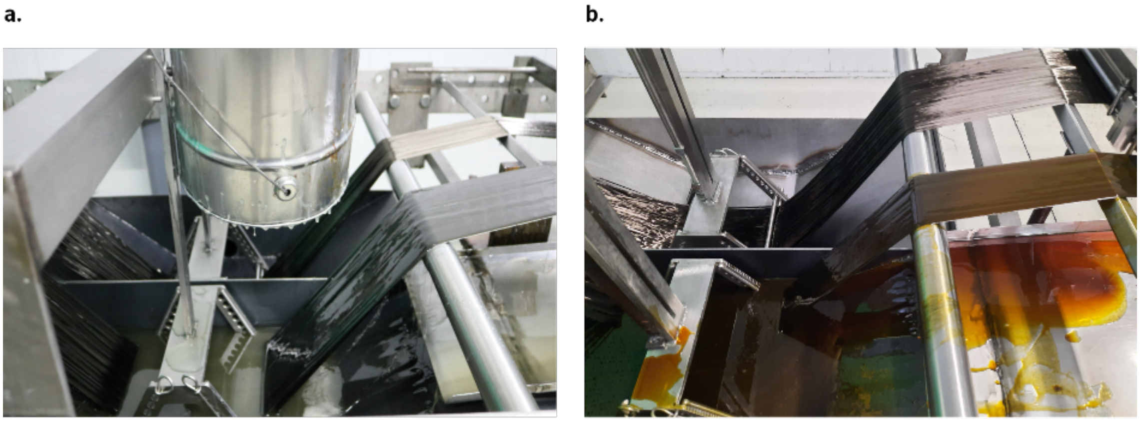

Figure 7.13: Carbon fibre impregnation of the: **a.** CF/VE, and **b.** bio-based CF/UP composites.

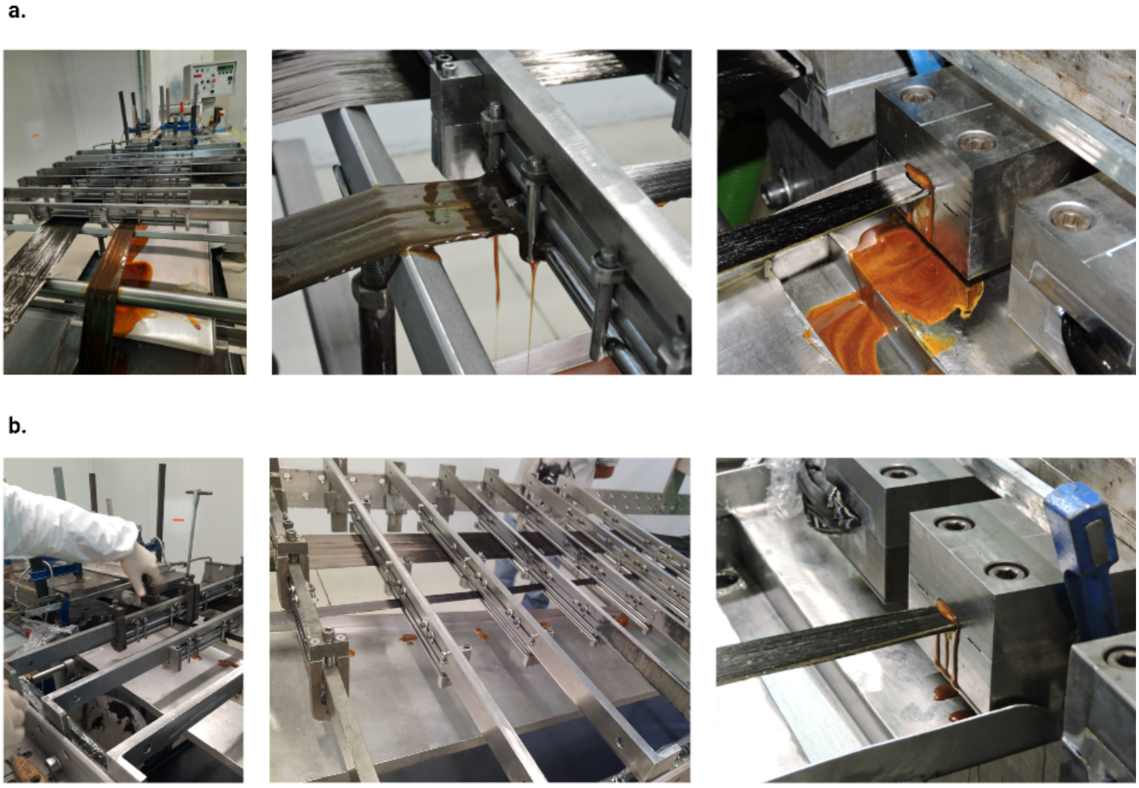

Figure 7.14: Preforming plates: **a.** before and **b.** after tightness adjustments.

The CF/VE and CF/UP composite strips were successfully produced after the above-mentioned viscosity and impregnation adjustments. In some segments of the strips, it was possible to observe a single longitudinal crack; this was more prevalent during the initial phase of production, having been mitigated by adding neoprene tabs to reduce the through-thickness compressive forces from the clamping of the strips at the pullers. In addition, during the preliminary pultrusion tests, several adjustments were made to the preforming plates' position to correct the warping of the strips. As shown in Figure 7.15, the production was stabilised when the strips showed a deviation from linearity within the company's usual quality control parameters. Finally, approximately 300 m of CF/UP composite strips were produced with average thicknesses of 1.36 mm, see Figure 16. The fibre (volume) fraction of both types of CFRP strips (Table 3) virtually matched, being 65% and 66% for the CF/VE and CF/UP strips, respectively.

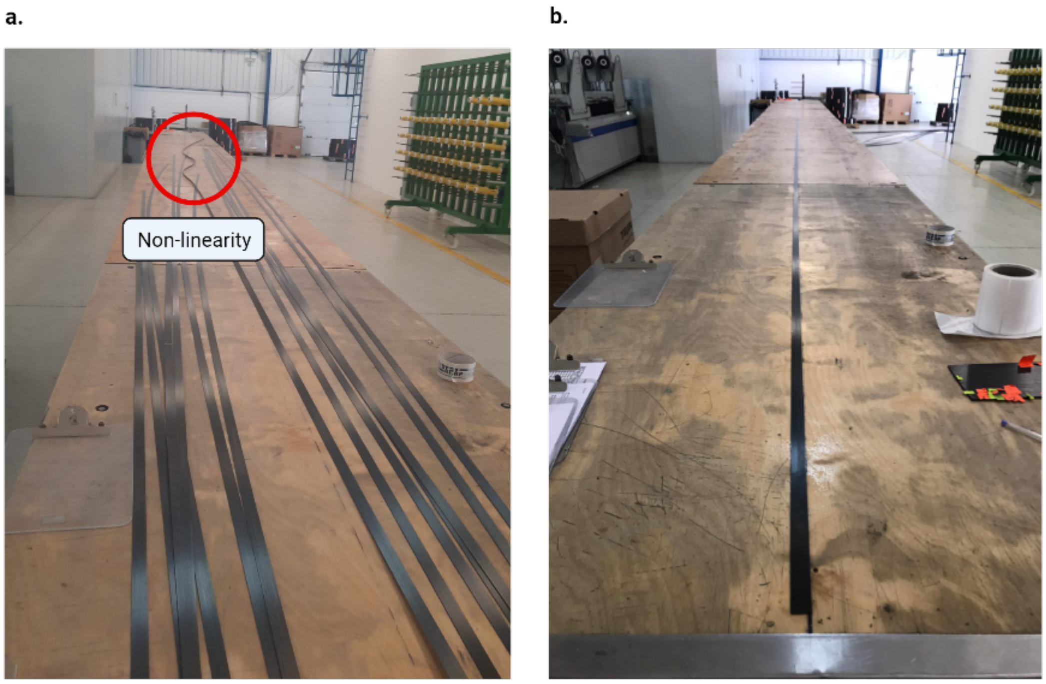

Figure 7.15: Pultruded composite strips: **a.** before and **b.** after linearity adjustments in the clamps.

Indeed, the bio-based pultruded CFRP strip prototype production in an industrial environment – by a partner company specialised in the manufacture of CFRP composite strengthening strips for the construction industry – showed the high technology readiness level of this solution. This is a main step forward made in the present research.

7.3.2 Mechanical behaviour

7.3.2.1 Hardness

The Barcol hardness measured for the bio-based UP resin was 42 comparing well with that of the VE (petrochemical) counterpart, which presented a Barcol hardness of 38. However, the bio-based CF/UP strips presented Barcol hardness of 69, *i.e.* 14% lower

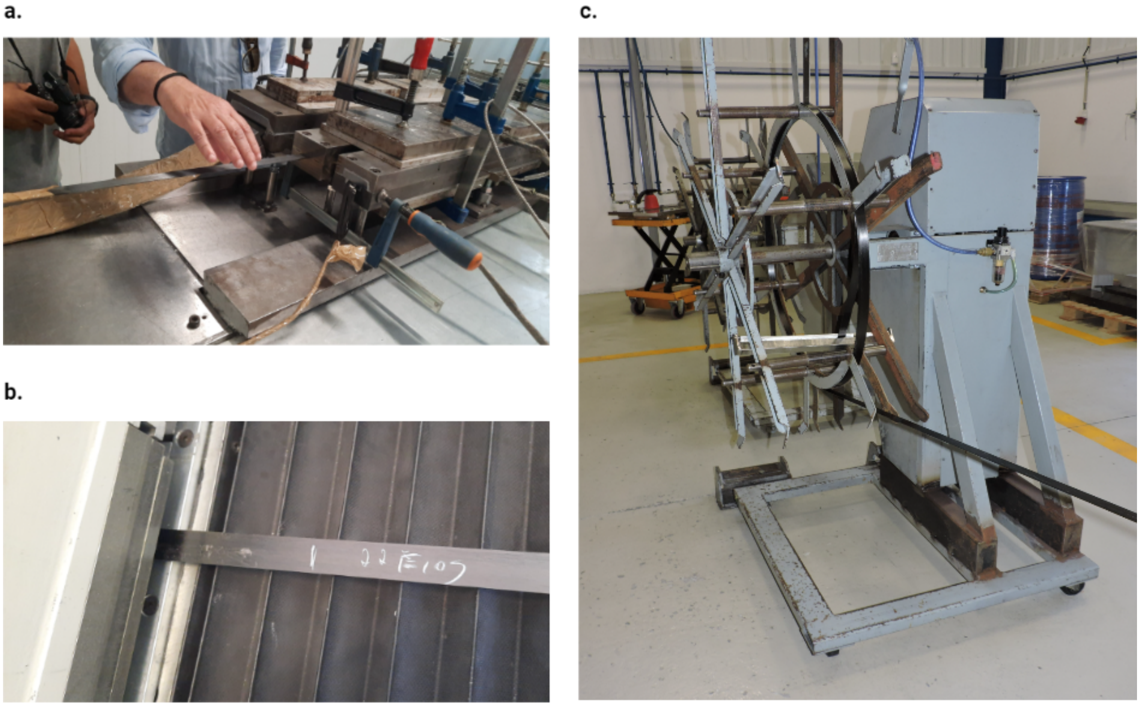

Figure 7.16: Bio-based CFRP strip successfully produced: **a.** CF/UP leaving the heating die; **b.** pultruded strip with 22 yarns; and **c.** winding the CF/UP strips into coils.

than the hardness obtained for the conventional CF/VE strips of 80. The higher addition of styrene (10 wt%) may explain, at least in part, the lower Barcol hardness of the strip produced with cured bio-based UP. Despite this relatively small difference, the hardness achieved by the bio-based system was considered adequate for the envisaged application.

7.3.3 Tensile behaviour

Figure 7.17 shows the tensile stress-strain nominal curves for CF/VE and CF/UP specimens. Both types of specimens exhibited linear response until failure, which occurred in a brittle manner, typical for conventional CFRP strengthening strips under tension. The tensile stress-strain curves presented very similar development for both conventional and bio-based CFRPs. All CFRP specimens exhibited an "explosive" failure, with generalised fibre rupture, as shown in Figure 7.18.

Table 7.3 provides a summary of the main results obtained from the axial tensile tests of the CF/VE and CF/UP specimens. The tensile strengths of the CF/VE (1964∼28 MPa) and CF/UP (2095∼145 MPa) strips were very similar – the average strength of the bio-based CFRP strip was 7% higher than its conventional counterpart. The tensile modulus of the CF/VE (172∼3 GPa) and CF/UP (167∼2 GPa) strips were also very similar, being about 3% higher in the former. By contrast, the average strain at break of the CF/VE strip (1.2∼0.1%) was about 14% lower compared with that of the CF/UP one (1.4∼0.2%) – for both types of composites, these figures are well below the strain at break of the corresponding resins, attesting their suitability for this type of reinforcement (*cf.* Table 7.1).

It is also worth noting the higher scatter of tensile strength (6.9% *vs.* 1.4%) and strain at break (7.1% *vs.* 8.3%) of the CF/UP strip with respect to the conventional one.

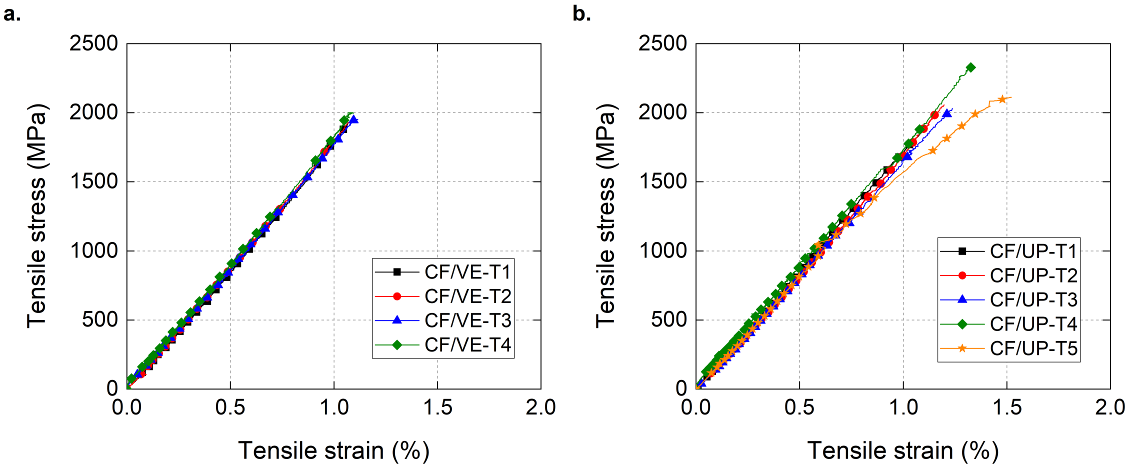

Figure 7.17: Nominal tensile stress-strain curves: **a.** CF/VE and **b.** bio-based CF/UP.

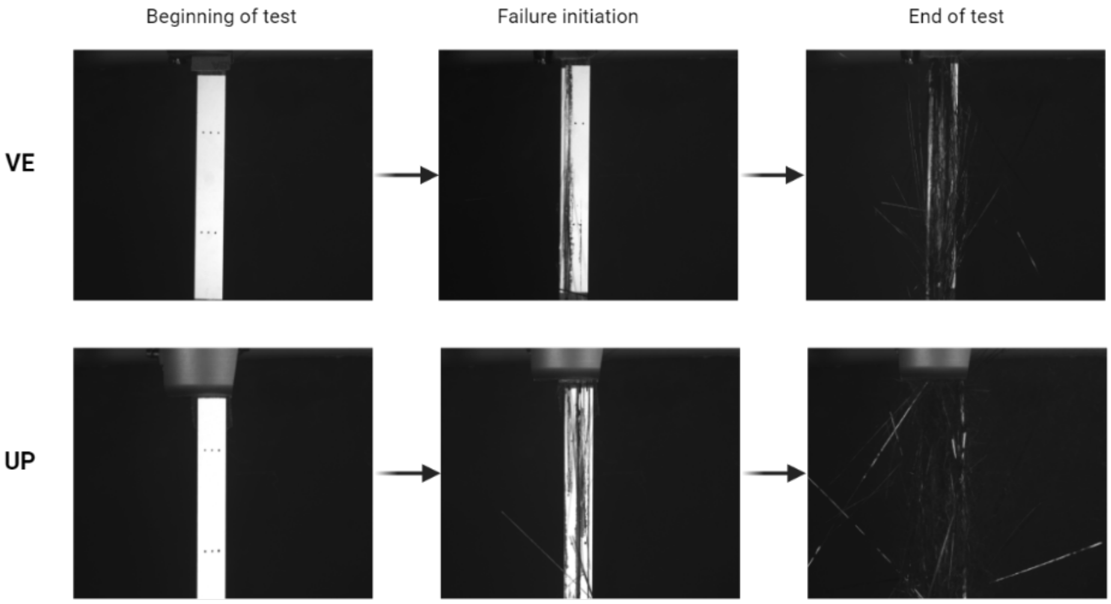

Figure 7.18: Failure modes in tension of representative CF/VE and CF/UP specimens.

Overall, the relative differences between the tensile behaviour of both types of composite strips were relatively limited, pointing out the potential of the bio-based CF/UP system to compete with its petroleum-derived counterpart, in terms of both tensile modulus and strength.

Figure 7.19 compares the results obtained in this study with other works reported in the literature, which used conventional thermoset resins to produce pultruded CFRP composites with fibre volume fraction ranging between 54% and 56% [61,83,84]. Tensile strength results for conventional pultruded carbon fibre reinforced phenolic (CF/PH) and carbon fibre reinforced epoxy (CF/EP), as well as bio-based counterparts, namely, carbon fibre reinforced furfuryl alcohol (CF/FA), are presented for comparison with the bio-based

Table 7.3: Fibre fraction, mechanical and thermomechanical properties of pultruded CF/VE and CF/UP strips.

Sample	Fibre fraction (%)	Barcol	Tensile strength (MPa)	Tensile modulus (GPa)	Strain at break (%)	T_g[a] (℃)	T_g[b] (℃)
CF/VE	65	80	1964±29	172±3	1.2±0.1	80	134
CF/UP	66	69	2095±145	167±2	1.4±0.1	78	140

[a] T_g from onset of storage modulus decay
[b] T_g from tan δ peak

CF/UP composite herein developed. Figure 7.19 shows that the CFRP composites studied herein exhibited higher tensile strength values than any of those studies. Finally, it is worth referring that the authors are unaware of any work reporting tensile strength values higher than those achieved here for pultruded CFRP composites manufactured with bio-based resins.

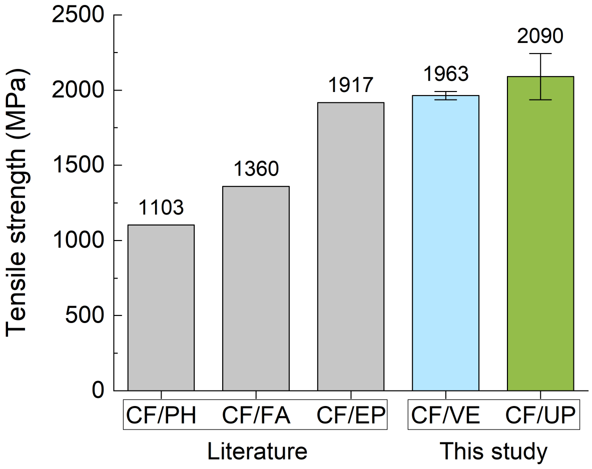

Figure 7.19: Comparison of tensile strength of pultruded CFRP composites mentioned in the literature (CF/PH [84], CF/FA [83], CF/EP [61]), and those developed in this study (CF/VE and CF/UP).

7.3.4 Thermomechanical behaviour

DMA tests were carried out to determine the thermomechanical properties of the CFRP strips and, together with the mechanical tests, to assess the potential for the use of the bio-based CFRP (CF/UP) strips to replace their petroleum-derived counterparts (CF/VE) in high-performance civil engineering applications, namely those located outdoors, where the temperature-dependence of mechanical properties is quite relevant. As mentioned, DMA tests were also performed on both types of neat resin specimens. Figure 7.20 presents the DMA curves for the storage modulus (E'), loss modulus (E''), and damping factor (tan δ) of the resin and composite specimens developed here, all as function of temperature.

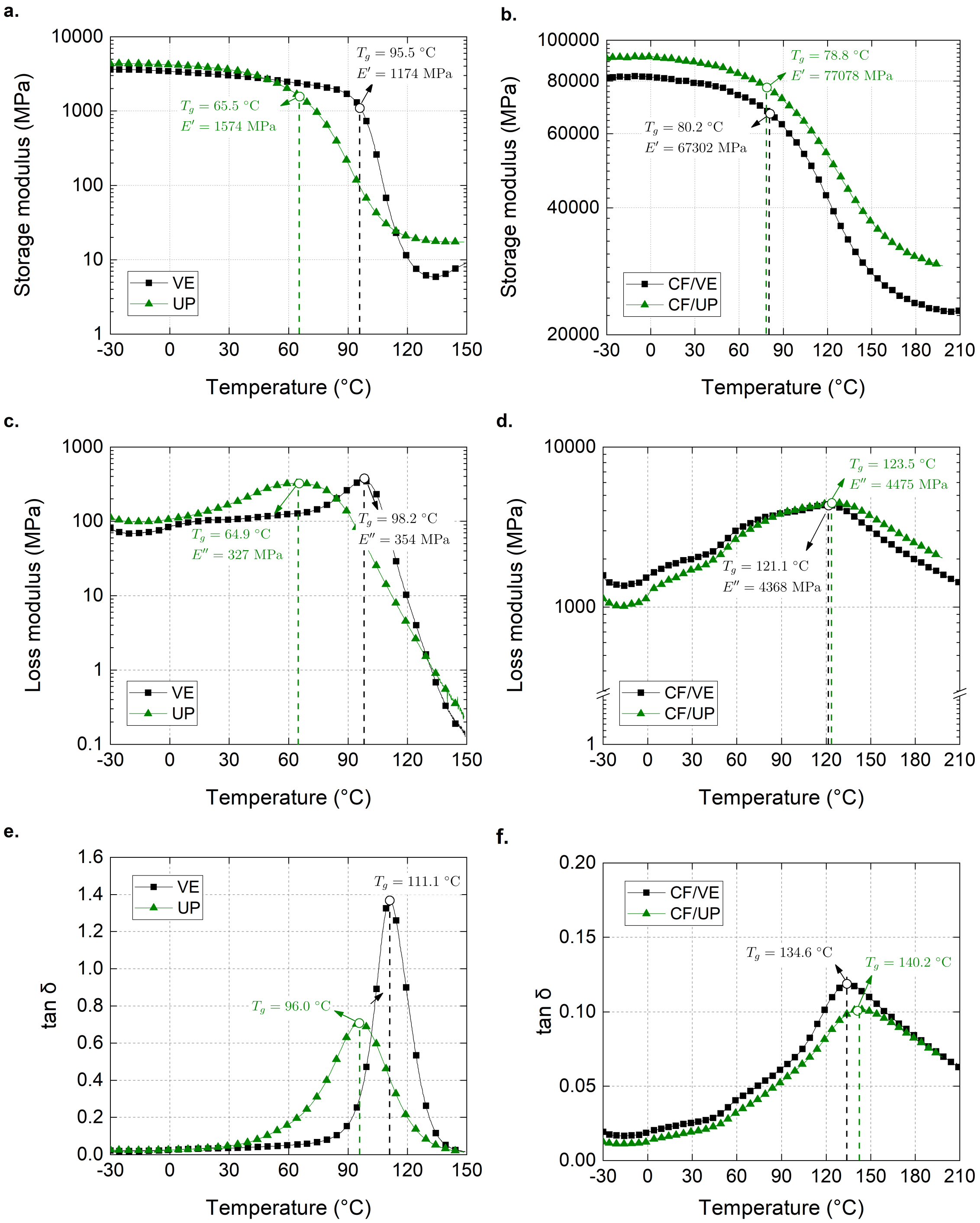

Figure 7.20: Thermomechanical properties of both types of resin and CFRP specimens.

The storage modulus curves of both types of composites and their corresponding resins present a well-defined and sharp drop with temperature increase across the glass transition region. The storage modulus of both "pairs" of curves (composite-resin) are quite consistent and so are the resulting estimates of T_g obtained from the onset value of the storage modulus decay – the results obtained prompt the following comments: (i) the storage modulus reduction of the conventional VE resin is more pronounced and occurs for higher temperature compared to the bio-based UP resin, resulting in T_g estimates of respectively 96 ℃ and 66 ℃ for VE and UP resins; (ii) for the corresponding composites, cured within the pultrusion die, these differences are much lower, with T_g estimates of CF/VE (80 ℃) and CF/UP (79 ℃) strips virtually matching; (iii) although the T_g estimate (from the onset of storage modulus decay) of the CF/UP is higher (20%) compared to its respective neat UP resin, the T_g of the CF/VE is lower (16%) compared to its respective neat VE resin – these differences should be due to the different cure kinetics underwent by each resin in post-curing (applied to the neat resins) versus the fast curing in the pultrusion die. While CFRP strips were not subjected to any post-curing and resin polymerization took place inside the heated die at 180 ℃ for about 3 minutes, the neat resins were post-cured at 100 ℃ for 4 hours – these procedures seem to have had different effects for the UP and VE resins, resulting in respectively higher and lower T_g estimates in their corresponding composites.

The loss modulus curves show no significant differences between the CF/VE and CF/UP strips regarding their capacity to dissipate energy for temperatures around 15 ℃ and 25 ℃. Figure 7.20 shows that as the temperature increases towards the glass transition, the energy dissipation remains very similar for the CF/UP (4475 MPa) and CF/VE (4368 MPa) strips. In addition, for both types of composites, the loss modulus curves present a wider shape and a higher peak than the corresponding resins.

The tan δ curves of both types of CFRP strips and the corresponding resins also present a typical development, with a well-defined peak in the glass transition, showing no signs of secondary relaxations, which attest the high curing degree of the materials. It is also worth referring that the CF/VE and CF/UP strips present similar T_g estimates, with that of the CF/VE strip (135 ℃) being 4% lower compared to the CF/UP one (140 ℃). In addition, the T_g estimates obtained from the tan δ peak for both CF/VE and CF/UP strips were higher than those obtained for the corresponding VE and UP neat resins, by respectively 21% and 46%.

Overall, the results obtained from the DMA tests show that the thermomechanical behaviour of the bio-based CF/UP strip is quite similar to the conventional CF/VE one, although their respective resins presented differences in thermomechanical behaviour. In addition, although the T_g of the CF/UP strip is slightly lower than that of the CF/VE one, it is still considered perfectly suitable for civil structural applications, with the environmental advantage of having a high bio-based content. In this respect, it is worth mentioning that the several guidelines for the design of FRP strengthening systems (*e.g.* [ACI]) recommend that the expectable service temperature does not exceed T_g – 20 ℃. The bio-based CFRP strip would thus allow a maximum service temperature of 58 ℃, which will not likely be exceeded in most climates.

7.4 Concluding remarks

This paper presented the pilot production, in an industrial context, of bio-based pultruded CFRP strips typically used for structural strengthening in civil engineering. The CFRP strips were manufactured with a high-performance bio-based unsaturated polyester resin developed in-house with raw materials derived from renewable sources. The bio-based CF/UP strip was characterised regarding its mechanical and thermomechanical properties, and compared with a CF/VE counterpart, produced with the same fibre architecture, and using a conventional petroleum-derived vinyl ester resin.

The bio-based pultruded CFRP strip was successfully manufactured, and a suitable impregnation of the carbon fibres with the bio-based unsaturated polyester resin was observed, which showed good potential to be used in the pultrusion technique. The results of the characterisation tests showed that the mechanical properties of the bio-based CFRP strip met or even exceeded those of its petroleum-derived counterpart. Furthermore, the glass transition temperature (T_g, defined from the onset of the storage module decay) of the bio-based CF/UP strip was very similar to that of the conventional resin, ensuring that it is fully compatible with the typical recommendations included in design guidelines for the maximum service temperature in outdoor applications.

Overall, the results obtained in this study show the technical potential of the bio-based pultruded CFRP strips developed in this study, which offer a more sustainable alternative to the CFRP strips currently based on resins produced with non-renewable resources. Future investigations should address other relevant aspects, such as the bond to concrete and the long-term durability.

7.5 References

[1] Lawrence C. Bank. *Composites for Construction: Structural Design with FRP Materials*. John Wiley & Sons, 1 edition, 2006.

[2] E. K. Gamstedt, M. Skrifvars, T. K. Jacobsen, and R. Pyrz. Synthesis of unsaturated polyesters for improved interfacial strength in carbon fibre composites. *Composites Part A: Applied Science and Manufacturing*, 33(9):1239–1252, 2002.

[3] S&P Clever Reinforcement. Vorgespannte Systeme: Verstärkung Eisenbahnbrücke - Aabachbrücke - Lachen, Switzerland. Technical report, 2020.

[4] S&P Clever Reinforcement. C-Laminates. Technical report, Elvas, Portugal, 2021.

[5] Amar K Mohanty, Singaravelu Vivekanandhan, Jean-Mathieu Pin, and Manjusri Misra. Composites from renewable and sustainable resources: Challenges and innovations. *Science*, 362(6414):536–542, 2018.

[6] Omar Faruk, Andrzej K Bledzki, Hans-Peter Fink, and Mohini Sain. Biocomposites reinforced with natural fibers: 2000–2010. *Progress in Polymer Science*, 37(11):1552–1596, 2012.

[7] M P Staiger and N Tucher. Natural-fibre composites in structural applications. In Kim Louise

Pickering, editor, *Woodhead Publishing Series in Composites Science and Engineering*, chapter 8, pages 269–300. Woodhead Publishing, 1st edition, 2008.

[8] Kin-tak Lau, Pui-yan Hung, Min-Hao Zhu, and David Hui. Properties of natural fibre composites for structural engineering applications. *Composites Part B: Engineering*, 136:222–233, 2018.

[9] Paul Wambua, Jan Ivens, and Ignaas Verpoest. Natural fibres: can they replace glass in fibre reinforced plastics? *Composites Science and Technology*, 63(9):1259–1264, 2003.

[10] Andrea Fernández, Marcello Santangelo-Muro, Juan P Fernández-Blázquez, Cláudio S Lopes, and Jon M Molina-Aldareguia. Processing and properties of long recycled-carbon-fibre reinforced polypropylene. *Composites Part B: Engineering*, 211:108653, 2021.

[11] Robert A Witik, Remy Teuscher, Véronique Michaud, Christian Ludwig, and Jan-Anders E Manson. Carbon fibre reinforced composite waste: An environmental assessment of recycling, energy recovery and landfilling. *Composites Part A: Applied Science and Manufacturing*, 49:89–99, 2013.

[12] Hamza Qazi, Richard Lin, and Krishnan Jayaraman. Fibre structure preservation in composite recycling using thermolysis process. *Resources, Conservation and Recycling*, 169:105482, 2021.

[13] Andrea Dorigato. Recycling of thermosetting composites for wind blade application. *Advanced Industrial and Engineering Polymer Research*, 4(2):116–132, 2021.

[14] Hess Kristen, Hinchcliffe Sean, and Srubar Wil V. Biobased FRPs for Retrofit and Rehabilitation of Civil Infrastructure, 2022.

[15] J. Jefferson Andrew and H. N. Dhakal. Sustainable biobased composites for advanced applications: recent trends and future opportunities – A critical review. *Composites Part C: Open Access*, 7:100220, 2022.

[16] Sripathi Dev Sharma Kopparthy and Anil N Netravali. Review: Green composites for structural applications. *Composites Part C: Open Access*, 6:100169, 2021.

[17] Boon Peng Chang, Amar K Mohanty, and Manjusri Misra. Studies on durability of sustainable biobased composites: a review. *RSC Advances*, 10(31):17955–17999, 2020.

[18] Michael P M Dicker, Peter F Duckworth, Anna B Baker, Guillaume Francois, Mark K Hazzard, and Paul M Weaver. Green composites: A review of material attributes and complementary applications. *Composites Part A: Applied Science and Manufacturing*, 56:280–289, 2014.

[19] Aaron T. Michel and Sarah L. Billington. Nonlinear Constitutive Model for Anisotropic Biobased Composite Materials. *Journal of Engineering Mechanics*, 140(11):4014083, 2014.

[20] Amod A Ogale, Meng Zhang, and Jing Jin. Recent advances in carbon fibers derived from biobased precursors. *Journal of Applied Polymer Science*, 133(45), 2016.

[21] Kirill Minchenkov, Alexander Vedernikov, Alexander Safonov, and Iskander Akhatov. Thermoplastic Pultrusion: A Review. *Polymers*, 13(2):36, 2021.

[22] Mak Kenneth and Fam Amir. Fatigue Performance of Furfuryl Alcohol Resin Fiber-Reinforced Polymer for Structural Rehabilitation. *Journal of Composites for Construction*, 24(3):4020012, 2020.

[23] Mohd Hafiz Zamri, Hazizan Md Akil, Azhar Abu Bakar, Zainal Arifin Mohd Ishak, and Le-

ong Wei Cheng. Effect of water absorption on pultruded jute/glass fiber-reinforced unsaturated polyester hybrid composites. *Journal of Composite Materials*, 46(1):51–61, 2011.

[24] Chin-Hsing Chen and I-Ken Chen. The unidirectional glass fiber reinforced furfuryl alcohol for pultrusion. II. Correlation of processing parameters for optimizing the process. *Journal of Applied Polymer Science*, 119(3):1788–1796, 2011.

[25] Xi Peng, Mizi Fan, John Hartley, and Majeed Al-Zubaidy. Properties of natural fiber composites made by pultrusion process. *Journal of Composite Materials*, 46(2):237–246, 2011.

[26] Chin-Hsing Chen and I-Ken Chen. The unidirectional glass fiber reinforced furfuryl alcohol for pultrusion. I. Process feasibility and kinetic analysis. *Polymer Composites*, 29(6):611–616, 2008.

[27] Hamed Velis Hedayati, Mohammad Golzar, and Omid Yousefzade. Composites based on HDPE, jute fiber, wood, and thermoplastic starch in tubular pultrusion die: The correlation between mechanical performance and microstructure. *Advanecs in Polymer Technology*, 37:3483–3491, 2018.

[28] John J. Palmese, Giuseppe R.; Yadav, Santosh K.; LaScala. Renewable Highly Biobased Polybenzoxazine Thermosets for Composite Appications, 2020.

[29] John J. Palmese, Giuseppe R.; Yadav, Santosh K.; LaScala. Renewable furan based polyimides for composite applications, 2018.

[30] Jens Erdmann. Bio-based carbon fibers – high-performance and sustainability for light-weight applications, 2019.

[31] N Saba, M Jawaid, M T Paridah, and O Y Al-othman. A review on flammability of epoxy polymer, cellulosic and non-cellulosic fiber reinforced epoxy composites. *Polymers for Advanced Technologies*, 27(5):577–590, 2016.

[32] Ellen Lackey, James G Vaughan, Kapil Inamdar, and Brittany Hancock. Statistical Characterization of Pultruded Composites with Natural Fiber Reinforcements – Part A: Fabrication. *Journal of Natural Fibers*, 4(4):73–87, 2008.

[33] James L Thomason and Jose L Rudeiros-Fernández. Thermal degradation behaviour of natural fibres at thermoplastic composite processing temperatures. *Polymer Degradation and Stability*, 188:109594, 2021.

[34] N K Kim, S Dutta, and D Bhattacharyya. A review of flammability of natural fibre reinforced polymeric composites. *Composites Science and Technology*, 162:64–78, 2018.

[35] M. W. Chai, S. Bickerton, D. Bhattacharyya, and R. Das. Influence of natural fibre reinforcements on the flammability of bio-derived composite materials. *Composites Part B: Engineering*, 43(7):2867–2874, 2012.

[36] K Mayandi, N Rajini, M Manojprabhakar, Suchart Siengchin, and Nadir Ayrilmis. Recent studies on durability of natural/synthetic fiber reinforced hybrid polymer composites. In Mohammad Jawaid, Mohamed Thariq, Naheed B T Durability Saba Fibre-Reinforced Composites and Hybrid Composites, and Life Prediction in Biocomposites, editors, *Woodhead Publishing Series in Composites Science and Engineering*, chapter 1, pages 1–13. Woodhead Publishing, 2019.

[37] Ehsan Bari, Jeffrey J. Morrell, and Asghar Sistani. Durability of natural/synthetic/biomass

fiber–based polymeric composites: Laboratory and field tests. In Mohammad Jawaid, Mohamed Thariq, and Naheed Saba, editors, *Durability and Life Prediction in Biocomposites, Fibre-Reinforced Composites and Hybrid Composites*, chapter 2, pages 15–26. Woodhead Publishing Series in Composites Science and Engineering, 2019.

[38] Michael George, Michael Chae, and David C. Bressler. Composite materials with bast fibres: Structural, technical, and environmental properties. *Progress in Materials Science*, 83:1–23, 2016.

[39] Darshil U Shah. Natural fibre composites: Comprehensive Ashby-type materials selection charts. *Materials & Design*, 62:21–31, 2014.

[40] Alessandro Gandini and Talita M Lacerda. From monomers to polymers from renewable resources: Recent advances. *Progress in Polymer Science*, 48:1–39, 2015.

[41] Paulien F. Harmsen, Martijn M. Hackmann, and Harriette L. Bos. Green building blocks for bio-based plastics. *Biofuels, Bioproducts and Biorefining*, 8(3):306–324, 2014.

[42] Jan-Georg Rosenboom, Robert Langer, and Giovanni Traverso. Bioplastics for a circular economy. *Nature Reviews Materials*, 7:117–137, 2022.

[43] U K Vaidya and K K Chawla. Processing of fibre reinforced thermoplastic composites. *International Materials Reviews*, 53(4):185–218, 2008.

[44] Winifred Obande, Conchúr M Ó Brádaigh, and Dipa Ray. Continuous fibre-reinforced thermoplastic acrylic-matrix composites prepared by liquid resin infusion – A review. *Composites Part B: Engineering*, 215:108771, 2021.

[45] Rui Zhang, Tianyun Li, Houbo Zhou, Huahua Huang, and Yongming Chen. Biobased transparent polyimides with excellent solubility and mechanical properties using myo-inositol derived diamines. *Reactive and Functional Polymers*, 128:91–96, 2018.

[46] Nassibeh Hosseini, Dean C. Webster, and Chad Ulven. Advanced biocomposite from highly functional methacrylated epoxidized sucrose soyate (MAESS) resin derived from vegetable oil and fiberglass fabric for composite applications. *European Polymer Journal*, 79:63–71, 2016.

[47] Aniruddha Nag, Mohammad Asif Ali, Makoto Watanabe, Maninder Singh, Kittima Amornwachirabodee, Shunsuke Kato, Tetsu Mitsumata, Kenji Takada, and Tatsuo Kaneko. High-performance poly(benzoxazole/benzimidazole) bio-based plastics with ultra-low dielectric constant from 3-amino-4-hydroxybenzoic acid. *Polymer Degradation and Stability*, 162:29–35, 2019.

[48] Kreisler S. Lau. High-Performance Polyimides and High Temperature Resistant Polymers. In Hanna Dodiuk and Sidney H. B. T. Goodman, editors, *Handbook of Thermoset Plastics*, chapter 10, pages 297–424. William Andrew Publishing, Boston, 3 edition, 2014.

[49] Jacek Andrzejewski, Amar K. Mohanty, and Manjusri Misra. Development of hybrid composites reinforced with biocarbon/carbon fiber system. The comparative study for PC, ABS and PC/ABS based materials. *Composites Part B: Engineering*, 200:108319, 2020.

[50] Noureddine Ramdani, Hamza Zaimeche, and Mehdi Derradji. Biobased thermally-stable aromatic cyanate ester thermosets: A review. *Reactive and Functional Polymers*, 168:105037, 2021.

[51] M. H. Irfan. *Chemistry and Technology of Thermosetting Polymers in Construction Applications*.

Springer Science+Business Media, Dordrecht, 1 edition, 1998.

[52] Frank R. Jones. Unsaturated Polyester Resins. In Marianne Gilbert, editor, *Brydson's Plastics Materials*, chapter 26, pages 743–772. Butterworth-Heinemann, 8 edition, 2017.

[53] Zhenyu Wang, Huijun Guo, Hang Zhou, Xinfeng Ouyang, Di Jiang, Jianhua Li, Qipeng Guo, Jun Tang, and Chuncai Yang. Effect of the Chain Structure of Self-Emulsifying Polyester Sizing Agent on ILSS of Carbon Fiber/Unsaturated Polyester Resin Composites. *Polymers*, 11(9), 2019.

[54] Abdelhak, Benaoum; Noureddine, Mahmoudi; Hacen, Mahmoudi. Improvement of the Interfacial Adhesion Between Fiber and Matrix. *Mechanics and Mechanical Engineering*, 22(4):885–894, 2020.

[55] Zijian Wu, Hongyu Cui, Lei Chen, Dawei Jiang, Ling Weng, Yingyi Ma, Xuejiao Li, Xiaohong Zhang, Hu Liu, Ning Wang, Jiaoxia Zhang, Yong Ma, Mingyan Zhang, Yudong Huang, and Zhanhu Guo. Interfacially reinforced unsaturated polyester carbon fiber composites with a vinyl ester-carbon nanotubes sizing agent. *Composites Science and Technology*, 164:195–203, 2018.

[56] Angela Daniela La Rosa, Giuseppe Recca, John Summerscales, Alberta Latteri, Gulia Cozzo, and Gianluca Cicala. Bio-based versus traditional polymer composites. A life cycle assessment perspective. *Journal of Cleaner Production*, 74:135–144, 2014.

[57] Juan P. Correa, Juan M Montalvo-Navarrete, and Miguel A Hidalgo-Salazar. Carbon footprint considerations for biocomposite materials for sustainable products: A review. *Journal of Cleaner Production*, 208:785–794, 2019.

[58] Amy Fitzgerald, Will Proud, Ali Kandemir, Richard J. Murphy, David A. Jesson, Richard S. Trask, Ian Hamerton, and Marco L. Longana. A Life Cycle Engineering Perspective on Biocomposites as a Solution for a Sustainable Recovery. *Sustainability*, 13(3), 2021.

[59] David Ayre. Technology advancing polymers and polymer composites towards sustainability: A review. *Current Opinion in Green and Sustainable Chemistry*, 13:108–112, 2018.

[60] C C M Ma, M S Yn, J L Han, C J Chang, and H D Wu. Pultruded fibre-reinforced furfuryl alcohol resin composites: 1. Process feasibility study. *Composites Manufacturing*, 6(1):45–52, 1995.

[61] C C M Ma, M S Yn, J L Han, C J Chang, and H D Wu. Pultruded fibre-reinforced furfuryl alcohol resin composites: 2. Static, dynamic mechanical and thermal properties. *Composites Manufacturing*, 6(1):53–58, 1995.

[62] SSUCHY. Sustainable structural and multifunctional biocomposites from hybrid natural fibres and bio-based polymers. Technical report, European Commission, 2022.

[63] Ecoxy. Bio-based recyclable, reshapable and repairable (3R) fibre-reinforced EpOXY composites for automotive and construction sectors. Technical report, European Commission, 2020.

[64] Matteo Andrea Lucherelli, Antoine Duval, and Luc Avérous. Biobased vitrimers: Towards sustainable and adaptable performing polymer materials. *Progress in Polymer Science*, 127:101515, 2022.

[65] Balaji Krishnakumar, Andrea Pucci, Prakash P Wadgaonkar, Indresh Kumar, Wolfgang H

Binder, and Sravendra Rana. Vitrimers based on bio-derived chemicals: Overview and future prospects. *Chemical Engineering Journal*, page 133261, 2021.

[66] Jie Zheng, Zhuang Mao Png, Shi Hoe Ng, Guo Xiong Tham, Enyi Ye, Shermin S. Goh, Xian Jun Loh, and Zibiao Li. Vitrimers: Current research trends and their emerging applications. *Materials Today*, 51:586–625, 2021.

[67] Yang Yang, Yanshuang Xu, Yan Ji, and Yen Wei. Functional epoxy vitrimers and composites. *Progress in Materials Science*, 120:100710, 2021.

[68] Xinxin Yang, Lizhen Guo, Xu Xu, Shibin Shang, and He Liu. A fully bio-based epoxy vitrimer: Self-healing, triple-shape memory and reprocessing triggered by dynamic covalent bond exchange. *Materials & Design*, 186:108248, 2020.

[69] Mikihiro Hayashi. Versatile functionalization of polymeric soft materials by implanting various types of dynamic cross-links. *Polymer Journal*, 53(7):779–788, 2021.

[70] Ibon Aranberri, Maite Landa, Edurne Elorza, Asier M Salaberria, and Alaitz Rekondo. Thermoformable and recyclable CFRP pultruded profile manufactured from an epoxy vitrimer. *Polymer Testing*, 93:106931, 2021.

[71] Hafeezullah Memon, Yi Wei, and Chengyan Zhu. Recyclable and reformable epoxy resins based on dynamic covalent bonds – Present, past, and future. *Polymer Testing*, 105:107420, 2022.

[72] Doo Hun Kim, Ayeong Yu, and Munju Goh. Oxidative chemical depolymerization of thermoset epoxy resin for green recycling. *Journal of Industrial and Engineering Chemistry*, 96:76–81, 2021.

[73] Carlos A Navarro, Yijia Ma, Katelyn H Michael, Hanna M Breunig, Steven R Nutt, and Travis J Williams. Catalytic, aerobic depolymerization of epoxy thermoset composites. *Green Chemistry*, 23(17):6356–6360, 2021.

[74] Yu-Yao Liu, Gan-Lin Liu, Yi-Dong Li, Yunxuan Weng, and Jian-Bing Zeng. Biobased High-Performance Epoxy Vitrimer with UV Shielding for Recyclable Carbon Fiber Reinforced Composites. *ACS Sustainable Chemistry & Engineering*, 9(12):4638–4647, mar 2021.

[75] Wouter Post, Arijana Susa, Rolf Blaauw, Karin Molenveld, and Rutger J I Knoop. A Review on the Potential and Limitations of Recyclable Thermosets for Structural Applications. *Polymer Reviews*, 60(2):359–388, apr 2020.

[76] Soraia Pimenta and Silvestre T Pinho. Recycling carbon fibre reinforced polymers for structural applications: Technology review and market outlook. *Waste Management*, 31(2):378–392, 2011.

[77] Mateus A. Hofmann, Abu T. Shahid, Mário A. Garrido, Maria J. Ferreira, João R. Correia, and João C. Bordado. Bio-based thermosetting polyester resin for high-performance applications. *ACS Sustainable Chemistry & Engineering*, Accepted(Manuscript ID: sc-2021-069697.R1), 2022.

[78] Mateus A. Hofmann, Mário Garrido, João R. Correia, and João C. Bordado. Development of high-performance biobased thermoset polyester using renewable building blocks from isosorbide, 1,3-propanediol, and fumaric acid. *Journal of Applied Polymer Science*, Submitted(Manuscript ID: app.20220135), 2022.

[79] ISO 1172. Textile-glass-reinforced plastics - Prepregs, moulding compounds and laminates - Determination of the textile-glass and mineral-filler content - Calcination methods, 1996.

[80] ASTM D2583. Standard Test Method for Indentation Hardness of Rigid Plastics by Means of a Barcol Impressor, 2013.

[81] ISO 527. Plastics - Determination of tensile properties - Part 5: Test conditions for unidirectional fibre-reinforced plastic composites, 2009.

[82] ASTM E1640-09. Standard test method for assignment of the glass transition temperature by dynamic mechanical analysis., 2009.

[83] Chen-Chi M. Ma. Process for pultruding fiber reinforced furan composites, 1996. `https://patents.google.com/patent/US5587034A/en`.

[84] Wen-cheng Ma, Chen-Chi M.; Shih. Process for pultruding fiber reinforced phenolic resin products, 1988. `https://patents.google.com/patent/US4873128`.

Part IV

Conclusions and perspectives

Chapter 8

Conclusions and perspectives

8.1 Conclusions

8.1.1 General remarks

The need to increase the sustainability of the plastics and fibre-polymer composites materials is a topic that has recently gained more attention. In fact, there is a demand from society for the development of innovative products with lower environmental impact, which can replace their counterparts derived from non-renewable sources. In this respect, some bio-based thermoplastic alternatives have been successfully developed. However, fibre-polymer composites – for structural applications in civil engineering – still lack thermoset matrices that provide the best balance between (i) sustainability, (ii) performance, and (iii) processing properties, enabling the use of current large-scale manufacturing techniques for high-performance components, namely vacuum infusion and pultrusion.

The primary research efforts regarding bio-based thermosets have focused on replacing (partially or totally) petroleum-derived monomers used in the main chain synthesis (pre-polymer) with renewable alternatives comprising the highest possible bio-content. This approach is similar to that adopted for the development of bio-based thermoplastics, particularly addressed to packaging an consumer product applications. However, thermoset polymers used in the composites industry are constituted by linear chains that need to be incorporated (diluted) into reactive monomers – typically low viscosity, toxic, petroleum derivatives, such as styrene – are used to decrease the resin (matrix) viscosity to ensure adequate impregnation of reinforcing fibres. This feature constitutes a constraint on the development of the linear chains suitable for bio-based thermosets; in fact, these linear chains must offer compatible functionality to ensure chain growth and guarantee its crosslinking with the reactive monomer.

In this context, a series of challenges that need to be overcome were found both in the literature and in the market of available bio-based thermoset resins. To the best of the author's knowledge, the bio-based thermoset resins presently available in the market that would have the potential to be used as a matrix in the fabrication of fibre-polymer composites for civil engineering structural applications still have low bio-contents, at most 30-35%.

Among these technical issues, whose resolution is decisive for the widespread acceptance of more sustainable fibre-polymer composites in civil engineering applications, the following particularly relevant needs were identified:

- development of a high-performance bio-based thermoset resin with a higher bio-content than those currently reported in the literature or available in the market, having adequate viscosity for impregnation of reinforcing fibres;
- evaluation of the processing properties of these bio-based resins in the production of prototypes of fibre-polymer composite components to validate their potential use at an industrial scale;
- characterisation of the properties of these materials (resins and composites) allowing for the production of more sustainable fibre-polymer composite structures.

In this context, the main objective of the work developed in this thesis was to contribute to the advancement in the development of more sustainable thermoset resins and fibre-polymer composites for civil engineering structural applications. Consequently, the study focused on the following main aspects:

- the design and synthesis of bio-based unsaturated polyester resins with high mechanical and thermomechanical performance;
- the production of fibre-polymer composites by vacuum infusion with one of the resin formulations developed in the thesis combined with synthetic glass fibres;
- the validation in an industrial environment of a prototype produced by pultrusion with one of the resin formulations developed in the thesis combined with synthetic carbon fibres;
- characterisation of the processing, mechanical and thermomechanical properties of the resins and their respective composites.

Globally, the objectives initially defined for developing the research were fulfilled. Therefore, the main conclusion drawn within the scope of this thesis is that, from a technical point of view, bio-based unsaturated polyester resins can potentially compete with their petroleum-derived counterparts to manufacture fibre-polymer composites intended for structural civil engineering applications. Specific conclusions and contributions to state of the art on the aforementioned research topics are presented in the following sections. Additionally, based on the experience in the development of bio-based composites acquired in this study, some additional considerations are made about potential alternatives to gradually increase the sustainability of the composites.

8.1.2 Synthesis of bio-based unsaturated polyester resins

The resins developed in this thesis were formulated based on a similar approach to those used in the development of bio-based thermoplastics, *i.e.*, replacing petroleum-based monomers (diacids and diols) – used in the synthesis of the main chain – with renewable counterparts. For this, a fine selection of these raw materials was carried out from a literature review. As a result, some of the main top-value added chemicals and monomers – compatible with the synthesis of unsaturated polyester – were selected and used: isosorbide 1,3-propanediol, and 2,5-furandicarboxylic acid. In addition, bio-based fumaric acid was used to provide the prepolymer with double bonds for further crosslinking with the reactive monomer (diluent) in the curing process.

In this thesis, bio-based prepolymers were synthesised from a catalysed bulk polycondensation reaction under a 10% excess of glycol over diacids. In this regard, the catalyst added to the mixture promoted reactions with residence time in the reactor between 6 and 8 hours, for a target degree of polymerisation and viscosity. Consequently, the prepolymers obtained were polyester with main chains consisting of few repeating units (∼6-8), which can be called oligoesters.

Subsequently, the prepolymers obtained were diluted in a mixture of reactive diluents. Such a mixture consists of a lower concentration of styrene (approximately 50% lower) when compared to conventional unsaturated polyester resins derived from petroleum, given its mixture in equal parts with 2-hydroxyethyl methacrylate. Finally, it is worth referring that the low degree of polymerisation oligoesters obtained from the syntheses may explain (in part) the fact that the viscosities are within an appropriate range for the composites manufacturing techniques tested here. In fact, a higher degree of polymerisation would have resulted in higher viscosities.

8.1.3 Using renewable raw materials

The building blocks synthesised in the course of this work showed distinct characteristics and properties, depending on the monomers selected for each formulation. The following specific conclusions were drawn for each of the raw material used in this study:

2,5-furandicarboxylic acid: the polyester prepolymers obtained from the FDCA-based building blocks were almost entirely bio-based (reaching 99.8% by weight). In addition, when FDCA entirely replaced PA in the prepolymer, the resulting cured unsaturated polyester resin exhibited the best thermomechanical properties, with the highest glass transition temperature. In fact, FDCA has been extensively studied to synthesise high-performance polymers, and its potential has been proven here in the UPRs obtained. However, it is worth referring that FDCA still has a very high cost, making this monomer uncompetitive in practice (in the short-term) for mainstream fibre-polymer composites – for example, in this thesis, the acquisition cost of FDCA, albeit at the laboratory scale, was about 30 times higher than its counterpart derived from oil, namely the phthalic anhydride.

Fumaric acid: an unsaturated acid that can be naturally formed or derived from agricultural by-products, such as sugarcane bagasse, was the key for incorporating bio-content among the other bio-based monomers tested in the thesis, with different formulations. As a result, formulations with higher crosslink density achieved higher mechanical and thermomechanical properties. The highest crosslink density was obtained from the highest ratio of fumaric acid (unsaturated) to saturated acids. As a consequence of the higher concentration of fumaric acid in the main chain, a successful balance between higher renewable content and high polymer performance was achieved for the respective formulations.

1,3-propanediol: Susterra® 1,3-propanediol used as a bio-based diol in the formulations tested in this thesis showed that, together with isosorbide concentrations, 1,3-propanediol is also a potential bio-based alternative for replacing ethylene glycol and propylene petroleum-derived glycol. 1,3-propanediol is commercially available today at a similar cost to its aforementioned non-bio-based counterparts. In this respect, unsaturated polyester resins comprising a partial content of 1,3-propanediol, together with other more rigid diols, are competitive in terms of cost as they have mechanical and thermomechanical properties that meet or exceed those of conventional resins, with the advantage of being more sustainable.

Dimer fatty acid: prepolymers synthesised from higher concentrations of dimerized fatty acid – namely, 25 mol% saturated acid concentration or PA:DFA = 0.75:0.25 – had too high viscosity, resulting in unsuitable resins for the impregnation of fibre reinforcements in the context of the vacuum infusion and pultrusion processes evaluated in this study. As a consequence of this limitation, prepolymers with ratios of 10% in mol of saturated acid concentration (PA:FA = 0.90:0.10) were evaluated, which were shown to have viscosities within typical ranges (820-860 cP) compared to their conventional counterparts. However, it was observed that the mechanical properties were lower – particularly the tensile strength and modulus of elasticity – when compared with the other bio-based resin formulations tested in this thesis (*cf.* Chapters 3 and 5). In fact, the long chains of DFA promoted higher flexibility in the unsaturated polyester main chain and may (in part) explain the lower mechanical properties of those formulations. The thermomechanical properties were also lower than the for the other bio-based resin formulations, but the differences were not statistically significant. Because of the properties presented by the UPRs formulated from DFA, it is possible to conclude that although the resins obtained had high bio-content, they are best suited for manufacturing components for applications where the structural requirements are less stringent. In addition, in spite of the limited mechanical properties of unsaturated polyester resins based on DFA, the supply chain of this raw material is potentially quite sustainable, given its origin (conifer tree $\rightarrow$ kraft pulp $\rightarrow$ crude taloil $\rightarrow$ DFA); thus it has a significant potential for use in fibre-polymer composites for construction.

Reactive diluents: all prepolymers synthesised in this thesis were incorporated with a mixture of reactive diluents comprising styrene and 2-hydroxyethyl methacrylate in equal parts. It is worth mentioning that the incorporation of the prepolymer with the mixture of reactive diluents showed that the total replacement of styrene by the alternative tested here (HEMA) is still impractical for the production of high-performance cured thermosets (since short crosslinks, specific of styrene are essential for the stiffness of the crosslinked structure).

8.1.4 Bio-based GFRP composites

Based on the results obtained from the different resin formulations, a bio-based unsaturated polyester resin developed in this thesis – namely, the UPR-D formulation (presented in Chapter 3) – was selected as a matrix for impregnating glass fibres in the production of bio-based GFRP composites by vacuum infusion. The criteria for its selection were aimed at achieving the best balance between sustainability, cost-competitiveness, mechanical, thermomechanical and processing properties compared to other formulations tested under the same conditions.

Two equivalent GFRP composite laminates were produced with the same dimensions, one made with (i) the selected bio-based unsaturated polyester resin, and the other with (ii) a comparable commercial petroleum-derived unsaturated polyester resin. As a result, the following results are highlighted, regarding the manufacturing process and the properties of the resulting composites:

- The bio-based resin required approximately 50 minutes to impregnate the fibres along the entire length of the laminate (approximately 1 m), while the commercial resin required 14 minutes. These differences are explained by the different viscosities of the bio-based resin (800 cP) compared to its commercial counterpart (300 cP);
- The bio-based GFRP laminate showed slightly higher tensile strength and considerably higher compressive strength than its conventional counterpart; however, differences in the modulus of elasticity were statistically insignificant;
- The in-plane and interlaminar shear strengths were also higher in the bio-based GFRP composite, attesting the bio-based resin's ability to impregnate the glass fibre reinforcement and to provide adequate fibre-matrix adhesion in the cured product;
- Although the glass transition temperature of the bio-based GFRP composite was slightly lower than its conventional counterpart (about 10%), it still exceeded the threshold of 60 ℃, which enables its use in most civil structural applications.

8.1.5 Bio-based CFRP composites

As for the GFRP composite, the UPR-D unsaturated polyester resin (developed in Chapter 3) was also selected as an impregnation matrix for producing a CFRP prototype produced by the pultrusion process in an industrial environment, namely at the facilities of the partner company S&P Clever Reinforcement.

The production follow-up and the processing, mechanical and thermomechanical properties of the bio-based resin and the bio-based CFRP strip prototype were compared with a well-established product from the company's standard production, namely a CFRP strip produced with a conventional petroleum-derived vinyl ester resin.

The manufacturing by pultrusion of the bio-based CFRP strips represented one of the biggest challenges and achievements of this thesis, as it allowed to further validate the use (at an industrial scale) of the developed bio-based unsaturated polyester resin, thus confirming that it offers a potential alternative to the petroleum-derived vinyl ester resin currently used by the above-mentioned company.

In this context, it is worth mentioning that the resin (initially produced in the laboratory) had to undergo viscosity adjustments during the preliminary phase of the pultrusion tests, since it had been stored for approximately eight weeks. Although this resin had been stored in dark flasks under an environment with controlled temperature and humidity, an increase in viscosity was observed after this storage period, requiring the addition of 10 wt.% of styrene concerning the total weight of the resin.

After this additional dilution, the resin was placed in an impregnation tank; some adjustments were also introduced in the pultrusion line to guarantee the straightness of the composite strips, and a few procedures were made aiming at a better impregnation of the fibres. After making these adjustments, the production process was successful, and around 300 meters of high-performance CFRP strips were produced using the bio-based unsaturated polyester resin developed in-house.

In the mechanical tests, the bio-based pultruded CFRP strips exhibited very similar (slightly higher) tensile strength than their conventional vinyl ester CFRP counterparts – approximately 2095 MPa *vs.* 1964 MPa, respectively. Likewise, the modulus of elasticity and tension at break were similar to those of the conventional CFRP strips. In addition, the bio-based pultruded CFRP strips exhibited a glass transition temperature that allows their use for service temperatures up to 58 °C.

8.2 Future developments

This section presents recommendations for future research, which basically fall into three main categories: (I) deepening some of the issues addressed in this thesis, (II) presenting alternative solutions to those studied here, and (III) identifying cross-cutting issues related to the topic of the thesis.

8.2.1 Issues regarding the bio-based resins developed here (I)

Concerning the improvement of the bio-based unsaturated polyester resins developed here, the following issues deserve further investigation:

- Study of the shelf-life of the bio-based unsaturated polyester resins. It is important to note that although radical inhibitors (namely, hydroquinone and toluhydroquinone) have been used in typical amounts – to avoid side reactions during synthesis and to prevent gelation after incorporation into the resin – at the time of opening the bottles of bio-based resins for use in pultrusion (after about eight weeks of storage), the resin showed a higher viscosity. The use of different reaction inhibitors – as well as their different concentrations – can promote a longer shelf-life;
- Alternative types and ratios of reactive diluents can be incorporated with the pre-polymers developed in this thesis. The main objective would be to make use of the already studied bio-based polyester main chains – mainly those with higher bio-content and with better properties, such as those based on FDCA – and to promote mechanical and thermomechanical improvements, as well as to introduce some additional bio-content to the resin, since some of these reactive monomers are bio-based. Furthermore, the production of bio-based resins free of toxic solvents should be pursued. Some examples of reactive monomers that can promote improvements in mechanical properties and T_g are short-chain acrylate-type or furan-based monomers;
- Development of unsaturated polyester resins based on lignin, which is a viable alternative for the synthesis of these resins with improved thermomechanical properties, especially at elevated temperature and under fire exposure, in relation to those developed here. This alternative is a relevant option, since lignin is one of the most abundant renewable materials in nature. Furthermore, lignin can be incorporated as a partial or almost total replacement of the diols tested herein in any of the formulations;
- New formulations of unsaturated polyester resins based on DFA should be tested, such as by introducing additional rigid blocks to the backbone, in order to minimise the resulting flexibility of the long-chain dimerized fatty acid.

8.2.2 Regarding alternative solutions (II)

With respect to the development of (i) new bio-based thermosetting resins, (ii) new fiber-polymer composites, and (iii) improvements in manufacturing techniques, the following issues warrant additional investigation:

- The development of GFRP composites using bio-based and photo-curable unsaturated polyester resins. For this, an ultraviolet die can be used in the pultrusion manufacturing process [1–3] to minimise the energy consumption spent in the conventional process. Some bio-based building blocks synthesised in this thesis can be used as a starting point;

- Design and experimental study of the vitrimerization of some of the bio-based unsaturated polyester resins developed here. This is a potential process to produce bio-based thermosetting resins capable of being reprocessed. A high-performance, bio-based thermosetting resin that is capable of being reprocessed could provide an even more relevant response to the demand for greener products and a more circular economy;
- The development of basalt fibre reinforced polymer (BFRP) composites, using some of the resin formulations tested here together with the appropriate types of sizing.

8.2.3 Other issues (III)

The following other issues related with the work developed in the present thesis are worth being investigated further:

- Some successful formulations tested here used ethylene glycol and other non-renewable monomers. However, the production of ethylene glycol from bioethylene is already a reality. Likewise, it is important to be aware of advances in the production of phthalic anhydride from renewable resources;
- Generally speaking, the shift from conventional thermosetting polymers to bio-based ones has a strong relationship with recent advances in biorefinery. Although this sector is relatively new when compared to the crude oil refinery, it has shown to be increasingly promising, given the demand for more sustainable products and energy sources; consequently, it is important to keep a close eye on its development, namely by assessing the potential of novel bio-based monomers, as well as taking advantage of the increasingly advantageous economies-of-scale that will continue to be achieved in this sector (*e.g.*, the cost of FDCA is expected to drop quite significantly in the coming years, as the increased demand and production should bring it closer to a commodity monomer status);
- The search for alternative raw materials that do not generate competition with the food industry;

The following other issues are worth being further investigated in terms of characterisation and evaluation:

- the work carried out in this thesis allowed to develop innovative fibre-polymer composites for structural applications. However, despite the positive results achieved in the thesis, the long-term behaviour of the composites still needs to be evaluated, especially under exposure to moisture and temperature (hygrothermal ageing), as well as to thermal and freeze-thaw cycles and UV radiation. In addition, evaluating the properties of bio-based unsaturated polyester resins subjected to these degradation agents will also provide relevant data about the potential performance of these composites for use in outdoor environments. Studies on the biodegradability of these bio-based composites are also relevant;

- life cycle assessment (LCA) of the composites developed herein is also relevant, considering the impacts generated from the extraction of raw materials to the manufacturing, exploration, and end-of-life phases of the different materials used in this study. Assessing the carbon footprint of fumaric acid (the major constituent of the resin), as well as of other renewable monomers used here (such as FDCA and isosorbide), is very relevant in this regard. Finally, these LCA studies should consider aspects such as gas emission, eutrophication, and other parameters regarding the environmental impacts of the bio-based resins and composites.

8.3 References

[1] Wenfang Shi and Bengt Rånby. Uv curing of composites based on modified unsaturated polyester. *Journal of Applied Polymer Science*, 51(6):1129–1139, 1994.

[2] Takashi Kanzaki. Pultrusion with cure by ultraviolet radiation, 1987. `https://patents.google.com/patent/US4861621A/en`.

[3] Iosu Tena, Aritz Esnaola, Mariasun Sarrionandia, Ibai Ulacia, J. Torre, and Jon Aurrekoetxea. Out of die ultraviolet cured pultrusion for automotive crash structures. *Composites Part B: Engineering*, 79:209–216, 2015.

Appendix

Appendix A

Prepolymer characterisation

A.1 Titration

Figure A.1 presents the titration procedures used for AN determination of the polyester prepolymers. The dicarboxylic acids and anhydrides used in the synthesis of the unsaturated polyesters were titrated with potassium hydroxide (KOH, 0.1 M) and phenolphthalein as titrant solution and indicator, respectively.

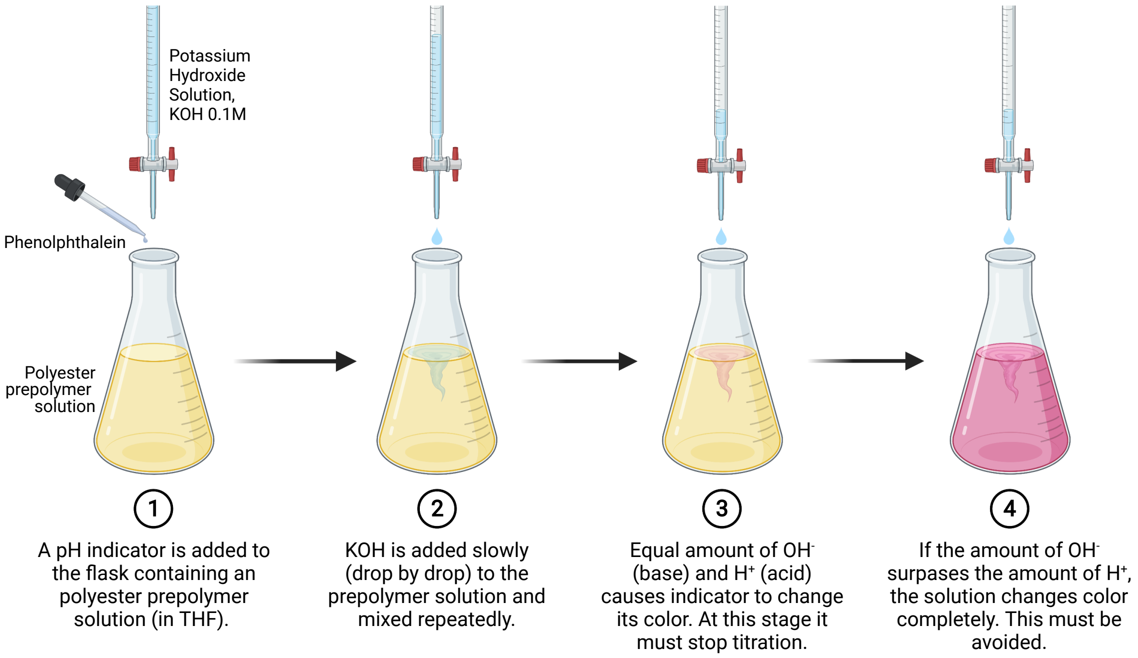

Figure A.1: Titration procedures for AN determination of the polyester prepolymers.

A.2 Kinetics

Commercial polyester resins for lamination of composites typically have acid numbers ranging from 25 to 50 mgKOH/g, whereas higher molecular weight isophthalic resins have acid numbers that range between 10 and 20 mgKOH/g. In acid-catalysed polyesterification systems, the following equation is considered for the rate of the reaction as a function of time,

$$-\frac{d[\mathrm{COOH}]}{dt} = [\mathrm{COOH}][\mathrm{OH}](k_3[\mathrm{COOH}] + k_{cat}[\mathrm{H}^+]) \tag{A.1}$$

where k_3 denotes a third-order rate constant for the uncatalysed reaction and k_{cat} is the rate constant for the catalysed process. By the definition of a catalyst, the $[\mathrm{H}^+]$ does not change throughout the course of the reaction and generally $k_{cat}[\mathrm{H}^+] \gg k_3[\mathrm{COOH}]$. As a result, Equation A.1 can be approximated by Equation A.2, in which the second-order rate constant k_2 is related to k_{cat} by the expression $k_2 = k_{cat}[\mathrm{H}^+]$:

$$-\frac{d[\mathrm{COOH}]}{dt} = k_2[\mathrm{COOH}][\mathrm{OH}] \tag{A.2}$$

Integration of Equation A.2 leads to:

$$\frac{1}{(1-p)} = k_2[\mathrm{COOH}]_0 t \tag{A.3}$$

Equation A.3 shows a dependence of the conversion on reaction time for a catalysed polyesterification, with the left side being the degree of polymerisation for balanced stoichiometric reactant ratios. However, in this study, an excess of glycol was used. Thus, the nonstoichiometric reactant ratios (r) were considered, resulting in $r = \mathrm{N_{COOH}}/\mathrm{N_{OH}} < 1$.

A.2.1 Conversion and degree of polymerisation

Tables A.1 and A.2 show the conversion (p) and the degree of polymerisation (X_n) from the AN values with the progress of the reaction.

Table A.1: Conversion (p) and degree of polymerization (X_n) from the AN values of the DFA-based polyester prepolymers.

Time	**AN (mgKOH/g)**			***p* (%)**			**X_n (a.u)**		
(min)	**UP-A**	**UP-B**	**UP-C**	**UP-A**	**UP-B**	**UP-C**	**UP-A**	**UP-B**	**UP-C**
0	477	452	457	0	0	0	1.00	1.00	1.00
180	72	70	64	85	84	86	5.11	4.99	5.4
240	62	63	57	87	86	87	5.68	5.42	5.82
300	59	58	54	88	87	88	5.91	5.74	6.08
360	55	54	48	88	88	89	6.17	6.03	6.57
420	55	52	43	88	88	91	6.18	6.19	7.03
480	47	44	-	90	90	-	6.82	6.92	-

Table A.2: Conversion (p) and degree of polymerization (X_n) from the AN values of the FDCA-based polyester prepolymers.

Time	**AN (mgKOH/g)**			***p* (%)**			**X_n (a.u)**		
(min)	**UP-A**	**UP-B**	**UP-C**	**UP-A**	**UP-B**	**UP-C**	**UP-A**	**UP-B**	**UP-C**
0	477	475	473	0	0	0	1.00	1.00	1.00
180	72	73	85	85	85	82	5.11	5.03	4.49
240	62	68	70	87	86	85	5.68	5.31	5.20
300	59	58	57	88	88	88	5.91	5.94	6.00
360	55	54	50	88	89	89	6.17	6.24	6.57
420	55	47	43	88	90	91	6.18	6.82	7.25
480	47	46	-	90	90	-	6.82	6.92	-

A.2.2 Theoretical molecular weights

Tables A.3, A.4, and A.5 show the nonstoichiometric reactant ratios and the theoretical molecular weights of the polyester prepolymers from the AN values.

Table A.3: Values used to estimate the theoretical molecular weights (in Chapter 3) from modified Carothers equation.

Sample	AN_0 **(mgKOH/g)**	r^a **(a.u)**	M_0^b **(Da)**
UP-A	482	0.9	191.5
UP-B	488	0.9	187.3
UP-C	491	0.9	184.3
UP-D	477	0.9	207.3
UP-E	480	0.9	201.2

[a] $r = N_{COOH}/N_{OH}$ is the nonstoichiometric reactant ratio

[b] Molecular weight of the structural (or repeating) unit, calculated from the weighted average of the components, as suggested by Sadler *et al.* [1]

Table A.4: Theoretical molecular weights from modified Carothers equation of the DFA-based polyester prepolymers.

Sample	AN_0 **(mgKOH/g)**	AN **(mgKOH/g)**	p **(%)**	r^a **(a.u)**	X_n **(a.u)**	M_0^b **(Da)**	M_n **(kDa)**
UP-A	477	47	90	0.9	6.82	216.2	1.48
UP-B	475	46	90	0.9	6.92	357.5	2.47
UP-C	473	43	91	0.9	7.03	357.5	2.53

[a] $r = N_{COOH}/N_{OH}$ is the nonstoichiometric reactant ratio

[b] Molecular weight of the structural (or repeating) unit, calculated from the weighted average of the components, as suggested by Sadler *et al.* [1]

Table A.5: Theoretical molecular weights from modified Carothers equation of the FDCA-based polyester prepolymers.

Sample	AN_0 **(mgKOH/g)**	AN **(mgKOH/g)**	p **(%)**	r^a **(a.u)**	X_n **(a.u)**	M_0^b **(Da)**	M_n **(kDa)**	M_w **(kDa)**
UP0	477	47	90	0.9	6.87	216.2	1480	2800
UP50	475	46	90	0.9	6.92	221.2	1530	2910
UP100	473	43	91	0.9	7.25	211.2	1530	2930

[a] $r = N_{COOH}/N_{OH}$ is the nonstoichiometric reactant ratio

[b] Molecular weight of the structural (or repeating) unit, calculated from the weighted average of the components, as suggested by Sadler *et al.* [1]

A.3 Molecular weight

Conventional calibration was done with three (vials) narrow polystyrene standards, where M_n (Da) was 266, 2140, 6320, 25000 for cap yellow, 435, 3260, 8420, 41200 for cap blue, and 1120, 4700, 14700, 59300 for cap black, according to a calibration table from PSS certificate of analysis information:

(`https://www.pss-polymer.com/fileadmin/pdf/product/pskitr1l-11.pdf`).

Figure A.2 shows the experimental procedures for the GPC tests.

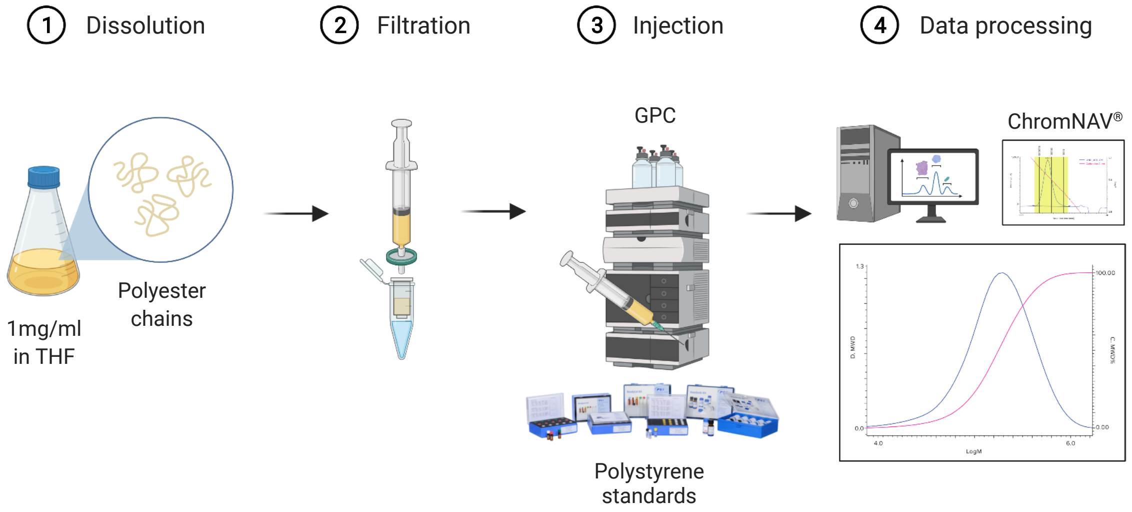

Figure A.2: GPC tests were performed in a JASCO™ equipment. Initially, polyester samples were dissolved in THF with approximate concentration of 1 mg/ml. After filtration, samples were injected into the system with columns filled of a monodisperse standard, namely, polystyrene crosslinked with divinylbenzene (gel). The data processing were performed by ChromNAV® software.

The signal as a function of retention time results obtained from the GPC tests as well as the molecular weight distribution curves of the prepolymers developed herein are presented next.

A.3.1 Prepolymers developed in Chapter 4

Figure A.3 shows the signal as a function of retention time results of the DFA-based unsaturated polyester prepolymers.

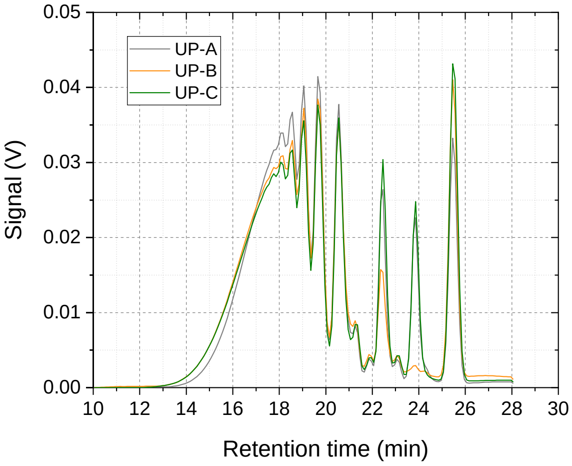

Figure A.3: GPC overlapping formulation curves of the DFA-based unsaturated polyester prepolymers.

Figure A.4 shows the molecular weight distribution curves of the DFA-based unsaturated polyester prepolymers.

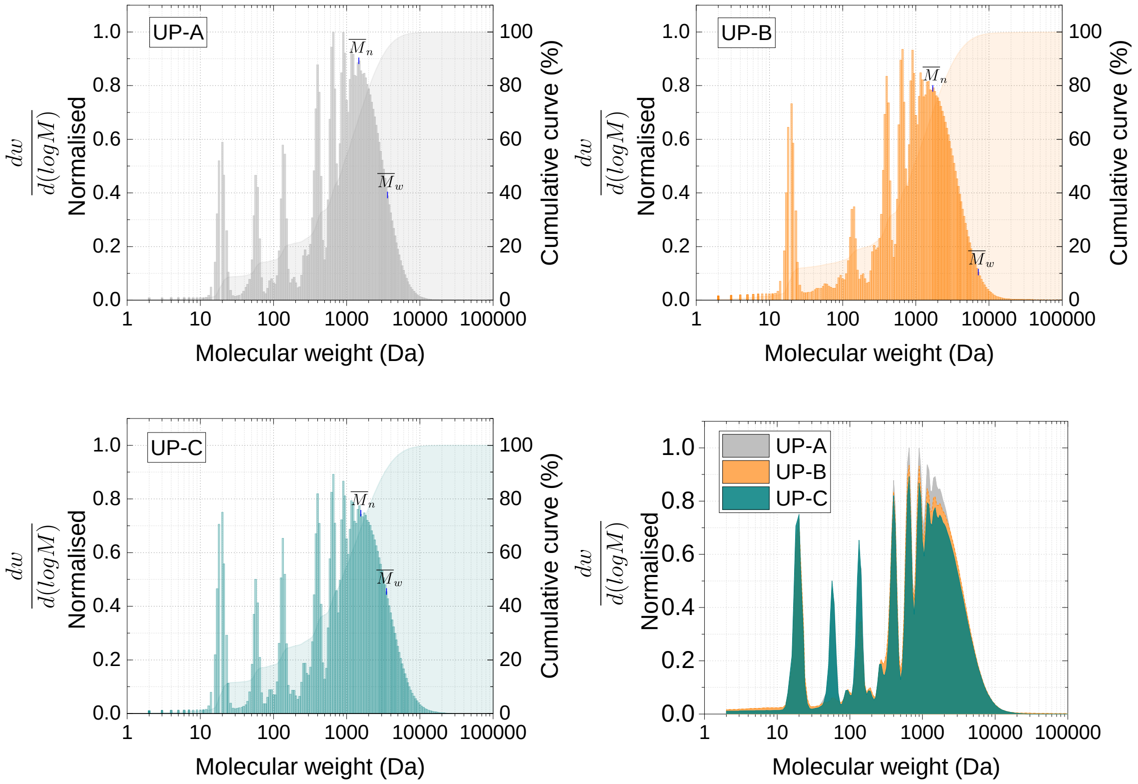

Figure A.4: Molecular weight distribution curves of the DFA-based unsaturated polyester prepolymers from the GPC analysis.

A.3.2 Prepolymers developed in Chapter 5

Figure A.5 shows the signal as a function of retention time results of the FDCA-based unsaturated polyester prepolymers.

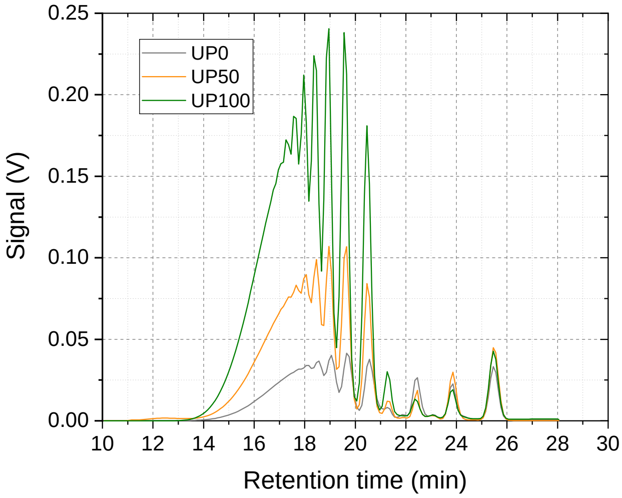

Figure A.5: GPC overlapping formulation curves of the FDCA-based unsaturated polyester prepolymers.

Figure A.6 shows the molecular weight distribution curves of the FDCA-based unsaturated polyester prepolymers.

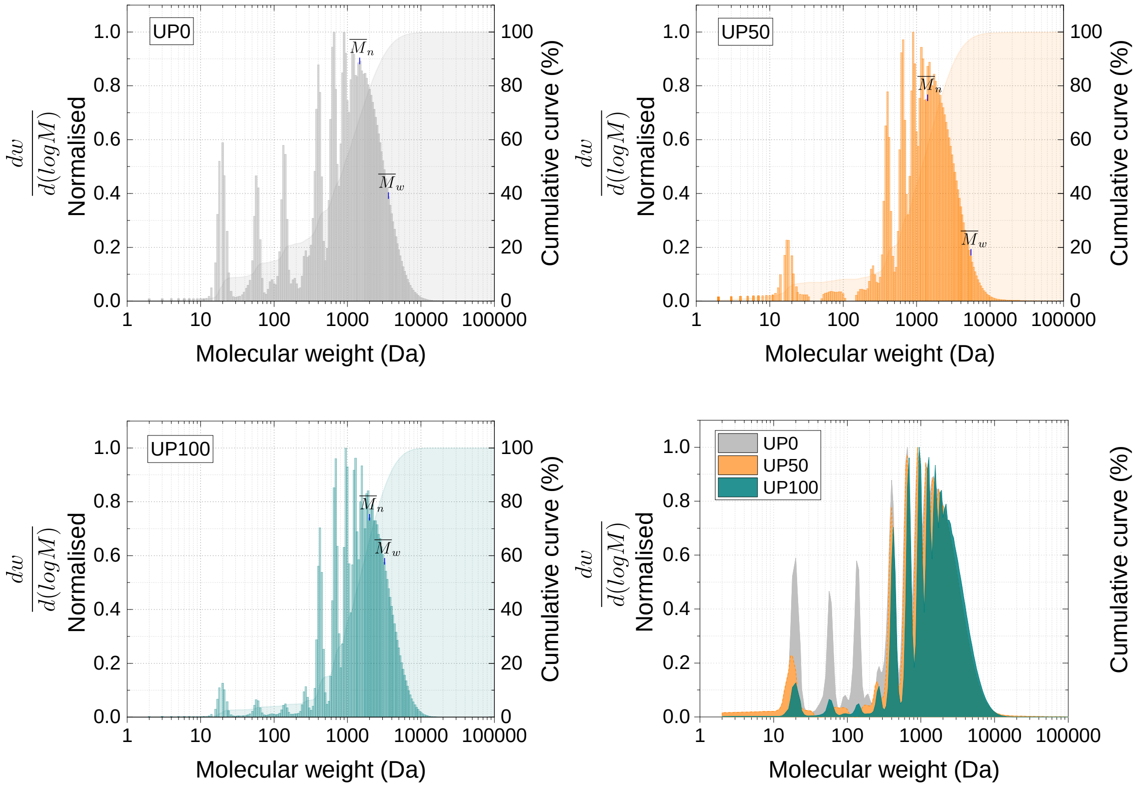

Figure A.6: Molecular weight distribution curves of the FDCA-based unsaturated polyester prepolymers from the GPC analysis.

A.4 Bio-based content

Tables A.6, A.7, and A.8 list the carbon content of the raw materials used in the synthesis of the polyester prepolymers.

Table A.6: Carbon content of raw materials used for the synthesis of bio-based polyester prepolymers developed in Chapter 3.

Monomer	**Formula**	M_w **(Da)**	C_w **(Da)**	C_w/M_w **(%)**
PA	$C_8H_4O_3$	148	96	64.9
FA	$C_4H_4O_4$	116	48	41.4
PDO	$C_3H_8O_2$	76	36	47.4
ISO	$C_6H_{10}O_4$	146	72	49.3
EG	$C_2H_6O_2$	62	24	38.7

Table A.7: Carbon content of raw materials used for the synthesis of DFA-based polyester prepolymers.

Monomer	**Formula**	M_w **(Da)**	C_w **(Da)**	C_w/M_w **(%)**
PA	$C_8H_4O_3$	148	96	64.9
DFA	$C_{36}H_{68}O_4$	564	72	12.8
FA	$C_4H_4O_4$	116	48	41.4
PDO	$C_3H_8O_2$	76	36	47.4
ISO	$C_6H_{10}O_4$	146	72	49.3

Table A.8: Carbon content of raw materials used for the synthesis of FDCA-based polyester prepolymers.

Monomer	**Formula**	M_w **(Da)**	C_w **(Da)**	C_w/M_w **(%)**
PA	$C_8H_4O_3$	148	96	64.9
FDCA	$C_6H_4O_5$	156	72	46.2
FA	$C_4H_4O_4$	116	48	41.4
PDO	$C_3H_8O_2$	76	36	47.4
ISO	$C_6H_{10}O_4$	146	72	49.3

Tables A.9 and A.10 indicate the biobased carbon and mass content of the polyester prepolymers regarding to groups (I) and (I) formulations developed in Chapter 3.

Table A.9: Bio-based carbon and mass content of the group (I) formulations developed in Chapter 3.

	UP-A		**UP-B**		**UP-C**	
Monomer	x_B **(%)**	m_B **(%)**	x_B **(%)**	m_B **(%)**	x_B **(%)**	m_B **(%)**
Phthalic anhydride	0	0	0	0	0	0
Fumaric acid	28.4	33.42	33.11	38.02	39.38	40.83
1,3-propanediol	11.76	12.09	12.19	12.22	13.59	12.31
Isosorbide	23.51	23.22	24.37	23.48	27.17	23.64
Ethylene glycol	0	0	0	0	0	0
Total	63.68	68.72	69.67	73.73	80.13	76.78

Table A.10: Bio-based carbon and mass content of the group (II) formulations developed in Chapter 3.

	UP-D		**UP-E**	
Monomer	x_B **(%)**	m_B **(%)**	x_B **(%)**	m_B **(%)**
Phthalic anhydride	0	0	0	0
Fumaric acid	31.82	37.18	34.67	39.93
1,3-propanediol	23.42	23.91	23.92	24.07
Isosorbide	23.42	22.96	23.92	23.11
Ethylene glycol	0	0	0	0
Total	78.66	84.05	82.51	87.11

Table A.11: Bio-based carbon and mass content of the DFA-based unsaturated polyester prepolymers.

	UP-A						**UP-B**						**UP-B**					
Monomer	W_i **(g)**	C_i **(g)**	x_{Bi} **(%)**	x_B **(%)**	m_{Bi} **(%)**	m_B **(%)**	W_i **(g)**	C_i **(g)**	x_{Bi} **(%)**	x_B **(%)**	m_{Bi} **(%)**	m_B **(%)**	W_i **(g)**	C_i **(g)**	x_{Bi} **(%)**	x_B **(%)**	m_{Bi} **(%)**	m_B **(%)**
PA	235.6	152.8	0	0	0	0	229.6	148.9	0	0	0	0	203.1	131.7	-	-	-	-
DFA	-	-	-	-	-	-	97.3	12.4	100	1.8	100	6.5	86.1	11	100	1.6	100	5.7
FA	557.7	230.8	100	31.8	100	37.2	503.3	208.3	100	30	100	33.6	534.1	221	100	32	100	35.6
PDO	358.6	169.9	100	23.4	100	23.9	339.8	161	100	23.2	100	22.7	343.4	162.7	100	23.5	100	22.9
ISO	344.4	169.8	100	23.4	100	23	326.3	160.9	100	23.2	100	21.8	329.8	162.6	100	23.5	100	22
Total	1500	725.3		78.1		84.1	1500	693.5		78.2		84.5	1500	691		99.7		86.2

Table A.12: Bio-based carbon and mass content of the FDCA-based unsaturated polyester prepolymers.

	UP0						**UP50**						**UP100**					
Monomer	W_i **(g)**	C_i **(g)**	x_{Bi} **(%)**	x_B **(%)**	m_{Bi} **(%)**	m_B **(%)**	W_i **(g)**	C_i **(g)**	x_{Bi} **(%)**	x_B **(%)**	m_{Bi} **(%)**	m_B **(%)**	W_i **(g)**	C_i **(g)**	x_{Bi} **(%)**	x_B **(%)**	m_{Bi} **(%)**	m_B **(%)**
PA	235.1	152.8	0	0	0	0	117.3	76.1	0	0	0	0	-	-	-	-	-	-
FDCA	-	-	-	-	-	-	123.6	57.1	100	8.1	100	8.2	246.2	113.6	100	16.7	100	16.4
FA	557.7	230.8	100	31.8	100	37.2	555.4	229.8	100	32.7	100	37	553.1	228.8	100	33.6	100	36.9
PDO	358.6	169.9	100	23.4	100	23.9	357.1	169.2	100	24.1	100	23.8	355.6	168.5	100	24.7	100	23.7
ISO	344.4	169.8	100	23.4	100	23	343	169.1	100	24	100	22.9	341.5	168.4	100	24.7	100	22.8
Total	1500	725.3		78.1		84.1	1500	703.2		88.9		91.9	1500	681.3		99.7		99.8

A.5 ^{1}H NMR study

^{1}H NMR spectra of the unsaturated (linear) polyester dissolved in acetone-d_6 were obtained using a Bruker Avance III a 500 MHz spectrometer equipped with a 5mm BBO resonance detection probe (see Figure A.7). The spectra were referenced using the solvent signals. The polyester prepolymers showed ^{1}H NMR peaks in agreement with the expected chemical shifts for individual constituents of the unsaturated polyesters.

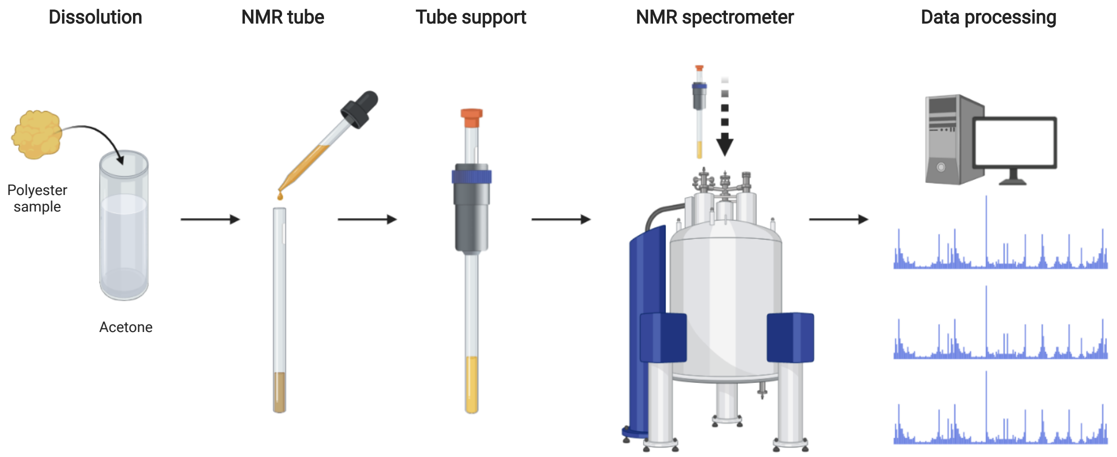

Figure A.7: NMR test procedures.

Figure A.8 presents ^{1}H NMR spectra of the DFA-based polyester prepolymers with the integration values.

a.

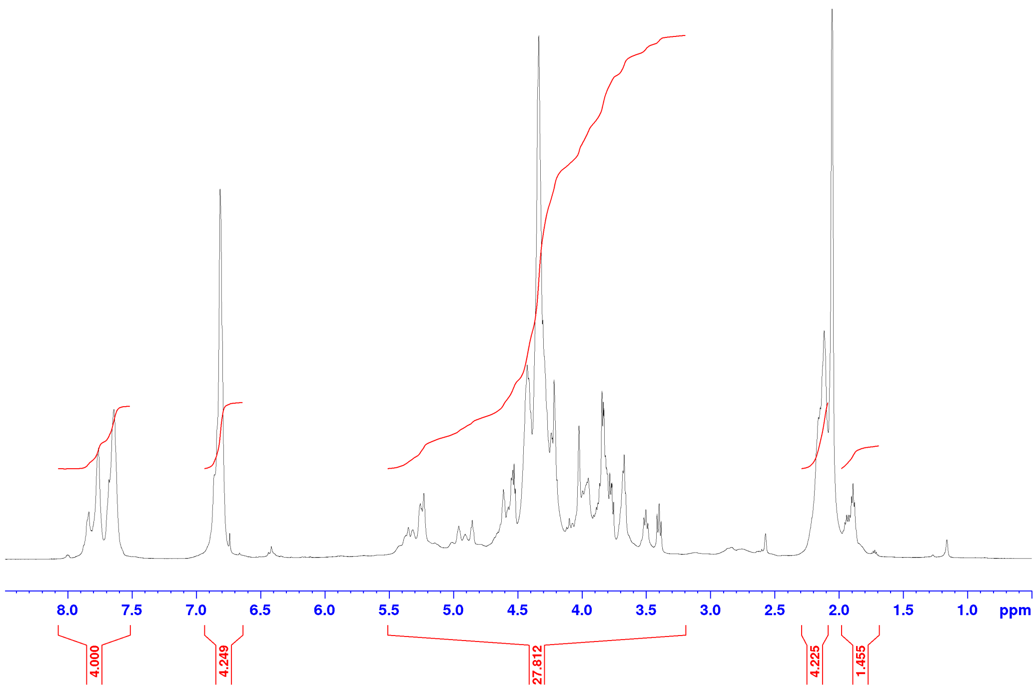

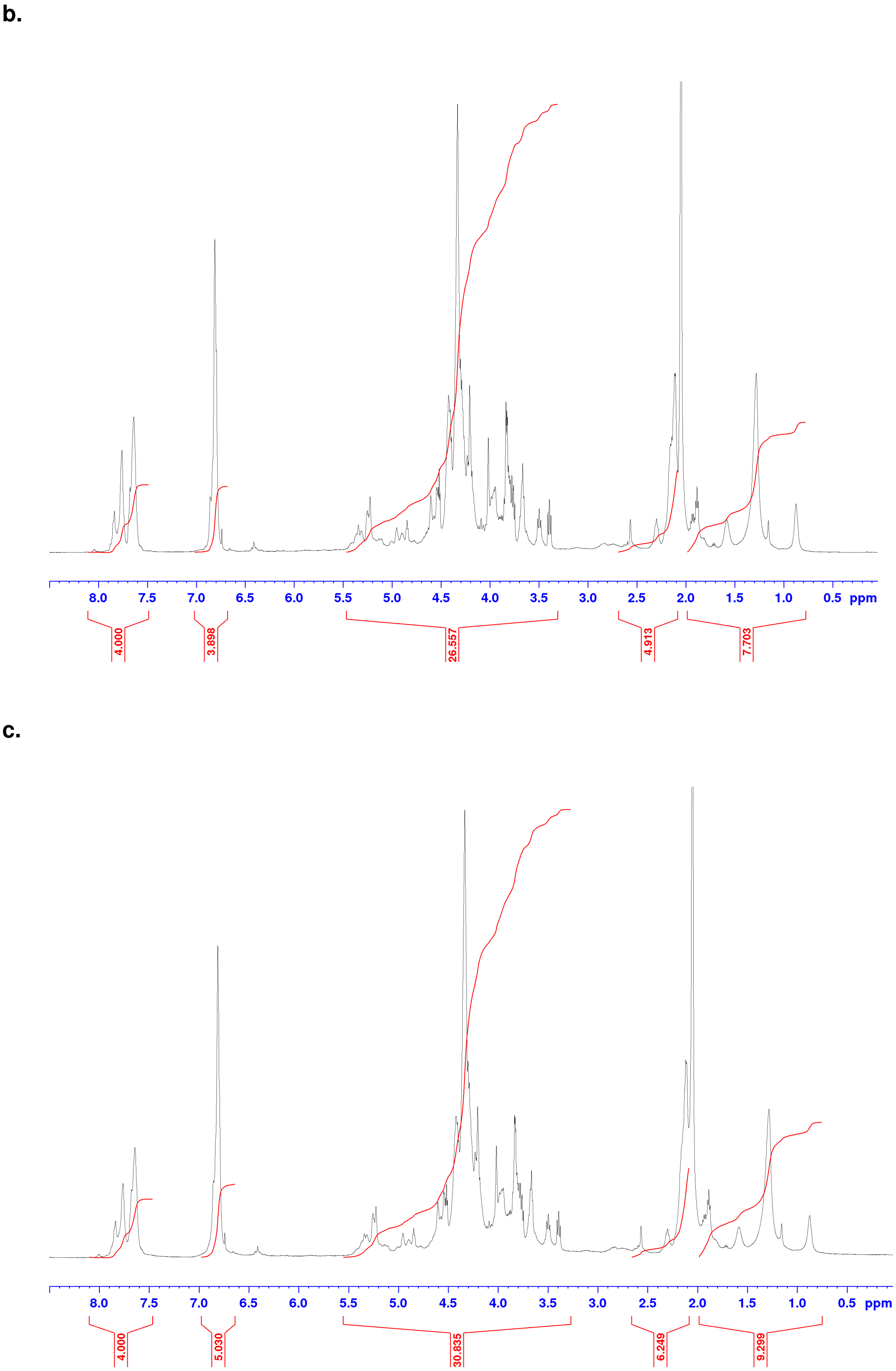

Figure A.8: ^{1}H NMR spectra of the DFA-based polyester prepolymers: **a.** UP-A; **b.** UP-B; and **c.** UP-C.

Figure A.9 presents ^{1}H NMR spectra of the FDCA-based polyester prepolymers with the integration values.

a.

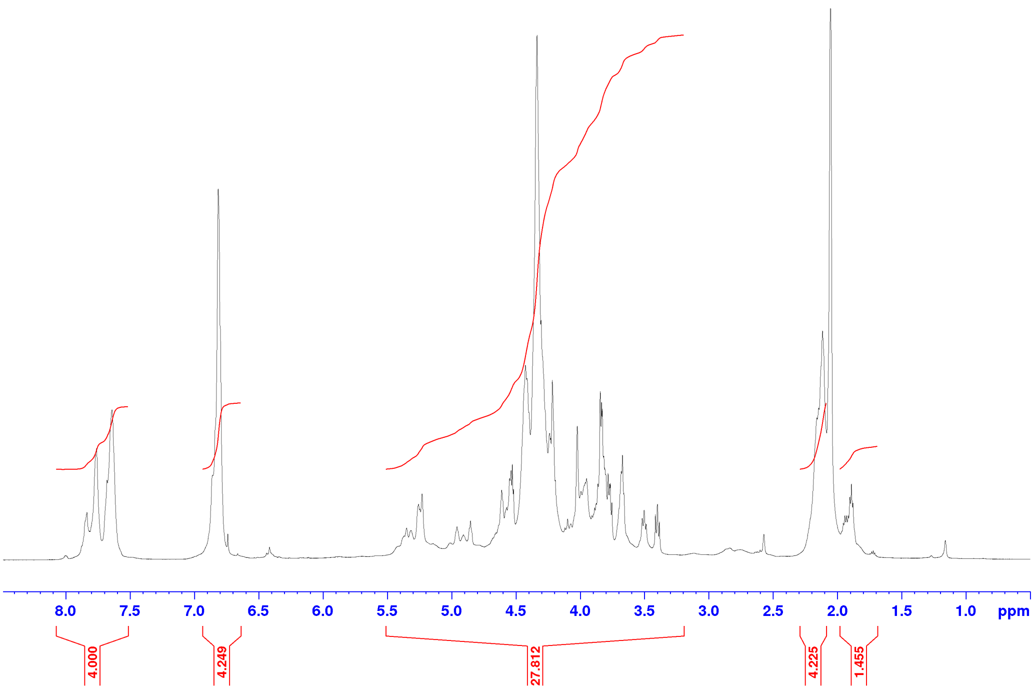
8.0
7.5
7.0
6.5
6.0
5.5
5.0
4.5
4.0
3.5
3.0
2.5
2.0
1.5
1.0
ppm
4.000
4.249
27.812
4.225
1.455

b.

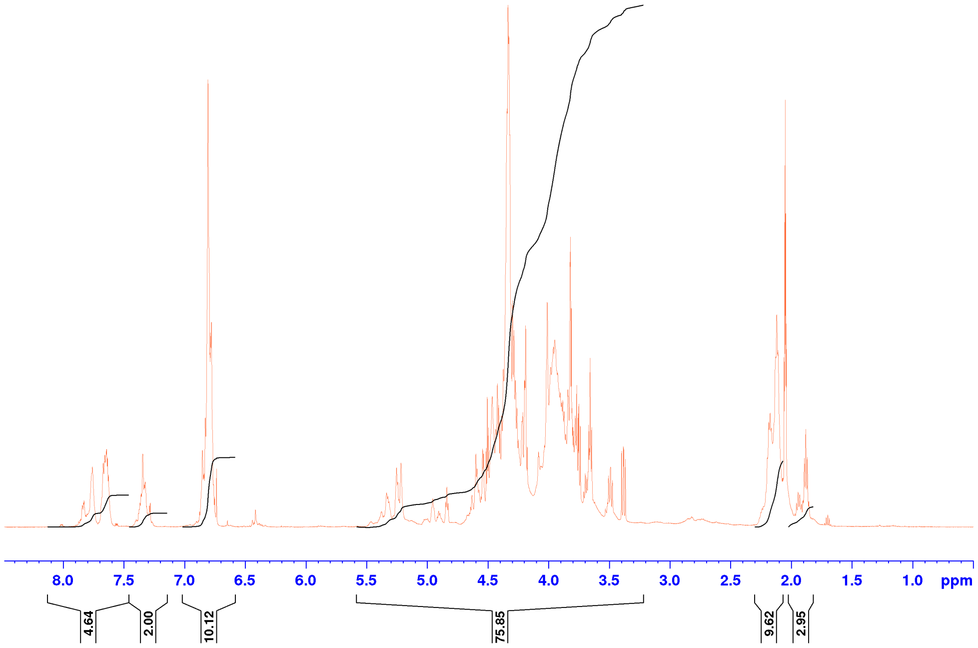
8.0
7.5
7.0
6.5
6.0
5.5
5.0
4.5
4.0
3.5
3.0
2.5
2.0
1.5
1.0
ppm
4.64
2.00
10.12
75.85
9.62
2.95

c.

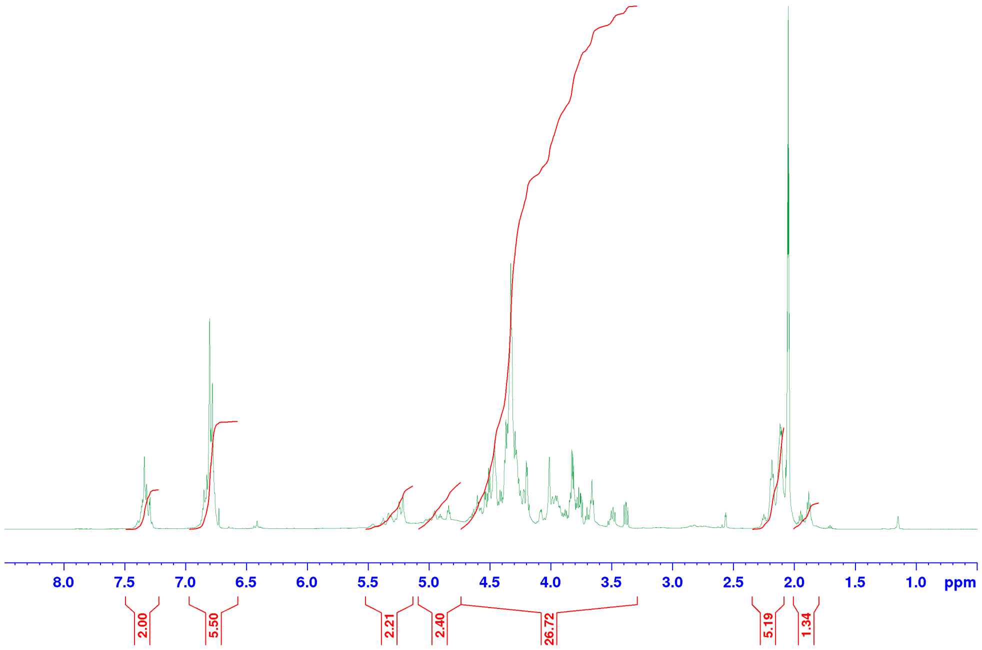

Figure A.9: ^{1}H NMR spectra of the FDCA-based polyester prepolymers: **a.** UP0; **b.** UP50; and **c.** UP100.

Tables A.13 and A.14 show the main resonances highlighting the regions, assignments, and the relative proportions of the constituents of the DFA- AND FDCA-based polyester prepolymers.

Table A.13: Main resonances from the ^{1}H NMR spectra of the DFA-based polyester prepolymers.

Region	Assignment	Integration/nr of protons/relative proportion		
		UP-A	**UP-B**	**UP-C**
7.84-7.65	C-*H* (phthalate)	4.00/4H/1	4.00/4H/1	4.00/4H/1
6.86-6.74	C-*H* (fumaric acid)	4.25/2H/2.12	3.90/2H/1.95	5.03/2H/2.52
1.64-0.79	C-H_2 and C-H_3 (dimer)	-	0.703/6H/0.12	0.986/6H/0.16
5.47-3.31	C*H*+CH_2 (ISO) and O-CH_2 (PDO) + C*H*=C*H* (DFA)	27.81/2.05 for ISO	26.56/1.93 for ISO	30.84/2.08 for ISO
2.35-2.08 and 1.97-1.82	-OCH_2CH_2CH_2O- from PDO	5.68/2H/2.84	5.43/2H/2.72	6.94/2H/3.47

Table A.14: Main resonances from the ^{1}H NMR spectra of the FDCA-based polyester prepolymers.

Region	Assignment	Integration/nr of protons/relative proportion		
		UP0	**UP50**	**UP100**
7.84-7.65	C-*H* (phthalate)	4.00/4H/1	4.64/4H/1.16	-
7.36-7.29	C-*H* (furan)	-	2.00/2H/1	2.00/2H/1
6.86-6.74	C-*H* (fumaric acid)	4.25/2H/2.12	10.12/2H/5.06	5.50/2H/2.75
5.48-3.36	C*H*+CH_2 (ISO) and O-CH_2 (PDO)	27.81/2.05 for ISO	75.85/6.32 for ISO	31.58/2.31 for ISO
2.28-2.07 and 1.97-1.82	-OCH_2CH_2CHH_2- from PDO	5.68/2H/2.84	12.56/2H/6.31	6.53/2H/3.26

A.6 Viscosity

Viscosity tests were performed on a Cone & Plate Viscometer Instrument from REL (Research Equipment London Ltd.), according to ISO 2884 [2] part 2, see Figure A.10. The viscosity of the polyester prepolymers was measured at 125℃ taking the average value of 3 measurements.

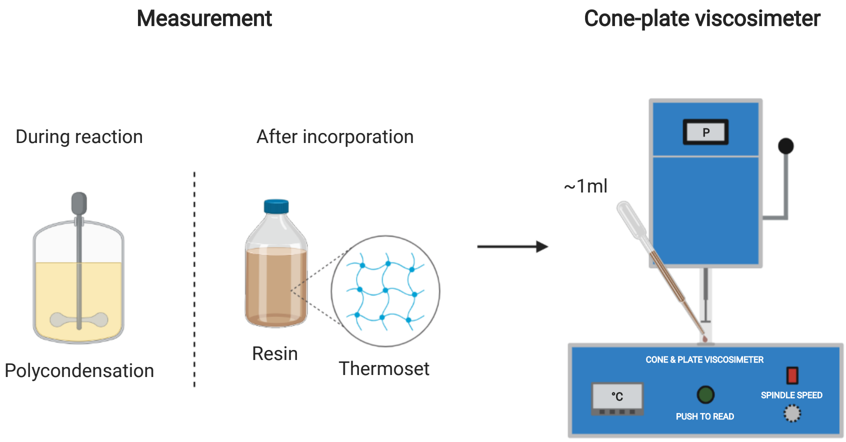

Figure A.10: Viscosity tests performed on a Cone & Plate Viscometer Instrument from REL (Research Equipment London Ltd.), by placing only two drops of resin on a surface that is then approached by a rotating cone (constant speed).

References

[1] Joshua M Sadler, Faye R Toulan, Giuseppe R Palmese, and John J La Scala. Unsaturated polyester resins for thermoset applications using renewable isosorbide as a component for property improvement. *Journal of Applied Polymer Science*, 132(30), 2015.

[2] ISO 2884:2003. Paints and varnishes — Determination of viscosity using rotatory viscometers – Part 2: Disc or ball viscometer operated at a specified speed, 2003.

Appendix B

Resin characterisation

B.1 Mechanical properties

B.1.1 Barcol hardness test

Barcol hardness tests were performed using the Barber Colman Barcol impresser, following ASTM D2583-13 [1]. The testing was conducted within 3 mm of the edge of the specimen. In order to produce an even distribution of force, plate specimens were continuously supported on a stiff, hard, and supportive surface to minimise false data due to bending in the material. Twenty-five tests were conducted on each sample plate. After the test, the average from results was calculated and taken as the Barcol hardness.

B.1.2 Tensile tests

Tensile test specimens were prepared according to part 2 of ISO 527 [2] with dumb-bell-shaped. The specimens were manufactured according to type 1A. The specimens have a prismatic form with reinforcement at the ends to avoid grip failure. The transition is made with a constant radius of 24±1 mm.

Tests were carried out in an Instron 8800D universal testing machine with 250 kN of load capacity and integrated load cell, under displacement control, at a speed of 2 mm/min. The specimens were gripped using a specific pressure, defined in order to minimise slipping of the specimens at the grips while avoiding the local crushing of the specimens. The displacements of six dots/targets (previously marked on the test specimens) were measured along 3 alignments ($1-2$, $3-4$ and $5-6$), through the video-extensometry technique, in which a high definition Sony$^{\text{TM}}$ video camera (model XCG 5005E, Fujinon – Fujifilm HF50SA-1 lens), and a LabView® computer software were used. Furthermore, the 3 alignments allowed to analyse the specimen thickness contraction used for the calculation of transverse strain and determination of the Poisson's ratio.

The specimens were tested under laboratory conditions with room temperature of 23±2 °C and 55±3 % relative humidity. For all specimens, width and thickness were measured with a digital micrometre at three points along the span to check tolerances and minimum area for axial stress calculation. From the test results, the average values of the tensile properties were obtained, namely, tensile strength, modulus of elasticity, and strain at break. Figure B.1 shows the tensile test setup.

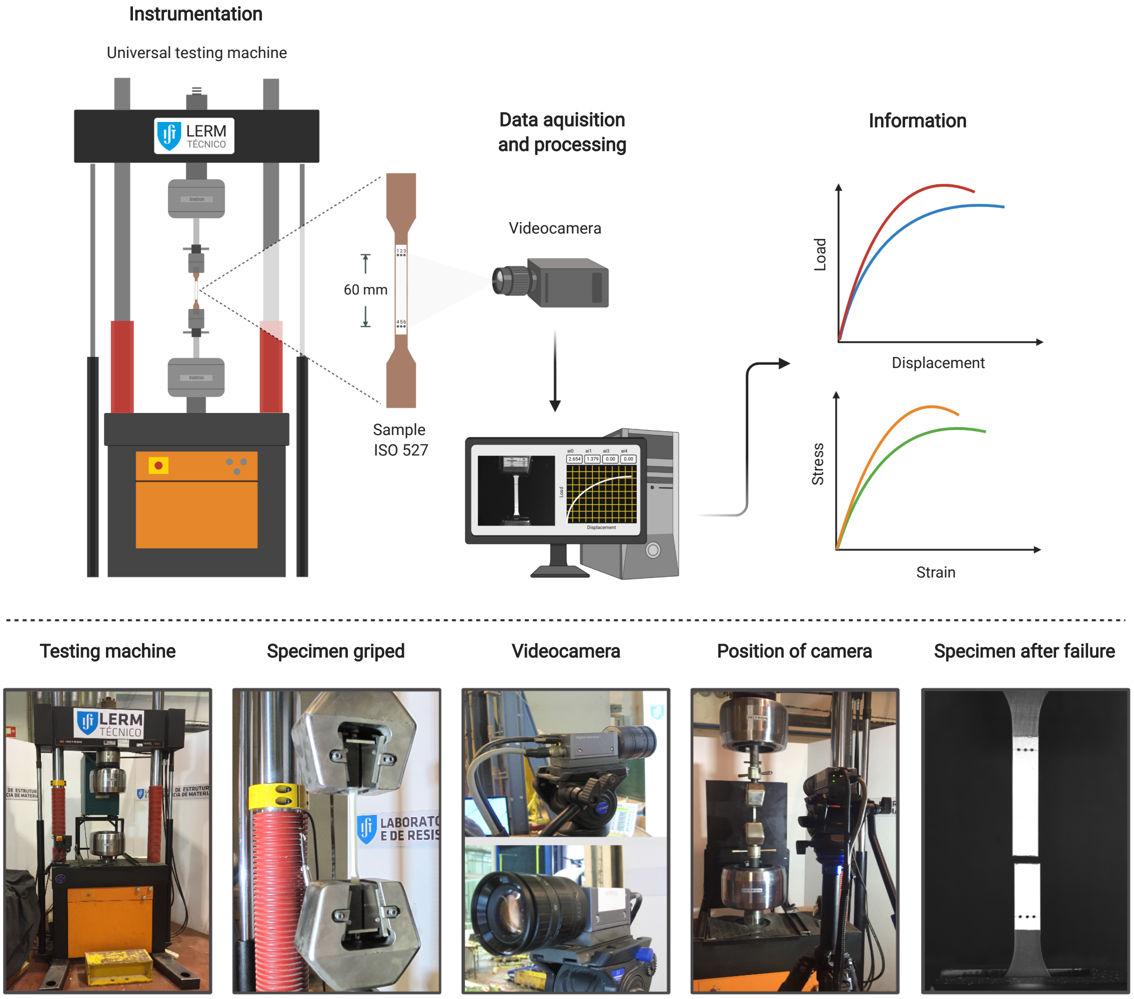

Figure B.1: Setup for tensile tests.

B.1.3 Compression tests

Compressive tests were carried out using a combined loading compression (CLC) test fixture performed to characterise the compression behaviour of the cured resins (thermosets). CLC comprises the transmission of loads to the specimen's central zone (gauge length) by applying a direct compression on the tops of the specimen and transferring load along the lateral face by a friction mechanism. The shape and dimensions of the specimens tested were established based on the ASTM D6641 [3], with 140 ± 3 × 12 × 5 mm (length, width and thickness). The universal testing machine and the camera and acquisition equipment described in the subsection B.1.2 were also used for the compressive tests. The tests were performed at a speed of 1 mm/ min. Figure B.2 shows the compresive test setup.

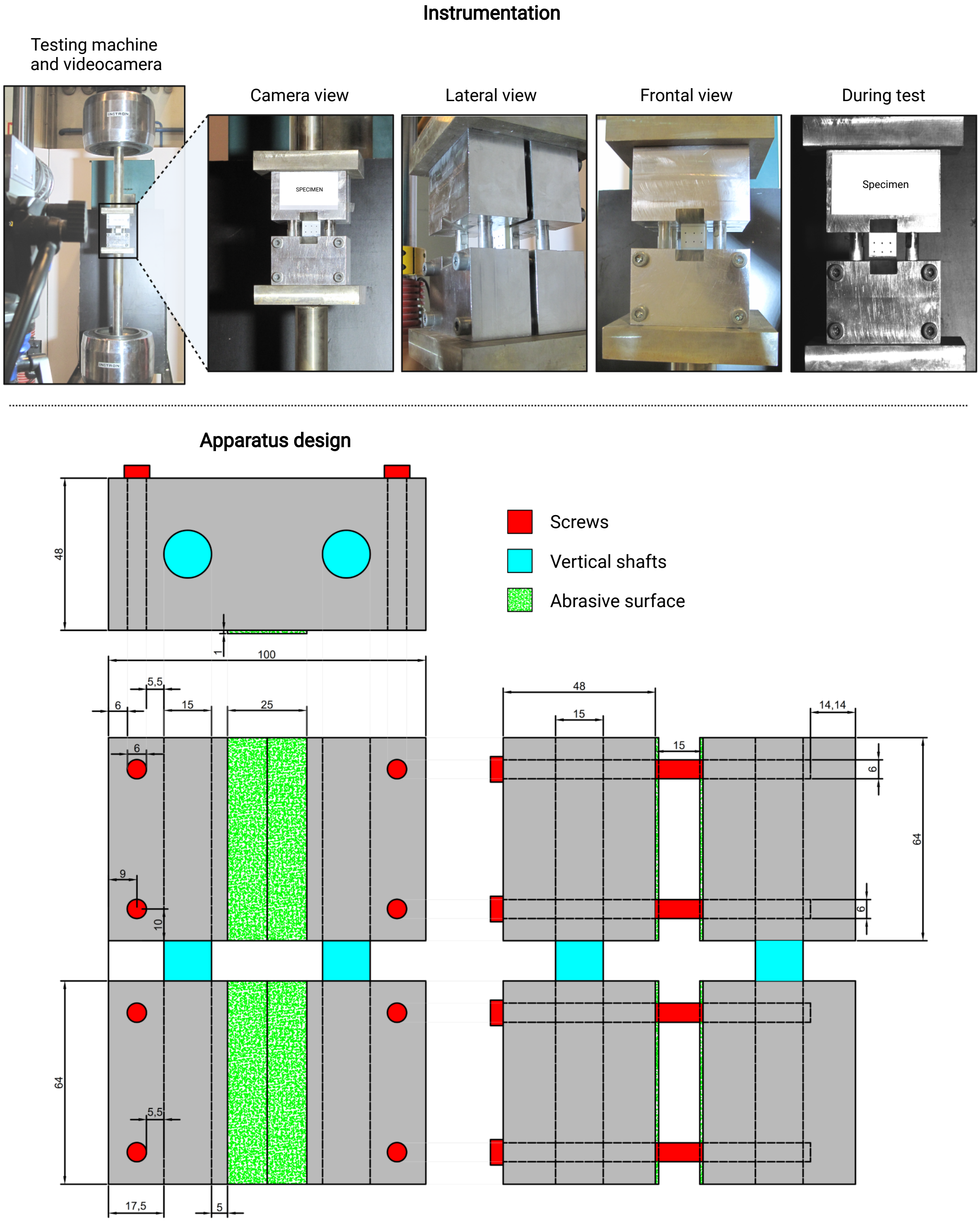

Figure B.2: Setup for compressive tests.

B.1.4 In-plane shear tests

The in-plane shear tests were performed according to ASTM D5379/D5379M, part 5 [4] (Iosipescu or V-notched beam method) - the axial loading of the two independent modules (which apply in-plane shear stresses) was applied under displacement control, at a rate of 2 mm/ min. Figure B.3 shows the in-plane shear test setup.

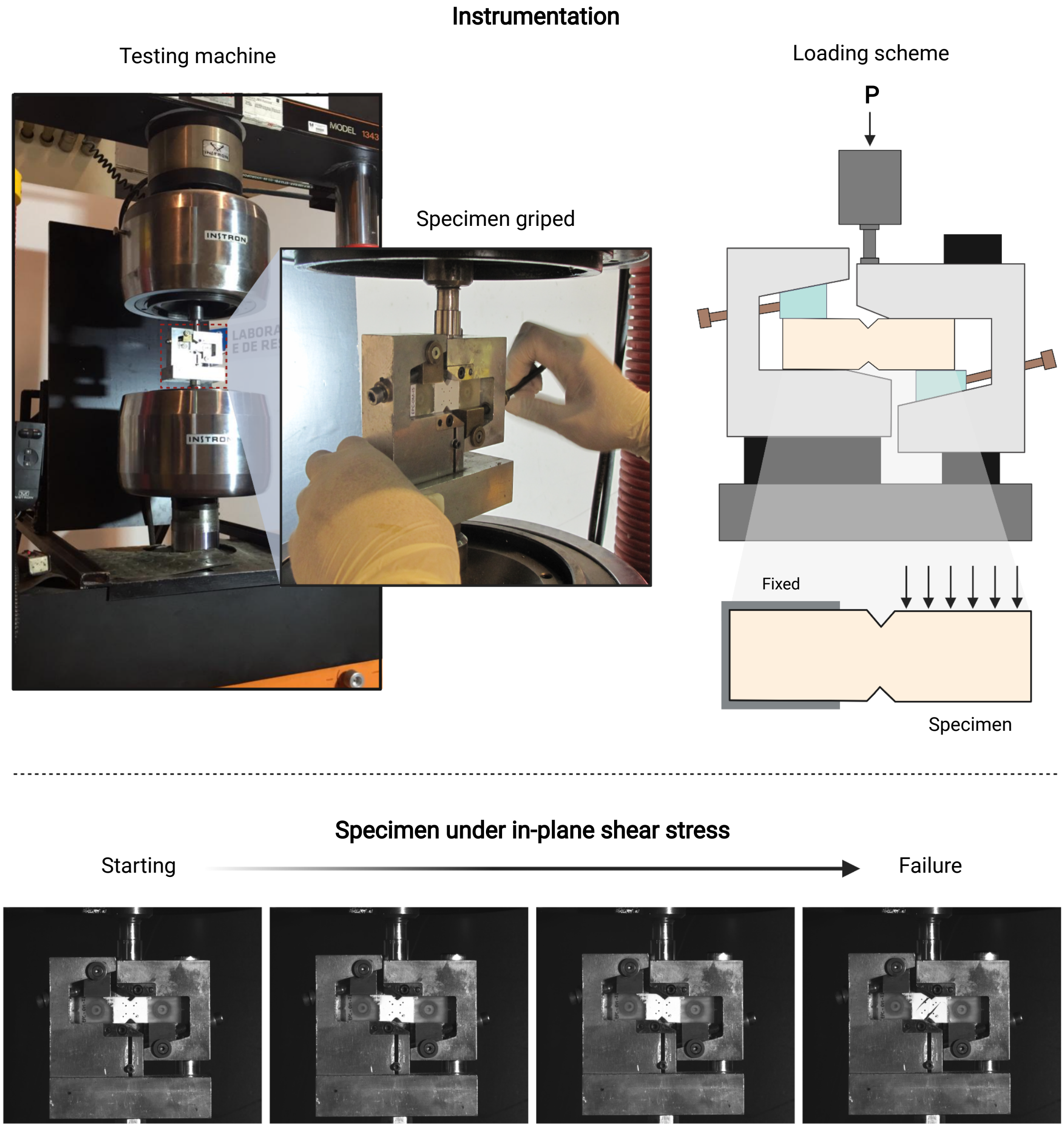

Figure B.3: Setup for in-plane shear tests.

B.2 Dynamic mechanical analysis

To measure the temperature-dependent viscoelastic properties, namely, the storage modulus ($E^{'}$), loss modulus ($E^{''}$), $\tan\delta$ and the glass transition temperature (T_g) of the unsaturated polyester resins, a DMA experiments were performed using a DMA Q800 (TA Instruments), according Figure B.4. Specimens with dimensions 60 mm × 10 mm × 4 mm were fabricated according to ASTM E1640-09 [5], and tested in a 35 mm dual cantilever clamp configuration, where a specimen is clamped at both ends and flexed in the middle. The specimens were subjected to a constant strain amplitude of 15 µm at a constant oscillation frequency of 1 Hz while submitted to a temperature sweep at a constant heating rate of 2 ℃/min, starting at –30 ℃ and ending at 150 ℃.

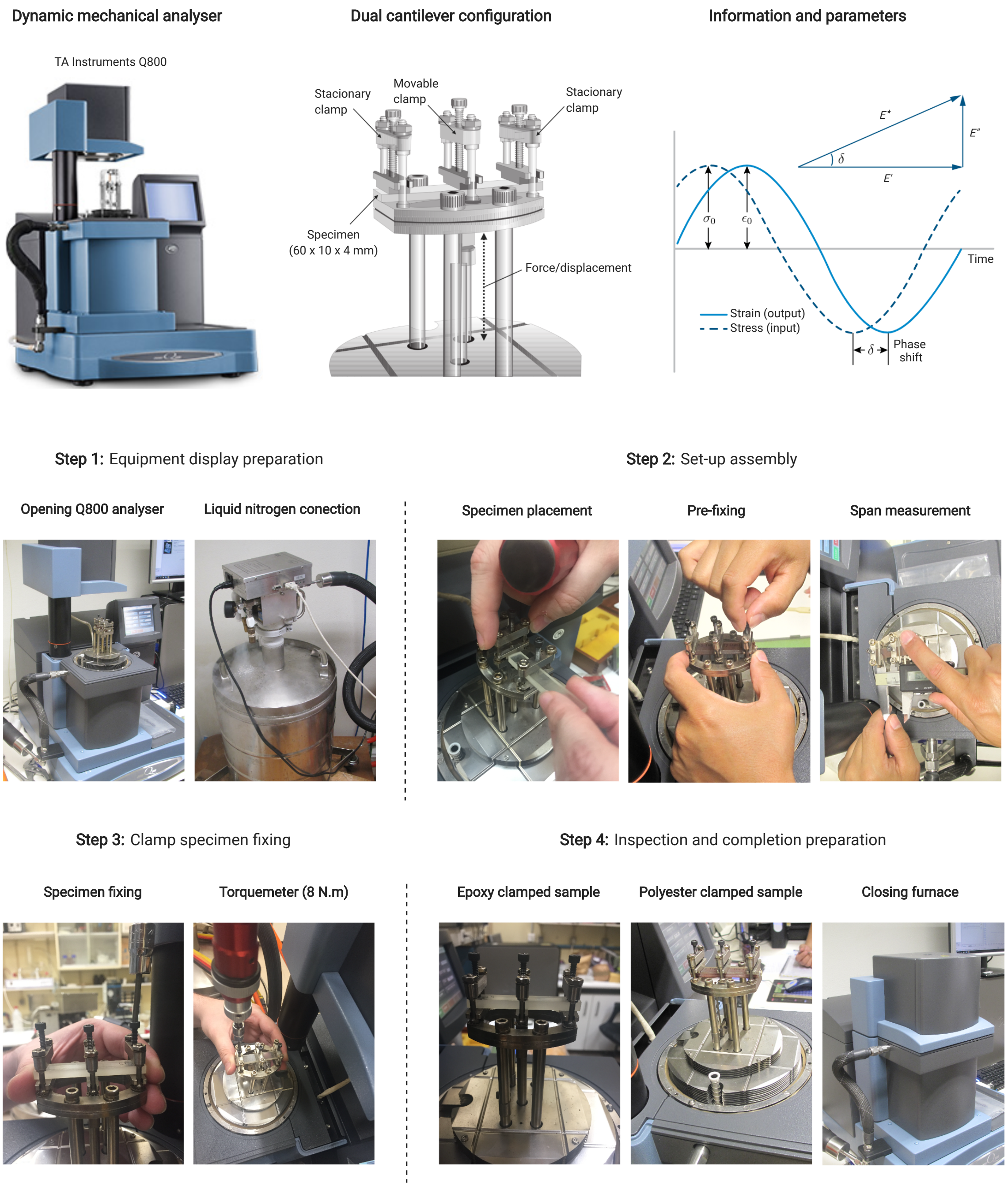

Figure B.4: DMA test setup in a TA Instruments Q800 equipment [6]. Test procedures are also illustrated in four main steps: (1) equipment display preparation, (2) set-up assembly, (3) clamp specimen fixing, and (4) inspection and completion preparation.

B.3 Characterisation of the commercial UPR

Crystic U 904 LVK from Scott Bader, a commercial orthophthalic UPR, was tested as reference resin for comparison with the bio-based UPR developed herein. The commercial UPR received equal cure and post-curing cycles to their bio-based counterparts; namely, MEKP was used as an initiator for free-radical polymerisation for the resin curing and, after exposure during 24 hours at room temperature, the specimens were post-cured during 4 hours at 100 ℃. The commercial UPR specimens were prepared followed standardised dimensions such as those from the bio-based UPRs. In addition, the mechanical and thermomechanical tests were carried out under the same conditions and procedures as the bio-based UPRs. Table B.1 shows the results obtained from the tensile, compressive, and shear tests of the commercial Crystic U 904 LVK resin, listing also its T_g (based on the value of the E' decay).

Table B.1: Mechanical and thermomechanical properties of the commercial UPR.

Resin	$\sigma_{t,max}$ (MPa)	E_t (GPa)	$\epsilon_{t,max}$ (%)	$\sigma_{c,max}$ (MPa)	E_c (GPa)	$\epsilon_{c,max}$ (%)	τ_{max} (MPa)	G (GPa)	γ_{max} (%)	T_g (℃)
Crystic	60.7	3.0	1.9	131.5	4.5	5.2	58.4	1.4	5.2	75.3

T_g measured from the onset storage modulus decay

References

[1] ASTM D2583-13a. Standard Test Method for Indentation Hardness of Rigid Plastics by Means of a Barcol Impressor, 2013.

[2] ISO 527-2. Plastics — Determination of tensile properties — Part 2: Test conditions for moulding and extrusion plastics, 2012.

[3] ASTM D6641/D6641M. Standard Test Method for Compressive Properties of Polymer Matrix Composite Materials Using a Combined Loading Compression (CLC) Test Fixture, 2009.

[4] ASTM D5379/D5379M. Standard Test Method for Shear Properties of Composite Materials by the V-Notched Beam Method, 2012.

[5] ASTM E1640–09. Standard test method for assignment of the glass transition temperature by dynamic mechanical analysis., 2009.

[6] TA Instruments. Q800 Dynamic mechanical analyser (DMA). `https://www.tainstruments.com/q800-dma/`, accessed February 2021.